Studies on Mathematical Models for Characterizing Plume and Drift Behavior From Cooling Towers

Volume 1: Review of European Research

EPRI

EPRI CS-1683
Volume 1
Project 906-1
Interim Report
January 1981

Keywords:
Cooling Tower Plumes
Plume Dispersion
Multiple Plumes
Plume Model
Mathematical Model

Prepared by
Argonne National Laboratory
Argonne, Illinois

ELECTRIC POWER RESEARCH INSTITUTE

Studies on Mathematical Models for Characterizing Plume and Drift Behavior From Cooling Towers
Volume 1: Review of European Research

CS-1683, Volume 1
Research Project 906-1

Interim Report, January 1981
Work Completed, December 1979

Prepared by

ARGONNE NATIONAL LABORATORY
Division of Environmental Impact Studies
9700 South Cass Avenue
Argonne, Illinois 60439

Principal Investigators
A. J. Policastro
M. Wastag

Prepared for

Electric Power Research Institute
3412 Hillview Avenue
Palo Alto, California 94304

EPRI Project Manager
J. A. Bartz

Water Quality Control and Heat Rejection Program
Coal Combustion Systems Divisio

ORDERING INFORMATION

Requests for copies of this report should be directed to Research Reports Center (RRC), Box 50490, Palo Alto, CA 94303, (415) 965-4081. There is no charge for reports requested by EPRI member utilities and affiliates, contributing nonmembers, U.S. utility associations, U.S. government agencies (federal, state, and local), media, and foreign organizations with which EPRI has an information exchange agreement. On request, RRC will send a catalog of EPRI reports.

NOTICE

Prepared by
Argonne National Laboratory
Argonne, Illinois

ABSTRACT

This report reviews recent research on cooling-tower plume dispersion carried out in Germany, Switzerland and France. A large quantity of good-quality laboratory and field data are available which can aid in the validation and improvement of cooling-tower plume models. Laboratory data from Electricité de France (EDF) provide basic parametric information on plume dispersion from one, two, and four towers of natural-draft type. Visible plume field data from Gardanne, Lünen and Neurath (supplemented by ambient profiles and tower-exit measurements) provide, in total, 24 new data cases for use in model validation and improvement studies.

Other data available include measurements at tower exit of liquid water emission rates, droplet-size spectra and temperature/velocity profiles. Profiles of velocity and temperature across the tower top at Neurath have revealed several distinct flow configurations depending on the wind speed at tower top.

Existing European models for cooling-tower plume dispersion are reviewed. Two of the most popular models (KUMULUS and FOG) are tested with field data and found to perform on par with the better U.S. models.

A two-year climatological study at Niederaussem presented interesting information on the long-term physical and biological effects of the cooling towers. A study of bacterial emissions of cooling towers using waste water revealed no significant adverse effects at and in the vicinity of the cooling towers.

Blank Page

EPRI PERSPECTIVE

PROJECT DESCRIPTION

Argonne National Laboratory is performing an effort to develop, improve, and validate mathematical models of cooling tower plumes. Emphasis is being placed on prediction of visible plume trajectory and deposition of saline droplet drift from the tower. Visible plumes and saline drift are environmental impacts of cooling towers that must be considered in power plant siting studies and licensing. A validated mathematical model of plume dispersion provides the industry with the tool required to make an assessment of environmental impact of the cooling tower.

This interim report, in five volumes plus an executive summary, describes results accomplished to date:

Executive Summary--Overview
Volume 1--Review of European Research
Volume 2--Single-Source Model
Volume 3--Drift Modeling of Single Sources
Volume 4--Multiple-Source Model
Volume 5--Drift Modeling of Multiple Sources

In a continuing effort, emphasis is being placed on developing a master model that is user-oriented and designed specifically for siting and licensing studies.

PROJECT OBJECTIVES

The goal of this effort is to develop, improve, and validate mathematical models of cooling tower plume dispersion for individual and clustered mechanical- and natural-draft cooling towers. The overall goal is to provide the utility planner with a tool for studies involving the environmental impact of cooling tower plumes.

PROJECT RESULTS

A model that has been developed and validated has prediction capabilities that are superior to other available mathematical models of cooling tower plume dispersion.

For example, in 77 percent of all cases of single sources that were studied, the model predicted a visible plume rise within a specified accuracy. This was the best performance among all available models (over a dozen) that were investigated.

This effort has also produced a useful review and summary of European research on cooling tower plume dispersion (Volume 1). Workshops in the fall of 1981 and in 1982 are being planned to disseminate to the industry the computer code that is being developed.

This series of volumes should be of value to utility planning engineers concerned with the impact of cooling tower plumes on plant siting.

John A. Bartz, Project Manager
Coal Combustion Systems Division

ACKNOWLEDGMENTS

Much of the information presented in this report was obtained through the cooperation and personal assistance of many individuals. Our thanks are extended to the following:

Dr. Hans Fuchs Dr. Pierre Brog Mr. Michael von Euw	Motor Columbus Consulting Engineers Baden, Switzerland
Dr. André Junod Dr. David Schneider	Swiss Meteorological Institute; Payerne, Switzerland
Dr. Dieter Haschke Dr. Fritz Gassmann Dr. Jan P. Trepp	Swiss Reactor Institute Würenlingen, Switzerland
Dr. Lionel Caudron	Electricité de France Chatou, France
Prof. Günter Ernst Dr. Walter Egler	Karlsruhe University, Karlsruhe Federal Republic of Germany
Dr. K. Nester	Reactor Institute, Karlsruhe Karlsruhe, Federal Republic of Germany
Prof. G. Dibelius Dr. A. Ederhof*	Technical University Aachen, Aachen, Federal Republic of Germany
Prof. Heinz Rögener Dr. Hans Brandes	Technical University, Hanover Hannover, Federal Republic of Germany
Prof. Werner Klug	Technical University, Darmstadt Darmstadt, Federal Republic of Germany

*Now at Brown, Boveri & Cie; Switzerland

Mr. Bruno Rudolf — German Weather Service
Offenbach, Federal Republic of Germany

We would also like to thank Dr. John Bartz of EPRI for his continued support and encouragement as technical monitor for the project. Finally, we would like to thank Dr. George McVehil for the many helpful comments and suggestions he made on a draft of this volume.

CONTENTS

Blank

ILLUSTRATIONS

TABLES

SUMMARY

This report reviews recent research on cooling-tower plume dispersion carried out in Germany, Switzerland, and France. Of interest are experimental data taken both in the laboratory and in the field which would aid in the validation and improvement of cooling-tower plume models. In addition, we sought to investigate the theory and performance of available European models for cooling-tower plume dispersion.

A large quantity of good quality experimental data were found to be available. Laboratory data from Electricité de France (EDF) provide basic parametric studies on plume dispersion from one, two, and four towers of natural-draft type. Measurements were made of plume trajectories and dilutions (through dye concentrations) under fixed tower and ambient conditions where K, the ratio of tower exit velocity to wind speed, was varied. The data show the important influence of the wake of the tower structure in increasing plume bending and increasing dilutions for larger winds. The effect of increasing the number of towers from 1 to 2 to 4 (in different geometric configurations) were also studied in terms of effects on trajectory and dilution.

Visible plume field data from Gardanne, Lünen, and Neurath (supplemented by ambient profiles and tower-exit measurements) provide, in total, 24 new data cases for use in model validation and improvement studies. The quality of the data range from fair to good. The data represent a large range in ambient conditions and levels of heat and moisture release. An intensive study involving in-plume measurements at Neurath (three towers) and Meppen (one tower) has provided considerable insight into the physics of dispersion from the visible and invisible plume. The visible portion of the plume was found to be at the topmost part of the plume, viewing it in a vertical plane; the visible portion is thereby not centered about the centerline of the invisible plume. In addition, small temperature and humidity effects at ground level were noticed from plumes from NDCTs under unstable atmospheric conditions.

European measurements of cooling tower exit conditions have included liquid water emission rates, droplet-size spectra, and temperature/velocity profiles. Field measurements on natural-draft cooling towers indicate that drift contributes about

20% to total liquid emission rates. Differences among measurements between different instruments applied at the same site, Neurath, are partially explainable as a result of temporal and spatial variations of liquid water emission in the tower. A competition among most European methods of measurement of liquid water and droplet spectra was made under controlled conditions at a lab tower. Results are not yet available. An empirical formula for liquid water emission (recondensate only) has been developed at the Technical University at Aachen. The formula is based on measurements made at lab and prototype towers of natural-and mechanical-draft type. The formula has been used for estimating tower liquid water emission for dates in which field data on visible plumes were acquired but no tower liquid water emission rates were measured.

Profiles of velocity and temperature across the tower top at Neurath have revealed several distinct flow configurations depending on the wind speed at tower top. At low winds, thermal instabilities result in cold air entering the tower affecting the mass, velocity, and temperature of the emission. At larger winds, puffing or vortices occur in the emitted plume. Implications for better tower design are discussed. Implications for plume modeling of these cold air incursions into the tower may be important due to the resulting alteration of tower exit conditions due to cold ambient air mixing in the tower.

European models for cooling-tower plume rise may be divided into two categories. The first refers to models developed for and commonly used for environmental impact analyses; the second classification are those models which are more complex in formulation and are expensive to run but were developed with the primary aim of representing internal plume dynamics in a microscopic level. The KUMULUS Model of Motor Columbus Consulting Engineers and the FOG Model of the Swiss Reactor Institute were tested by us with field data from single and multiple natural-draft cooling towers. The KUMULUS Model (recalibrated version) performed as well as any available American model. FOG Model predictions tended to give visible plumes that were shorter and of lower rise than the observed visible plume data. In spite of this systematic behavior, the FOG Model performed on par with the better U.S. models.

The only major climatological study carried out in the U.S. and Europe was performed during the period 1972-1974 at Niederaussem, a 1500 MWe plant containing both natural and mechanical-draft cooling towers. Some conclusions from the physical measurements follow. First, plume shadowing was imperceptibly small beyond 1000 m from the towers; interestingly, however, irradiation along the sunny side of the visible plume is <u>increased</u> by 5-10% across a considerable area by reflection by

the plume fog droplets, which appear to be white. Second, temperatures are almost always higher and relative humidities lower on the lee side of the power station than corresponding values on the upwind side. The cause of the increased temperature on the lee side is mainly the waste heat emitted by the power station itself, probably the boiler house, rather than the cooling towers. Third, results seem to indicate (yet not proven conclusively) that precipitation around the cooling towers is a little higher than at a greater distance and that the cooling tower plume occasionally led to an intensification of the precipitation in the immediate vicinity of the cooling tower complex. Fourth, a shortening of the leaf wetting duration on the lee side of the power station was also found.

A comprehensive study was carried out in the Federal Republic of Germany to assess the possibility of germs being emitted from cooling towers when waste water was being used for cooling. The study encompassed many field tests on existing wet cooling towers (inside and in the vicinity of the towers) where measurements of micro-organism concentrations and types were made. These tests were supplemented mainly with germ concentration measurements carried out on a laboratory cooling tower. No risk of infection was found from the lab or field studies and should not occur, in general, for towers with modern drift eliminators.

Section 1

INTRODUCTION

Much research has been carried out in Europe in the area of environmental impact of evaporative natural- and mechanical-draft cooling towers. Much of the valuable information acquired has not been made available to researchers in the U.S. Of special interest is the laboratory and field data which have been acquired to aid in the understanding of cooling tower vapor plume dispersion. Also of interest are the mathematical models for plume dispersion which are commonly used for environmental impact analyses. This report summarizes the most important studies carried out to date and reviews the direction of present work.

Since the major limitation on the improvement in the state of the are of plume modeling is the quality and quantity of the data base, a combined European and American data base on cooling tower plumes provides special advantages for model improvement. In addition, a review of the better European plume models provides an expanded fund of ideas from which a better choice of assumptions for improved plume (and drift models) can be made.

This report is divided into four parts. Section 2 reviews instrumentation and measurements commonly made on natural- and mechanical-draft cooling towers. Those measurements are mainly for tower exit conditions and are used as: (a) part of the input data to plume (and drift) models and (b) information on the thermal performance of the towers themselves. Section 3 describes European laboratory and field data acquired on cooling tower plumes. Section 4 reviews the available plume models. Section 5 evaluates two of the most popular European cooling-tower plume models with American and European field data.

Blank

Section 2
INSTRUMENTATION AND MEASUREMENTS OF TOWER EXIT CONDITIONS

INTRODUCTION

Much of the published work studying the character and quantity of emissions from cooling towers has been done in the Federal Republic of Germany. (A good discussion of the kinds of wet and dry cooling towers in operation in Europe may be found in Refs. (1 - 3). Considerable insight has been gained in understanding the physics of plume formation inside the tower and in quantifying the liquid water emissions from cooling towers.

In the area of liquid water emission from towers, German measurements have confirmed that the water given off by the evaporative towers consists of two kinds of droplets:

1. those which have arisen by recondensation during the evaporative cooling process in the cooling tower and are accordingly designated "recondensation droplets". The recondensate droplets are generally less than 10 μm in diameter and contain negligible quantities of salts
2. those which have arisen from spraying and are called "drift" or "spray" droplets. Drift droplets are generally larger than 40 μm in diameter and contain salts that were present in the cooling water.

The theory of droplet growth predicts that the recondensation droplets, which are the only ones responsible for the visibility of the vapor plume inside and outside the tower, are nearly the same size and that the rate of fall of those recondensation droplets will not greatly exceed 1 cm/s. As a result, these droplets would be deposited far from the tower if they did not evaporate entirely. The drift size ranges are, of course, larger and are independent of the thermodynamics of the tower but are a function of the internal characteristics of the tower and the kind of drift eliminators in use. Measurements on the mass flow rate for each type of droplet (recondensate, drift) have been made on prototype towers in Germany as well as measurements of the drop size distribution for both the recondensate and drift drops.

The drift droplets are only important in drift deposition and have no effect on plume dispersion. The recondensate droplets are important in that they provide the

initial liquid loading to the plume and affect the character of the visible plume. Recondensate liquid emission generally ranges from 0.5 - 2.0 g/kg dry air. This kind of range can lead to significant differences in visible plume lengths under summer conditions; visible plumes are less sensitive to that range in initial liquid water loading under winter conditions. Unfortunately, U.S. measurements of plumes from cooling towers (Paradise, Chalk Point, and Amos sites) have not included determination of liquid water emission. That omission lowers the overall quality of the data sets and in some summer cases makes it very difficult to predict visible plume characteristics without an estimate of that initial liquid water loading. Although summer plumes are generally small, a consistent theory of plume dispersion is sought which can predict plumes from all seasons. Selected European data have included these measurements. Field data for plumes which do not include tower exit liquid water measurements may be improved through the use of a fairly accurate empirical correlation for recondensate liquid water emission, recently developed from measurements made in Germany. That interesting relationship, developed from prototype measurements, was the result of work at the Institute of Steam and Gas Turbines at Aachen and is presented below (4 - 6).

In addition to field measurements on liquid water emission from towers, advancements have been made in the theory of evaporative cooling. Work at the Technical University at Hanover has permitted a reasonably accurate predictive model of the condensate load of the plume. That tower model (by Poppe (7)) was tested with field data at a prototype tower and performed fairly well.

Of great interest to plume modelers is the work done at the University at Karlsruhe in which detailed measurements were made in time of velocity and temperature at the exit plane of an operating NDCT. Surprising patterns, especially concerning flow instabilities were observed which may have profound implications on plume dispersion. Those results too will be reviewed below.

Selected measurement methods on tower exit conditions and some sample results will be described below. The instrumentation to be discussed here have been employed in two types of studies: (1) basic studies on the theory of evaporative cooling, and (2) large coordinated plume mapping surveys where such instruments have been used to provide measurements on tower exit conditions.

METHODS FOR MEASUREMENT AND RESULTS OF LIQUID WATER EMISSION FROM COOLING TOWERS

Throttle Calorimeter (Prof. H. Rögener, and Mr. H. Brandes, Technical University, Hannover) (8 - 10)

The throttle calorimeter measures the total droplet load (recondensate plus drift contributions) of the plume at the point of measurement, usually taken just above the drift eliminators. A diagram of the instrument and a diagrammatic representation of its physical principle appears in Figure 2-1. The principle employed is based on the following. A thermodynamic peculiarity of gases (including moist gases) is that they do not change their temperature during adiabatic throttling (reduction in pressure by, for example, use of a vacuum pump) as long as such gases do not contain any water droplets. However, if that air did contain water in droplet form, then the water droplet/air mixture would actually cool during the throttling. Thus, supersaturated air would go over into an unsaturated state as a result of the lowering of its pressure. In fact, the droplet load can be computed directly from measurements on the exact amount of cooling that occurred.

During the throttling, the partial pressure of the water vapor is lowered in the same ratio as the total pressure of the mixture. In this way, the partial pressure of the water vapor becomes smaller than the saturation pressure associated with the given temperature. As a result, the droplets evaporate and provide additional water vapor which the air absorbs. In this process, the droplet/air mixture provides the necessary warmth for the evaporation itself and the mixture accordingly cools. If the pressure in the throttle is lowered so far that the water droplets completely evaporate, then the originally present droplet content can be determined in a simple manner from the temperatures before and after the throttling occurred. The throttling calorimeter thus reacts to the droplet content only and thus its sensitivity and accuracy can be made quite high.

An advantage to the method lies in the fact that the temperature difference referred to above can be determined very precisely by means of a thermoelectric pile (difference in temperature between two thermocouples). The local plume temperature, which is actually the inlet temperature to the calorimeter, is also a necessary input to the formula for evaluation of liquid water emission. That temperature can be measured with moderate accuracy without significantly influencing the total uncertainty of the measurement. A simple analytical expression for the droplet load appears in Ref. (9), p. 51; only the plume temperature and thermocouple temperature difference are required input variables to that formula. Interestingly, the actual pressure and humidity state after throttling is not significant.

In the field, the instrument is hung downwards into the upward plume flow in the cooling tower so that a partial stream can enter isokinetically (at the same velocity and direction as the upward plume flow). Within the instrument itself, the throttle path is insulated against heat exchange with the environment. Ten minute to half-hour periods of time are required at a fixed location for one set of readings. Strip chart recordings from the thermocouples in the throttled section (actually there are 6 thermocouple elements set up in front and 6 behind the throttle) indicate when all drops have evaporated. [If a droplet has not completely evaporated and strikes a thermocouple, the thermocouple temperature no longer reads dry-bulb and jumps to wet-bulb value.] Clearly, the temperature difference measurable at the throttle is not constant but has a fluctuating mean value which varies with time. It is estimated that the maximum uncertainty of the measurement method is $\pm$ 0.05 g/kg dry air.

It should be noted that one instrument provides only a point value of water loading during a 10-30 minute period. The location chosen for measurement may not, of course, represent the mean value of liquid water loading over the tower cross section. Recall also that the throttle calorimeter provides total water loading, i.e., recondensate plus drift droplets. Additional means must be available to distinguish the separate contributions of recondensate and drift to the total liquid water loading. Interestingly, a mechanical-draft cooling tower (MDCT) run under zero heat load provides no recondensation droplets but identical drift liquid mass emission as the positive heat load case. Thus, an estimate of the relative contributions of the recondensate and drift portions of the total liquid water emission for a MDCT may be made with the knowledge of (a) the zero load liquid water emission and (b) the full heat load liquid water emission. No such simple method of estimating the liquid recondensate contribution to the total liquid water emitted is possible for natural-draft cooling towers. Measurements of the liquid loading for one of three towers at Neurath (300 MWe) in the period Oct.-Dec. 1973 yielded values varying from 0.38-3.32 g water/kg dry air for total liquid emission.

It is interesting to note that one of Rögener's students (Poppe (7) in his Ph. D. Thesis) has developed a mathematical model to predict the recondensate load from a natural-draft cooling tower. Simulating the cooling tower (e.g., Neurath) as a pure counter-current heat and mass transfer system (air flowing upwards into narrow channels on whose walls the water to be cooled runs down as a film), Poppe wrote continuity equations for dry air and water along with an energy balance for a cross-section of the tower. The ordinary-differential equation system which resulted determined the state change which the air undergoes. As soon as the air has

reached the limit of saturation, its additional state change is described by a slightly different set of equations. Input to the model are: cold water temperature, hot water temperature, ambient dry bulb and wet bulb temperatures, air pressure, air flow through the tower, and water flow through the tower. The integration of the coupled differential equations from the cold water temperature to the hot water temperature yields the state of the vapor emerging from the inner components of the tower. Results are in terms of water content, specific enthalpy, and weight of water evaporated. All equations for the model are presented in the Ph.D. thesis of Poppe (7). A short review of the model equations is given in Ref. (9). [The computer code for the model is not presently available although the authors are willing to run their program for those interested.] The Poppe model was compared to throttle calorimeter water loading measurements at Neurath. There generally was less than a 50% difference between predictions and observations. It should be noted that drift contributions (not predicted by Poppe's model) to total liquid loading of the plume at tower exit to about 20% based on other measurements at Neurath (9). There were other difficulties in judging the model/data comparisons since the throttling calorimeter measures the "instantaneous" (over 10-30 min period) and local value of liquid loading at its measurement location, which, under certain circumstances may vary considerably from the associated time and space mean values predicted by the Poppe model. Results of some other measurements with the throttling calorimeter are presented by Bung (11).

Another published comparison of Poppe model predictions to field data is reproduced in Table 1. Here the total droplet content measured at exit to a natural draft cooling tower (equipped with drift eliminators) is compared to the content of recondensation droplets to be expected according to the calculations of Poppe. The agreement here is quite good. The influence of the outside air state on the intensity of the vapor plume appears clearly. In this case, the droplets found in the plume at tower exit appear to have been formed predominately (or nearly exclusively) because of recondensation.

Diffuse Light Probe (Prof. G. Dibelius and Dr. A. Ederhof, Institute for Steam and Gas Turbines, Aachen (4 - 6))

The diffuse light probe is an optical system which is used to measure the droplet size spectrum for droplets in both the recondensate and drift size ranges. Through integration over the entire drop spectrum, the total water load of the emitted plume may be computed from the measurements.

The measurement principle for the probe is illustrated diagrammatically in Figure 2-2. The image of the arc of a strong light source is formed across a lens, the aperture 1, and the objective 1 in a plane at the scattering volume. If a droplet in a stream of droplets passes through that light beam, then the light is scattered by it, i.e., it acts as an independent light source for an observer who views this droplet. The intensity of the scattered light observed at a solid angle θ is a measure of the size of the scattering droplet. The frequency of occurrence of that scattered light pattern determines the concentration of that size droplet in the flow stream. For the measurement probe designed, the observation is carried out 90° to the direction of illumination.

The scattering volume is the volume cut out by both ray paths. It can be enlarged or reduced over wide limits, as required. The larger the scattering volume chosen, the more accurate is the measure of concentration of the larger droplet sizes. The scattered lateral diffuse light in the direction of observation is conducted on a second light path across the objective 2, the aperture 2, and a prism to a photo-multiplier, which transforms the light pulses into voltage pulses. With the aid of an oscillograph and pulse height analyzer, these impulses are recorded according to their size and number. With the aid of a previously set up calibration curve, the particle sizes are determined from this.

The pulse width, i.e., the retention time of the particles in the scattering volume, is a measure of the particle velocity. From the summation of all the particle weights which fly through the cross section of the scattering volume (located perpendicular to the direction of movement of the particles) per unit of time, the particle weight per unit time and area can be calculated. For the measurement of water droplets in air, this is the local liquid flow rate.

Figure 2-3 shows the measurement probe as constructed. The probe is connected by cables to the cooling tower during data acquisition. Measurements have been made at the tower top and also above the drift eliminators. See Figure 2-4 for location of diffuse light probe at the Neurath natural-draft cooling tower. At the tower top, measurements are usually taken at 5 m steps along two cables traversing the tower diameter in two perpendicular directions. Previous measurements above the drift eliminators were less difficult due to available walkways and thus the probe was is able to be brought to the desired measurement location by hand. Measurement time ordinarily amounts to several minutes per measurement point (for droplets in the recondensate range). With the presence of the larger (and rarer) drift drops, this

measurement time is protracted considerably. Longer measurement times can, of course, lead to other questions such as synopticity of measurements. The probe may be set at four sampling volumes (choice of 2 probe heads, each with a choice of 2 apertures). The sampling volumes allow measurements of drop diameters in the approximate ranges: $0 < D_0 \leq 70$ μm; $70 \leq D_0 \leq 150\text{-}200$ μm; $150\text{-}200 \leq D_0 \leq 500$ μm; and $D_0 \geq 500$ μm. Any number of droplet bins within each of those four ranges may be reported. The probe is often combined with an anemometer for vertical speed determination and a temperature sensor. The updraft velocities so measured aid in calculating the liquid mass flow per unit air mass flow of plume out of the tower.

Figures 2-5 and 2-6 show sample measurements with the diffuse light probe. Presented are droplet size spectrum measurements at the Staudinger MDCT for full load (solid line, denoted "full load"). Note that two frequency maxima Figure 2-5 are clearly distinguishable. This is typical of Dibelius-Ederhof measurements made to date. The two distributions are separated by an intermediate range of droplet sizes with very small droplet counts. Clearly, the droplet range 2-10 μm refer to recondensate droplets and the range 40-80 μm to drift droplets for that MDCT. Since the results of Figures 2-4, 2-5 and 2-6 were determined on a ventilator (mechanical-draft) cooling tower, the recondensation process could almost entirely be suppressed if there were no heat load from the power station but maintaining the standard air throughput. In such a case, then, the only drops to be measured would be drift droplets. Results of such measurements also appear in Figure 2-5 with the dotted line referring to measurements made under zero heat load conditions. The river water used in the discharge cooling (pumps operating only) in this case was somewhat warmer than the air. Accordingly, it was slightly cooled in the cooling tower so that some slight recondensation still appears. The ejection of large droplets is, however, almost completely independent of the thermal load. Thus the light probe has shown that recondensed and drift droplets can thus be separated by means of the droplet size range for an MDCT. This was also confirmed by Dibelius and Ederhof from theoretical considerations of the mechanism of the origin of the droplets.

Dibelius and Ederhof have made numerous measurements with their diffuse light probe at natural-draft, mechanical draft, and experimental towers. They have found an interesting empirical correlation between the recondensate liquid emission and tower and ambient parameters. The correlation is presented in Figure 2-7. The graph is from Dibelius and Ederhof; (6) the mathematical formula was developed at ANL to represent that graph. The same correlation should apply for both NDCT and MDCT prototype applications. Recent measurements at the NDCT at Meppen in the Federal

Republic of Germany indicated additional verification for the correlation. The correlation provides that the more efficient a tower is on a particular date in dissipating the waste heat, the less recondensate liquid emitted by the tower. We have used the formula presented in Figure 2-7 as a predictive tool to estimate the liquid recondensate emitted from NDCTs and MDCTs in cases where other plume data were acquired but the measurements did not include liquid recondensate emission.

A study (4) of the recondensate emitted during the Neurath study from Oct.-Dec. 1973 yielded some interesting facts about the recondensate liquid water emission from one of the three 300 MWe towers in operation.

1. Condensate flow distributions at different points along a diameter traverse at the tower top showed marked variations. There was a decrease in liquid recondensate emission starting from the lee side of the tower to the side exposed to the wind. The condensate flows are not only subject to local spatial variations across the tower, but to a strong degree to temporal variations. These temporal variations are caused by periodic irruptions of cold air which come in from outside the tower and can penetrate very deeply into the chimney part of the tower. The determination of tower mean values of the liquid recondensate is made difficult due to the various uncertainties resulting from such marked variations. These cold air irruptions are very much wind-dependent which help explain the often-noted wind-directional dependency of the condensate flow distribution across the tower.
2. Larger condensate drop sizes were observed more in the summer than in autumn. The weight of the droplets whose diameter is greater than 5 μm for the summer measurement is about 50%; for the autumn measurements, in contrast, it is less than 2%. In regions of the tower exit where the condensate is less, the average drop diameter is larger. This is a result of separation effects as a result of cold air irruptions: smaller droplets follow a directional change of the air flow more easily than do larger drops.
3. Autumn measurements showed that the droplet spectra, measured above the inner components of the tower, hardly differ from those at the cooling tower top for the same tower operational conditions. The droplets are only slightly larger at the tower top, about 0.1 μm larger in average diameter due to the slight coagulation of droplets on the way to the top. Thus not much growth occurs for these droplets in their travel from the drift eliminators up to the tower top.
4. It is remarkable that the condensate flow differs greatly depending on updraft air velocity and air temperature differences in the tower which together lead to "cold" spots or "warm" spots. It was found that when there are low plume temperatures and high updraft velocities at cold spots, the condensate load of the air is reduced to about 6% or less of the corresponding value at the "warm" spots. Sometimes no condensate is emitted from the cold spots. These cold air bundles are locally fixed and might result from the wind influence.

5. In the transition from complete load on the tower to partial load, the recondensate drop size distribution changes to somewhat larger droplets. Also, there was found to be a 15-fold increase in condensate emitted at points on the tower exit where there are no drift eliminators below.

6. For winter measurements, the recondensate liquid water emission rate over the inner components of the tower was quite uniform across the tower. The average diameter was always still small but clearly greater than in the autumnal measurement; the condensate load was higher than in the autumnal measurement.

Heat Probe (W. Roller and Prof. G. Ernst; Institute for Technical Thermodynamics; University at Karlsruhe) (12)

This instrument provides another measure of the droplet load of the plume in the cooling tower. The heat probe has been applied in the winter of 1973, the summer of 1974, the summer of 1975, the winter of 1976 and summer of 1976 in various weather conditions in cooling tower C of the Neurath Power Station. It has been applied at the tower exit plane and the plane just above the drift eliminators.

The measurement principle of the device (see Figure 2-8) is as follows: A partial stream from the plume with a temperature of θ_1 (state "1" in Figure 2-8) is heated up so that all the water droplets evaporate. After the heating, state "2" is measured with an aspiration psychrometer. If the saturation moisture x_s corresponding to the entrance temperature θ_1 of the plume is subtracted from the absolute moisture x_2, then one obtains the droplet load x_{F1} of the plume.

This droplet load consists of recondensate and drift droplets; the heat probe cannot distinguish between these. Note the similarity to the throttling calorimeter: both instruments work by evaporating all water droplets in the plume sample. However, the throttling calorimeter evaporates them by setting up a very low pressure environment. The heat probe evaporates all drops by heating. The heat probe requires measurement of the wet and dry bulb temperatures of the sample after heating. The throttling calorimeter requires only the dry bulb temperature measurement in the parcel state at low pressure (in addition to the plume dry bulb temperature upon entrance to the calorimeter). The droplet content, as determined by the heat probe, is calculated as the difference between two water vapor contents. This, in general, appears as a relatively small difference between two large numerical values. The measurement apparatus accordingly cannot achieve the sensitivity and accuracy of the throttling calorimeter.

The structure of the heat probe is also given in Figure 2-8. At the entrance to the aluminum tube, which is 1 m long with inner diameter 50mm and heat-insulated, a jacket heating area 1500 mm long is tightly screwed on. In the interior of the tube, about 130 mm from the lower end, spirally arranged turbulence plates are rigidly connected to the aluminum pipe. Above the turbulence plates, the tube is filled up to the flange with aluminum wool on whose surface the water droplets are separated and evaporated.

The plume is suctioned in isokinetically. The capacity of the jacket heating area, which is continuously adjustable up to 800 watts, produces enough heat in the aluminum tube and in the turbulence plates that all the water droplets suctioned in are evaporated. The flange provided with a heat-insulating seal thermally separates the "evaporator section" from the "measurement section."

In the "measurement section", a blower moves the heated and unsaturated plume through a turbulence screen to the aspiration psychrometer. The psychrometer and the plume thermometer are mounted as a unit on a slide rail. The cheesecloth sheath on the wet bulb thermometer is supplied with distilled water from the vessel in the lower part of the rail.

The resistances of all platinum thermometers are calibrated with a water triple-point cell and a accurate measuring bridge (1ppm). For this reason, values up to about 50°C can be measured with an accuracy of $\pm$ 1/100 C. Higher temperatures do not occur during the measurements. Although the probes have a height of about 1.2 m, they are light enough to be suspended on horizontally stretched wire cables. Another advantage of their low weight is their short thermal adjustment time, of about 2-3 minutes.

The above discussion of the measurement principle and probe assumed that the plume air was saturated. This is true generally for natural draft cooling towers. However, for low thermal load and relatively high air velocities in the inner components of a ventilator (MDCT) cooling tower, it can happen that the plume is not saturated at the measurement location, in spite of the presence of cooling tower droplets which may be carried along. In that case, an additional measurement must be made: the wet bulb temperature of the plume sample entering the heat probe. Two cases are possible. If the plume sample after heating is supersaturated, then the difference in vapor contents yields the droplet load after saturation of the plume air. If, on the other hand, the plume sample after heating is subsaturated, then the difference

in vapor contents represents the greater moisture which must be added to the initial plume sample to achieve saturation under equilibrium conditions. Details on these possibilities are discussed further in Ref. (12). In all, the droplet load is measured by the heat probe with an accuracy of 0.1 g/kg dry air.

An improvement in the measurement system was made and was first employed during the summer of 1975. The three thermometers employed in each heat probe were interrogated at the same time rather than individually as done previously. This shortened the time of interrogation for the 4 or 8 heat probes often used for measurements on one cooling tower. Interrogation of all eight heat probes then would last only 24-80 seconds. This improvement was necessary considering the temporally varying plume temperatures.

In the winter of 1973 and the summer of 1974, measurements were carried out with four heat probes in the cooling tower top and four above the inner components of the cooling tower. In the other measurement programs, 8 heat probes were sometimes used at the same time, all located above the inner components of the cooling tower. In any case, after one interrogation cycle, the temperatures of the ambient air, the cold water and the warm water were measured and recorded for the purpose of setting up a correlation similar to Figure 2-7. The droplet loads measured by the individual heat probes are determined for each interrogation cycle. For the measurements at cooling tower C at Neurath, results agreed, on the average, when done simultaneously at the cooling tower top and over the inner components of the tower.

In Figure 2-9, the mean values of the droplet load X_{Fl} are shown representing 3402 interrogation cycles (21,630 individual measurements). The data points represent measurements of the droplet load of the plume at different times of the year. The droplet load x_{Fl} of the plume is plotted as a function of the difference of the mean water temperature θ_{Wm} (arithmetic mean value from the warm water temperature and the cold water temperature) and the ambient temperature θ_U.

For conditions in the summer (small differences between the mean water temperature θ_{Wm} and the environmental temperature θ_U), the droplet load of the plume is lower than it is in the winter. The measurement points "P" indicate droplet loads x_{Fl} for a cooling water flow reduced by about 30%. The measurement points "T" characterize the droplet load x_{Fl} of the plume with a capacity of the turbine reduced by about 45%.

Conductivity-Condensation Method (Prof. G. Ernst, Institute for Technical Thermodynamics, University at Karlsruhe) (3, 13)

This method permits the separation of liquid load on the plume into recondensate and drift components. It also provides an independent measure on the total liquid water emitted by the tower. Figure 2-10 provides a sketch of the apparatus used.

This conductivity-condensation apparatus cools the wet plume air that passes through it by means of ice water. The droplets in the plume sample which are enlarged due to the condensation process occurring in the apparatus are separated from the air in a helical tube. The drift contribution is determined from an equation of balance of ionized impurities passing through the apparatus; a measure of these impurities is taken to be the electrical conductivity.

In this conductivity-condensation method, a part of the plume is suctioned and cooled in the pipe helix. A film of condensed water forms in which the droplets present in the plume are separated. This film is collected in a condensate vessel. Across a second piping not shown in Figure 2-10, the droplets which separate onto the inner wall of the suction funnel are conducted into the condensate vessel. The suctioned air flows into the funnel with the rate of the ascending plume. The air flowing out of the condensate vessel contains only water vapor in the saturation state. Its temperature, θ_1, and its pressure, p_1, are measured, so that its moisture content x_{so} can be calculated. The air mass m_{Ltr} suctioned through the apparatus (not including the contribution of water) is determined with a gas meter; the mass m_F of the collected condensate is determined with a balance.

From the measurements just described, we can compute the moisture x_1 of the entering plume from the simple formula

$$x_1 = x_{so} + \frac{m_F}{m_{Ltr}} \qquad (2\text{-}1)$$

and the condensate load of the plume from

$$x_{Fl} \simeq x_1 - x_s\,(\theta_1, p_1) \qquad (2\text{-}2)$$

Here, the saturation moisture content x_s of the plume (corresponding to temperature θ_1 and pressure p_1) is subtracted from the moisture x_1 of the plume. The conden-

sation loads thus determined agrees with those measured by the heat probes in a satisfactory manner. The differences amount to about $\pm$ 0.3 g/kg.

The moisture content and condensate load of the plume are computed above. A determination of the drift loading follows from a balance on the electrical conductivity. The balance requires knowledge of

- Mass of collected condensate, m_F
- Air mass suctioned through the apparatus during the period of time that the condensate was accumulated, m_{Ltr}
- Electrical conductivity of liquid in the condensate vessel, σ_F
- Electrical conductivity of the cooling water entering the cooling tower, σ_m
- Moisture content of the surrounding air, x_U, and
- Electrical conductivity of the moisture in the surrounding air, σ_U.

The conductivity balance equation can be solved for x_m to yield

$$x_m = \frac{m_F}{m_{Ltr}} \cdot \frac{\sigma_F}{\sigma_m} - x_U \cdot \frac{\sigma_U}{\sigma_m} \qquad (2\text{-}3)$$

Further details are presented in Ref. (13).

This apparatus is clumsy in comparison to the heat probes. It is not very well suited for measurements of the condensate load at several places at the same time or even at the cooling tower top. Above all, the apparatus best serves to determine the proportion of the drift water in the plume which is not removed by the drift eliminators. Since the value of this magnitude can vary quite markedly across the inner components of the tower, its mean value for the entire cross section of the cooling tower only leads to a relative accuracy of about $\pm$ 40%.

The conductivity-condensation method implicitly assumes that the electrical conductivity of drift droplets is equal to the conductivity of the cooling water. This is a reasonable assumption since droplet spectra measurements by Dibelius and Ederhof (presented earlier) on NDCTs have also shown that drift droplets do not grow or evaporate between the location of the drift eliminators and the tower top. Apparently, the time of travel from drift eliminators to tower top is too small for significant droplet growth to be possible. For the same reason, we expect that drift droplets will not be able to grow or evaporate significantly between formation and capture by the conductivity-condensation apparatus.

Results of some measurements at Neurath in 1973 will now be given. For three measurement programs (July, Sept./Oct., and Dec. 1973) which include 74 measurement periods, mean values of the measurements of the condensate load $\bar{x}_{Fl}$ of the plume are presented (Ref. (13)):

for summer and autumn $\bar{x}_{Fl} = 2.0$ g/kg

for winter $\bar{x}_{Fl} = 1.7$ g/kg

The bar over x refers to averaging done across the tower to achieve a single value for the survey and also to averaging done over surveys carried out within the same season. These condensate loads are, of course, carried along with the moisture of the emerging air of the plume.

On the average, about 0.3 g cooling water per kg dry air was found to be entrained as drift based on the conductivity-condensation method. This corresponds to a flow of drift water of about 2 kg/s or 0.02% of the cooling water flow. The drift emission rate was found to be about 20% of the liquid recondensate emission rate, using the conductivity-condensation apparatus.

Measurements from the diffuse light probe presented earlier indicated that the condensate load in winter was larger than in summer and both were larger than measurements during autumn. The conductivity-condensation apparatus shows the measurements about even among seasons. Although the diffuse light probe is probably more accurate in such determinations, other confusing features are present such as spatial and temporal variations of the plume state in the cooling tower. It also should be kept in mind that competing instrumentation were not present at the same time (and same location) in the tower. Simultaneous measurements between instruments is the best method of intercomparison. See below for a discussion of the available comparisons of all these competing methods of measurement of recondensate loading, drift loading, and droplet-size spectra. Clearly, there is much disagreement over which of these competing instruments is superior for cooling tower measurements.

Double Calorimeter (H. Dittrich and Prof. G. Ernst, Institute for Technical Thermodynamics, University at Karlsruhe) (14)

This method is quite promising for measuring total liquid droplet load but at present no tower measurements have been made. The apparatus is not set up to distinguish drift and recondensate liquid water. A prototype of the probe is presently under construction.

The measurement principle is based on the difference in specific heats between supersaturated and unsaturated air. An interesting feature of supersaturated moist air is its high specific heat, caused by the heat of evaporation of the liquid water. An example should illustrate this: if to supersaturated air with a droplet load of 1 g/kg and a temperature of 30°C, sufficient heat is introduced (under isobaric conditions) that the saturation state is achieved, i.e., that all the water evaporates, then the temperature increases by 0.6°C to 30.6°C. If the same heat is introduced to unsaturated air, then its temperature increases from 30°C to 33°C, that is by 3°C. The double calorimeter first heats the wet and the dry plume in two heating chambers connected in series.

The two heating chambers are connected in sequence to a measurement apparatus, in the manner shown in Figure 2-11. The plume is suctioned through both heating chambers. In the first chamber, the supersaturated plume is converted into the unsaturated state by the heat flow $\dot{Q}_1$. In the second heating chamber, the unsaturated air is heated by the heat flow $\dot{Q}_2$ to determine the mass flow. Only three temperatures and the two heat capacities have to be measured.

In the first chamber, the entrance state is given by the temperature θ_1, the droplet load x_F, and the water vapor content x_{D1}. If we assume thermodynamic equilibrium, then the water vapor content x_{D1} is equal to the saturation moisture content at the temperature θ_1. At the exit of the first chamber, all the liquid water is evaporated; there remains only the vapor content x_{D2}, which is greater than x_{D1} by x_F. The temperature θ_2 here is higher than the dewpoint temperature. The heat flow Q_1 which has to be supplied for this change of state can be easily calculated as a function of: the mass flow of dry air suctioned through, the specific heats of air and water vapor, the heat of evaporation, and x_{D1}, x_F, θ_2, θ_1.

In the second chamber, heating of the stream of unsaturated moist air is shown. Here the vapor content x_{D2} remains constant; only the temperature changes. The heat flow $\dot{Q}_2$ which is introduced may be computed from the mass of dry air flow through the chamber along with the two specific heats, x_{D2}, θ_3 and θ_2. Assuming we know $\dot{Q}_1$ and $\dot{Q}_2$ along with θ_1, θ_2, θ_3, and the two specific heats, our energy equations for each of the two chambers can be solved for the plume initial water content, x_F.

The measurement accuracy to be expected is very good. In order to determine the droplet load with an accuracy to 0.1 g/kg, the temperatures must be exactly measured to about 0.06°K. This does not represent a problem. With the use of the

precise measurement apparatus and calibration thermometers, this accuracy should easily be exceeded. The heating capacity ratio K must also be known to about 1%, in order to guarantee the accuracy of 0.1 g/kg for the determination of the droplet load under standard operating conditions. This is achieved by connecting the heating coils for both chambers in series. K is then equal to the ratio of the two heating resistances $K = R_2/R_1$.

By suitable selection of the resistance material, this ratio can be kept constant to an accuracy of 0.1%. Heat losses which also influence the ratio K can be kept sufficiently small by appropriate design measures.

The expense for the apparatus is quite minimal. In addition to two heating chambers and three thermometers, only an air suction ventilator which overcomes the slight pressure loss in the probe is required. If the ventilator is connected to a strong motor, the probe is not susceptible to many disturbances and should operate without maintenance. Because of the compact structure, the weight and size can be kept small enough to make it possible to install the probe in the cooling towers easily. As the connection to the outside, only a multiwire cable is required. As noted earlier, a prototype of the double calorimeter is presently under construction.

Discussion of the Alternative Methods of Measurement of Liquid Water Emission from Cooling Towers

As presented above, a number of different methods are available and have been employed in Europe for the measurement of liquid water emission (recondensate and drift) from natural and mechanical-draft cooling towers. It should be noted that most of them (the calorimetric methods: throttling calorimeter, heat probe and the double calorimeter) only provide total liquid emission and are unable to separate the recondensate and drift contributions to the total liquid water emission. Only for mechanical-draft cooling towers under zero heat load conditions will the contribution of the recondensate drops disappear. However, the conductivity-condensation method and diffuse light probe were able to separate recondensate and drift.

A sixth method is available, a full discussion of which is not given since we do not have many details. Older, unpublished measurements of the Technical Monitoring Association of Essen have indicated that the cyclone separator determines the recondensation droplets only partially, but is able to determine the drift droplet contribution to total liquid water emission. Assuming that these two components of the liquid emission are completely separated, one may obtain the proportion of the drift droplet mass of the plume from the mass and the electrical conductivity of the

eliminated water (see Figure 2-12), the conductivity of the cooling water, and the mass of suctioned off vapor plume. For practical reasons of measurement, the two related methods of conductivity-condensation and conductivity-cyclone separation are best able to measure the drift droplet content directly above the droplet eliminators and not the content at the cooling tower exit. In addition, droplet content at the tower exit may possibly have been changed by recondensation or reevaporation or by coagulation with recondensation droplets. However, measurements from the diffuse light probe at Neurath have indicated that, at least for the recondensate droplets, such increases in droplet sizes are negligible as droplets rise from drift eliminators to the tower top.

Two other methods deserve some mention here. The first involves the use of sensitive paper. The procedure generally involves the use of specially prepared filter paper in which water droplets collected from the plume leave colored spots, and from the size of the spots, the diameter of the droplets is determined. From the number of the spots, the quantity of the droplets contained in the plume is determined. Droplets below about 25-50 μm in diameter will not generally be recorded.

The second method sometimes used is the photographic method in which droplet sizes and concentrations are determined from a photograph of the plume sample. This method has problems in that the sampling volume is not well known. Also, large drops can mask smaller drops behind them. Furthermore, the precise size of the oblong-shaped droplets (seen by photograph) provides some difficulty in size determination.

Table 2-2 summarizes European (mainly German) methods of measurement for drift water content of the plume (applied at the tower exit or above the drift eliminators). Estimated measurement uncertainties and smallest droplet content measurable are also listed. The lowest droplet contents measurable with the aforementioned methods (except with the less accurate heat probe), according to a rough estimate, are probably between 0.002 and 0.01 g_{water}/kg_{plume}.

Table 2-3 provides examples of the kinds of numbers obtained from measurements of the drift emission (does not include recondensate contribution) of plumes (at the tower exit or above the drift eliminators) with the various instrumentation described above. From Table 2-3, drift emission rates were never more than 0.2% of the cooling water flow for any of the natural draft or mechanical-draft cooling towers tested. The remaining values fit into two groups: in one group, the values are between 0.01 and 0.02%, and for the other, they are approximately between 0.002

and 0.004%. Installation No. 10 refers to a tower for the chemical industry and not a standard power station. It is thought that 0.01% of the circulating water might be state-of-the-art for German towers. However, values of an order of magnitude less have been observed. Those lower values probably need verification by additional measurements.

During June 1978, the German EPA has sponsored an evaluation of the methods described above to determine which method is state-of-the-art. An experimental mechanical-draft cooling tower, already set up at the Technical University at Hanover for basic studies on tower heat and mass transfer, was used to make comparison tests of the different methods. This experimental tower was meant to represent a real tower by providing a model of a section of a real tower. In that tower, water and air-flux quantities were adjusted between a number of values; the drift and recondensate liquid water content could be measured at the top of the tower. The experimental tower had the major characteristics of a European natural-draft cooling tower including vertical plates (24 of them spaced the same distance apart as in a real tower, but 90 cm deep instead of 120 cm), drift eliminators, and the vertical updraft (from a fan, not from natural draft, however). The laboratory model did, however, lack the small area where the cooling water is sprayed to the top of the vertical plates. The tower had 10,000 m^3/hr air flow with inlet water temperatures which could be varied easily from about 7°C-60°C. Variations in tower inlet conditions were made about 10 times a day to permit different cases for measurement. There were five days of testing encompassing about 60 different sets of tower conditions. The ranges in tower conditions permitted the range in liquid water emission from a low of 0.00006 to a high of 5g/kg. Cases with and without drift eliminators were set up.

The measurement methods tested were: throttling calorimeter, diffuse light probe, photographic method, heat probe, conductivity-condensation method, sensitive paper, photographic method, and the cyclone. The PILLS system of the Environmental Systems Corporation (Knoxville, Tennessee USA) was also to be used for comparison measurements as well except that it arrived damaged from the plane trip from the U.S. ESC employed sensitive paper instead during the study. A duct above the drift eliminators had 2 large holes inserted in it to allow two groups at a time to carry out their measurements simultaneously.

A report on the comparison of measurements was to be issued in early 1979. However, disagreements resulted as to the standard of comparison and the methodology used in the carrying out of the tests. It has been agreed to repeat the tests in mid 1979.

MEASUREMENTS AND RESULTS OF VELOCITY AND TEMPERATURE MEASUREMENTS AT THE COOLING TOWER EXIT

Prof. Ernst and his colleagues at Karlsruhe have been studying the flow and temperature field at the tower exit of a natural-draft cooling tower and how that flow and temperature field varies with ambient conditions, mainly the wind speed at tower top. The results have been very surprising and have led to much new information and insight. A system of temperature and updraft velocity sensors was set up at 11 points at the exit to one of the three NDCTs at Neurath. On high-grade steel cables, 11 measurement units were suspended; each consists of a hydrometric vane (for updraft velocity) and a platinum resistance thermometer. The design and the distribution of the units over the cross section of the cooling tower are shown in Figure 2-13. Each measurement unit hangs vertically so that the anemometers measure the vertical component of the velocity of the plume; from those 11 velocity measurements, the cooling tower discharge flow may be computed.

During the field program of the summer/autumn of 1973 at Neurath block C, the temperatures and the velocities at the 11 measurement points were recorded for periods of about 20 minutes. At each measurement location, 20 to 30 measurement values for temperature and updraft velocity were made per survey. In the winter, this rate was reduced to 10 values for each measurement point with measurement rounds of 8 minutes duration.

Analysis of the data showed several characteristic formations of the plume at the tower exit at Neurath depending on the magnitude of the ambient wind speed (see Figure 2-14 for illustration).

Under calm conditions or a low wind velocity, a cold air ring lies in the cooling tower and surrounds the plume causing a vertical pressure gradient in the tower, equal to the pressure gradient outside the tower (diagram a in Figure 2-14). Due to this cold air ring, the plume is accelerated as a free buoyant flow; i.e., as if the upper end of the cooling tower stack containing the cold air ring were not present. For a low cross wind (0.5-2 m/s), a cold air wedge forms in the cooling tower on the side exposed to the wind (diagram b in Figure 2-14); the form, position and size of this wedge can vary. Here also, the part of the cooling tower in which the plume is accelerated as a free buoyant flow does not contribute to the suctioning of the air from the environment through the inner components of the tower. The influence of the top part of the tower is essentially lost. For a cross wind of medium velocity (2-5 m/s), some cold air irrupts into the cooling tower and moves horizontally as well, often up to the center of exit opening. In rare cases, this

cold air can form a plug across the entire cross section for a short period of time. In general, this cold air which is lying flat narrows the exit of the plume so greatly that it gets shifted out by the plume in pulses, with the ambient air flowing back in the tower periodically (diagram c in Figure 2-14). At a high wind velocity (5-10 m/s), an inner vortex appears on the side of the cooling tower exposed to the wind, at the top (diagram d in Figure 2-14). The position of the vortex changes less and less with increasing wind velocity but with increasing wind velocity, the diameter of the vortex becomes increasingly smaller. This inner vortex partially closes off the exit cross section, and with a sudden abatement of the wind can be shifted out by the plume. At very high wind velocities (10-20 m/s), the plume appears on the lee side of the cooling tower in a flat shape with a relatively high exit velocity (diagram e in Figure 2-14). At the same time, a large part of the plume is suctioned across the top edge of the tower into the low pressure areas to both sides of the cooling tower and moves downwind in the form of two edge vortices. A noticeably bifurcated plume appears.

Figures 2-16 through 2-19 illustrate these results further. Figure 2-16 sketches a cold air irruption under the conditions of Figure 2-14 (diagram c). A weak gust of wind causes a narrowing of the plume for about 30 seconds. The static pressures left and right of the dividing line are the same; the higher specific gravity of the cold air is compensated for by the inertial forces of the accelerated plume flow. A rough estimate in this case gives a temperature of about 25°C for a stable cold air irruption provided (a) the irruption occurs over a short period of time, (b) the irruption is of 25 m depth, (c) the plume accelerates from 4.3 to 5.5 m/s within this 25 m height difference, and (d) the plume temperature is 30°C.

Figure 2-17 presents a summary of velocity measurements in the tower exit cross section for a wind velocity of 5 m/s; this case was also presented in Figure 2-14 (diagram c). For each of the 11 measurement points, $\bar{w}$ refers to the mean vertical velocity, w_{max} is the maximum vertical velocity, w_{min} is the minimum vertical velocity, and θ is the mean plume temperature during a period of 5 minutes of measurement. Thus, Figure 2-17 does not represent an instantaneous record of a stable cold air irruption over a short period of time. However, one can recognize clearly how the rates on the side exposed to the wind vary and are, in part, negative, while the flow on the lee side is quite steady. The lower temperatures measured on the side exposed to the wind allow us to conclude that at the cooling tower top, the plume did occupy that area for most of the time.

Figure 2-18 illustrates a large wind case. Here the flow is not influenced by the

thermal instabilities that occur for the lower winds, but instead is influenced by complicated turbulence systems. Here, a characteristic inner vortex occurs inside the tower. The inner vortex is wind-driven and rotates on the side exposed to the wind. This vortex significantly reduces the exit cross section for plume emission. In this way, relatively high flow rates must occur in the free cross section of the tower exit plane. The higher momentum flow of the plume requires increased ascending force, so that the total temperature level in the cooling tower must increase to provide the additional buoyancy. The inner vortices consist of plume parcels with a small mixture of cold air, as can be seen from the temperature distribution. These mixed parcels are continuously fed by the plume within the tower yet empty on both sides of the cooling tower through the boundary vortex sketched in Figure 2-19.

During 1976 and 1977, further detailed measurements have been made at the natural draft cooling tower C of the Neurath power station in order to study the relationship between the wind velocity at the height of the cooling tower top and the plume flow in the top. As with the other measurements, ten hydrometric vanes were suspended on steel cables (Figure 2-13 and 2-15). In addition, a wind measurement device was installed (Figure 2-15) on a steel cable at a height of about 115 m in the center between the towers C and E. It consisted of two hydrometric vanes which were arranged in a cross.

During a measurement period of 5-10 minutes duration, the velocity and direction of the plume ("upwards" or "downwards") at the tower exit were recorded simultaneously every 1 1/2 seconds at all ten measurement points at the tower top. In addition, the wind velocity and wind direction were measured and recorded. The temperature of the plume above the inner components, the ambient temperature, the ambient moisture and the air pressure were also measured. A total of 130 such field surveys were performed at different times of the year and for different operating conditions of the cooling tower. For each measurement survey, about 300 instantaneous profiles of the exit velocity were made which may be related to the associated velocity and direction of the wind. Thus, a total of about 40,000 instantaneous flow profiles are available for evaluation. As a sample of the results, Figures 2-16 through 2-19 present (a) the wind speed, (b) a local flow velocity of the plume at measurement location 11, and (c) the average flow velocity derived from ten local updraft velocities of the plume, all plotted against time. Clearly, large variations in tower exit velocity occurs as a result of strong variations in the ambient wind speed.

A complete evaluation of the measurements is not yet completed. As an intermediate

result, however, Prof. Ernst finds that the plume flow is most strongly impeded when the velocity of the wind at the height of the tower top is about equal to the velocity of the plume at tower exit; that is, for wind velocities between about 2.5 and 5 m/s at Neurath. At low wind velocities, thermal instabilities at the cooling tower top can result in irruptions of cold air into the tower. As noted earlier, those thermal instabilities occur from the fact that the vertical pressure gradient inside the tower is smaller in magnitude than the pressure gradient in the surrounding air outside the tower. Clearly, warmer air inside the cooling tower is of lower density.

Ernst notes that the adverse effect of these thermal instabilities can probably be removed or reduced if the upper part of the cooling tower is narrowed (rather than expanded outwards as is common for NDCTs of hyperbolic type). with such a design, the magnitude of the pressure gradient within the cooling tower crown is greater than outside, as a result of the acceleration of the plume, so that the following is true:

$$\left|\frac{\partial p}{\partial z}\right|_{\text{inside}} > \left|\frac{\partial p}{\partial z}\right|_{\text{outside}} .$$

For high wind velocities, such a narrowed contour at the tower exit would act as a sort of guideplate by deflecting the wind upwards, so that the formation of the inner vortices which narrow the cross section would be hindered. By means of additional wind guideplates pointing upward, the effect could be reinforced.

By means of these corrective measures, Ernst believes that a lower cooling tower height (than in the designs used to date) may be employed while still providing the same cooling tower capacity. He believes that the top 10-20 m of existing towers are not being fully utilized.

Ernst's study of the flow and temperature distribution at the tower exit of the common hyperbolic NDCT has two main impacts, one in terms of modeling, and the other in terms of design. In the first area, we are made aware that the tower exit profiles are not at all uniform (top-hat) as all mathematical models assume. For low winds, the full tower exit cross-section is not being used by the plume due to the cold air wedge penetrating the tower outlet. For moderate winds, a portion of this cross section is also cut off. Due to the cold air often penetrating the tower for moderate and high winds (usually a very transient and intermittent process), additional mixing is occurring inside the tower leading to a reduced overall tower plume temperature at exit than expected assuming no ambient air flow interference. As a

result, the plume buoyancy is lowered and the corresponding buoyant uplift is less. The mass of air emitted by the tower will be enlarged (including now plume plus ambient air penetrating the tower) for these cases (moderate to large winds) when transient penetrations of cold air occur. Thus, the true tower exit conditions may be quite different than ordinarily assumed and will be quite variable in space and time. Ernst also has noted that the character of the ambient/plume interaction inside the tower is reflected in the plume character at distances far downwind of the tower. For example, consider those cases where the wind is strong enough to periodically constrict the plume's exit from the tower (Diagram c in Figure 2-14 along with those cases in which the wind speed is approximately equal to the tower exit velocity). Ernst notices that the plume exits the tower in puffs with those puffs remaining as individual convective cells even at far distances downwind. In these cases large amounts of cold air flows into the tower and then out, enlarging the mass of the plume and causing it to exit as puffs. Thus the character of the air intrusion into the tower will affect plume behavior outside the tower, according to Ernst. The precise functional correlation between tower exit variables and ambient wind speed is very important to determine but Ernst has found the relationship very difficult to define due to the intermittency of the air intrusions.*

The second area of impact of the Ernst work is in the design of natural draft cooling towers. Ernst's studies have shown that the topmost portion of a NDCT of hyperbolic type (diverging outlet) is not effective in providing upward draft to the plume, due to the divergent shape of the top of the tower, encouraging cold air intrusions. He has recommended a shorter tower of convergent-shaped top (also less expensive to build) which he expects to provide the same overall thermal performance. Two towers are planned in the Federal Republic of Germany with this convergent-top shape. The towers will be for the 700 MWe coal-fired Bergkamen plant for Steag (utility) and a tower for the 1200 MWe nuclear plant Schmehausen.

---

*The mixing of cold ambient air into the tower probably does not change the mean heat emission or buoyancy flux from the tower. However, the plume will undergo additional entrainment and this entrainment happens to occur at (or inside) the tower exit rather than in the free air. It may well be then that cold air intrusions have an important effect on plume dynamics as Ernst states, but it is not certain at this point that plume models must necessarily take cold air intrusions into account in order to predict correct gross plume characteristics.

SUMMARY

European measurements of cooling-tower exit conditions have centered around liquid water emission rates, droplet-size spectra, and temperature and velocity profiles. These data have been taken as part of cooling-tower performance tests and as supportive studies to cooling-tower plume mapping surveys.

There are several measurement methods employed for total liquid water emission rates. The calorimetric methods cannot distinguish between recondensate and drift contributions. The conductivity-condensation method and the diffuse light probe (measuring droplet size spectra) are capable of distinguishing the two contributions. Field measurements on natural draft cooling towers indicate that drift contributes about 20% to total liquid emission rates. Recondensate emissions (droplets less than about 10μm) are important in the determination of visible plume length (under summer conditions especially, based on model sensitivity studies) while the drift emission rate (droplets larger than about 40μm) is important in determining ground-level deposition rates. Differences among measurements between different instruments at Neurath are partially explainable as a result of temporal and spatial variations of liquid water emission in the tower. It is not known, at present, which instrument is superior for the measurement of liquid water emission and drop spectra. A competition among all methods was made under controlled conditions at a lab tower at the Technical University at Hannover in 1979. Results are not yet available.

An empirical formula for liquid water emission (recondensate only) has been developed at the Technical University at Aachen. The formula is based on measurements made at lab and prototype towers of natural- and mechanical-draft type. The formula is useful for estimating tower liquid water emission for dates in which field data on visible plumes were acquired but no tower liquid water emission rates were measured.

Profiles of velocity and temperature across the tower top at Neurath have revealed several distinct flow configurations depending on the wind speed at tower top. At low winds, thermal instabilities result in cold air entering the tower affecting the

mass, velocity, and temperature of the emission. At larger winds, puffing or vortices occur in the emitted plume. Implications for better tower design are discussed. Implications for plume modeling of these cold air incursions into the tower may be very important due to the resulting alteration of tower exit conditions due to cold ambient air mixing in the tower.

REFERENCES

1. K. Spangemacher. Wet Cooling Towers. IN: Thermal Load of Bodies of Water and of the Atmosphere. VDI Report No. 204. pp. 10-25. 1973.

2. J. Buxmann. Dry Cooling. IN: Thermal Load of Bodies of Water and of the Atmosphere. VDI Report No. 204. pp. 26-40.

3. G. Ernst. Cooling Towers, Design and Plume Behavior. IN: International Advanced Course. Heat Disposal from Power Generation. International Centre for Heat and Mass Transfer. Dubrovnik, Yugoslavia. pp. 1/27 - 8/27. August 23-28, 1976.

4. G. Dibelius and A. Ederhof. Measurements of the Droplet Size Spectrum and the Condensate Load of the Air. IN: Studies on a Natural Draft Wet Cooling Tower. VDI Report. Vol. 15. No. 5. Ed. G. Ernst. pp. 37-48. July 1974.

5. G. Dibelius and A. Ederhof. Diffuse Light Measurement Technique for Determination of Droplet Spectra and the Output of Liquid Water from Cooling Towers. IN: Wet Cooling Towers: Thermal Principles and Measurements. VDI Report 298. VDI - Verlag GmbH. Seminar held in Dusseldorf. Ed. H. Rögener. pp. 10-16. May 25, 1977.

6. G. Dibelius and A. Ederhof. Correlation Experiments for Recondensed and Entrained Water Cooling Towers. IN: Wet Cooling Towers: Thermal Principles and Measurements. VDI Report 298. VDI - Verlag GmbH. Seminar held in Dusseldorf. Ed. H. Rögener. pp. 17-22. May 25, 1977.

7. M. Poppe. Heat and Mass Transfer in Evaporative Cooling in Countercurrent and Crosscurrent Cooling Towers. Doctoral Dissertation, Technical University Hanover. VDI Research Issue 560. 1972.

8. H. Rögener. Physics of Recooling. IN: Thermal Load of Bodies of Water and of the Atmosphere. VDI Report No. 204. pp. 1-9. 1973.

9. H. Brandes, H. Rögener, M. Pollack, and M. Poppe. Measurement and Calculation of the Condensate Load of the Cooling Tower Plume. IN: Studies on a Natural Draft Wet Cooling Tower. VDI Report. Vol. 15. No. 5. Ed. G. Ernst. pp. 49-57. July 1974.

10. H. Rögener and H. Brandes. Determination of Spray Droplet Ejection from Ventilator Cooling Towers with the Throttling Calorimeter. IN: Wet Cooling Towers: Thermal Principles and Measurements. VDI Report 298. VDI - Verlag GmbH. Seminar held in Dusseldorf. Ed. H. Rögener. pp. 37-41. May 25, 1977.

11. W. Bung. Droplet Ejection Before and After Installation of a Droplet Trap at a Natural Draft Cooling Tower. IN: Wet Cooling Towers: Thermal Principles and Measurements. VDI Report 298. VDI - Verlag GmbH. Seminar held in Dusseldorf. Ed. H. Rögener. pp. 42-48. May 25, 1977.

12. W. Roller, E. Baer, H. Dittrich, G. Ernst, and D. Wurz. Determination of the Droplet Load of the Cooling Tower Plume with Heat Probe. IN: Wet Cooling Towers: Thermal Principles and Measurements. VDI Report 298. VDI - Verlag GmbH. Seminar held in Dusseldorf. Ed. H. Rögener. pp. 29-36. May 25, 1977.

13. E. Baer, H. Dittrich, G. Ernst, W. Roller, and D. Wurz. Measurements of the Operating Behavior of the Cooling Tower. IN: Studies on a Natural Draft Wet Cooling Tower. VDI Report. Vol. 15. No. 5. Ed. G. Ernst. pp. 16-37. July, 1974.

14. H. Dittrich. Double Calorimeter for Determination of Droplet Load in Cooling Tower Plumes. IN: Wet Cooling Towers: Thermal Principles and Measurements. VDI Report 298. VDI - Verlag GmbH. Seminar held in Dusseldorf. Ed. H. Rögener. pp. 23-28. May 25, 1977.

15. E. Baer, D. Wurz, and G. Ernst. Studies of Plume Flow in the Tops of Natural Draft Cooling Towers. IN: Wet Cooling Towers: Thermal Principles and Measurements. VDI Report 298. VDI - Verlag GmbH. Seminar held in Dusseldorf. Ed. H. Rögener. pp. 169-186. May 25, 1977.

Table 2-1.

Measured and calculated droplet content of the plume of a natural draft cooling tower. (The measurements were carried out by the Rheinisch-Westfälischen Technischen Überwachungs-Verein).

Experiment		I	II	III
Ambient air temperature	°C	13.36	15.73	20.19
Water content of the ambient air	g/kg	8.29	8.68	9.37
Warm water temperature	°C	35.69	36.55	37.52
Cold water temperature	°C	22.80	23.37	24.39
Ratio of air throughput to water throughput		1.10	1.15	1.18
Cooling water throughput	m^3/h	34.240	34.300	34.270
Droplet content of the plume relative to dry air	measured,	1.09	0.85	0.25
	calculated g/kg	1.03	0.67	0.25

Note: Measurements include recondensate and drift contributions. Predictions are from the Poppe model and represent the recondensate contribution only.

Table 2-2.

Methods for measurement of the drift water content of the plume

Device	*Principle*	*Use*	*Smallest Measurable Droplet Content*	*Measurement Uncertainty*	*Literature*
			g_{water}/kg_{plume} estimated values		
Throttling calorimeter	Adiabatic expansion of a partial plume stream up to complete evaporation of the droplets carried along, temperature differences measure the cooling.	Only for plumes without recondensation droplets . . . measures total liquid emission only	0.010	± 0.005	1
Diffuse light measurement probe	Determination of the size of the individual droplets from the intensity of the diffuse light pulse. Determination of the drift droplet content from pulse count and pulse intensity.	For every type of plume . . . separates drift and recondensate contributions and also measures total liquid water emission	0.002	± 0.001	4
Heat probe	Heating of a partial plume stream up to complete evaporation of the droplets carried along; psychometric determination of the absolute moisture and comparison with the saturation moisture for the incoming plume temperature.	Only for plumes without recondensation droplets . . . measures total liquid emission only	0.28	± 0.10	2
Conductivity/ condensation apparatus	"Washing out" of a measured partial plume stream in a condensation vessel; measurement of the increase of conductivity. Calculation of the drift water content of the plume from the conductivity of the cooling water.	For every type of plume . . . separates drift and recondensate contributions and also measures total liquid water emission	0.005	± 0.003	3
Cyclone separator	Centrifuging out of the droplets from a partial plume stream throughput. The electrical conductivity of the separated water and of the circulating cooling water is used.	For every type of plume . . . but the smaller droplets are difficult to capture	0.01	± 0.005	5
Sensitive paper	Collection of the droplets on adhesive paper; measurement and examination of the "water spots".	For every type of plume . . . but measures drop size distribution above about 50µm drop diameter	0.002	± 0.001	6

References for Table 2	Methods of Measurement of the Drift Water Content of the Plume
1. Rögener, H.U. G. Kowollik	Measurement of the droplet ejection of cooling towers. Brennstoff-Warne-Kraft (BWK) 15 (1963) p. 270-271.
Chinira, C.	A thermodynamic method for determination of the droplet content of wet air. Brennstoff-Warne-Kraft 25 (1973) pp. 31-38.
Brandes, H. H. Rögener M. Pollack M. Poppe	Measurement and calculation of the condensate load of the cooling tower plume. In: Studies on a natural draft wet cooling tower. Progress Report VDI-Z, Series 15, No. 5, pp. 36-41.
2,3. Baer, E. H. Dittrich G. Ernst W. Roller D. Wurz	Measurements of the operating behavior of a cooling tower. In: Studies of a natural draft wet cooling tower. Progress Report VDI-Z, Series 15, No. 5, pp. 15-27.
4. G. Dibelium A. Ederhof	Measurement of the droplet size spectrum and the condensate load of the air. In: Studies of a natural draft wet cooling tower. Progress Report VDI-Z, Series 15, No. 5, pp. 28-36.
5. Henning, H. U. S. Kliemann	Precipitation and fog formation from cooling towers. Energie u. Technik 3 (1971) pp. 87-90 and 4 (1971) pp. 112-115.
6. Martin, A. F. R. Berber	Some water droplet measurements inside cooling towers. Atmospheric Environment Vol. 8 (1974) No. 4, pp. 325-336.
Morton, V. M. P. M. Foster	The design of the droplet sampling devices for measurements in cooling towers. Atmospheric Environment Vol. 8 (1974) No. 4, pp. 361-372.

Table 2-3.
Measured drift droplet content

Installation	Measurement Method	Operating Mods of the Tower	Drift Droplet Ejection (in tenths of a % of the cooling water flow)	Literature
1. Natural draft cooling water	Cyclone separator	Full thermal load	0.1	1
2. Ventilator cooling tower (small test MDCT)	Throttling calorimeter	Without thermal load	0.15	2
3. Ventilator cellular cooling tower (MDCT)	Throttling calorimeter	Without thermal load	0.20	3
4. Natural draft cooling tower	Diffuse light probe	Full thermal load	0.18	4
5. Natural draft cooling tower	Diffuse light probe	Full thermal load	0.10	5
6. Ventilator cooling tower (MDCT)	Diffuse light probe	Full thermal load	0.02-0.04	
		Without thermal load	0.02-0.04	6
7. Natural draft cooling tower	Condensation/conductivity apparatus	Full thermal load	0.20	7
8. Natural draft cooling tower	Sensitive papers	Full thermal load	0.02-0.20	8
9. Natural draft cooling tower	Guarantee. Information not yet published	Full thermal load	0.02	9
10. Ventilator cellular cooling towers (MDCTs) for acid and brine cooling	Not given	Full thermal load	0.005	10

References for Table 3	Measured Drift Droplet Content
1. Bung, W.	Result of droplet ejection measurement on a natural draft cooling tower 130 m high. Techn. Überwechung 15 (1974) No. 3, p. 83-87.
2. Rögener, H. H. Brandes M. Pollack	Unpublished measurements on a test cooling tower. (1975)
3. Bremdes, H. H. Rögener	Unpublished measurements on a ventilator cellular cooling tower. (1976)
4. Dibelius, G.	Unpublished measurements on a natural draft cooling tower. (1976)
5. Dibelius, G.	Unpublished measurements on a natural draft cooling tower. (1976)
6. Dibelius, G.	Unpublished measurements on a ventilator cooling tower. (1976)
7. Baer, E. H. M. Dittrich G. Ernst W. Roller D. Wurz	Measurements of the operating behavior of the cooling tower. In: Studies of a natural draft wet cooling tower. Progress Reports, VDI-Z, Series 15, No. 5.
8. Martin, A. F. R. Barber	Some water droplet measurements inside cooling towers. Atmospheric Environment Vol. 8, No. 4 (1974) pp. 325-336.
9. Pell, J.	The chalk point cooling tower project, Environmental effects of cooling systems at nuclear power plants. Proceedings of a Symposium, Oslo 26-30, August 1974. International Atomic Energy Agency, Vienna 1975.
10. Kliemman, S.	State of the art and possible developments in cooling tower construction from the point of view of various influences on the environment. VGB Kraftwerkstechnik 55 (1975) pp. 375-381.

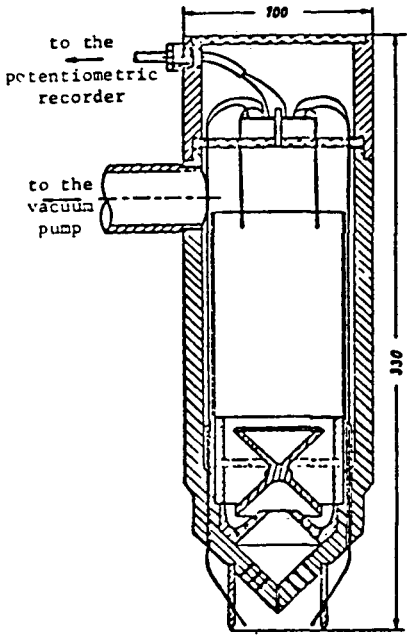

Throttling calorimeter [Source: From Rögener and Brandes (10).]

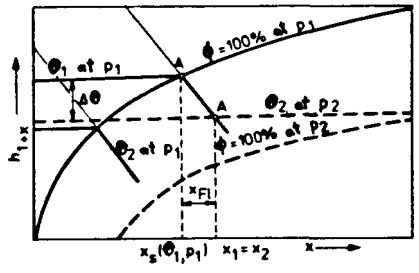

h,x — Diagram for determination of the total droplet.

A **State of the wet air upon entrance into the probe**

A **Saturation state of the air upon entrance into the probe**

Δϑ **Cooling of the air in the measurement path.**

X_{FL} **Condensate load of the wet air**

(Institute for Thermodynamics, Hannover)

Figure 2-1. Schematic diagram of throttling calorimeter and its measurement principle. [Source: From Brandes et al. (9).]

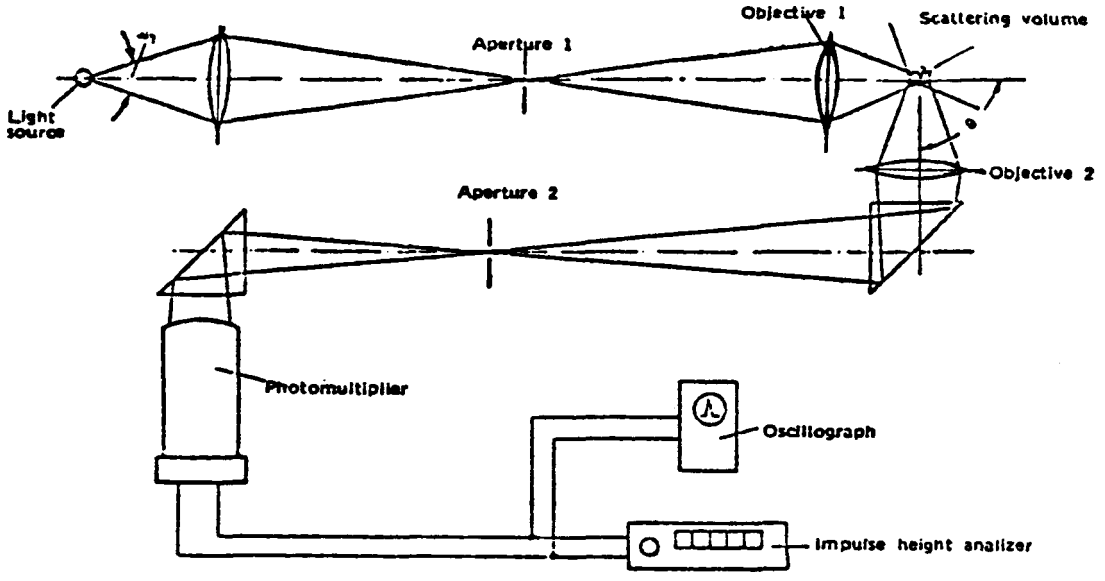

Figure 2-2. Diagram of the principle of the diffuse light measurement probe. [Source: From Dibelius and Ederhof (4).]

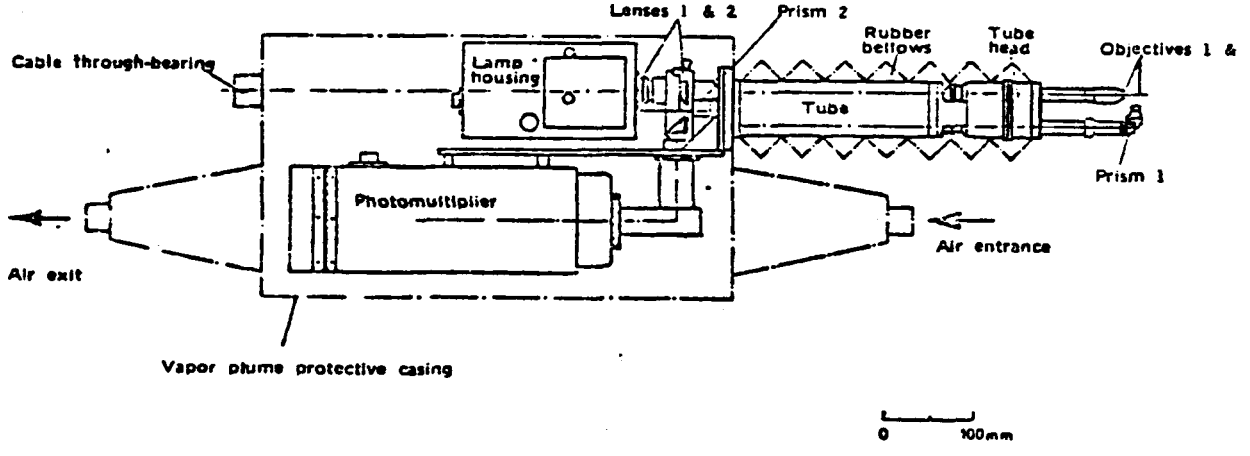

Figure 2-3. Diffuse light measurement probe (design "Neurath"). [Source: From Dibelius and Ederhof (4).]

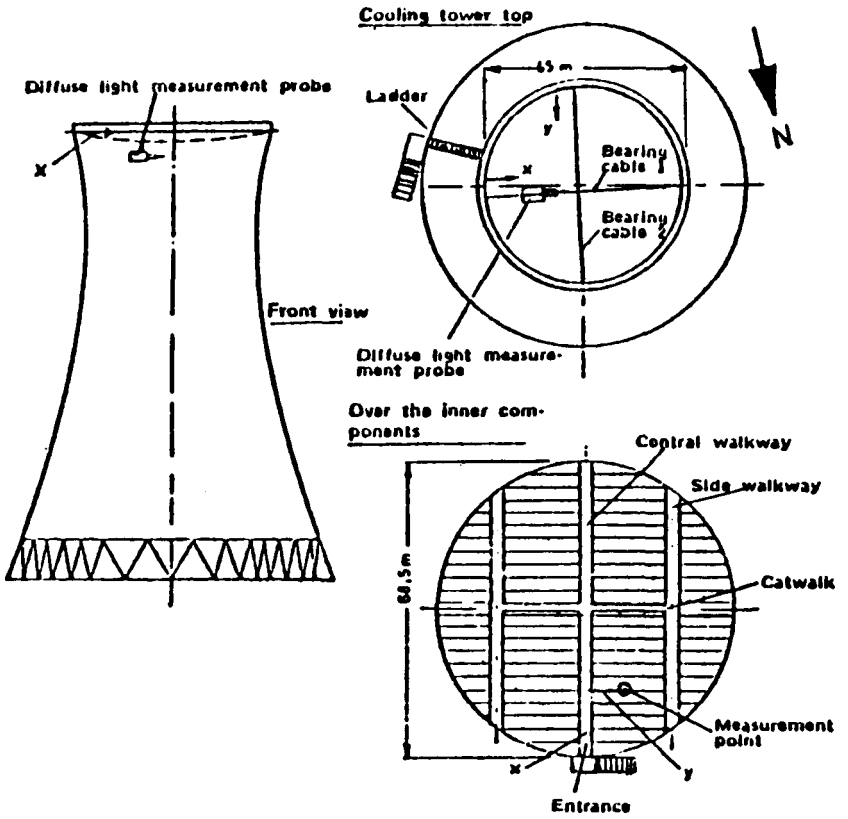

Figure 2-4. Measurement arrangement in the cooling tower. [Source: From Dibelius and Ederhof (4).]

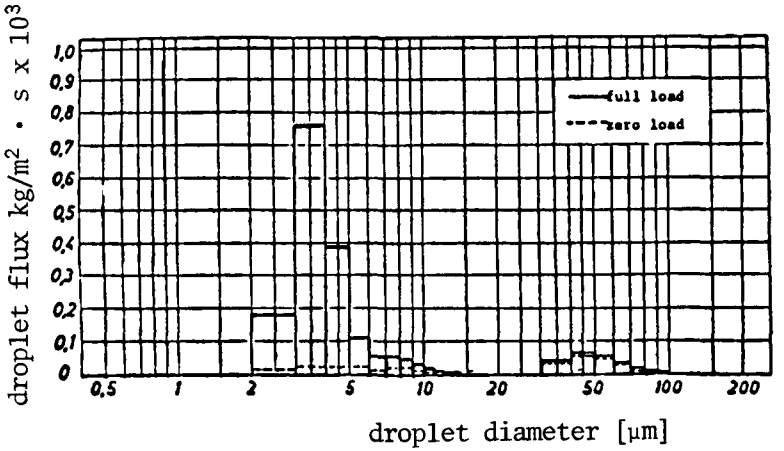

Figure 2-5. Droplet flux distribution across the cooling tower diameter. [Source: From Dibelius and Ederhof (5).]

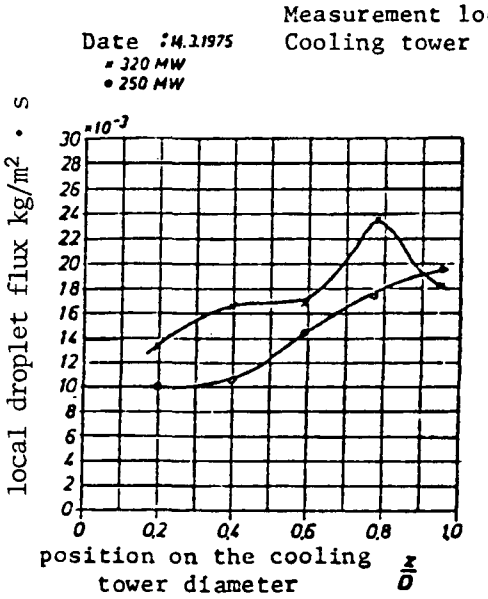

Figure 2-6. Droplet flux distribution for full load and zero load. [Source: From Dibelius and Ederhof (5).]

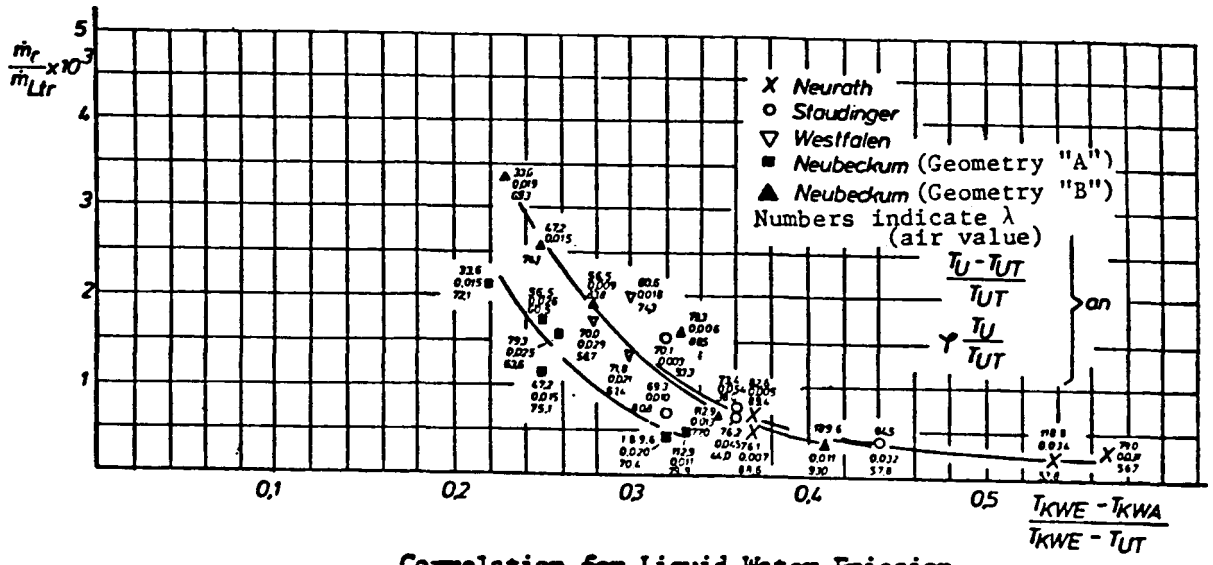

Correlation for Liquid Water Emission

$$\frac{\dot{m}_r}{\dot{m}_{Ltr}} \cdot 10^3 = \frac{2.39}{(1.0 - 7.95\ X)^2}$$

where

$\frac{\dot{m}_r}{\dot{m}_{Ltr}}$ = liquid water emission in g water/g air

$$X = \frac{T_{KWE} - T_{KWA}}{T_{KWE} - T_{UT}}$$

where

T_{KWE} = hot water temperature

T_{KWA} = cold water temperature

T_{UT} = ambient dew point temperature

$T_{KWE} - T_{KWA}$ = temperature range of tower

$T_{KWE} \approx$ plume exit temperature + 5°C

Figure 2-7. Empirical expression for liquid water emission from natural-draft cooling towers.

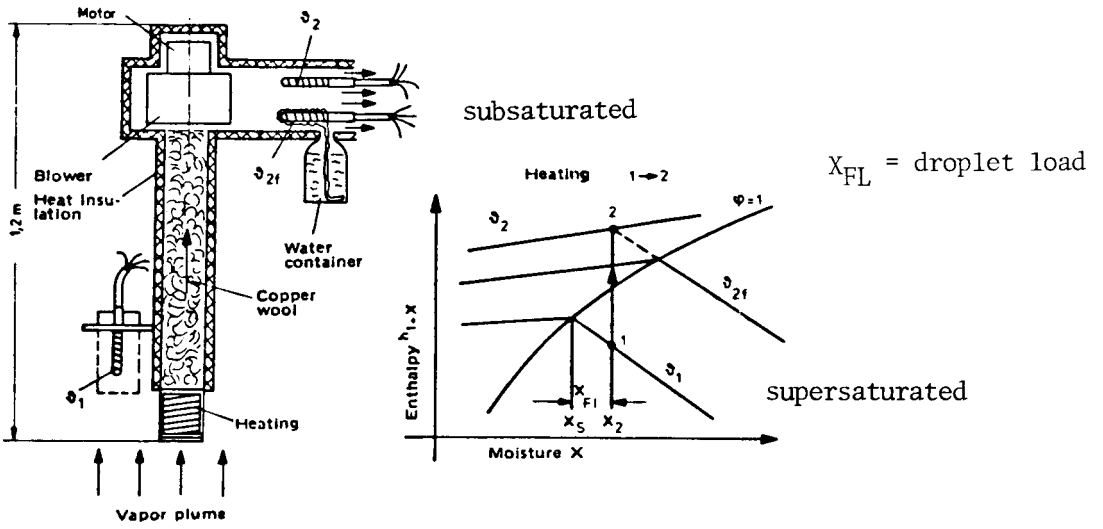

Figure 2-8. Diagram of the heat probe and representation of the measurement principle. [Source: From Roller et al. (12).]

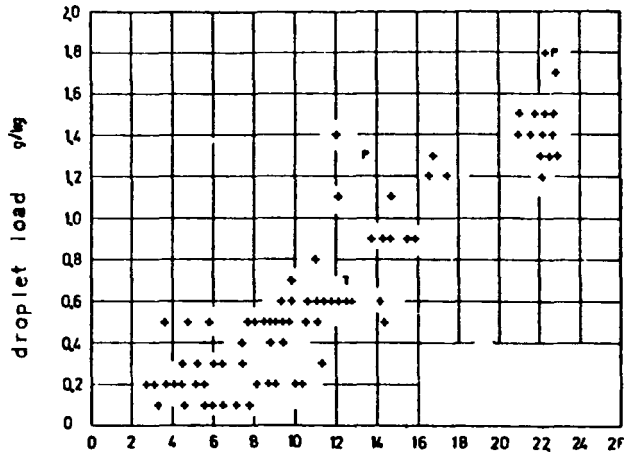

difference between mean water temperature θ_{Wm} and ambient temperature θ_U in C°

Droplet load X_{FL} of the plume.

P: reduced cooling water flow rate.

T: reduced turbine power.

Figure 2-9. Correlation between ambient and tower parametric and droplet load X_{FL} of the plume. [Source: From Roller et al. (12).]

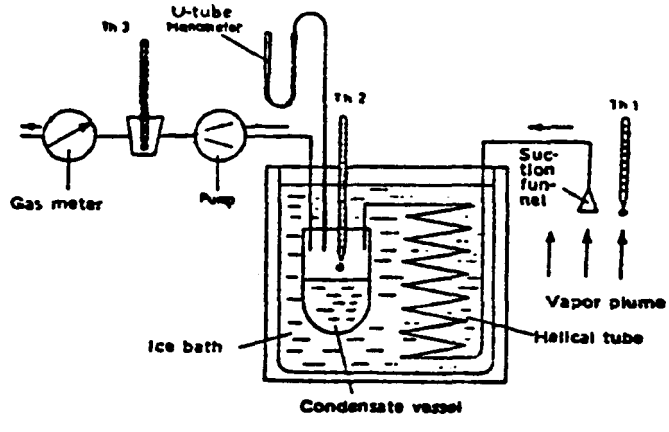

Figure 2-10. Apparatus for determination of water entrained by the air in the cooling tower. (conductivity-condensation method). [Source: From Baer et al. (13).]

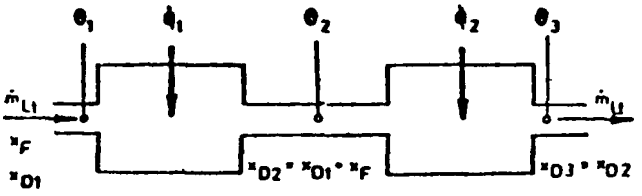

ϕ_1 = supplied heat flow into first chamber (heating supersaturated air)

ϕ_2 = supplied heat flow into second chamber (heating unsaturated air)

θ_1 = plume sample temperature (entrance state)

θ_2 = plume sample temperature in Chamber II

θ_3 = plume sample temperature upon exit from Chamber II

$\dot{M}_{LT}$ = mass flow rate of air through the double calorimeter

X_{D1} = water vapor content at the entrance state

X_{D2} = water vapor content of plume air in Chamber II

X_{D3} = water vapor content of plume sample upon exit from Chamber II

X_F = initial water vapor content of plume (to be measured)

Figure 2-11. Serial connection of two heating chambers. (double calorimeter method). [Source: From Dittrich (14).]

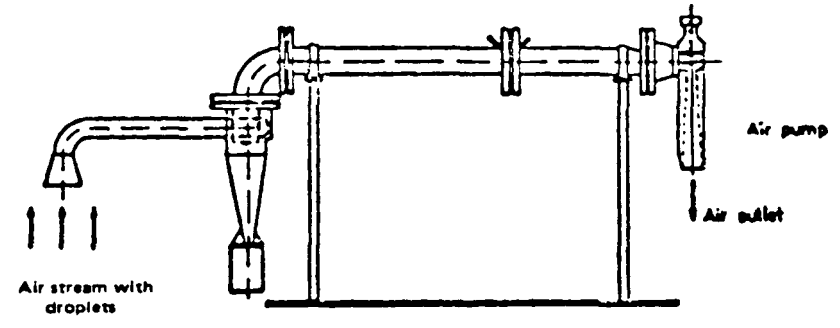

Figure 2-12. Cyclone Separator (Balcke-Dürr).

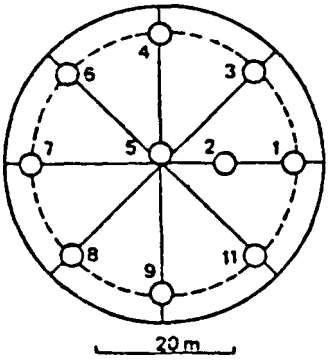

Figure 2-13. Arrangement of the velocity measurement devices at the tower exit of tower C at Neurath. [Source: From Baer, Wurz and Ernst (15).]

Figure 2-14. Plume configuration at the top of a natural draft cooling tower and its dependence on various wind velocities measured at the height of the cooling tower top. [Source: From Baer, Wurz and Ernst (15).]

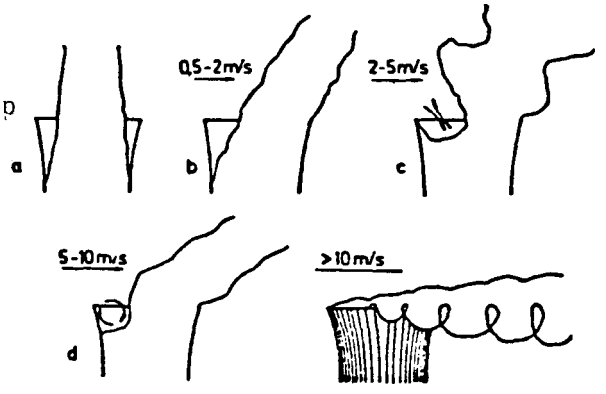

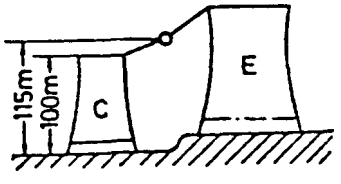

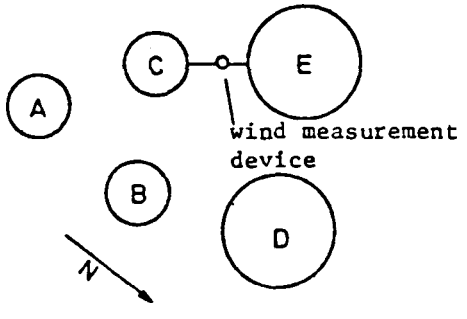

Figure 2-15. Arrangement of the wind measurement device at the height of the cooling tower top. [Source: From Baer, Wurz and Ernst (15).]

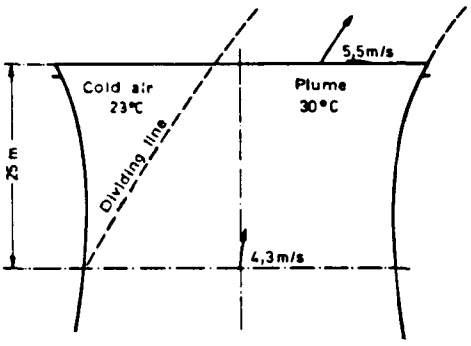

Figure 2-16. Diagram of cold air irruption. [Source: From Baer et al. (13).]

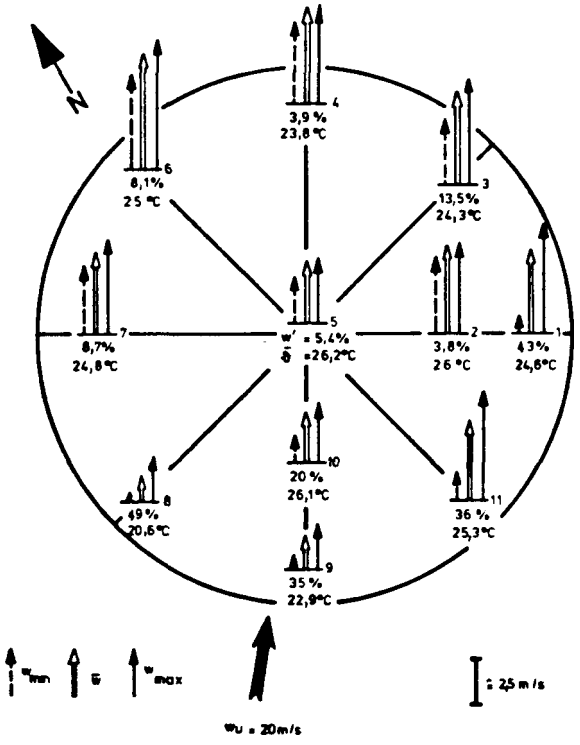

Figure 2-18. Flow relationships and temperature distribution at the cooling tower top for a wind velocity of 20 m/s. [Source: From Baer et al. (13).]

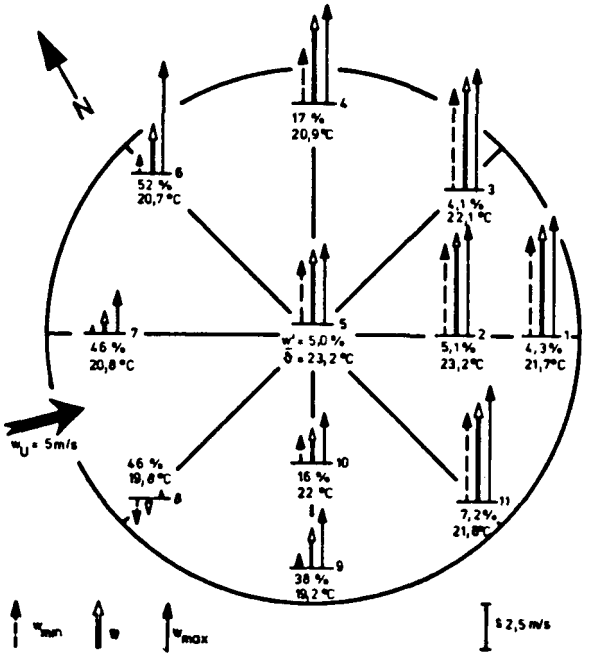

Figure 2-17. Flow relationships and temperature distribution at the cooling tower top for a wind velocity of 5 m/s. [Source: From Baer et al. (13).]

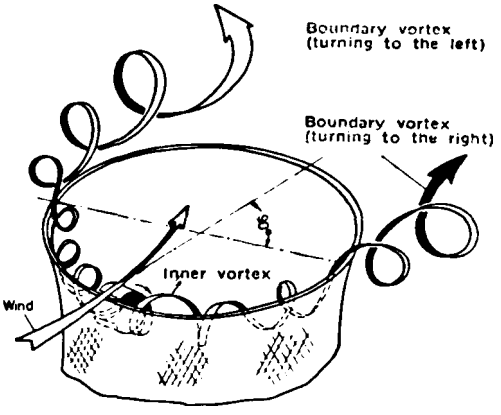

Figure 2-19. Diagram of the inner and boundary vortex formation at the cooling tower top. [Source: From Baer et al. (13).]

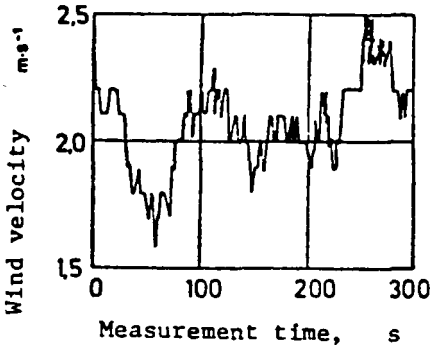

Figure 2-20. Wind velocity at the height of the cooling tower top plotted against time. [Source: From Baer, Wurz and Ernst (15).]

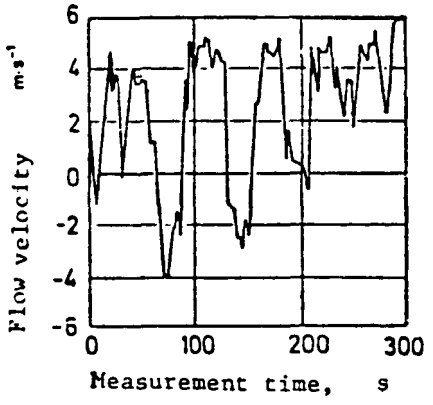

Figure 2-21. Local flow velocity at the measurement point 11 plotted against time (compare Figure 2-20). [Source: From Baer, Wurz and Ernst (15).]

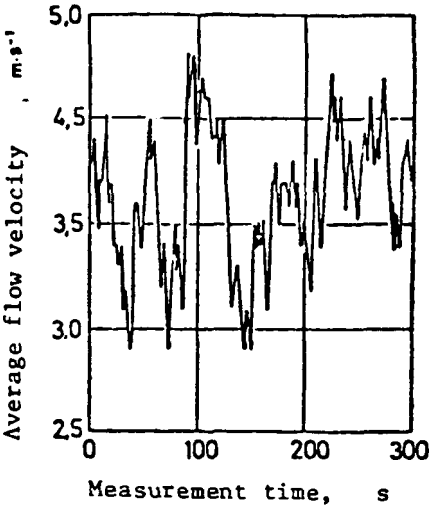

Figure 2-22. Average flow velocity of the plume in the cooling tower exit plotted against the time. [Source: From Baer, Wurz and Ernst (15).]

Section 3

LABORATORY AND FIELD DATA ON COOLING TOWER PLUMES

INTRODUCTION

Much laboratory and field data have been acquired in Europe which aid in the understanding of cooling tower vapor plume dispersion. Due to the large expense in acquiring prototype data on plumes, the good-quality European data in this area are indispensible and actually provide an excellent complement to the available American data. Since a major limitation on the improvement in the state of the are of modeling has been the quality and quantity of the data base, the combination of European and American data bases on cooling tower plumes provides special advantages for model improvement. Thus, the experimental data acquired in Europe by the French, Swiss, and Germans on cooling tower plumes provide an important and crucial complement to the laboratory and field data available in the U.S.

LABORATORY DATA (ELECTRICITÉ DE FRANCE)

The best quality and most useful lab data on cooling-tower plume dispersion were taken by Electricité de France (EDF) (1). Their study was carried out in a hydraulic flume and was aimed at (a) a better understanding of the physics of natural-draft cooling-tower plume dispersion through basic parametric tests, and (b) providing experimental data for calibration and verification of the EDF cooling tower plume models. The EDF lab data have special advantages in that the ranges in physical parameters modeled by EDF were precisely those of NDCT effluent. Lab studies available in the U.S. (e.g., Fan, (2) Keffer and Baines (3); see discussion below) for single source vertical jets do not have similar non-dimensional parameters (densimetric Froude number and velocity ratio). Second, in the EDF studies, the cooling tower structure itself was present in the flow and was suitably scaled along with the effluent. As a result, the effects of downwash of the tower structure were treated. Third, the EDF lab studies included tests which involved multiple-tower configurations.

Among the tests carried out were measurements on plumes from 1, 2, and 4 towers of equal size. The regime of interest for NDCT plumes is $0.3 \leq K \leq 2$ and $F_o \sim 0.5$. Here F_o is the initial densimetric Froude number of the tower effluent and K is

the ratio of the tower exit velocity to wind speed at tower height.* It should be noted again that most available lab studies on plumes and jets treat different ranges of parameter space (K, F) and also do not account for the effect of the wake of a structure like a cooling tower in its effect on plume trajectory and dilution characteristics. Among the most well-known of the previous lab studies was one done by Fan (2); Fan studied weakly buoyant jets in weak currents, $4 \leq K \leq 16$ and $10 \leq F_o \leq 40$. Of special interest to Fan was the jet centerline trajectory and jet dilution. Keffer and Baines (3) studied isothermal jets ($F=\infty$), mainly jet centerline trajectories, where $2 \leq K \leq 10$. The EDF study is especially important since it covers the range of F_o and K of interest in the field for NDCTs and also studies the multiple tower plumes.

Viollet (1) presents a large quantity of interesting data from the EDF studies. Some of his special test series related to:

1. the effect of jet Reynolds Number on dispersion for $F_o = 0.5$, $k = 2$, and $\alpha = 0$ (α is the exponent in the power-law wind speed variation with height above ground. As expected, the jet Reynolds number, R_o, is not a significant factor above a value 2×10^4.
2. measurements on centerline trajectory and dilution for plumes from 1, 2, and 4 towers, each tower with $F_o = 0.8$. For these runs, $0.33 \leq K \leq 2$, $\alpha = 0.25$, $R_o = 2 \times 10^4$, and $H/D_o = 1.85$ (H_o = height of tower, D_o = tower exit diameter). In the case of two towers, the wind is directed perpendicular to the axis of the towers. In the 4-tower cases, the towers were located in a diamond shape with the wind directed towards the left tower or else the 4 towers were located at vertices of a parallelpiped with the wind direction parallel to the two parallel bases. Some results are shown in Figures 3-1 through 3-6.

Figure 3-1 presents the plume concentration isopleths for a single tower and $F_o = 0.8$, $\alpha = 0.25$, and $H/D_o = 1.85$. In the lab, dye was injected into the tower effluent. Measurements of dye concentration were made throughout the plume and related to the initial dye concentration at discharge. We see from Figure 3-1 that the plume trajectory bends over more rapidly with increasing wind (decreasing K). However, at any given X/D_o, there is no monotonic trend in dilution (determined from dye concentration measurements) with variation in K. The minimum dilution occurs with $K \approx 0.5$. This data trend is a systematic behavior that any plume model should be able to represent. Figure 3-2 replots those trends for trajectory and dilution.

The influence of K on plumes from two towers is seen in Figure 3-3 and follows the trend seen for the single tower cases. Plume isocontours in the plane perpen-

*In volumes 2-5, K is defined as the ratio of the wind speed at tower height to the tower exit velocity.

dicular to the wind at X/D_0 = 5 are given in Figure 3-4 for three values of K. The cross-sections are horseshoe-shaped as expected.

In Figure 3-5, we see very little difference between both 4-tower configurations. Clearly, the increase from 1 to 2 to 4 towers leads to a higher trajectory (due to greater buoyancy) and less dilution for any fixed distance downwind. Figure 3-4 shows the 0.05 and 0.01 concentration isopleths for the two-tower case revealing their usual horseshoe-shape within a plume cross-section. In the single tower case, a lower F_0 leads to a delay in the appearance of the horseshoe-shaped proviles (from the $F_0=\infty$ case), yet that shape is found to remain a longer distance downwind. Also, the higher the F_0, the more rapid the bendover (due to the lower jet buoyancy); however, less dilution is noted for a fixed distance downwind. This latter influence diminishes with increasing current.

It should be noted that experimental data had been obtained by EDF in two other general categories: isothermal jets and jets in a stratified environment. Ref. (1) provides the details. Also important in the EDF study is the measurement of velocity profiles for the isothermal cooling tower plume cases; these velocity measurements give a better picture of jet dilution and the effect of the wake of the tower. Information on other EDF work may be obtained from Refs. (4) through (10).

FIELD DATA

Gardanne Natural-Draft Cooling Tower (Visible-Plume Data) (1), (4), (5), (7)

Field data on visible plume rise from a single NDCT were obtained at this 250 MWe power plant located at the bank of the Rhône River. The measurement campaign was undertaken during one week and a complete set of information on the plumes is given for five cases in Ref. (1). This old tower does not have drift eliminators. However, this should not affect the amount of liquid recondensate emitted by the tower since these small size droplets are not influenced by the presence of drift eliminators. The recondensate emission can be an important parameter if plume visibility is being predicted. Viollet (1) suggests that the recondensate liquid emission from the tower be taken as σ_o = 2.9 g/kg. [The tower manufacturer for Gardanne expects the total liquid emission to range from 0.1 - 0.5% of the circulating water flow rate. Taking a mean of 0.3% and assuming half is drift and half is recondensate, Viollet expects 0.15% of the cooling water flow to be a representative number for liquid emission from the recondensate. This translates to σ_o = 2.9 g/kg.] Viollet also expects a saturated plume at exit. Details on the

means of measurement of ambient profiles and tower exit conditions are not given in Ref. (1). The Gardanne measurement campaign is treated in detail in Ref. (7); however, that reference was unavailable to us. A sample of the visible plume outline with concomitant tower exit and ambient conditions is given in Figure 3-7. Each of the five data sets presented in Ref. (1) represents plumes from a weak source under weak stratification and relatively strong wind conditions. One case, however, represents a weak wind and weak stratification.

Lünen Natural-Draft Cooling Tower (Visible-Plume Data) (11)

Field data on visible plume rise from a single NDCT were obtained at the 335-MW_e fossil-fired plant at Lünen, West Germany, during the winter of 1972. The field measurement program was carried out as a joint effort of the Swiss Meteorological Institute and the German Meteorological Service. This single NDCT is located in nearly level terrain but in an industrial area. There are four sets of data encompassing tower-outlet conditions, vertical ambient profiles taken at the site, and visible plume outlines. Eight additional sets with ambient profiles from an off-site weather station were also available.

Visible plumes were recorded using 16-mm motion pictures taken at one frame per second and 35-mm stills taken at an unspecified rate. Visible plume outlines were obtained by time-averaging as many as 30 of these photographs. Ambient conditions (dry bulb, relative humidity, and wind speed) were determined by radiosonde-equipped free balloons tracked by a double-theodolite system. Tower-exit conditions were inferred from measurements made at 11 locations in a horizontal cross section of the tower just above the drift eliminators. The measurements of tower-exit conditions appear to be good, although the lack of information on the initial plume humidity and initial liquid water is troublesome. The ambient profiles are limited in that time-averaged measuremets were not made. The quality and representativeness of the visible plume outlines are uncertain, although we believe that the averaging method is probably adequate. The time coordination between the photographs, the ambient profiles, and the measurement of tower-exit conditions was good; also, the overall measuring period for the tower-outlet conditions was a relatively short, 1/2 to 3/4 hour. All four data sets from Lünen taken in the first series were acquired under high-wind conditions but under a variety of ambient temperatures and humidities. An example of one of those sets of data from Lünen is given in Figure 3-8.

Neurath Natural-Draft Cooling Tower (Visible Plume Data) (12)

The Neurath fossil-fired power plant is located in the region west of the Rhine river between Bonn, Cologne, and Aachen in West Germany. At the time of the measurements, each of the three 300-MW_e units dissipated its heat to one of three NDCTs. The centers of the three towers form an equilateral triangle 114 m on a side. Seven complete data sets were acquired on five dates during the period September 28 to December 16, 1973. Each set of observations includes the following measurements for the one instrumented tower.

1. entrance and exit temperature of the cooling water and cooling-water flow rate.
2. exit temperature and exit speed of the plume at 11 locations at the tower crown.
3. ambient profiles of temperature, relative humidity, and wind speed taken by using radiosonde-equipped free balloons. (On two observation dates, wind-speed measurements from a nearby German Weather Service station were used.)
4. visible plume outlines extracted from one or more photographs taken at the time of the ambient profiles. Each photograph was taken at approximately right angles to the wind direction. (The visible plume outlines were "sketched" from photographs, aided by written comments taken at the time of the survey. The published report does not make this procedure clear.) We consider the visible plume outlines the weakest part of the data set.

In addition to the four items listed above, several data sets include measurements of the total liquid-water content in the plume above the drift eliminators (recondensate plus drift), droplet-size spectra at the tower crosn, relative humidity of the plume at the tower crown, and the velocity distribution across the tower crown. When winds were not too strong, supplemental data on ambient conditions near the ground, as high as 178 m above the tower top, were taken by a radiosonde-equipped tethered balloon.

It is generally assumed that all three towers have identical exit conditions since they are identical towers and were run under the same power load, despite lack of measurements on two of the three towers. An example of one set of data from Neurath is given in Figure 3-9.

Neurath/Meppen Natural-Draft Cooling Towers (In-Plume Measurements) (13) - (17)

The goal for these field experiments was to obtain field data, mainly in-plume measurements, for the calibration and verification of models for cooling tower plume dispersion. Two campaigns were conducted at the cooling towers at Neurath (900 MWe) in 1974 and also two campaigns were made at the single cooling tower at

the Meppen power station (600 MWe) in 1975. Many different types of measurements were made covering the ambient meteorology and the plume variables themselves. A schematic of the measurement systems used is given in Figure 3-10. The major groups cooperating in the data acquisition were DFVLR-Institute for Atmospheric Physics in Oberpfaffenhofen, West Germany (in-plume measurements); the German Weather Service in Offenbach (ambient conditions); and the Swiss Reactor Institute in Würenlingen, Switzerland (data reduction).

The main source of measurements was a powered glider equipped with high-resolution instruments that measured temperature, vapor pressure, pressure/altitude, and vertical acceleration (from which vertical speed may be computed) at any location in the plume or in the ambient. The vapor pressure (humidity) measurements were made with the Lyman Alpha Method. The system was operated by DFVLR-Institute for Atmospheric Physics. The equipment used is similar to those employed by investigators at Penn State University in their ongoing measurement studies of the Keystone plumes here in the U.S. In-plume measurements were made with the glider at horizontal transects directed normal to the plume centerline. Typically 20-25 penetrations were made at each of 2-5 downwind distances, i.e., in 2-5 planes normal to the wind. Reduced data involved instantaneous values of temperature, specific humidity, and updraft velocity along each horizontal transect. The powered glider sometimes was used to provide vertical ambient profiles as well. A radar system was used to locate the glider in space at any time. In some of measurement surveys, the German Weather Service or personnel from the Testing Station of the German military were present to provide radiosonde profiles in the ambient for wind speed (direction), temperature, and humidity with height.

The powered glider, however, was used only for elevations above 200 m above the ground due to the presence of transmission lines. Below 200 m (actually 0-500 m), remote-controlled model planes (measurement drones) were used to measure ambient temperature and humidity along with horizontal profiles through the plume. Measurement values were transmitted by telemetry to a center on the ground.

At times, dropsondes were released from a separate DO-27 plane 1500-2000 m above the ground to provide a vertical ambient or plume profile; temperature and humidity measurements with time were telemetered to the ground. A DO-27 plane also measured aerosol concentrations as well as sulfur content (mainly SO_2) in the ambient and determined the general position of the plume in space and its structure. A tethered kytoon was used, when feasible, to get a vertical sounding of pressure, temperature and humidity beneath, through, and above the plume. (A "chaff cloud"

experiment was planned but not carried out in which the turbulent spreading of the plume could be observed by dropping short aluminum strips in the tower exit. The spreading of this cloud of aluminum dipoles was to be observed photographically on the radar screen to determine spreading behavior). In order to study the effects of the plume on the ground, horizontal transects at ground level were made with a radiosonde for temperature, humidity and pressure. Transport was accomplished by car or walking; the results were transmitted to the telemetry center. A second instrument called a "Wommel" was used; it is a portable meteorological station with high resolution recorders for wind, temperature, humidity and atmospheric pressure. The Wommel was transported on the ground. A series of infrared photographs of the plume were also taken from the ground and from the airplane (DO-27).

Details on the field measurements are given in Refs. (13) - (19) and samples of complete data reduction for two data surveys appear in Ref. (15). A complete tape of measurements may be obtained from DFVLR-Institute for Atmospheric Physics. We have a copy at ANL.

A small sample of the large amount of plume data acquired is given in Figures 3-11 and 3-12 representing transects through the Meppen plume of Feb. 16, 1975 (1506-1704) for distances of 0.5 and 0.7 km downwind. The horizontal lines in the middle of each figure represent transects parallel to the ground. All transects were made in the same vertical plane at 0.5 km (Fig. 3-11) and 0.7 km (Fig. 3-12) downwind of the tower. In the middle section of each of the two figures, the horizontal axis represents the lateral distance as measured from the center of the Meppen tower. The vertical axis presents vertical height measured above the ground. The actual measured ambient temperature profile is also plotted in the middle section of each figure along with the dry adiabatic lapse rate, presented for reference purposes. The section of the figures on the right presents values of the maximum and average vertical velocity as measured along the associated horizontal transect through the plume. The maximum vertical velocity refers to the local maximum measured over the transect, whereas the average value is the spatial-average taken over the length of the transect. The left section of each figure presents, for each transect,

(a) the local ambient specific humidity at the height of the transect

(b) the difference of plume and ambient specific humidities at the height of the transect, and

(c) the difference of plume and ambient temperatures at the height of transect.

The ambient moisture profile is presented for reference in each of the left subfigures.

A short discussion of these data will follow in order to provide a sample of the kind of insight that can be gained from these data sets. These two figures show clearly that the vertical cross-section of the plume can be defined; also, traverses at these two vertical planes allow the determination of the rising properties of the plume and the growth of the plume cross sectional area with considerable accuracy. Figures 3-11 and 3-12 represents a case with a weak wind and partially unstable atmosphere; i.e., neutral stratification below a marked inversion which began at about 600 m above ground.

The vertical distribution of the specific humidity shows thorough mixing of the ambient atmosphere. Even with the short distance separating the two vertical sections (200 m) of Figures 3-11 and 3-12, the rising effect of the entire plume is detectable. The distribution of the vertical velocity on the right-hand side of Figure 3-12, as expected, shows the largest values in the region of unstable stratification for both mean values (open circles) and maximum values (crosses); the jumps in vapor pressure (or specific humidity) are also the greatest at those points.

In general, the determination of the geometry of the plume is critically dependent on whether or not, based on local ambient conditions, the plume has disintegrated into a series of individual convective elements or puffs. The data have shown that with stable stratification, it is possible to determine, quite accurately, the increased cross-sectional plume surface area with increasing distance from the cooling tower. One case with large ambient stratification indicated that the relative error in plume cross-section determination can be lower than 10%. When thermal stratification is beginning near the ground, natural convection of warm air parcels occurs and the plume under unstable ambient conditions becomes split into a chain of individual convective elements or puffs. This creation of puffs occurs even at small distances from the cooling tower whether or not the plume has already become invisible. In case a plume is reduced to a series of puffs, numerous horizontal traverses in a cross-section are required in order to determine, by statistical means, the "mean" 3-D spatial geometry of the plume. This applies to Figures 3-11 and 3-12. Crossings at 0.5 km showed that the plume was visible and hence may be called a plume in the usual sense, while a study of the cross-section indicated that the "plume" has its dynamic and thermodynamic point of concentration below the visible part. That observation can be generalized in that the Neurath and Meppen measurements showed that the visible part of the plume always represents only the uppermost level of the plume. The plume dispersion generally occupies the entire space down to near the ground but with greatly decreasing intensity.

Some of the interesting findings from the data analysis at Neurath and Meppen follow.

1. the structure of the temperature and humidity rises above ambient are similar to each other in shape and magnitude in any cross-section normal to the wind direction (see Figure 3-13).
2. in each traverse, discontinuous lateral boundaries of the plume are indicated by abrupt changes in temperature and humidity. Fortak (14) states that top-hat profiles of temperature and humidity are apparently more appropriate than Gaussian distributions since Gaussian distributions do not show such an abrupt interface with the ambient.
3. in the central part of the plume cross section and on its boundaries, a circulation acts in such a way that outward movement occurs along the outer boundaries of the plume. This boundary circulation is often completely lacking or is undetectable (with the measurement system used) in the lower and upper levels of the plume. The circulations noted are the counter-rotating vortices representing a bifurcated plume often observed in the laboratory.
4. close to the ground, all thermodynamic effects, unlike the dynamic ones were found to be negligibly small.

From the field measurements, a schematic model was proposed for the dispersing plume. The gain in plume mass, which is necessary for its ascent and spread with increasing distance from the cooling tower, takes place mainly on the underside of the plume and begins right upon exit from the tower. Due to upward buoyancy of the plume, it is only under very unstable stratifications that plume properties can extend to near ground level. Lateral exchange of properties between plume and the environment, however, are relatively insignificant. The plume's behavior with regard to rise and spreading depends on the input of mass and air at the underside.

The field measurements also showed that details of the ambient structure of the atmosphere have a very great influence on plume development in all cases. In many cases, small inversion layers within very narrow vertical limits have a great effect on the ascending behavior of the plume even if an inversion breakthrough results.

Two reports are available which help one to employ the Neurath and Meppen data for mathematical model studies. The first is by Trepp (17); this report correlates all traverses by glider to actual field distances for a number of the Neurath surveys. In this way, each traverse can be located physically with respect to the cooling tower. Trepp also processes the data on temperature, moisture, and turbulence. The report is indispensible for one using the data. However, a small amount of additional data reduction work needs to be done since each plume traverse provides only "instantaneous" plume variables. Vertical velocities, temperature differences above ambient, and moisture differences above ambient are best used

by models if they are averaged over the plume width defined by that traverse. Nester (18), in his use of this Neurath/Meppen data has done some of this data reduction. For each traverse, he has averaged those three quantities along a traverse and plotted those variables (one value per traverse) with vertical distance above the ground . . . for all traverses in a given vertical plane. This leads to a vertical profile of temperature excess, moisture excess, and vertical velocity. Done for each vertical plane that measurements were made leads to 3-D picture of the plume dispersion. Additionally, this reduction process also locates a centerline and a plume width. The plume width actually varies with traverse as well as vertical plane downwind.

Several cautions should be noted with these data.

1. no tower exit conditions were measured during the field surveys. This limits the use of the data. Trepp and Gassmann of the Swiss Reactor Institute employ a mathematical model of thermal performance of a crossflow cooling tower in order to obtain tower exit conditions on the dates in-plume data were measured. That tower model was calibrated to previous tower performance data at Neurath. That tower model is available from the Swiss Reactor Institute. Nester also provides those exit conditions (from a simple tower performance model of his own) from available tower and ambient variables measured on the dates of plume measurements. Nester states that the lack of knowledge of these exit variables is not crucial. His own plume model (to be reviewed later) is sensitive to reasonable changes in these numbers by only about 10%. This is a problem which we feel remains uncertain.
2. Nester notes that the specific humidities measured are valid only when the Lyman Alpha system did not traverse the visible plume during the study. The Lyman Alpha system was not set up to handle liquid droplets striking the system and undoubtedly the slow evaporation of those droplets from the instrument biased future specific humidity measurements in the same study (even though later traverses may have been in the invisible part of the plume). In cases where the glider did traverse the visible plume with the Lyman Alpha system, moisture contents were measured to be factors of 2-3 too high. Nester notes that even in cases where only the invisible plume was sampled, the shape of the vertical specific humidity profile at any vertical cross-section will be correct although the magnitudes themselves of the specific humidity differences would not be correct.
3. vertical velocities in some cases appeared to be rather large and perhaps untrustworthy.

A complete set of Neurath data (after data reduction and analysis) including estimated tower exit conditions will be published soon by Trepp. A good discussion of data limitations will be provided. In all, these Neurath and Meppen data are the first in-plume data of reasonable quality to be published and should be very useful for model testing and model development.

Meppen and Amos Natural-Draft Cooling Towers (Visible Plume and In-Plume Measurements (10) and (19)

EDF has recently carried out two major field studies at operating NDCTs. Since French towers are in operation only for small plants (250 MWe), data from larger foreign towers were felt to be necessary to support model validation and improvement programs ongoing at EDF at Chatou. The results of both studies are presently unavailable; the results of the Amos studies should be published in the open literature in the near future.

The Meppen study (10) was carried out at the 600 MWe plant between March 14 - April 2, 1977 in the Federal Republic of Germany. The site is ideal in that only a single tower is operating in open area unobstructed by buildings, other than the fossil-fired power station itself and the stack. Measurements obtained were

1. visible plume outlines taken by photogrammetry employing two sets (of two) automatic stations.
2. exit conditions from the tower including (i) drop-size spectra for recondensate and drift droplets (the optical system of Dibelius and Ederhof was used) and (ii) the thermodynamic and dynamic flux of air from the tower exit (plume temperature, velocity and direction of the effluent).
3. physical and microphysical plume characteristics, taken by a helicopter by making traverses through the plume for temperature and droplet spectra. Water vapor concentrations were measured in the plume by means of LIDAR.
4. ambient profiles of wind speed, pressure, temperature, and humidity determined as a function of altitude by means of aerological soundings.

Organizations which took part in this study were: EDF (Division of Meteorology Applied to Atmospheric Pollution), Bonnenberg and Drescher Society in Germany, Technical School Aachen (Prof. Dibelius), Universities of Aix-la-Chapelle and Munich, Dynamics and Microphysics Laboratory (LDMA) of Clermont-Ferrand and CEV of Bretigny-sur-Orge. A sample of some of the data taken is given in Figure 3-14.

The Amos study (19) was carried out by EDF in cooperation with Smith-Singer Meteorologists (now Meteorological Evaluation Services Inc.) of Amityville, New York. Measurements at the Amos site in West Virginia were made on the MWe total). Measurements on the plumes included visible plume outlines by the photogrammetric method and balloon and aircraft soundings of atmospheric variables. No in-plume measurements were made. Some of the plume and ambient field data (not complete sets, however) are available at MES (from Mark Kramer) but these data are not in publishable form at this time.

SUMMARY

A large quantity of good quality laboratory and field data are available on cooling-tower plume dispersion from French, German, and Swiss sources. Laboratory data from Electricité de France provide basic parametric studies on plume dispersion from one, two, and four towers of natural-draft type. For the parametric lab studies, measurements were made of plume trajectories and dilutions (through dye concentrations) under fixed tower and ambient conditions where K, the ratio of tower exit velocity to wind speed, was varied. The effect of the tower wake in adding dilution is especially notable. The effect on dilution and trajectory of (a) varying F_0 for the single tower case and (b) adding additional towers in different geometric configurations was also studied.

Visible plume field data from Gardanne, Lünen, and Neurath (supplemented by ambient profiles and tower-exit measurements) provide, in total, 24 new data cases for use in model validation and improvement studies. The quality of the data range from fair to good. The data represent a large range in ambient conditions and levels of heat and moisture release.

An intensive study involving in-plume measurements at Neurath (three towers) and Meppen (one tower) has provided considerable insight into the physics of dispersion from the visible and invisible plume. Measurements of plume temperature, humidity, and vertical velocity have been made in 3-5 vertical planes downwind. Selected data from Neurath have been fully reduced. The major disadvantage to the data is that tower exit conditions were not measured. However, predictions of tower exit variables can be made from available plant and tower operational data.

REFERENCES

1. Pierre-Louis Viollet. Study of Jets in Transverse Currents and in Stratified Environments. Doctoral Dissertation. Curie University. Paris, France. February 1977. (in French)

2. L. N. Fan. Turbulent Buoyant Jets into Stratified or Flowing Ambient Fluids. Report No. KH-R-15. W. M. Keck Laboratory of Hydraulics and Water Resources. California Institute of Technology. 1967.

3. J. F. Keffer and W. D. Baines. The Round Turbulent Jet in a Cross Wind. Journal of Fluid Mechanics. Vol. 15. pp. 481-496. 1963.

4. L. Caudron. Study of Plumes from Cooling Towers (Calculations and Experimental Data). Report E 44/78.19. Electricité de France. Hydraulics Laboratory. Chatou, France. (in French)

5. P. L. Viollet. The Structure of Buoyant Jets Emitted Vertically in Different Types of Environments. Electricité de France. Hydraulics Laboratory. Chatou, France. Presented at Von Karman Institute for Fluid Dynamics. Lecture Series 1978-7. Pollutant Dispersal in the Environment. Brussels, Belgium. May 8-12, 1978.

6. J. Chevalier. Some Hydrodynamical Problems Encountered in Nuclear Power Plants. Journal of Hydraulic Research. Vol. 15, No. 2. pp. 125-136. 1977.

7. J. L. Bringuier, C. Charpentier, A. Hodin, and A. M. Lanquette. Cooling Towers: Dispersion of Visible Plumes and Review of Field Data Acquired at Gardanne. Report E 32/76.16. Electricité de France. 1976.

8. L. Caudron and A. Darles. Schematic Study of Visible Plumes from Wet Natural-Draft Cooling Towers of 2 and 4 Towers of 900 MWe. Report E 44/77.17. Electricité de France. Hydraulics Laboratory. Chatou, France. May 1977.

9. Pierre-Louis Viollet. Physical Structure and Numerical Modeling of Plumes from Cooling Towers. Report E 44/78.15. Electricité de France. National Hydraulics Laboratory. Chatou, France. April. 1978.

10. Electricité de France. Study of Plumes from Cooling Towers: Meppen Study - RFA. IN: Electricité de France. Department of Research and Investigation. Report of Activities - 1977. Hydraulics Laboratory. Chatou, France. pp. 22-24. 1978.

11. Eidgenossiche Kühlturm Kominission. Bericht der Arbeitsgruppe über die Meteorologischen Auswirkugen der Kühltürme - Meteorologische Messerie am Standort Lünen. Payrne, Switzerland. May 1973.

12. W. Caspar and H. Scharrer. Measurements of the Atmospheric Conditions and Observation of the Cooling Tower Plume. IN: Studies on a Natural Draft Wet Cooling Tower. VDI Report. Vol. 15. No. 5. Ed. G. Ernst. pp. 57-69. July 1974.

13. F. Gassmann, D. Haschke, and W. Solfrain. Measurements on Cooling Tower Plumes (Part 1): Mathematical Simulation and Significance of the Measurements. EIR Report No. 295. Würenlingen, Switzerland. April 1976.

14. H. Fortak. Measurements on Cooling Tower Plumes (Part 3): Three-Dimensional Measurements on Cooling Tower Plumes. Jül - 1250. DFVLR - Institute for Atmospheric Physics. Oberpfaffenhofen, Federal Republic of Germany. November 1976.

15. H. Fortak et al. Measurements on Cooling Tower Plumes (Part 4): Results of Measurement Programs on the Cooling Towers of the REW Power Stations of Neurath and Meppen. Jül - 1250 (Part 4). DFVLR - Institute for Atmospheric Physics. Oberpfaffenhofen, Federal Republic of Germany. May 1976.

16. H. Borchardt, F. Gassmann, D. Haschke, F. Rudin, and J. P. Trepp. Measurements on Cooling Tower Plumes (Part 2): LIDAR Measurements on Cooling Tower Plumes. EIR Report No. 302. Würenlingen, Switzerland. June 1976.

17. J. P. Trepp. Flight Measurements on Cooling Tower Plumes: Measurement Data from the Neurath II Measurement Program on Wet Natural Draft Cooling Towers. Report TM-ST-509 (Supplement to EIR Report No. 351). Würenlingen, Switzerland. June 1976.

18. K. Nester. Personal Communication. Kernforschungszentrum Karlsruhe, Federal Republic of Germany. September 1978.

19. M. Kramer. Personal Communication. Meteorological Evaluation Services, Inc. Amityville, New York. 1978.

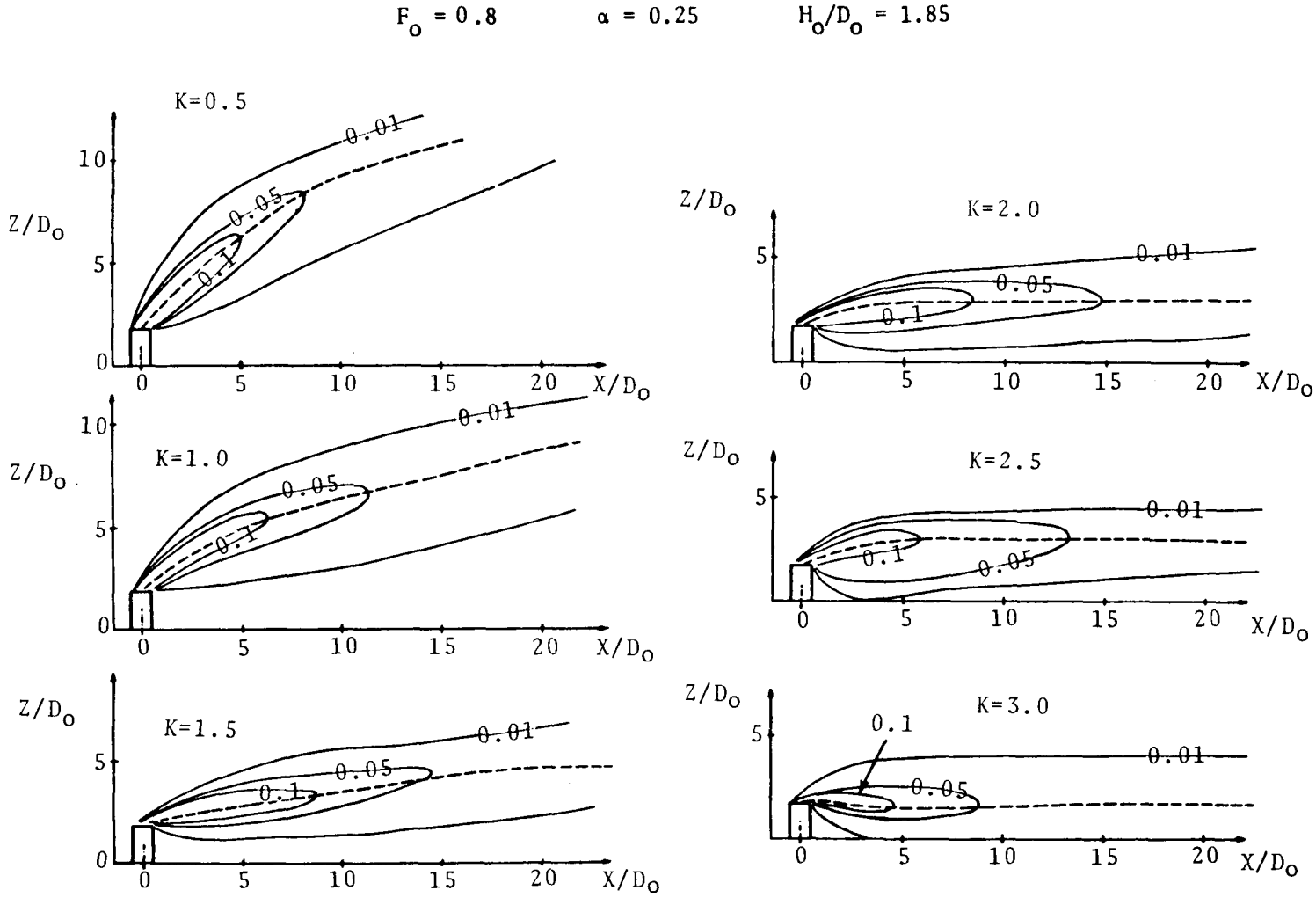

Figure 3-1. Parametric laboratory study of isoconcentration contours of a NDCT plume...variation in K. [Source: From Viollet (1).]

Influence of K for $F_0 = 0.8$ $\quad 2 \geq K \geq 0.33$

$H_0/D_0 = 1.85$; $\quad \alpha = 0.25$

$R_0 = 2.10 \cdot 10^4$

Discharge geometry:

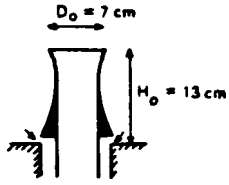

Legend:

* K = 2
\+ K = 1
x K = 0.66
o K = 0.5
◐ K = 0.4
◑ K = 0.33

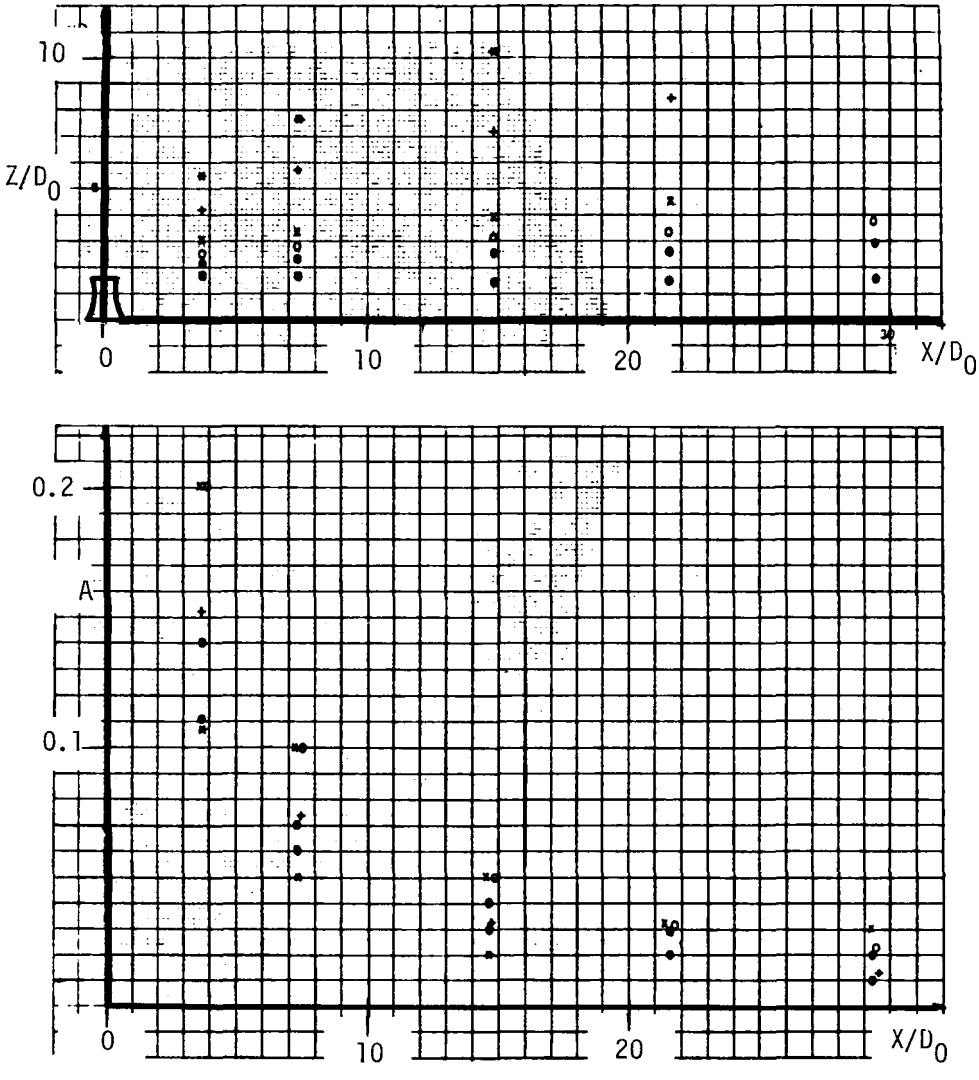

Figure 3-2. Comparison of trajectory variation and centerline concentration decay for parametric study in Figure 3-1. [Source: From Viollet (1).]

Influence of K for a 2-Discharge Group - $F_o = 0.65$

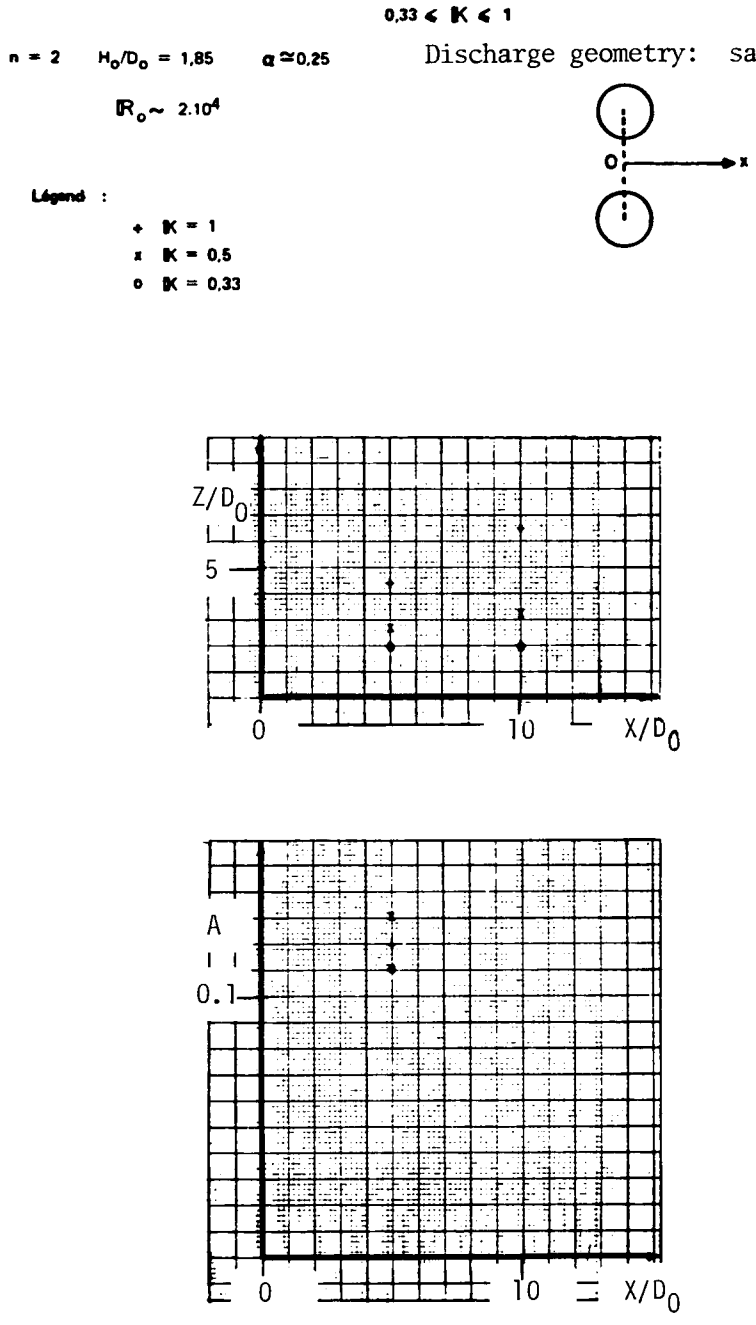

Figure 3-3. Comparison of trajectory variation and centerline concentration decay for parametric study of two natural-draft cooling towers . . . variation in K. [Source: From Viollet (1).]

Interaction of 2 Jets. Isoconcentrations in a Plane Perpendicular to the Current at $X/D_o = 5$

2 towers separated by one diameter

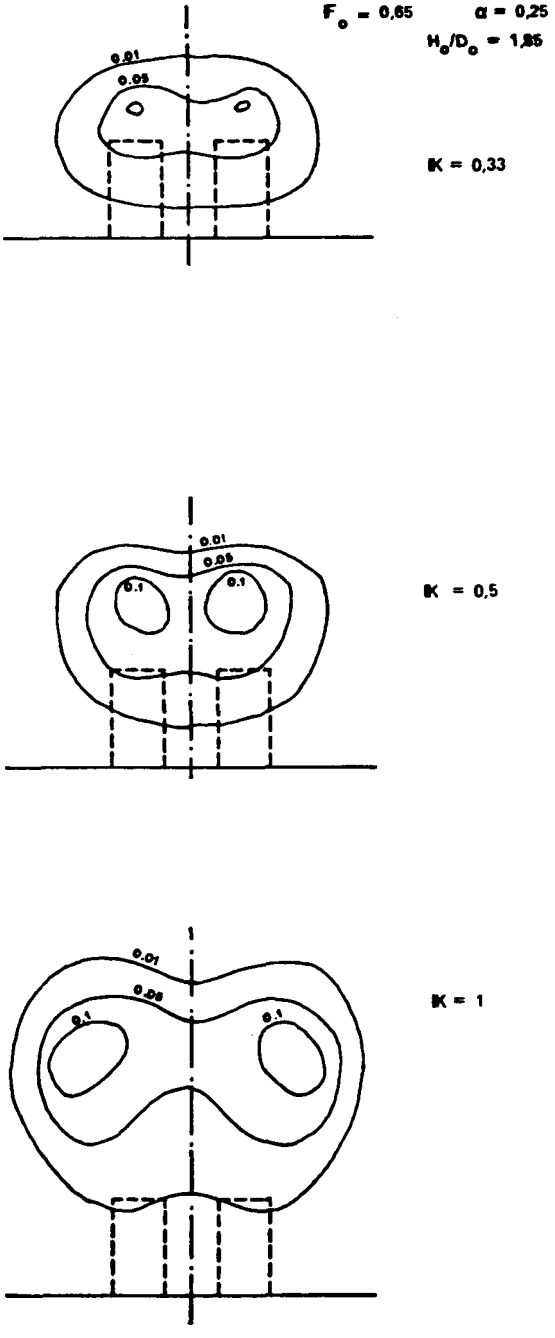

Figure 3-4. Comparison of isoconcentration contours at $X/D_Q = 5$ for a two tower configuration . . . variation in K. [Source: From Viollet (1).]

Influence of K for a 4-Discharge Group - $F_o = 0.8$

Discharge geometry: same as in Fig. 2

$H_o/D_o = 1.85$; $\alpha = 0.25$

$R_o = 2.10 \cdot 10^4$

$0.33 \leq IK \leq 2$

Discharge arrangement:

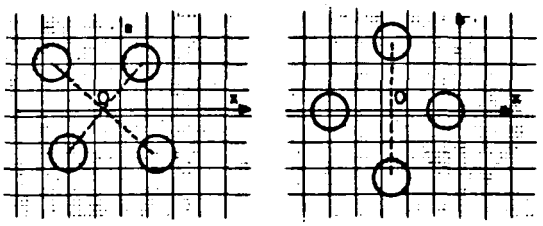

Legend:

	Arrangement
+ IK = 2	a
x IK = 2	b
o IK = 1	a
● IK = 1	b
◐ IK = 0.5	a
◑ IK = 0.5	b
⅄ IK = 0.33	a
Y IK = 0.33	b

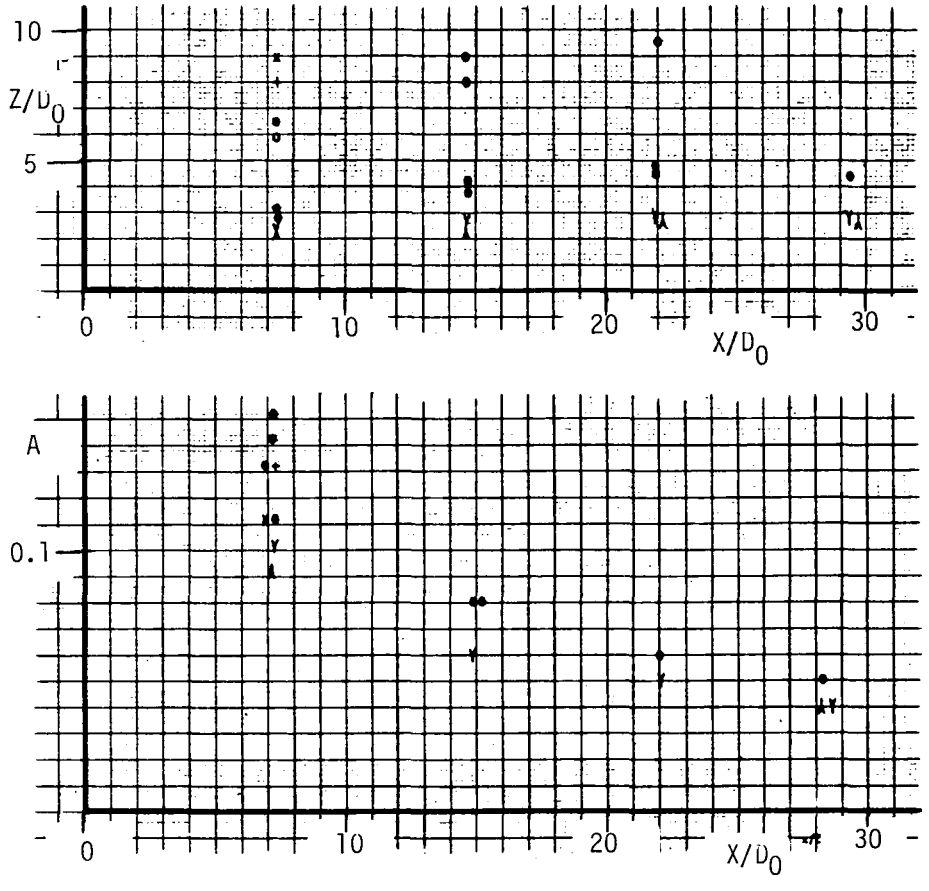

Figure 3-5. Comparison of trajectory variation and centerline concentration decay for parametric study of four natural-draft cooling towers . . . variation in configuration of towers and in K. (Source: From Viollet (1).]

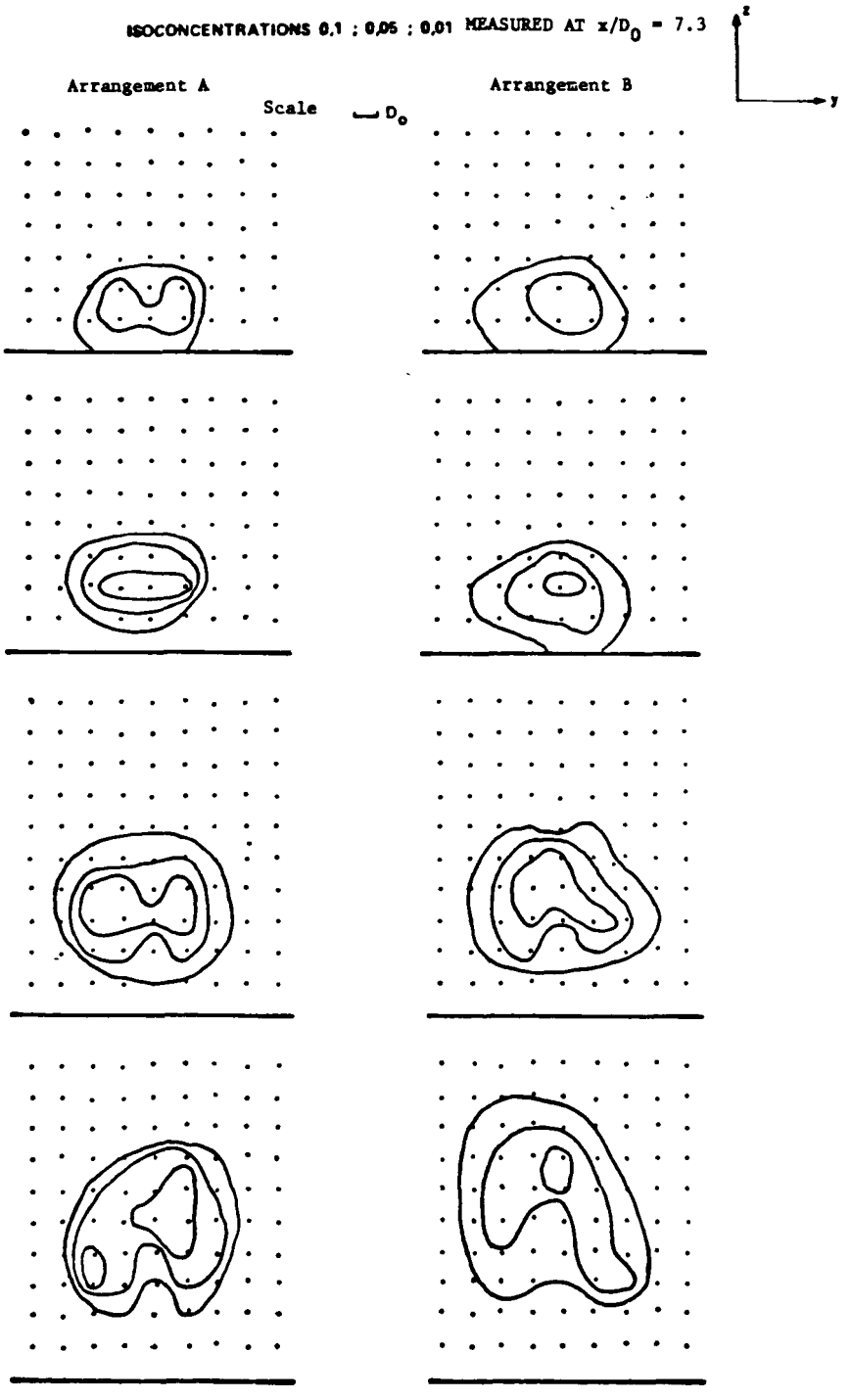

Figure 3-6. Comparison of isoconcentration contours at X/D_0 = 7.3 for the two four-tower configurations. [Source: From Viollet (1).]

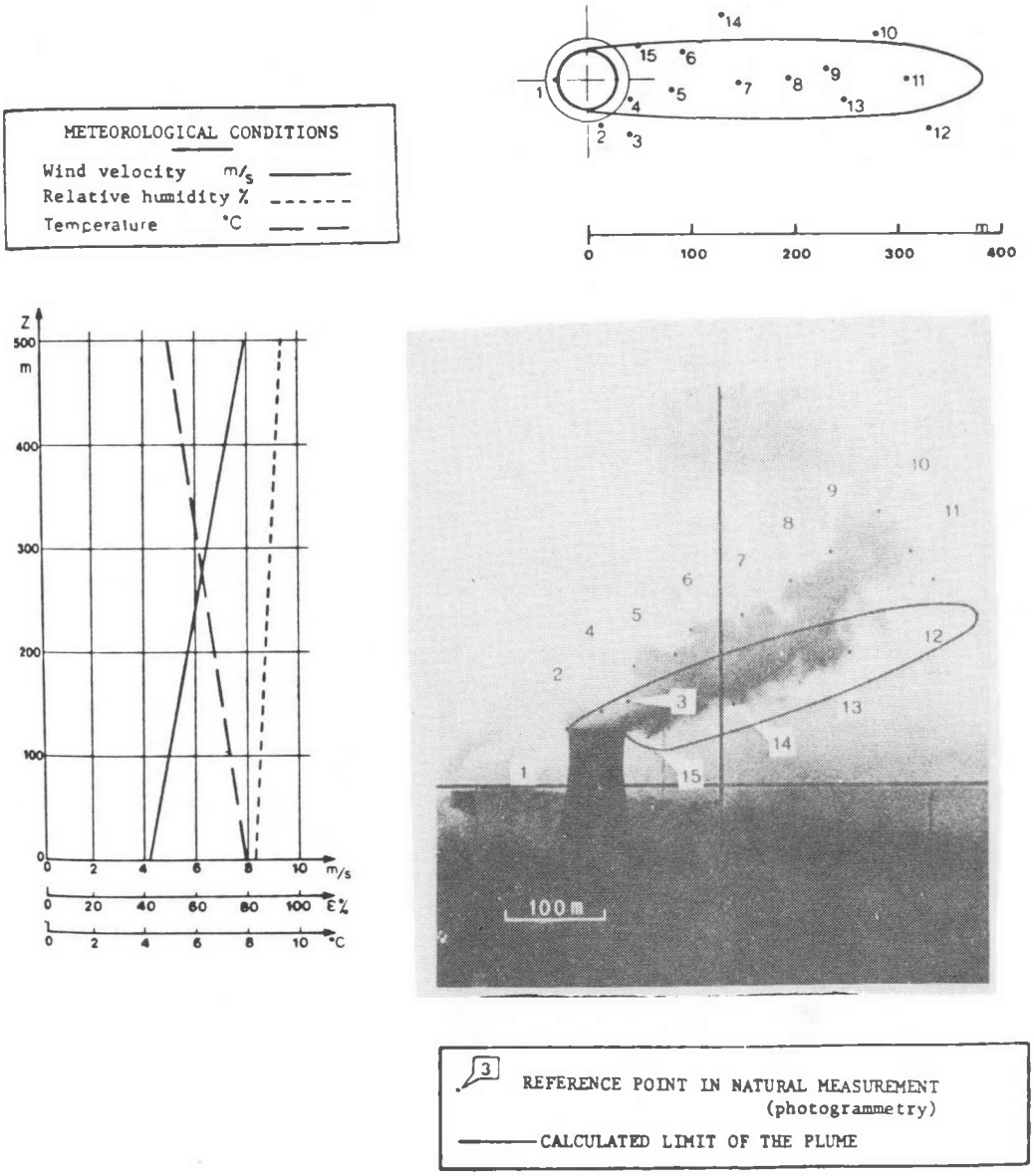

Tower Exit Conditions:

height of tower - 120 m

exit diameter of tower - 59 m

exit velocity - 2.8 m/s

difference between exit temperature and ambient temperature at tower height - 14.2 °C

estimated recondensate liquid emission - 2.9×10^{-3} g/g dry air

Figure 3-7. Sample of plume data from Gardanne . . . visible plume outline, tower exit conditions, ambient profiles . . . December 9, 1975 (0930 Hrs). [Source: From Viollet (1).]

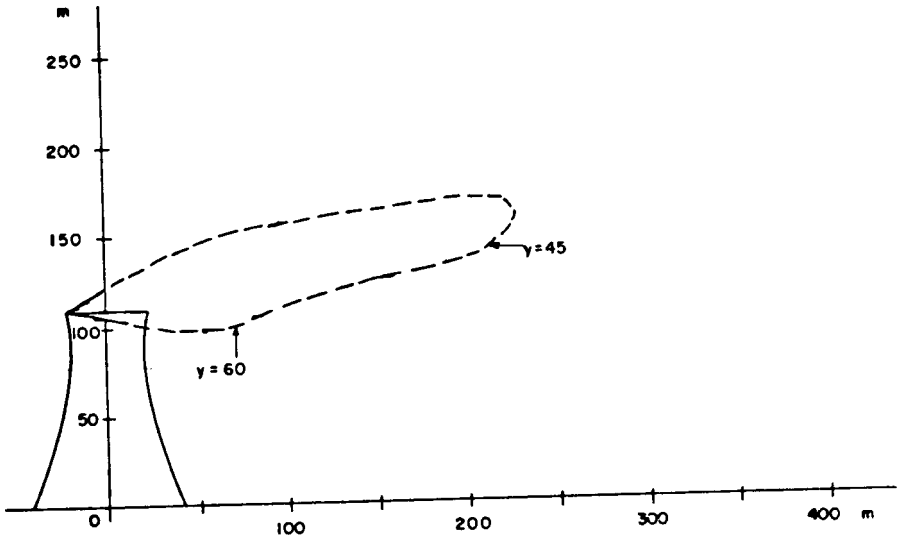

Ambient Profile

Height m	Temperature °C	Relative Humidity %	Wind Speed m/s
0	7.4	54	5
166	6.8	64	9
225	6.3	67	10
411	4.4	69	14
506	3.3	70	16
812	1.2	72	11
919	1.4	78	15
1019	1.1	80	--
1147	1.1	78	--
1430	-0.8	82	--

Tower exit conditions

height of tower - 109.3 m
exit diam. of tower - 51.3 m
exit velocity - 4.42 m/s
exit temp. - 25.0 °C
recondensate liquid emission - not measured

Figure 3-8. Sample of plume data from Lünen . . . visible plume outline, tower exit conditions, ambient profiles . . . November 30, 1972 (1300 Hrs). [Source: From Eidgenössiche Kühlturm Kominission (11).]

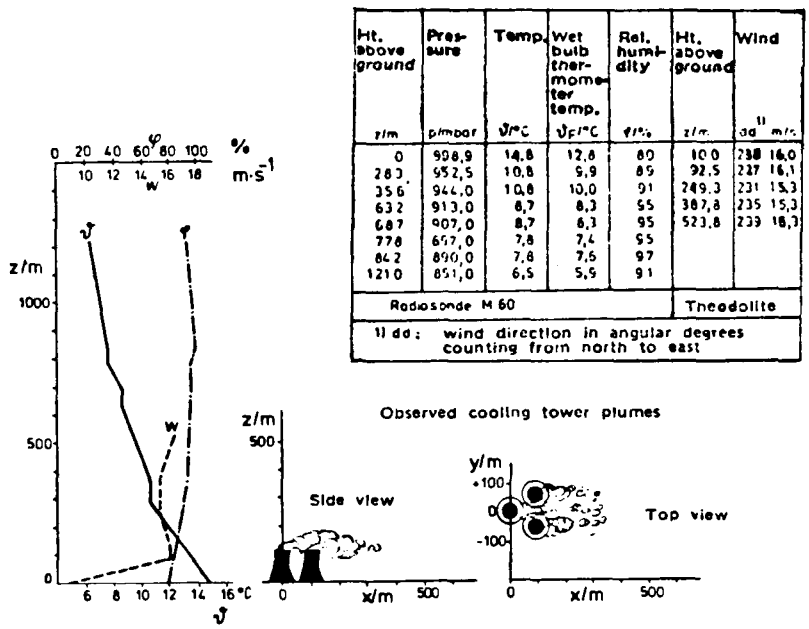

Tower Exit Conditions (1300 Hrs):

height of tower - 100 m

exit diameter of tower - 44.6 m

exit velocity - 3.72 m/s

exit temperature - 31.6 °C

recondensate liquid emission - not measured

Figure 3-9. Sample of plume data from Neurath . . . visible plume outline, tower exit conditions, ambient profiles . . . September 28, 1973 (1500 Hrs). [Source: From Caspar and Scharrer (12).]

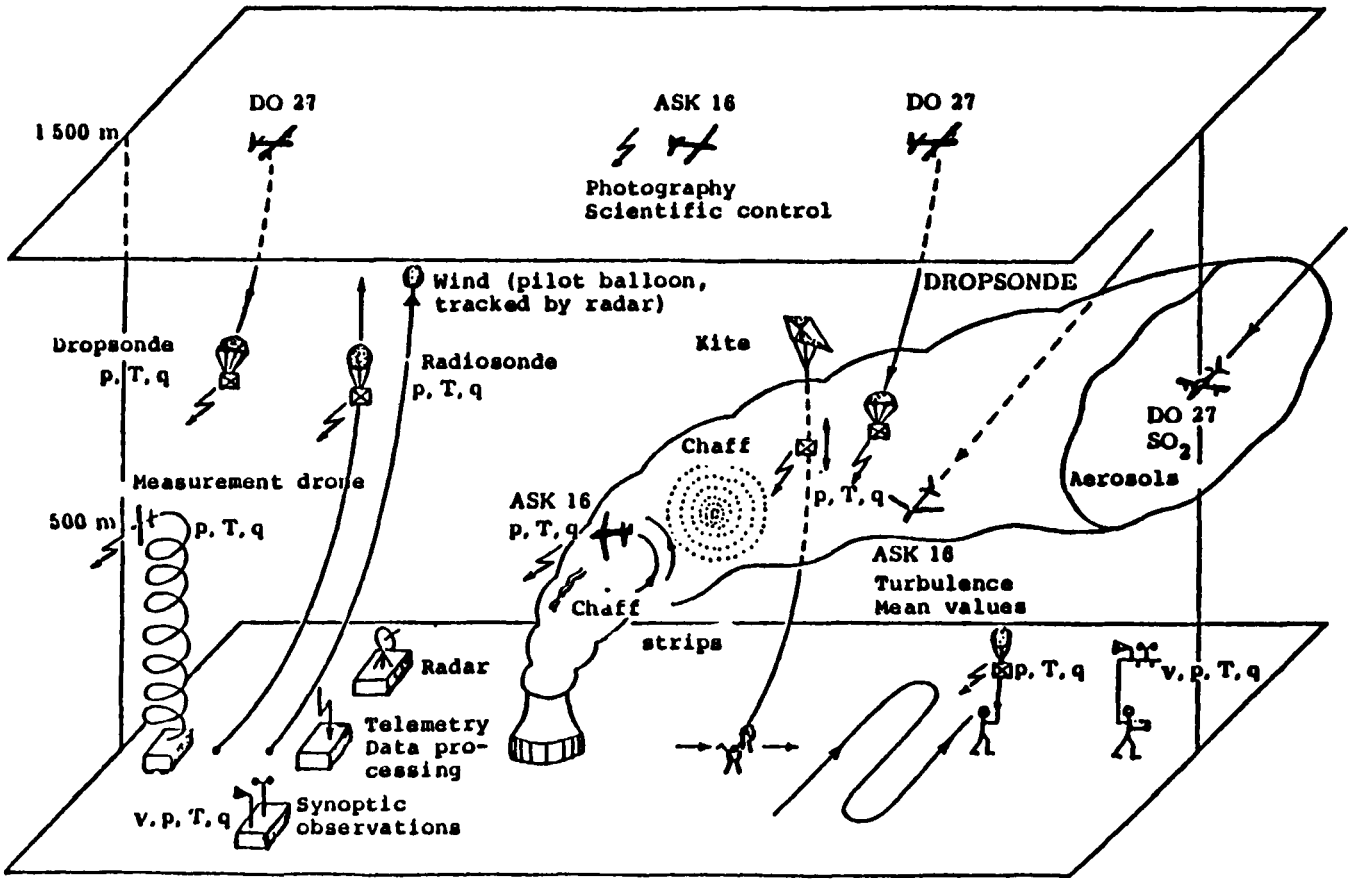

Figure 3-10. Schematic of measurement methods employed in 1974-1975 Neurath and Meppen Studies. [Source: From Fortak (14).]

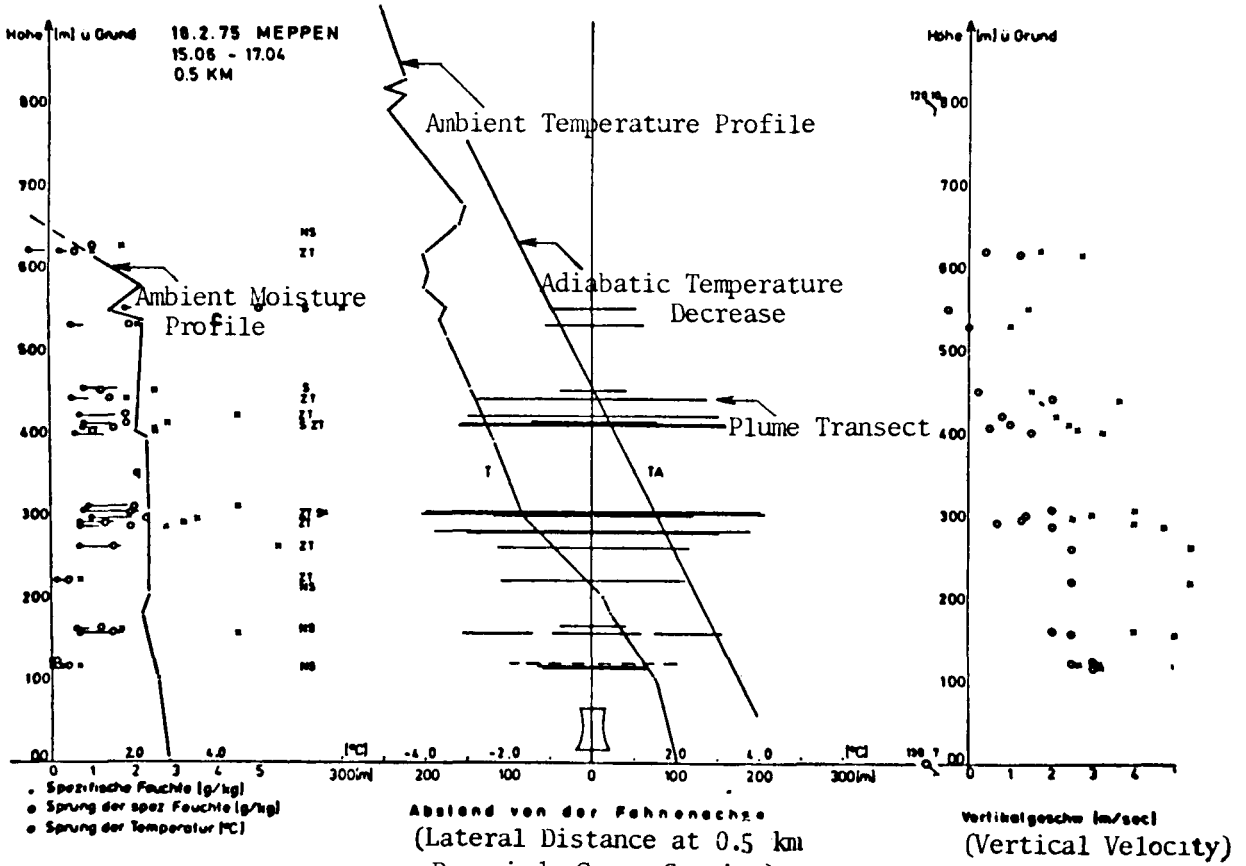

Legends:

Left:

- Specific Humidity of Ambient (g/kg)
- Difference of Plume Specific Humidity Above Ambient (g/kg)
- Difference of Plume and Ambient Temperature (°C)

Middle:

S : Visible
ZT : Partially Visible
NS : Invisible

Right:

x Maximum Vertical Velocity
o Average Vertical Velocity

Figure 3-11. Vertical distribution of vertical velocity (right), specific humidity (middle) and temperature differences above ambient (left) for Meppen plume. Feb. 6, 1975 (1506-1704 Hrs) . . . 0.5 km from tower. [Source: From Fortak (14).]

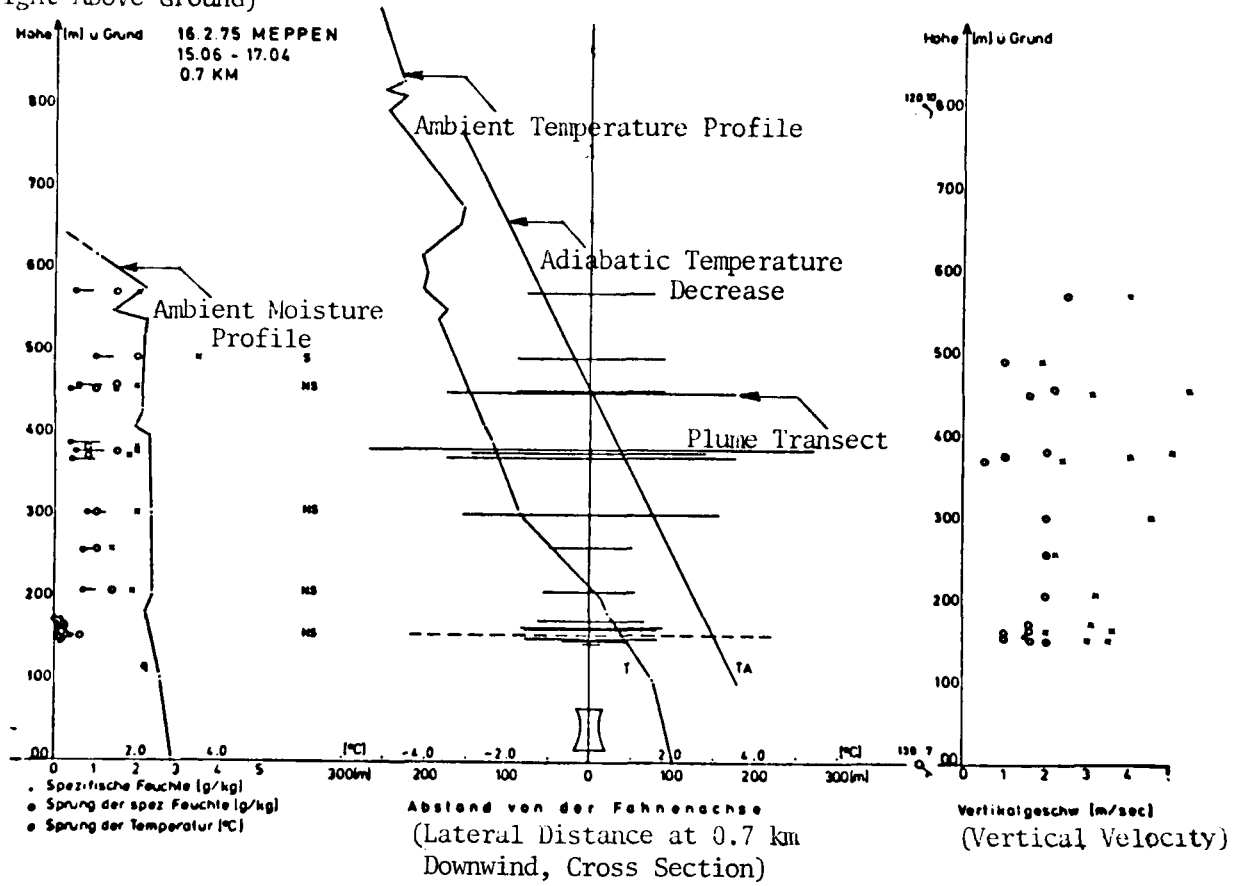

Legends:

Left:

- Specific Humidity of Ambient (g/kg)
- Difference of Plume Specific Humidity Above Ambient (g/kg)
- Difference of Plume and Ambient Temperature (°C)

Middle:

S : Visible
ZT : Partially Visible
NS : Invisible

Right:

x Maximum Vertical Velocity
o Average Vertical Velocity

Figure 3-12. Vertical distribution of vertical velocity (right), specific humidity (middle) and temperature differences above ambient (left) for Meppen plume. Feb. 16, 1975 (1506-1704 Hrs) . . . 0.7 km from tower. [Source: From Fortak (14).]

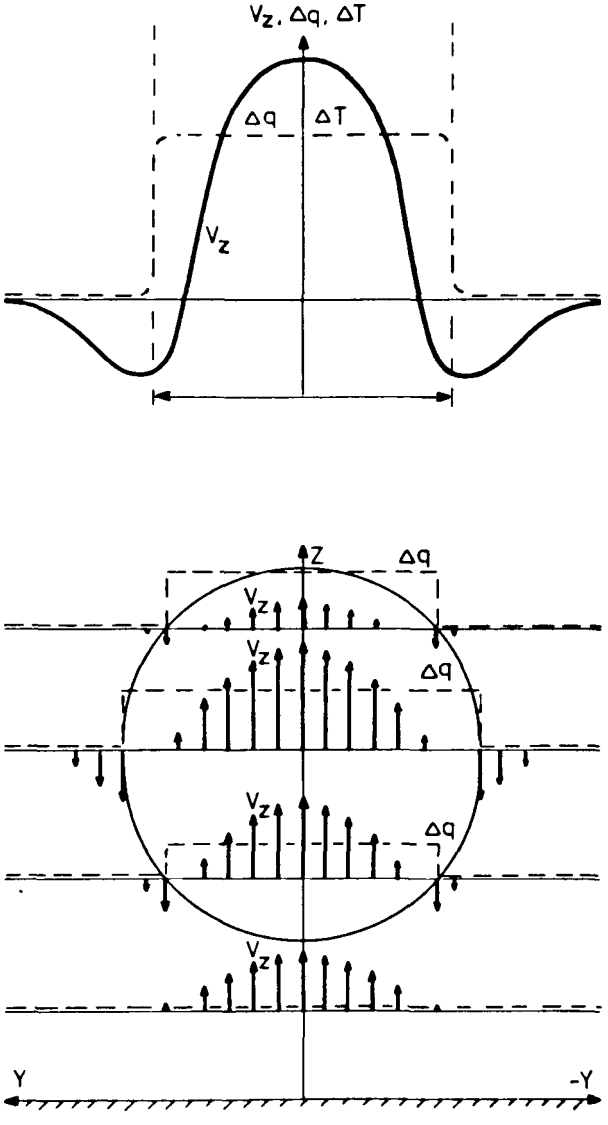

Figure 3-13. (a) Typical horizontal traverse through Neurath or Meppen plume showing distribution of vertical velocity, humidity and temperature elevation above ambient (top). (b) Variation of above distributions with distance from cooling tower (bottom). [Source: From Fortak (14).]

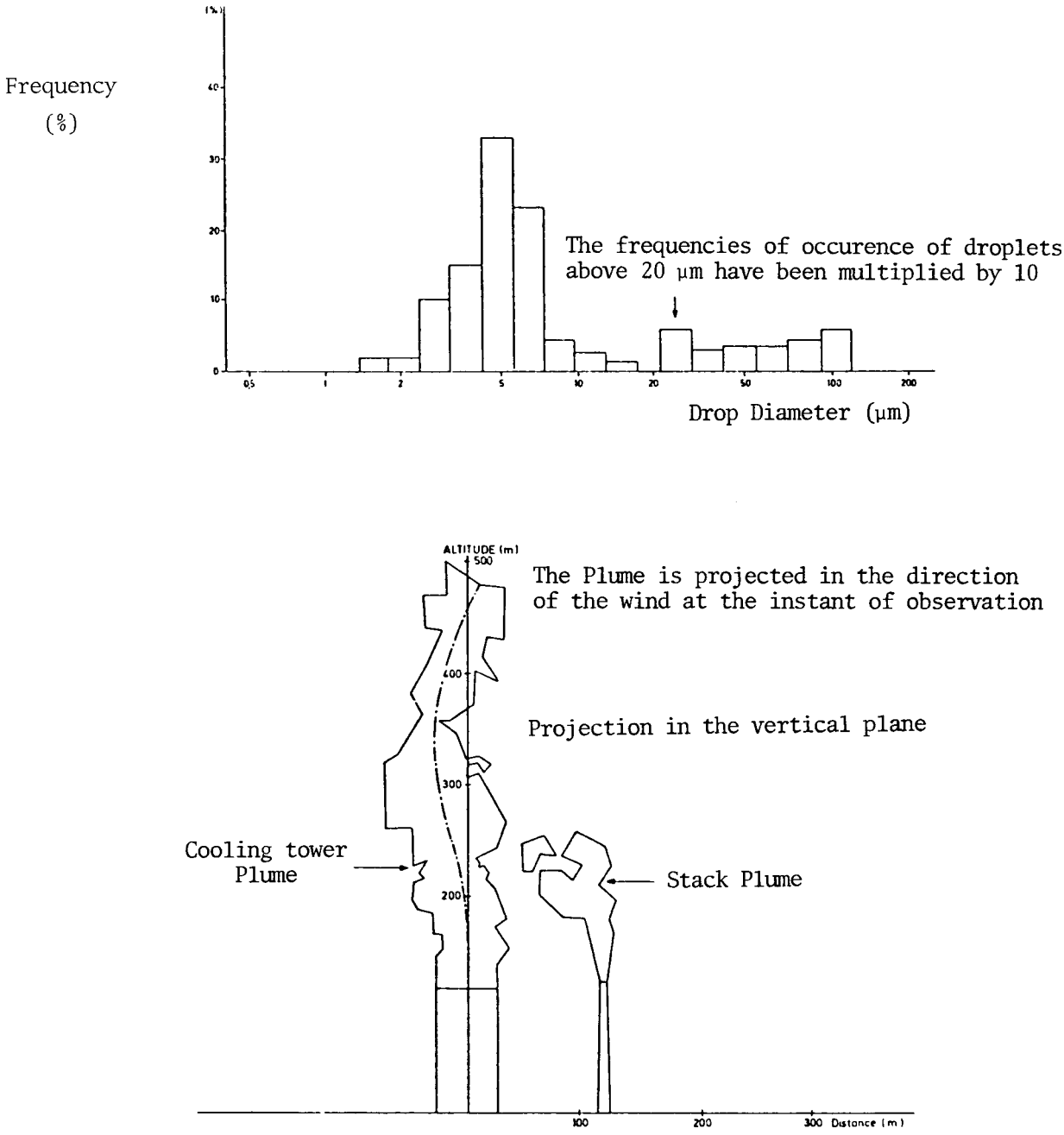

Figure 3-14. (a) Droplet-size distribution as a function of drop diameter at exit of Meppen tower. Recondensate and drift drops are included . . . Meppen, March 29, 1977 (1245 Hrs). (b) Photogrammetric determination of visible plume . . . Meppen, March 29, 1977 (1556 Hrs). [Source: From Electricite de France (10).]

Section 4

MATHEMATICAL MODELS FOR COOLING TOWER PLUME DISPERSION

European models for cooling tower plume and drift dispersion may be divided into two categories. The first category refers to models developed for and commonly used for environmental impact analyses (KUMULUS (1, 2); FOG (3, 4); SMOKA (5, 7); and PANACH/MYKES (8, 12)); the second classification are those models which are more complex in formulation and are expensive to run but were developed with the primary aim of representing internal plume dynamics on a microscopic level (WALKÜRE (13, 14) and the model by Egler (15, 16)). The French models (PANACH (8, 12) and MYKES (8, 12) actually span both categories. The formulation of each model will be reviewed briefly below.

Our study of the European models provides us with an expanded view on model approaches and assumptions. The best method to evaluate these European models is to test them with experimental data. Section 5 of this report evaluates the KUMULUS and FOG models through model/data comparisons. Other models were still under development (SMOKA, Egler model, WALKÜRE) or proprietary and not available (PANACH/MYKES) for our validation study. Each model will now be described briefly.

KUMULUS (P. Brog and M. Von Euw; Motor-Columbus Consulting Engineers, Baden, Switzerland) (1, 2)

The KUMULUS Model predicts plume dispersion from single and multiple cooling towers of natural or mechanical-draft type. The model has an associated drift deposition code (BIG BEN) which has been used to predict drift from towers located on the more polluted European rivers and also for the proposed Indian Point Unit 2 towers on the Hudson River in the U.S. The plume model has been continually improved over the past seven years and has been calibrated to selected European and American field data. The KUMULUS Model is the most popular model employed in environmental impact analyses of cooling towers in Switzerland and the Federal Republic of Germany. The BIG BEN Model is of relatively recent origin and has not been calibrated with experimental data.

The single tower plume model is similar in development to the work of Weinstein and Davis (17). The bent-over plume assumption is made. The equations of conservation of vertical momentum and enthalpy follow Weinstein and Davis. Unique features of the model include (a) an entrainment function which attempts to account for jet mixing, atmospheric turbulence, and additional mixing due to the wake of the tower, (b) an elliptical plume cross-section which is a function of ambient stability, and (c) an additional empirical drag force on the plume which is effective under large wind conditions and provides additional plume bending due to the effect of the wake of the tower.

The BIG BEN Model is described in some detail in Refs. (1, 18). The model has a very simple plume rise formulation and a simple breakaway criterion. Its assumption that droplet temperatures after breakaway assume the temperature of the ambient dry bulb is not correct and will lead to much too rapid an evaporation process (18). Additional information on the BIG BEN Model is presented in Ref. (18).

The use of the KUMULUS and BIG BEN Models for environmental impact analyses involve the making of predictions over a season or the full year. An important component in the application of the KUMULUS/BIG BEN Models then is the method of treatment of the ambient meteorology in the preparation of seasonal or annual predictions of plume characteristics or drift deposition patterns about the tower. This is a very difficult problem; the KUMULUS Model provides an advancement in the methodology of such seasonal/annual predictions. The ambient meteorology at a site (seasonal or annual) is reduced to 90 representative ambient profiles with associated frequencies based upon their occurrence in a given season and wind direction. The KUMULUS or BIG BEN Model is then run only for those 90 cases and the results combined based upon those frequencies for the season under study. Although questions arise on how best to set up the methodology to choose the most appropriate 90 cases, the ideas behind this approach are fundamentally sound. Earlier methodologies in the field employed on oversimplified plume or drift model and computer runs for every meteorological observation taken at the site; as a result, an extremely large number of calculations is required, requiring the use of an inexpensive, and often oversimplified plume and drift model in order to keep computer costs manageable.

FOG (F. Gassmann, J. P. Trepp and D. Haschke; Swiss Reactor Institute, Würenlingen, Switzerland) (3, 4)

This model is of the one-dimensional integral type and has been employed in a number of environmental impact analyses in Switzerland. Recent measurements of in-plume data from Neurath and Meppen have been acquired for calibration of the model.

The model consists of two parts: the rising plume (entrainment portion) and the diffusion part. The rising part is characterized by a mean plume velocity which is greater than the turbulent intensity of the free atmosphere. In the diffusion part, atmospheric turbulence is predominant. A sketch of the division of the plume, as modeled by FOG, is given in Figure 4-1.

The rising part or entrainment part of the model follows the ideas of Weinstein and Davis as do other U.S. models such as Hanna (19), Orville (20), and EG&G (21). Characteristics of this part of the model are

1. bent-over plume assumption,
2. top-hat plume profiles; circular plume cross-sections,
3. an entrainment velocity proportional to the vertical velocity and local jet angle with the horizontal, and
4. detailed plume thermodynamics treated by allowing for changes of state from moist air to liquid water to ice crystals if conditions warrant.

The bent-over plume assumption removes the need for a horizontal momentum equation.

A unique feature to the model is the idea of detrainment which is applied to both the buoyant jet and atmospheric diffusion parts of the model. As the vapor plume rises, it entrains ambient air, yet loses a small amount of its mass to the ambient air on the lee side of the plume due to the turbulence of the free atmosphere. Clearly, the net difference between entrainment and detrainment is the important quantity in determining the plume variables of interest within the rising buoyant jet. Yet, the fate of air "detrained" at each plume cross-section does show some additional effects. The FOG Model treats the detrained moisture at each slice of the plume as a "source" of moisture for dispersion downwind by ambient turbulence. If, for instance, the plume from tower top to maximum rise is divided into 50-100 sections, each normal to the plume centerline, then each of those 50-100 plume slices is the location of a small source of moisture "detrained" by atmospheric turbulence. Moisture dispersion from each of those sources (as well as the one large source located at the last calculated ascending parcel at maximum rise) is computed for fixed distances downwind. In this calculation, the effects of each of those sources is superimposed for any downwind distance of interest. FOG calculations show that for the Neurath towers under conditions of high ambient atmospheric instability, there would be small moisture increases (above ambient levels) at the ground.

The FOG theory of detrained sources leading to moisture elevations in the lee of the plume downwind has actually been verified with field data acquired at Neurath. Figure 4-2(a) shows measurements of ground-level moisture and temperature elevations made by means of a portable ground sonde. The sonde traversed laterally under the plume at a distance of 750 m downwind. Figure 4-2(a) shows the fluctuations in moisture and temperature which appear at one location over a period of 3 minutes. Figure 4-2(b) shows the lateral distribution of excess moisture content on the ground derived from the field data. The measurements were fit to a Gaussian distribution from which, by integration, the total moisture excess at the given distance could be determined. Model predictions using FOG for that distance showed fairly good agreement between ground-level moisture data.

It should be noted that the ground measurements at Neurath were also supplemented by model airplane ("measurement slave") measurements and the power glider (ASK-16) measurements mentioned in Section 2. The vertical distribution of water content above ambient could be computed from those three complementary measurement sources. This distribution is illustrated in Figure 4-2(c). (From that distribution, Trepp and Gassmann of the Swiss Reactor Institute were able to check the total water balance of the plume since the water emission rate from the cooling towers and stacks was known. This confirmation helped prove the consistency of the measurements.) The shape of the measured vertical distribution in Figure 4-2(a) was also predicted by the FOG Model. That distribution is useful for potential tuning of the spreading predicted by a plume model. Further validation of the FOG Model appears in Section 5.

Figures 4-3, 4-4 and 4-5 present some results of the FOG model. Figure 4-3 presents a plume calculation with FOG showing in (a) the vertical variation in plume kinematic and thermodynamic variables at different distances downwind, and in (b) isopleths of moisture content in the plume along with the visible portion of the plume (shaded area). Figure 4-4 shows calculated plumes such as can be formed by a wet NDCT and a dry NDCT (about 1800 MWe each) under identical atmospheric conditions. (The fact that the plume is visible in the dry tower case should be noted). A verification run of the model with field data at Neurath is given in Figure 4-5. The goal of the research with the FOG Model (and also the ultimate goal of the field measurements at Neurath and Meppen) is to simulate the atmospheric effects of wet and dry towers of various designs and sizes by mathematical models and hence to clarify quantitatively the climatic changes from cooling towers that are significant. Further discussion on dry tower application of the FOG Model appears in Refs. (3, 4).

An older model developed at the Swiss Reactor Institute is the PLUMEFF code (22). In this model, the cooling tower plume is simulated in a two-dimensional time-dependent format where the steady state solution is of interest (nonzero wind only). The equations of motion, continuity, and those that describe the transport of heat, water vapor, and water droplets are solved by finite difference techniques. Turbulent transfer is represented either by a constant eddy viscosity or by the Prandtl mixing-length hypothesis. Condensation, evaporation, coagulation, breaking and gravitational effects of water droplets relative to air are included. The size distribution of the water droplets is given as a discrete spectrum of five droplet sizes. For each time step, the model calculates the temperature, velocity, relative humidity, cloud and rainwater content for each grid point.

In cases of a nonzero wind, the plane of solution is the longitudinal-vertical plane through the tower centerline. Unfortunately, a NDCT must be considered as an infinite slot, which is not realistic. For calm conditions, however, cylindrical coordinates in r and z are used with time providing a realistic treatment of the geometry of the tower. A major limitation to the model is the lack of knowledge on the choice of eddy diffusivity coefficients. A sample prediction of the PLUMEFF Model for zero wind conditions is given in Figure 4-6. (Work on the PLUMEFF Model has been halted with all attention centered on the one-dimensional FOG Model.)

PANACH and MYKES (L. Caudron and P. Viollet; Electricité de France, Paris) (8 - 12)

These two computer models have been employed to predict plumes from single and multiple natural draft cooling towers by EDF. Both models employ a finite-difference solution to a simplified form of the governing equations of plume motion. PANACH, a steady state model, applies to plumes in a windy environment while MYKES, a time-dependent model, applies to plumes in calm ambient atmospheres. Both models have been calibrated to field and laboratory data.

The PANACH Model solves the three-dimensional equations of continuity, momentum (x,y,and z), temperature and passive tracer concentration. The equations are simplified by dropping all diffusion terms in the x-direction (wind direction) as well as the gradient of pressure with x. The equations now become a parabolic set in x and, as a consequence, a marching solution in the wind direction can be made starting from the tower exit plane (x=0).

The equations are solved from step x to step x+Δx using a method of fractional steps based upon the work of Chorin (22). The order of solution of the governing equations is

1. solve for the U velocity at x+Δx (U is the velocity in the downwind direction x) from the horizontal momentum equation using information at x,
2. estimate V and W at x+Δx from the y and z momentum equations assuming all gradient terms are zero,
3. solve for pressure by solving a Poisson equation in y and z,
4. correct the estimates of V and W, and then
5. temperature and concentration are solved at x+Δx. This step from x to x+Δx is now complete.

Marching takes place along the direction of the wind (the x axis) from the exit plane. At each step along x, all plume variables are computed for the associated y-z plane. Only one sweep along x is needed. Several features of this solution need be mentioned. First, this parabolic solution precludes any fundamental treatment of the very near field which involves plume bendover in the presence of the tower structure. Simplifications to achieve parabolic form of the governing equations prevent the PANACH Model from handling recirculative motions in the x-direction. Thus tower downwash cannot be accounted for directly. Caudron and Viollet define the initial vertical plane for calculation as located at the tower exit centerline and of width D_o (tower exit diameter) and height h_o. The h_o and kinematic variables at the plane are defined from simple conservation laws which introduce a new parameter λ representing the amount of dilution assumed to take place in the very near field. The amount of dilution employed in the model for the very near field is known through previous model calibrations. The second feature that requires discussion is the use of constant eddy viscosities and eddy diffusivities which do not vary in space and time in the model. Dependent upon the initial variables (exit diameter, exit velocity, number of towers, etc.) diffusion coefficients are presented and are assumed constant during plume calculation. Estimates for these numbers have been determined mainly through previous calibration. Although Caudron and Viollet recognize that constant values are a large oversimplification, they find that they are satisfied with the calibration results they achieved with them. Third, the model treats condensation and evaporation in a unique way. PANACH solves a temperature and a passive tracer equation of identical form. However, in the temperature equation, the temperature is replaced by an enthalpy expression and the passive tracer in its equation is assumed to be liquid water concentration. At each point downwind, these two quantities along with the Clausius-Clapeyron equation determine if the plume is visible there or not.

Results presented as calibration or validation runs of the model appear quite impressive. Single tower plume predictions show the characteristic bifurcated nature of the plume and show realistic-looking velocity and concentration profiles at cross sections to the wind. Field data comparisons have been made by EDF to data at Gardanne, Neurath, and Amos. A sample comparison of the PANACH model to Gardanne field data has been shown in Section 2. The wide use of field data for calibration makes it difficult to assess the overall predictive capability of the model. No model/data comparisons are presented by EDF which are stated to be purely verification runs (i.e., no calibration involved).

The MYKES Model is the time-dependent version of the PANACH code. By replacing x by time t and U = 1, a model for the stagnant ambient case is obtained. The model employs cylindrical coordinates and assumes an axisymmetric jet.

EDF also has developed a simple closed-form integral model (12) for plume dispersion. Under assumptions of bent-over plume, top-hat profiles, circular cross sections, and entrainment defined as a constant times the vertical velocity, Caudron and Viollet solve simple ordinary differential equations of vertical momentum, conservation of mass, and conservation of heat energy. A closed-form solution is provided for unstable, stable, and neutral ambient conditions, assuming the temperature profile in the vertical direction is linear. The model has been used mainly for interpretative purposes and to provide physical insight. A complete discussion of that model and a brief description of the PANACH and MYKES Models appears in Ref. (12).

WALKÜRE (K. Nester, Kernforschungszentrum Karlsruhe) (13, 14)

This model has many similarities to the PANACH Model of EDF. It is steady-state and three-dimensional and follows a parabolic numerical approach; i.e., integration is carried out in steps in x starting from the vertical plane at the tower exit. Nester makes the bent-over plume assumption thereby eliminating the need for the horizontal momentum equation. In each subsequent x, plume variables in the y-z plane are computed. The model solves seven partial differential equations numerically by finite differences for calculation of the relevant plume variables. The following list shows the relation between the equations and the variables:

differential equations	variables
vorticity stream function	velocities perpendicular to the direction of transport

enthalpy	temperature
vapor and cloud water content (droplets without fall speed)	cloud water content water vapor content
rain water content (droplets with fall speed)	precipitation
turbulent kinetic energy rate of dissipation	turbulent diffusion coefficients

WALKÜRE employs the work of Kessler (23) on the physical processes of cumulus clouds to model the growth and evaporation of droplets and other thermodynamic processes in cooling tower plumes. The model was originally set up following the cooling tower model of Taft (24). Subsequent changes from that theory have been in the area of the thermodynamics (mentioned above) and in the modeling of the eddy viscosities and eddy diffusivities. In this latter area, the empirical expressions employed in the early development of WALKÜRE have been replaced by the k, ε model of Spalding. The WALKÜRE model can treat multiple towers and does yield realistic-looking cross-sectional predictions of velocity, temperature, and concentration. Disadvantages to the model include (1) its inability to treat the initial plume bending correctly with the parabolic approach . . . the parabolic method also cannot account for effects caused by recirculative eddies in the downwind direction. It cannot therefore treat tower downwash effects from a fundamental point of view. (One-dimensional integral models cannot do so either unless empirically). Thus, it is questionable if the initial conditions at the first vertical plane will be accurate. (2) like PANACH and MYKES it is expensive to run due to the finite-difference techniques used. Computer runs for a complete site evaluation ($\sim$ 100 runs at least) would be very costly. Use of the k $\sim$ ε turbulence model adds two more differential equations to solve and additional expense. Limited validation (14) to field data at Meppen, however, showed reasonable agreement of plume predictions with the predicted trajectory slightly lower than observed trajectories. Although the model provides more detail at each plume cross section than integral models, its advantages over the 1-D models are questionable. The model is yet to be validated with a wide range of plume data.

The model is set up to treat drift deposition as well but the model is costly to use since one new equation must be solved for each bin in the droplet size spectrum.

SMOKA (B. Rudolf; German Weather Service; Offenbach, Federal Republic of Germany) (5 - 7)

This is another 1-D integral model with many similarities to other models but with a few important differences. The model solves equations of conservation of mass,

vertical momentum, enthalpy, liquid water and total water. The bent-over plume assumption is made and circular plume cross sections are assumed. Entrainment is assumed to be composed of two terms: one resulting from self-induced turbulence and the other from ambient turbulence. Both terms are assumed operational from the tower exit downwind; of course, the jet-induced turbulence term becomes less important as downwind distance increases and the ambient turbulence term becomes relatively more important with downwind distance. The ambient turbulence term is defined locally from the ambient profiles through a Richardson number criterion. Several empirical constants defined from model calibration are included in the ambient turbulence formulation. The second significant feature of the model is the treatment of plumes from multiple towers. Details are not presently available on the precise methodology but we know that the merging of plumes is taken into account in the equations of continuity and vertical momentum. The model also treats downwash effects of buildings upwind of the towers for the larger wind speeds. The method is empirical and the formulation was fixed by model calibration to data at Neurath. The model is presently undergoing further improvement. At present, the model has been calibrated to 5 sets of data at Neurath. The model also employs a subroutine to predict tower exit conditions when not available for natural-draft cooling towers, wet/dry cooling towers, and natural-draft dry cooling towers. A sample run of the model is presented in Figure 4-9.

It should be noted that the SMOKA Model will eventually replace the use of the KUMULUS Model by the German Weather Service for environmental impact analyses for German power plants. The KUMULUS Model actually took the place of the simple TOWER Model (25, 26). The TOWER Model is based on the Weinstein-Davis (17) theory in the near field and a simple solution of the convective-diffusion equation for the diffusion phase. The model, however, did not compare favorably with other models in earlier European validation studies.

MODEL BY W. EGLER (Institute of Thermodynamics; University at Karlsruhe) (15, 16)

This model is also a 3-D finite difference simulation of cooling tower plumes following the parabolic approach. The model is not yet completed but some interesting computations have already been made. The model may perhaps be considered more as an interesting application of turbulence theory than a practical model for cooling-tower design or environmental assessment. The model assumes a bent-over plume with hydrostatic and Boussinesq approximations. It uses a second-order closure model following the Launder-Rodi approach which accounts for the effect of buoyancy in the

turbulence theory. The model solves the following differential equations at each step downwind

1. Vorticity transport equation
2. Poisson equation for the stream function

} solution for velocities v,w

3. Energy equation

4-6. Equations for the turbulence energies in the three space coordinates; i.e., three components of the Reynolds stresses, $\overline{u_1'^2}$, $\overline{u_2'^2}$, $\overline{u_3'^2}$

7. Equation for the energy dissipation rate, ε

8. Covariance of the enthalpy, $\overline{h'^2}$

9. Covariance of the water content fluctuations, $\overline{y'^2}$

Plume thermodynamics is accounted for in the energy and enthalpy covariance equations. Total liquid water is treated but is not broken down into cloudwater and hydrometeor components.

Computations with the model have been undertaken with a 25 x 25 grid normal to the wind where steps along this wind direction are taken. One sample calculation required 1/2 hour on the UNIVAC 1108. Disadvantages of the model involve (a) the problem of defining correct boundary conditions at the initial plane of integration, (b) the difficulty in treating low wind cases with the parabolic method since no convergence occurs and unstable solutions result as downwind integration is attempted, and (c) the incapability of the model to treat tower downwash conditions since circulations in the x-direction cannot be treated by parabolic models. The model will be Walter Egler's Ph.D. Thesis under the supervision of Prof. G. Ernst. A sample result of the model in its present form is given in Figures 4-7 and 4-8.

REFERENCES

1. Motor Columbus Consulting Engineers and the Environmental Systems Corporation. The KUMULUS Model for Plume and Drift Deposition Calculations for Indian Point No. 2. Knoxville, Tennessee. October 1977.

2. P. Brog and N. Bhargava. Special Problems in the Simulation of the Plume of Hybrid Cooling Towers: IN: Wet Cooling Towers: Thermal Principles and Measurements. VDI Report 298. VDI - Verlag GmbH. Seminar held in Dusseldorf. Ed. H. Rögener. pp. 132-141. May 25, 1977.

3. F. Gassmann, D. Haschke, and W. Solfrain. Measurements on Cooling Tower Plumes (Part 1): Mathematical Simulation and Significance of the Measurements. EIR Report No. 295. Würenlingen, Switzerland. April 1976.

4. J. P. Trepp, F. Gassmann, and D. Haschke. Plume Spread Models of the Swiss Confederation Institute for Reactor Research; Comparison with Measurement Results. IN: Wet Cooling Towers: Thermal Principles and Measurements. VDI Report 298. VDI - Verleg GmbH. Seminar held in Dusseldorf. pp. 109-116. May 25, 1977.

5. Bruno Rudolf. Ein Numerisches Modell Zur Berechnung Der Wolkenbildung Über Einem Kühlturm. Meteorologisches Institut der Universität Bonn. 1974.

6. B. Rudolf and K. Fraedrich. Convection Above Cooling Towers. German Meteorological Service. Annalen der Meteorologie. Vol. 9. pp. 65-68. 1974.

7. Bruno Rudolf. Description of the Model SMOKA for Calculating Cooling Tower Emissions and Their Effects. German Meteorological Service. October 1978.

8. Piere Louis Viollet. Study of Jets in Transverse Currents and in Stratified Environments. Doctoral Dissentation. Curie University. Paris, France. February 1977.

9. L. Caudron. Study of Plumes from Cooling Towers (Calculations and Experimental Data). Report E 44/78.19. Electricité de France. Hydraulics Laboratory. Chatou France 1978. (in French).

10. Pierre Louis Viollet. The Structure of Buoyant Jets Emitted Vertically in Different Types of Environments. Electricité de France. Hydraulics Laboratory. Chatou, France. Presented at Von Karman Institute for Fluid Dynamics Lecture Series 1978. Pollutant Dispersal in the Environment. Brussels, Belgium. May 8-12, 1978.

11. L. Caudron and A. Darles. Schematic Study of Visible Plumes from Wet Natural-Draft Cooling Towers of 2 and 4 Towers of 900 MWe. Report E44/77.17. Electricité de France. Hydraulics Laboratory. Chatou, France. May 1977.

12. Pierre-Louis Viollet. Physical Structure and Numerical Modeling of Plumes from Cooling Towers. Report E 44/78.15. Electricité de France. National Hydraulics Laboratory. Chatou, France. April 1978.

13. K. Nester. WALKÜRE. Simulation der Wirbel struktur der Ablufströmung aus Kühltürmen mit einem Rechenprogramm. KFK 2249. Kernforschungszentrum Karlsruhe. February 1976.

14. K. Nester. Personal Communication. Kernforschungzentrum Karlsruhe. Karlsruhe, Federal Republic of Germany. August 1978.

15. W. Egler. Basic Concept of a Prediction Model for the Cooling Tower Plume. IN: International Advanced Course. Heat Disposal from Power Generation. International Center for Heat and Mass Transfer. Dubrovnik, Yugoslavia. pp. 1/28 - 16/28. August 23-28, 1976.

16. W. Egler and G. Ernst. Three-Dimensional Spread Model. IN: Wet Cooling Towers: Thermal Principles and Measurements. VDI Report 298. VDI - Verlag GmbH. Seminar held in Dusseldorf. Ed. H. Rögener. pp. 117-131. May 25, 1977.

17. A. I. Weinstein. Numberical Model of Cumulus Dynamics and Microphysics. Journal of Atmospheric Science. Vol. 27. 1970.

18. A. J. Policastro, W. E. Dunn, M. Breig, and J. Ziebarth. Evaluation of Mathematical Models for Salt-Drift Deposition from Natural-Draft Cooling Towers. Draft Report. Division of Environmental Impact Studies. Argonne National Laboratory. Argonne, Illinois. February 1979.

19. S. R. Hanna. Predicted and Observed Cooling Tower Plume Rise and Visible Plume Length at the John E. Amos Power Plant, Atmospheric Turbulence and Diffusion Laboratory. ATDL Contribution File No. 75/21. Oak Ridge, Tennessee. November 1975.

20. L. E. May, Orville, H. D., and J. H. Hirsch. Application of a Cloud Model to Cooling Tower Plumes and Clouds. Institute of Atmospheric Sciences, South Dakota School of Mines and Technology. Rapid City, South Dakota. 1975.

21. EG&G. Potential Environmental Modifications Produced by Large Evaporative Cooling Towers. Final Report. Contract No. 14-12-542. Federal Water Pollution Control Adm. Boulder, Colorado. 1970.

22. A. J. Chorin. The Numerical Solution of the Navier-Stokes Equations for an Incompressible Solution. Bulletin Amer. Math. Soc. Vol. 73. 1967.

23. E. Kessler. On the Distribution and Continuity of Water Substance in Atmospheric Circulations. Meteorological Monographs. Vol. 10. American Meteorological Society. Boston. 1969.

24. James Taft. Numerical Model for the Investigation of Moist Buoyant Cooling-Tower Plumes. IN: Cooling Tower Environment - 1974. Available as CONF - 740302 from NTIS. Springfield, Virginia. 1975.

25. W. Ott. Physical Numerical Model for Determination of the Meteorological Environmental Influence of Cooling Towers. Meteorologische Rundschau. Vol. 26. pp. 97-102. 1973.

26. P. Brog and W. Ott. Plume Propagation Calculations. IN: Studies on a Natural Draft Wet Cooling Tower. VDI Report. Vol. 15. No. 5. Ed. G. Ernst. pp. 69-77. July 1974.

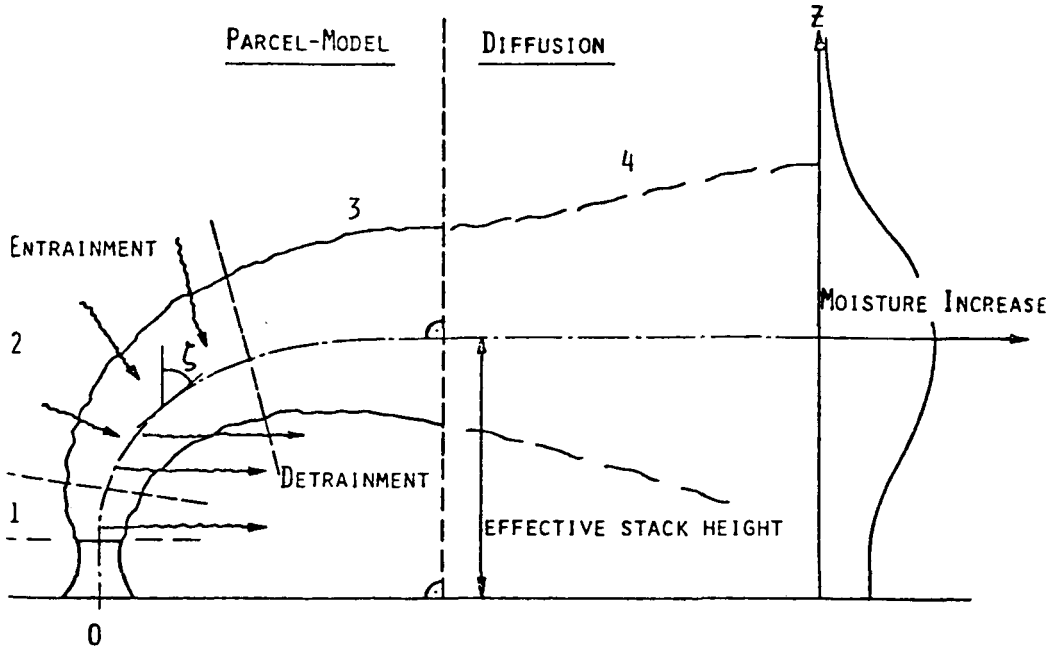

Regions		Parameter for	
No.	Name	Entrainment	Detrainment
1	vertical stage	α , δ	δ
2	bending over stage	α, γ, δ	δ
3	bent over stage	γ, δ	δ
4	pseudocloud stage	Diffusionsparameter	

Figure 4-1. Division of plume as modeled by FOG. [Source: From Gassmann, Haschke and Solfrain (3).]

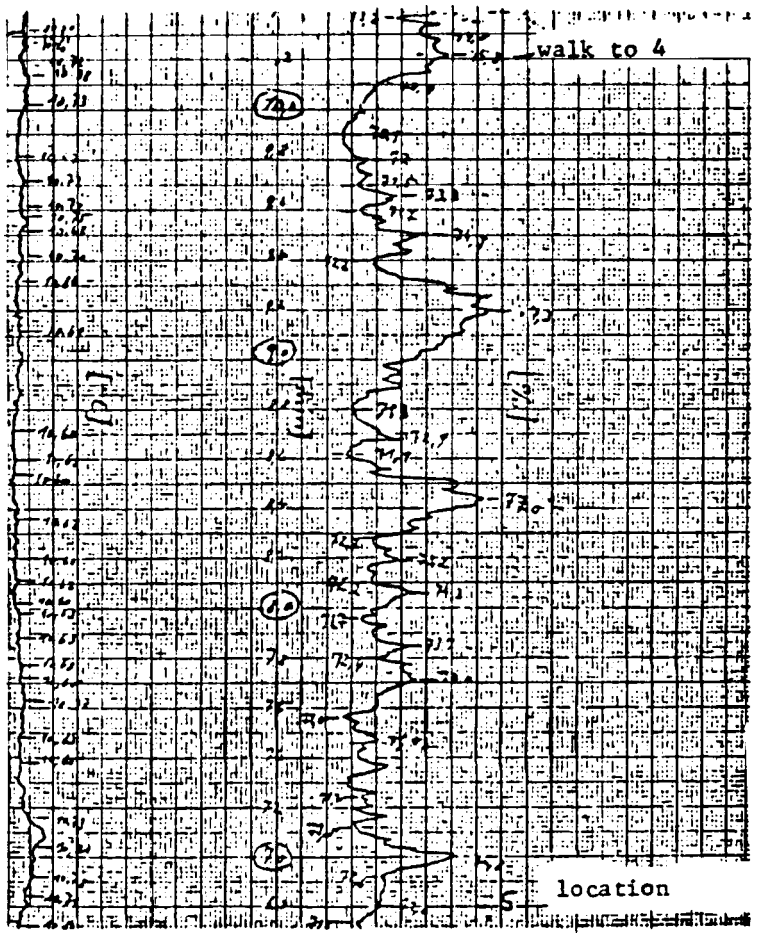

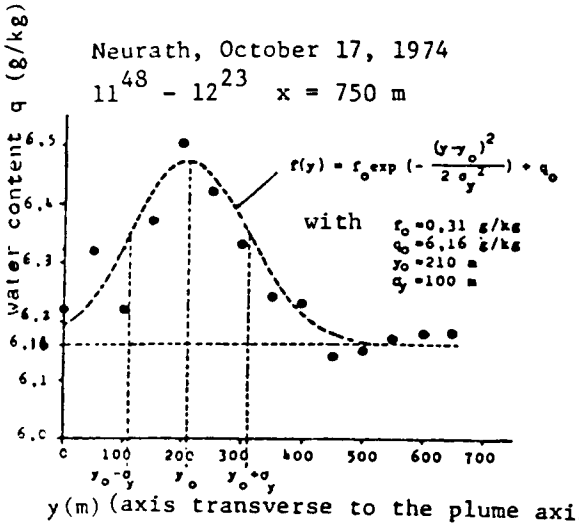

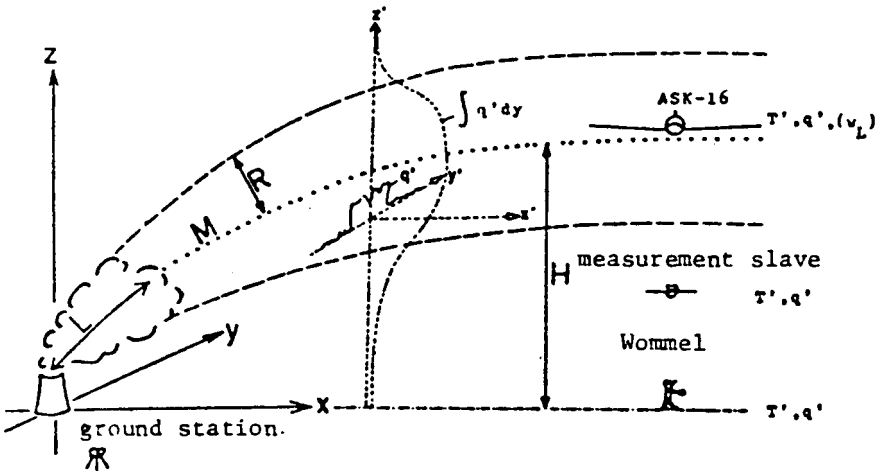

Figure 4-2. (a) Sample of measurements at one location on ground from ground sonde (left).
(b) Evaluation of ground sonde measurements (upper right).
(c) Measurement slave, and Wommel (lower right). [Source: From Trepp, Gassmann and Haschke (4).]

a) Rising computations

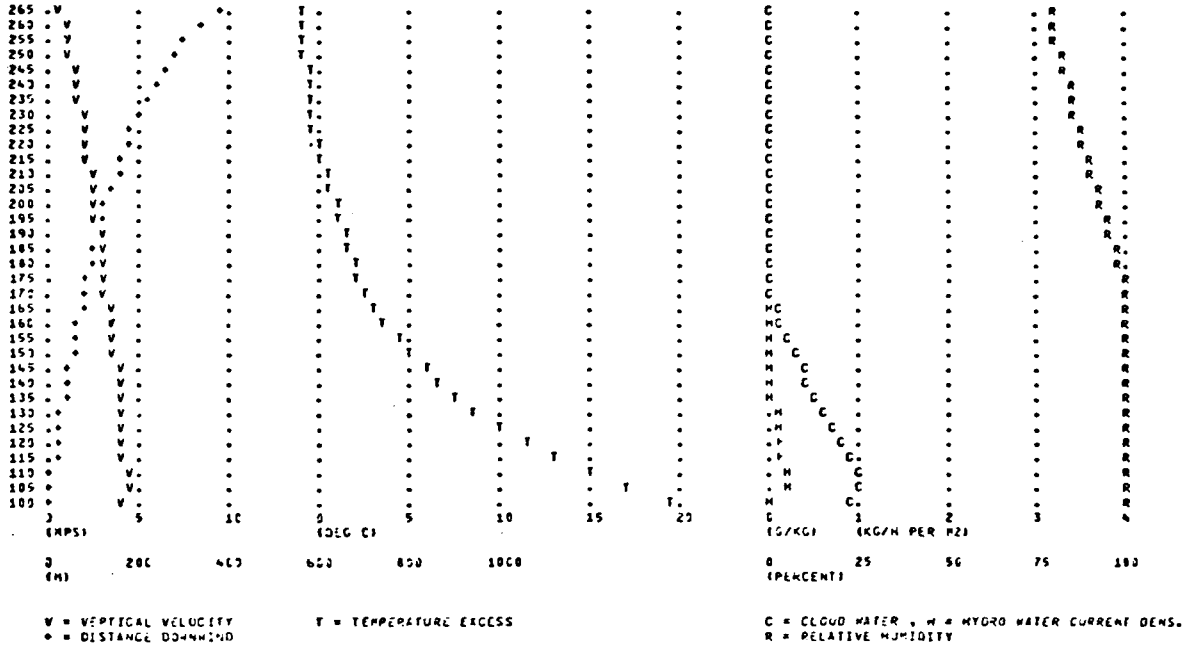

b) Humidity increases

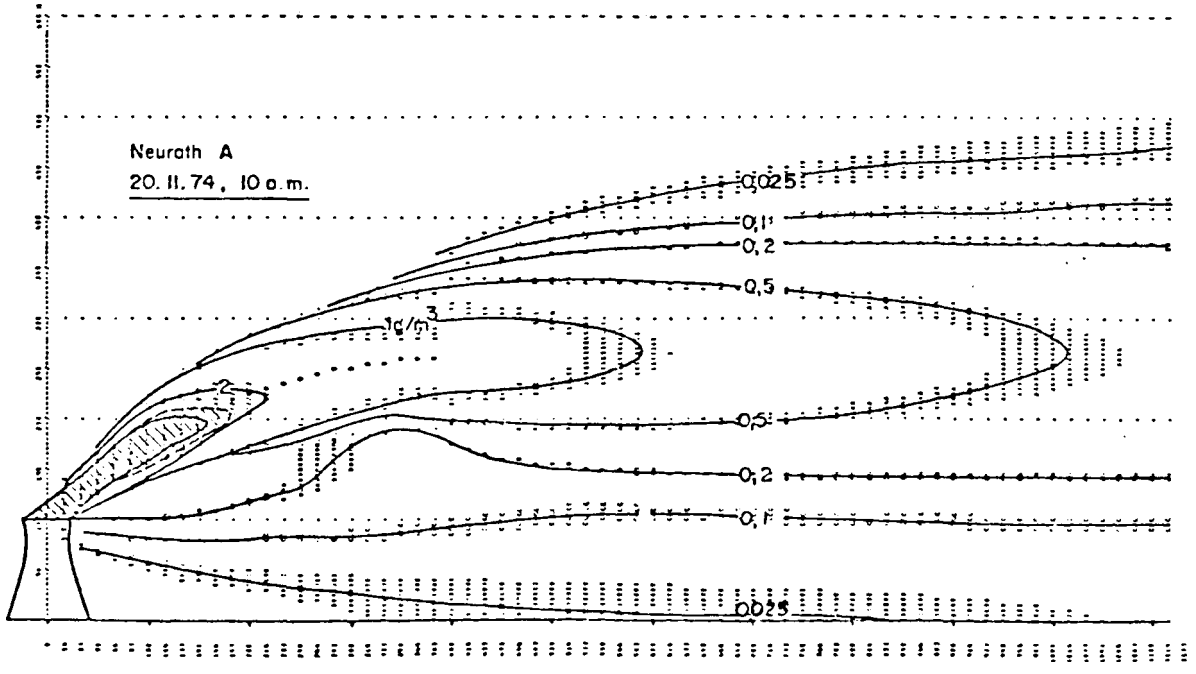

Figure 4-3. Computation of the plume of a single cooling tower of the Neurath Power Station on 11/20/74, 10 hrs. CET . . . FOG model. [Source: From Gasmann, Haschke and Solfrain (3).]

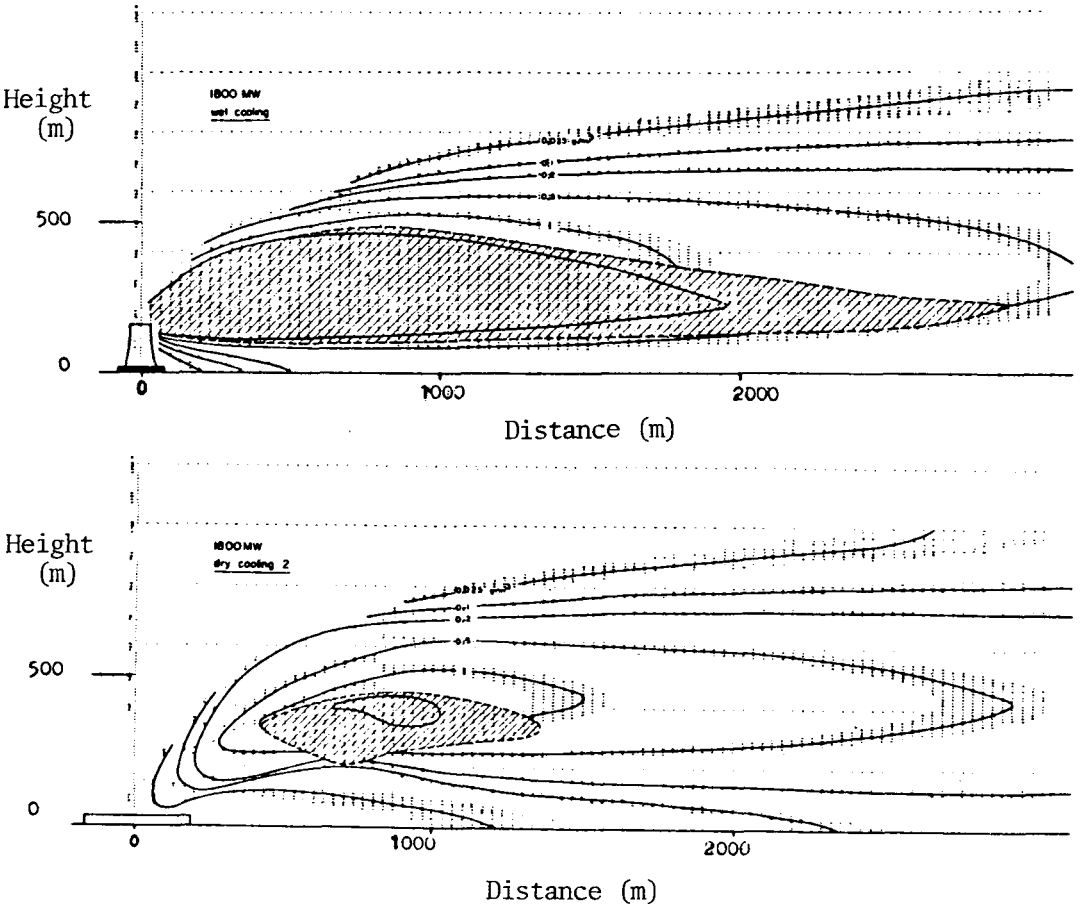

Figure 4-4. Calculation with the plume model FOG: comparison of a wet (top) with a dry cooling tower (bottom) of equal capacity (additional water content; visible plume, compact; visible plume shreds.) [Source: From Trepp, Gassmann and Haschke (4).]

Figure 4-5. Calculation with the plume model FOG: comparison with photographed plume (visible plume, compact; visible plume shreds). [Source: From Trepp, Gassmann and Haschke (4).]

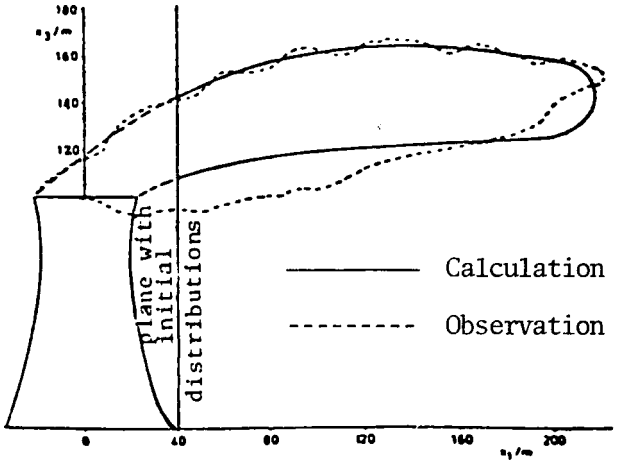

Figure 4-7. Calculated and observed outline of the visible plume in the vertical plane of symmetry. Block C, Neurath power station, September 28, 1973, 3:00 p.m. [Source: From Egler and Ernst (16).]

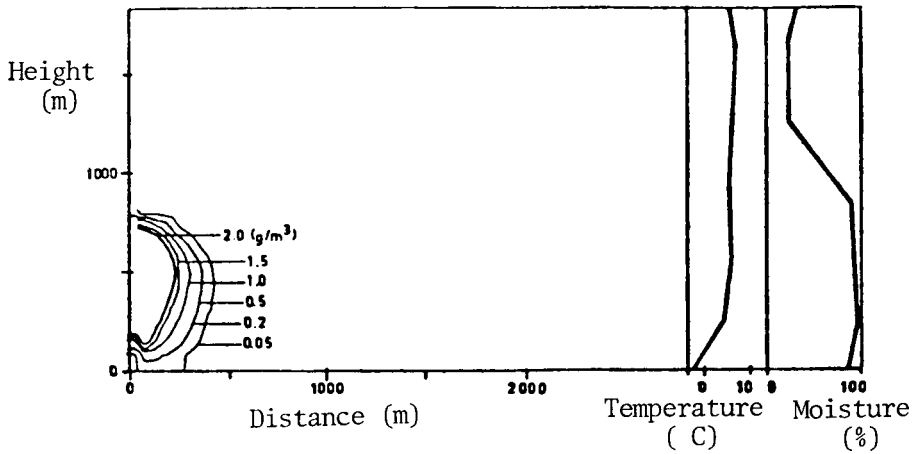

Figure 4-6. Calculations with the plume model PLUMEFF for a wet cooling tower (additional water content). [Source: From Trepp, Gassmann and Haschke (4).]

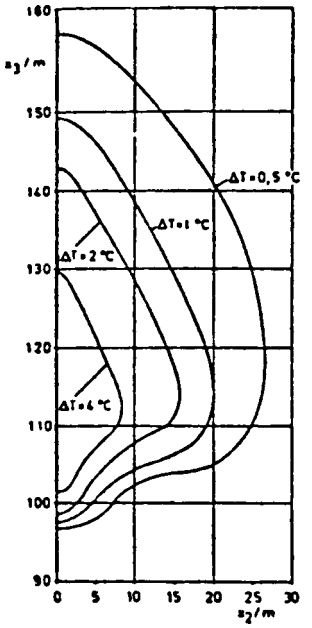

Figure 4-8. Excess temperature of the plume above the environmental temperature at the same height, 42 m downstream from the initial distributions for the right half of the plume. Block C Neurath power station, September 28, 1973, 3:00 p.m. [Source: From Egler and Ernst (16).]

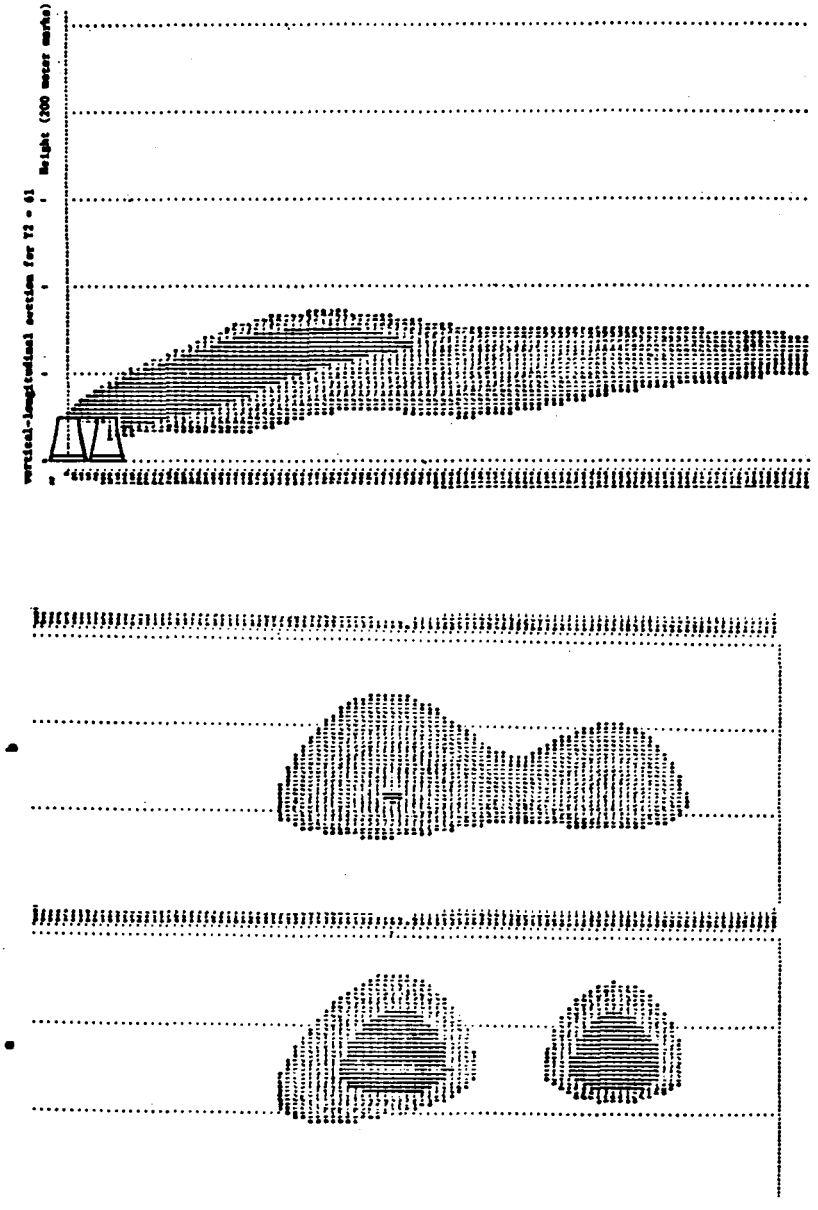

Figure 4-9. (a) Vertical-longitudinal section through the calculated SMOKA plumes from a cooling tower group. (b) Vertical cross-section through the calculated plumes of a cooling tower group . . . (a) before and (b) after merging. [Source: From Rudolf (7).]

Section 5

EVALUATION OF THE KUMULUS AND FOG MODELS FOR COOLING TOWER PLUME DISPERSION

This chapter presents an evaluation of the KUMULUS (1) and FOG (2) Models by means of model/data comparisons of those models to our visible-plume data from single and multiple towers. We chose those two models for evaluation for the following reasons. First, those models along with the PANACH/MYKES Model (3) of Electricité de France (EDF) are the most popular and commonly used models for cooling-tower plume prediction in Europe. Other models are either not appropriate for environmental-impact work because they are mainly research tools (e.g., WALKÜRE (4), Egler Model (5)) or the models are still under development (e.g., SMOKA (6)). We sought to include the EDF Model in our study here but EDF representatives declined. They would, in fact, prepare calculations for us for our test cases only if we had data for a plant larger in power output than the Amos Plant (2900 MWe) in West Virginia. Since data for towers with such a large heat output has never been acquired, we could not meet that condition. A second reason for our special interest in the FOG and KUMULUS Models is that the development of those models is by the integral approach which we also planned to employ (see Vol. 2). Both models also employ a consistent theory of development. Those theories provided additional ideas for evaluation.

This chapter presents model/data comparisons of those two models to the single-tower data of Lünen, Chalk Point, and Paradise, and multiple-tower data of Neurath and Amos. Information on these data is given in Vol. 2. The KUMULUS Model predictions were carried out by Dr. Pierre Brog and Mr. Michael von Euw of Motor Columbus Consulting Engineers of Baden, Switzerland. The KUMULUS Model is proprietary to Motor Columbus; details on the model formulation are available from Ref. (1) but the computer code and empirical constants are not available. We provided them with tower exit and ambient conditions and they provided us with a listing of the computer output including a line-printer plot of the visible plume. We employed an electronic digitizer to extract the plume outline from the output to a form suitable for plotting. It should be noted that Motor Columbus made computations with their model at two different times. Early in 1978, they provided us predictions for all our single-tower cases. Summary plots of visible-plume rise and visible-plume length revealed that the KUMULUS Model predicted visible plume length quite well but consistently overestimated visible plume rise. Overall performance of the model

was only fair-to-good. At their request, we provided them with the observed visible-plume outlines so that they could recalibrate their model. In late 1978, a new set of model predictions for single- and multiple-tower plumes was sent to us computed from the recalibrated KUMULUS Model. We present predictions with the recalibrated KUMULUS Model along with summary plots of both the original and recalibrated versions.

FOG Model predictions have been made by ANL with the FOG computer code which has been provided to us by Drs. F. Gassmann and J. P. Trepp of the Swiss Reactor Institute. Visible-plume predictions were also presented in the computer output in terms of line-printer plots which we digitized for our plotting purposes. Computer calculations were made employing recommendations on parameters presented in the FOG user's manual and with additional clarifications made in telephone conversations with Drs. Gassmann and Trepp.

Figures 5-1 through 5-24 present the KUMULUS and FOG model/data comparisons for the single-tower data of Lünen, Chalk Point, and Paradise. Figures 5-25 through 5-42 present the multiple-tower model/data comparisons for the Neurath and Amos sites. Figure 5-43 presents a comparison of the overall predicted versus observed visible-plume lengths and rises for the uncalibrated KUMULUS Model made early in 1978 for single-tower cases. The tendency to overpredict visible plume rise is consistent. Figure 5-44 presents the same comparison but with the recalibrated version of the model. Improvement is dramatic and the overall comparison is, indeed, quite good. Close examination of individual figures and the summary graph of Figure 5-44 reveals that the model plumes have a slight tendency to be low and long. For short observed plumes (plumes less than about 500 m), the model predictions tend to be shorter than the observed data. For long observed plumes, the model tends to predict longer plumes. These long predicted plumes occur generally under high humidity conditions. Also noticeable in the graphs is the tendency of the KUMULUS Model to predict the reappearance of the plume after it has disappeared earlier. A summary of the multiple-tower length and rise predictions is given in Figure 5-45. The model's overall performance for multiple tower plume cases is not as good as single-tower predictions with multiple-tower plume predictions having a clear tendency to be low but balanced in length. The predicted plumes from the multiple tower probably do not merge as they should because they are too low. Although low, the predicted plumes are balanced in length. A few Amos cases were not able to be predicted by the model.

A summary of the FOG Model predictions compared to field data is given in Figures 5-46 and 5-47 for single tower and multiple tower cases, respectively. Clearly, the FOG Model predictions are not as accurate as the KUMULUS prediction; however, the FOG Model has not been calibrated to large quantities of field data that have been used in calibrating the KUMULUS Model. The consistency shown in the predictions indicates that a calibration of coefficients to our data should make significant improvements in the overall model performance. Overall, the model predictions for single tower cases show visible plumes that are generally short and low. In multiple-tower applications, the merging criterion is over-simplified: all sources are combined into one before plume calculations begin. An interesting feature of the plume predictions should be mentioned. As noted in a discussion of the model in Section 3, the model assumes the rising plume to be a source of detrainment. Sometimes this added moisture in the lee of the plume is enough to cause visibility in a short region downwind of the rising plume.

One of the FOG Model authors, F. Gassmann, had the following comments upon examination of the results of our model/data comparisons for the FOG Model:

1. his experience with the FOG Model indicated that it predicts plume rise with high accuracy. The fact that our model/data comparisons showed a consistent trend for the model to predict a low visible plume rise is due to the fact that predicted visible plume length was short in these cases,
2. model/data comparisons for visible plume length can sometimes be misleading because,
   - -- the visible length can change between 100 m and several kilometers in a few minutes, as time-lapse films show. That means that it is possible to have two very different photographs of plume lengths for the same sounding,
   - -- the measurement of humidity can be inaccurate. If a sounding gives for example a relative humidity of 90%, it could in reality as well be 95% or 85% and that difference can change calculation plume lengths by an order of magnitude. An example of an effect like that could be the situation of Fig. 5-24. Another difficult parameter is the wind speed. For the example in Fig. 5-33, (AMOS - Case 15), the vertical shape of the observed plume is the proof that there was almost no wind. Measured wind data, however, indicated a wind speed of 4.9 m/sec from ground to 900 m above ground.

We agree with Gassmann's comments but wish to add that

1. model/data comparisons to visible plume outlines to our complete set of 39 single tower and 26 multiple-tower cases usually provided an accurate picture of model performance for models previously tested. We were usually able to trace reasons for underprediction

or overprediction to specific model assumptions. In addition, the systematic behavior of a model to overdilute or underdilute was replicated when models were compared with single phase laboratory data. The underprediction of visible plume length and rise may be due to lack of an optimal calibration of entrainment coefficients.

2. there are indeed data sets among our 65 which raise questions about data accuracy (see Vol. 2). However, the behavior of a model with the entire data base has, in the past, revealed systematic trends that were valid based upon scrutiny of the plume theory used in the model. Errors in relative humidity of $\pm 5\%$ are important for the higher relative humidities ($\sim 90\%$) but less important for the lower ambient humidities. If indeed model errors are random, it would have been impossible for a deterministic theory to represent the visible plumes as well as the recalibrated KUMULUS Model has. We suspect that data errors do not allow us to predict visible plume length and rise better than a factor of 1.5-2.0 for 90% of our data cases. Clearly then, data errors are a factor but model/data comparisons with 65 data cases have provided a consistent test of a model.

A comparison of FOG and KUMULUS Model performance to American models (8 - 22) appears in Tables 5-1 and 5-2. The recalibrated KUMULUS Model's performance is on par with any of the U.S. Models. It should be remembered that the KUMULUS Model was calibrated to this data base; some American Models (Winiarski-Frick, Orville, Hanna, and Slawson (Closed Form)) were also calibrated to selected data as well. Further details on the American models appears in Ref. (23). Further testing of the KUMULUS Model appears in Vol. 2 of this report.

REFERENCES

1. Motor Columbus Consulting Engineers and the Environmental Systems Corporation. The KUMULUS Model for Plume and Drift Deposition Calculations for Indian Point No. 2. Knoxville, Tennessee. October 1977.

2. F. Gassmann, D. Haschke, and W. Solfrain. Measurements on Cooling Tower Plumes (Part 1): Mathematical Simulation and Significance of the Measurements. EIR Report No. 295. Würenlingen, Switzerland. April 1976.

3. Pierre-Louis Viollet. Study of Jets in Transverse Currents and in Stratified Environments. Doctoral Dissertation. Curie University. Paris, France. February 1977. (in French)

4. K. Nester. WALKÜRE. Simulation der Wirbel struktur der Abluftströmung aus Kühltürmen mit einem Rechenprogramm. KFK 2249. Kernforschungszentrum Karlsruhe. February 1976.

5. W. Egler and G. Ernst. Three-Dimensional Spread Model. IN: Wet Cooling Towers: Thermal Principles and Measurements. VDI Report 298. VDI - Verlag GmbH. Seminar held in Dusseldorf. Ed. H. Rögener. pp. 117-131 May 25, 1977.

6. Bruno Rudolf. Description of the Model SMOKA for Calculating Cooling Tower Emissions and Their Effects. German Meteorological Service. October 1978.

7. F. Rudin. Programs FOG1PLT and FOG2PLT for Plotting Cooling Tower Plumes Calculated by the FOG1 Program. Technical Report TM-ST-564. Wurlingen, Switzerland. October 1978.

8. P. M. Wigley and P. R. Slawson. The Effect of Atmospheric Conditions on the Length of Visible Cooling Tower Plumes. Atmospheric Environment. Vol. 9. 1975.

9. P. R. Slawson and J. H. Coleman. Natural-Draft Cooling-Tower Plume Behavior at Paradise Steam Plant. Waste Heat Management and Utilization Conference. Miami Beach. May 1977.

10. J. Weil. The Rise of Moist Buoyant Plumes. Journal of Applied Meteorology. 13. pp. 435-443. June 1974.

11. W. E. Frick. The Influence of Stratification on Plume Structure. Master's Thesis. Atmospheric Sciences Department. Orgeon State University. June 6, 1975.

12. L. Winiarski and W. Frick. Methods of Improving Plume Models. IN: Cooling Tower Environment -- 1978 Proceedings. A Symposium on Environmental Effects on Cooling Tower Emissions. May 2-4, 1978. Power Plant Siting Commission. Maryland Department of Natural Resources. Report PPSP-CPCTP-22. WRRC Special Report No. 9. May 1978.

13. L. Winiarski. Important Considerations in a Simple Numerical Plume Model. Second Conference on Waste Heat Management and Utilization. Miami Beach. May 1977.

14. M. E. LaVerne. Oak Ridge Fog and Drift Program (ORFAD) User's Manual. ORNL/TM-5021. 1976.

15. S. R. Hanna. Predicted and Observed Cooling Tower Plume Rise and Visible Plume Length at the John E. Amos Power Plant. Atmospheric Turbulence and Diffusion Laboratory. ATDL Contribution File No. 75/21. Oak Ridge, Tennessee. November 1975.

16. Y. J. Tsai and C. H. Huang. Evaluation of Varying Meteorological Parameters on Cooling-Tower Plume Behavior. Symposium on Atmospheric Diffusion and Air Pollution. AMS Publication. Boston, Massachusetts. pp. 408-411. 1972.

17. K. B. Batty. Sensitivity Tests with a Vapor Plume Model Applied to Cooling Tower Effluents. Master's Thesis. Department of Meteorology. Penn State University. November 1976.

18. J. L. Lee. A Numerical Simulation of Atmospheric Convection Caused by Heat Dissipation at Large Power Centers. American Meteorological Society. Third Symposium on Atmospheric Turbulence, Diffusion and Air Quality. October 26-29, 1976.

19. R. V. Calabrese, J. Halitsky, and K. Woodard. Prediction of Temperature and Moisture Distributions in Cooling Tower Plumes. Pickard-Lowe-Garrick Inc., Washington, D.C. 1974.

20. D. W. Stephen and W. J. Moroz. Plume Rise from Wet Cooling Towers in Strong Winds. Engineering Research Bulletin B-107. Center for Air Environment Studies. Penn State University, University Park, Pennsylvania. September 1972.

21. J. Saame. "An Analytical Investigation of the Formation and Dispersion of Fog Plumes from a Natural Draft Water Cooling Tower for Various Meteorological Conditions." Master's Thesis. Department of Mechanical Engineering. University of Pittsburgh. 1971.

22. L. E. May, H. D. Orville, J. H. Hirsch. Application of a Cloud Model to Cooling Tower Plumes and Clouds. Institute of Atmospheric Sciences, South Dakota School of Mines and Technology, Rapid City, South Dakota. 1975.

23. A. J. Policastro, R. A. Carhart, S. E. Ziemer, and K. Haake. Evaluation of Mathematical Models for Characterizing Plume Behavior from Cooling Towers. Vol. 1. Dispersion from Single and Multiple Source Natural Draft Cooling Towers. Division of Environmental Impact Studies. Argonne National Laboratory. U.S. Nuclear Regulatory Commission Report NUREG/CR-1581. June 1979.

Table 5-1.

Comparison of Performance Statistics of KUMULUS and FOG Models for 39 Sets of Single-Tower Visible Plume Data from Lünen, Chalk Point, and Paradise and 26 Sets of Multiple-Tower Visible Plume Data from Neurath and Amos.

Statistical Measure*	Visible Plume Rise			
	Single Tower		Multiple Tower	
	KUMULUS	FOG	KUMULUS	FOG
N_2	27	23	19	21
N_5	35	36	25	25
$\bar{\rho}$ log	1.50	1.65	1.64	1.43
$\bar{\rho}$ s.m.	0.95	0.85	0.83	1.23
$.2 \leq \rho_i \leq 1.0$	19	27	20	14
$1.0 \leq \rho_i \leq 5.0$	16	9	5	11

Statistical Measure*	Visible Plume Length			
	Single Tower		Multiple Tower	
	KUMULUS	FOG	KUMULUS	FOG
N_2	27	15	10	11
$N_{2.5}$	30	22	13	
N_5	33	32	23	17
$\bar{\rho}$ log	1.59	2.02	2.17	1.82
$\bar{\rho}$ s.m.	1.11	0.76	1.34	0.72
$.2 \leq \rho_i \leq 1.0$	20	25	13	15
$1.0 \leq \rho_i \leq 5.0$	13	7	10	2

* see Table 5-2 for definitions

Table 5-2.

Performance statistics for KUMULUS and FOG Models as compared to fifteen U.S. single-tower models for prediction of visible plume rise and visible plume length.

	Model	Range of ρ_i	N_2	N_5	N_F	$\bar{\rho}=\frac{1}{n}\sum\rho_i$	σ_1	$\rho_2 = 10^{1/n\sum\lvert\log \rho_i\rvert}$	σ_2
Visible Plume Rise	Slawson-Wigley	0.01-6.78	17	30	0	0.83	0.68	1.89	0.20
	Slawson (Closed Form)	0.01-7.38	20	32	0	0.96	0.71	1.77	0.18
	Weil	0.09-6.07	16	32	0	0.74	0.64	2.05	0.19
	Frick	0.07-3.83	16	37	0	0.61	0.59	2.19	0.20
	Winiarski-Frick	0.13-6.50	31	37	0	0.83	0.36	1.49	0.13
	Winiarski-Frick (1977)	0.10-4.79	24	37	0	0.70	0.71	1.86	0.15
	ORFAD	0.56-7.93	5	11	27	2.34	1.29	2.27	0.19
	Hanna	0.23-11.00	30	38	0	1.27	0.82	1.60	0.16
	Tsai-Huang (Stone & Webster Engr. Corp.)	0.01-10.57	24	32	0	0.92	0.49	1.52	0.14
	Lee-Batty	0.11-9.96	19	32	1	0.92	0.75	1.88	0.23
	Lee (NUS)	0.21-12.97	29	38	0	1.09	0.67	1.64	0.17
	Calabrese-Halitsky-Woodard (Pickard-Lowe-Garrick Inc.)	0.10-10.61	18	29	8	1.52	1.01	1.86	0.18
	Stephen-Moroz	0.23-20.52	24	35	0	1.44	0.97	1.68	0.19
	Saame	0.47-9.70	17	36	2	2.08	0.94	2.01	0.17
	Orville	0.44-34.87	23	35	0	1.74	1.20	1.78	0.20
	KUMULUS	0.03-2.60	27	35	1	0.95	0.49	1.50	0.14
	FOG	0.14-8.00	23	36	1	0.85	0.52	1.65	0.19

	Model	Range of ρ_i	N_2	$N_{2.5}$	N_5	N_F	$\bar{\rho}=\frac{1}{n}\sum\rho_i$	σ_1	$\rho_2 = 10^{1/n\sum\lvert\log \rho_i\rvert}$	σ_2
Visible Plume Length	Slawson-Wigley	0.00-6.50	7	11	24	0	0.72	0.77	2.33	0.19
	Slawson (Closed Form)	0.00-22.87	13	19	27	0	1.15	1.09	2.12	0.17
	Weil	0.01-24.27	5	7	19	0	0.52	0.54	2.85	0.19
	Frick	0.03-0.61	3	4	15	0	0.36	0.13	2.99	0.15
	Winiarski-Frick	0.08-2.39	23	27	33	0	0.79	0.49	1.77	0.15
	Winiarski-Frick (1977)	0.06-1.79	14	20	30	0	0.66	0.45	2.11	0.20
	ORFAD	0.32-16.18	0	0	2	17	2.49	2.17	3.79	0.09
	Hanna	0.19-2.90	21	23	27	11	1.21	0.71	1.57	0.15
	Tsai-Huang (Stone & Webster Engr. Corp.)	0.01-4.90	19	21	28	6	1.68	1.08	1.81	0.19
	Lee-Batty	0.00-3.93	8	14	24	2	0.85	0.90	2.27	0.15
	Lee(NUS)	0.00-0.94	5	7	21	2	0.41	0.22	2.76	0.20
	Calabrese-Halitsky-Woodard (Pickard-Lowe-Garrick Inc.)	0.04-541	13	19	27	8	1.27	0.95	1.90	0.17
	Stephen-Moroz	0.10-383	16	18	23	13	1.41	0.98	1.60	0.19
	Saame	0.09-24.35	11	19	28	2	0.75	0.81	2.21	0.15
	Orville	0.27-17.04	20	23	32	0	1.72	1.22	1.72	0.22
	KUMULUS	0.01-75.38	27	30	33	1	1.11	0.80	1.59	0.16
	FOG	0.08-12.93	15	22	32	1	0.76	0.76	2.02	0.17

Notes: ρ_i is defined as the ratio of predicted to observed (either length or height as indicated)
N_2 is the number of times the prediction is within a factor of 2, i.e., $0.5 < \rho_i < 2.0$
$N_{2.5}$ is the number of times the prediction is within a factor of 2.5, i.e., $0.4 < \rho_i < 2.5$
N_5 is the number of times the prediction is within a factor of 5, i.e., $0.2 < \rho_i < 5.0$
N_F is the number of failures of the model in 39 data sets
σ_1 is the standard deviation of the ρ_i distribution
σ_2 is the standard deviation of the $|\log \rho_i|$ distribution

Table 5-3.

Performance statistics for KUMULUS and FOG Models as compared to six U.S. multiple-tower models for predictions of visible plume rise and visible plume length.

	Model	Range of ρ_i	N_2	N_5	N_F	$\bar{\rho}$	σ_1	ρ_2	σ_2
Visible Plume Rise	Hanna	0.24-5.50	19	25	0	1.17	0.63	1.51	0.15
	Slawson-Wigley	0.12-3.27	13	20	0	0.98	0.71	1.71	0.16
	ORFAD	0.44-3.73	0	3	23	2.07	1.34	2.58	0.11
	Lee (NUS)	0.19-7.25	19	24	0	1.10	0.50	1.56	0.14
	ORVILLE	0.38-66.25	18	25	0	1.59	1.06	1.72	0.18
	Calabrese-Halitsky-Woodard (Pickard-Lowe-Garrick Inc.)	0.23-2.31	9	17	9	0.92	0.62	1.84	0.21
	KUMULUS	0.21-1.81	19	25	1	0.83	0.42	1.64	0.21
	FOG	0.23-5.00	21	25	1	1.23	0.88	1.43	0.18

	Model	Range of ρ_i	N_2	N_5	$N_{2.5}$	N_F	$\bar{\rho}$	σ_1	ρ_2	σ_2
Visible Plume Length	Hanna	0.08-3.03	9	11	9	13	1.05	0.69	1.54	0.18
	Slawson-Wigley	0.01-2.46	5	13	8	0	0.80	0.67	2.24	0.19
	ORFAD	14.42-39.46	0	0	0	23	0.0	0.0	1.0	0.0
	Lee (NUS)	0.0-1.20	2	7	2	6	0.48	0.39	2.89	0.27
	ORVILLE	0.02-21.83	11	18	14	1	0.93	0.67	1.84	0.19
	Calabrese-Halitsky-Woodard (Pickard-Lowe-Carrick Inc.)	0.03-1.06	7	10	7	9	0.69	0.29	1.67	0.23
	KUMULUS	0.03-4.61	10	23	13	1	1.34	1.20	2.17	0.20
	FOG	0.06-9.17	11	17	13	5	0.72	0.51	1.82	0.16

Notes: ρ_i is defined as the ratio of predicted to observed (either length or height as indicated)
N_2 is the number of times the prediction is within a factor of 2, i.e., $0.5 < \rho_i < 2.0$
$N_{2.5}$ is the number of times the prediction is within a factor of 2.5, i.e., $0.4 < \rho_i < 2.5$
N_5 is the number of times the prediction is within a factor of 5, i.e., $0.2 < \rho_i < 5.0$
N_F is the number of failures of the model in 26 data sets
σ_1 is the standard deviation of the ρ_i distribution
σ_1 is the standard deviation of the $|\log \rho_i|$ distribution

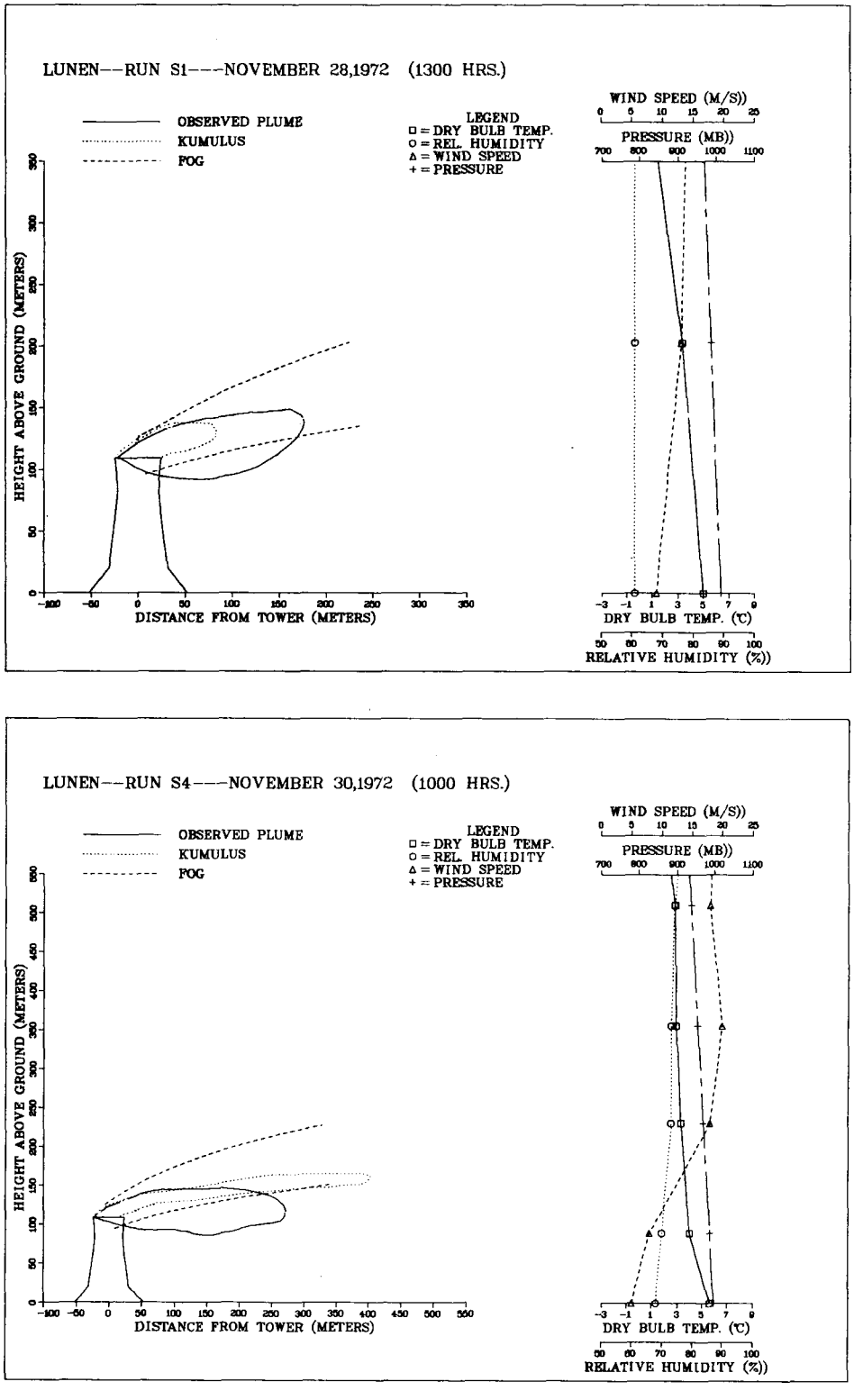

Figure 5-1. Comparison of predictions of KUMULUS and FOG models to observed visible-plume outlines at Lünen . . . cases S1 and S4.

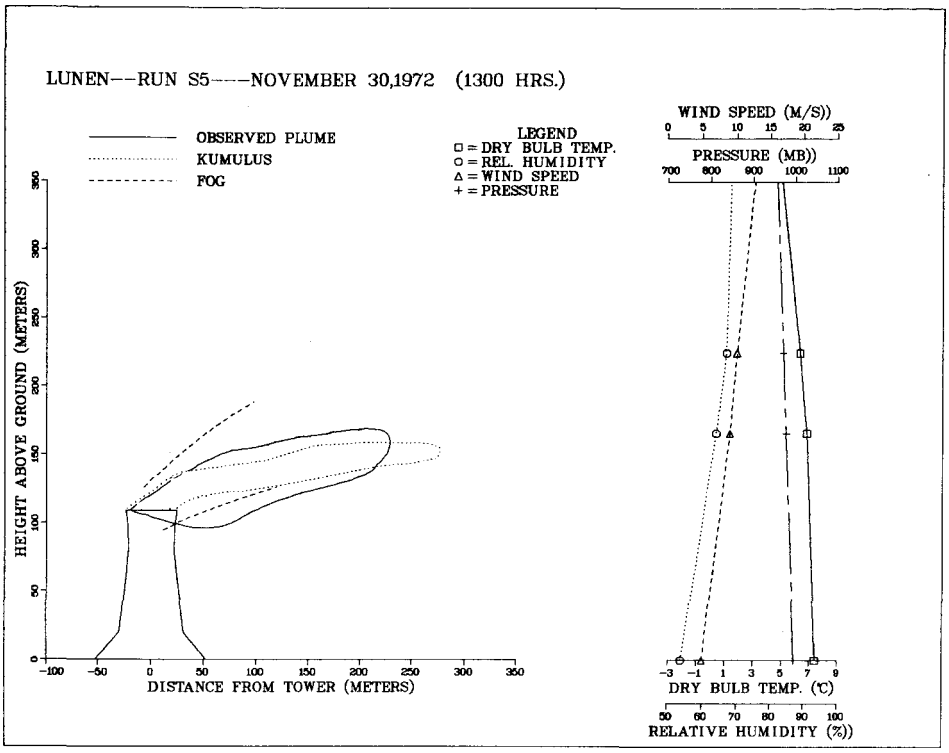

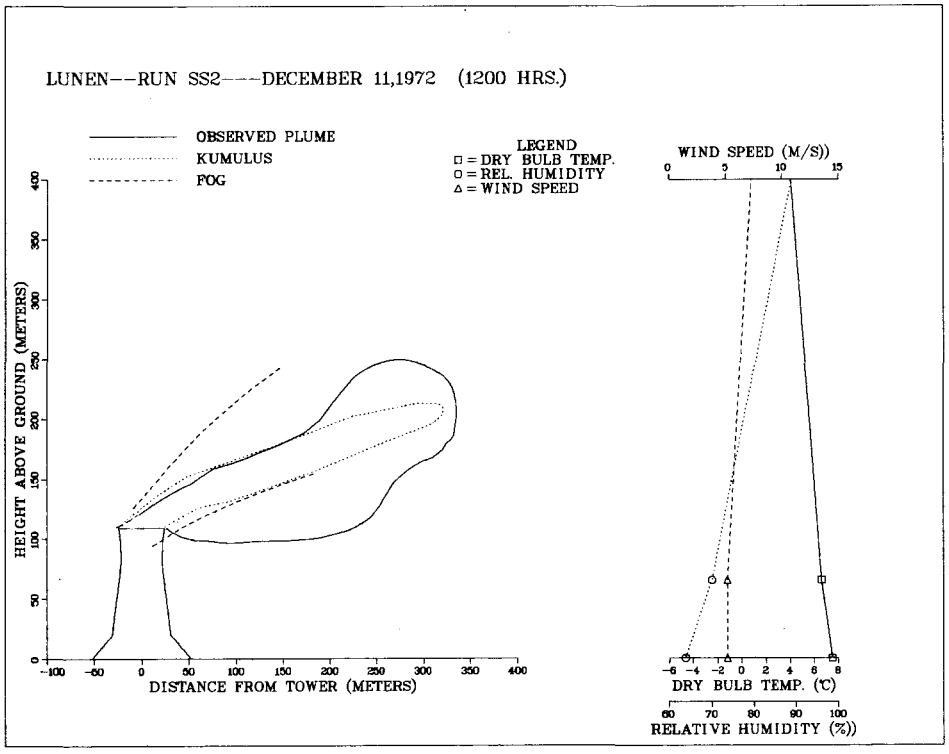

Figure 5-2. Comparison of predictions of KUMULUS and FOG models to observed visible-plume outlines at Lünen . . . cases S5 and SS2.

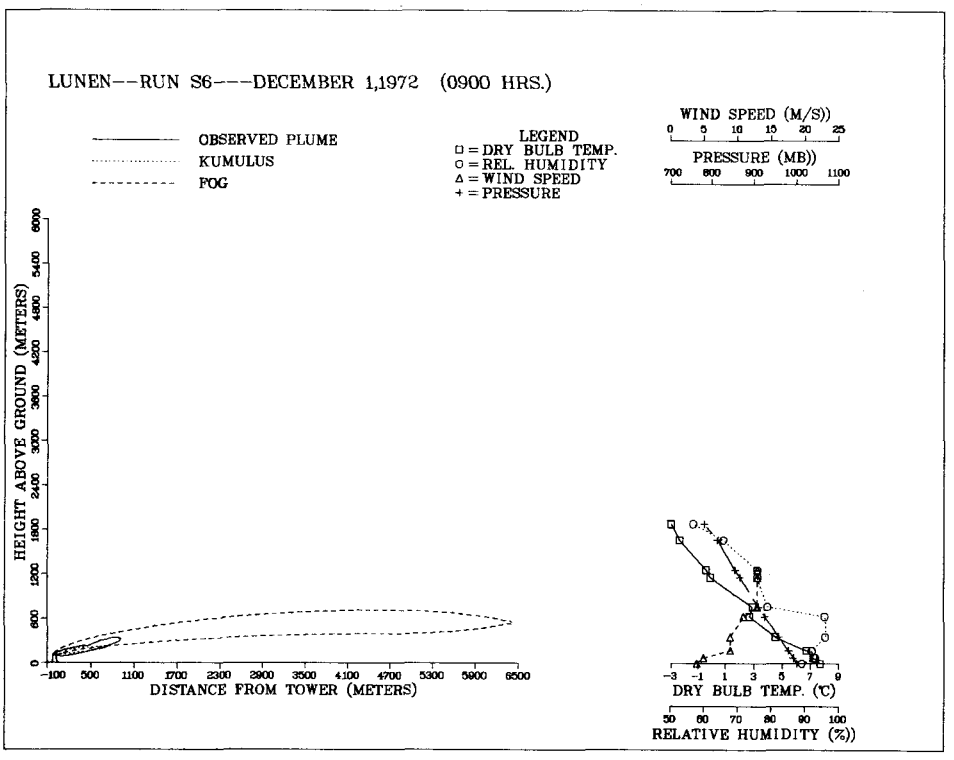

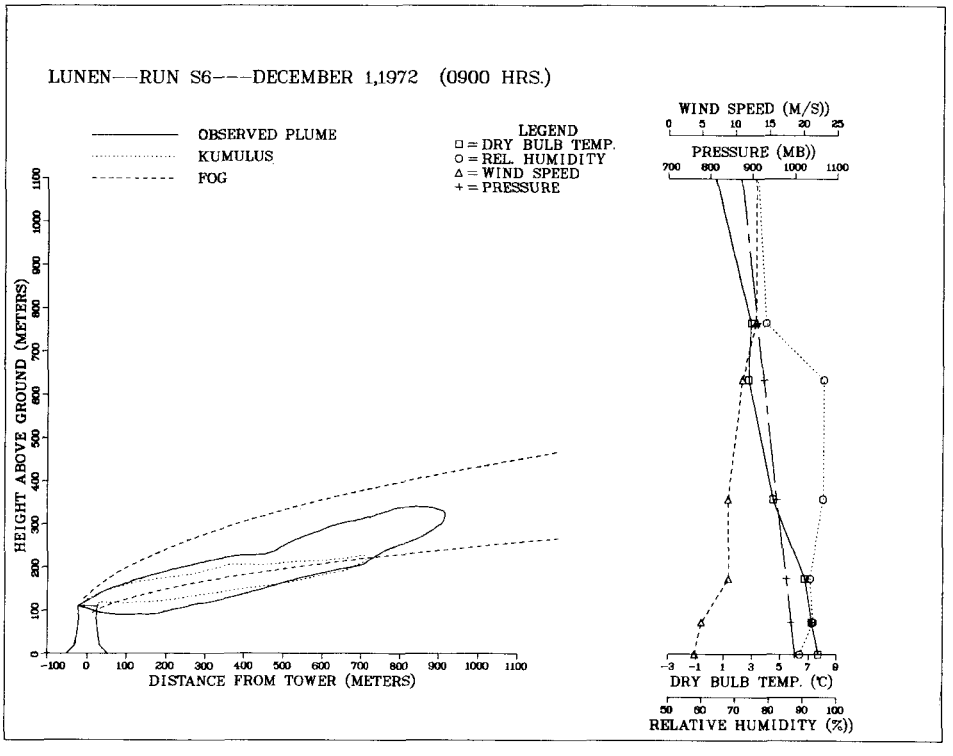

Figure 5-3. Comparison of predictions of KUMULUS and FOG models to observed visible-plume outlines at Lünen . . . case S6.

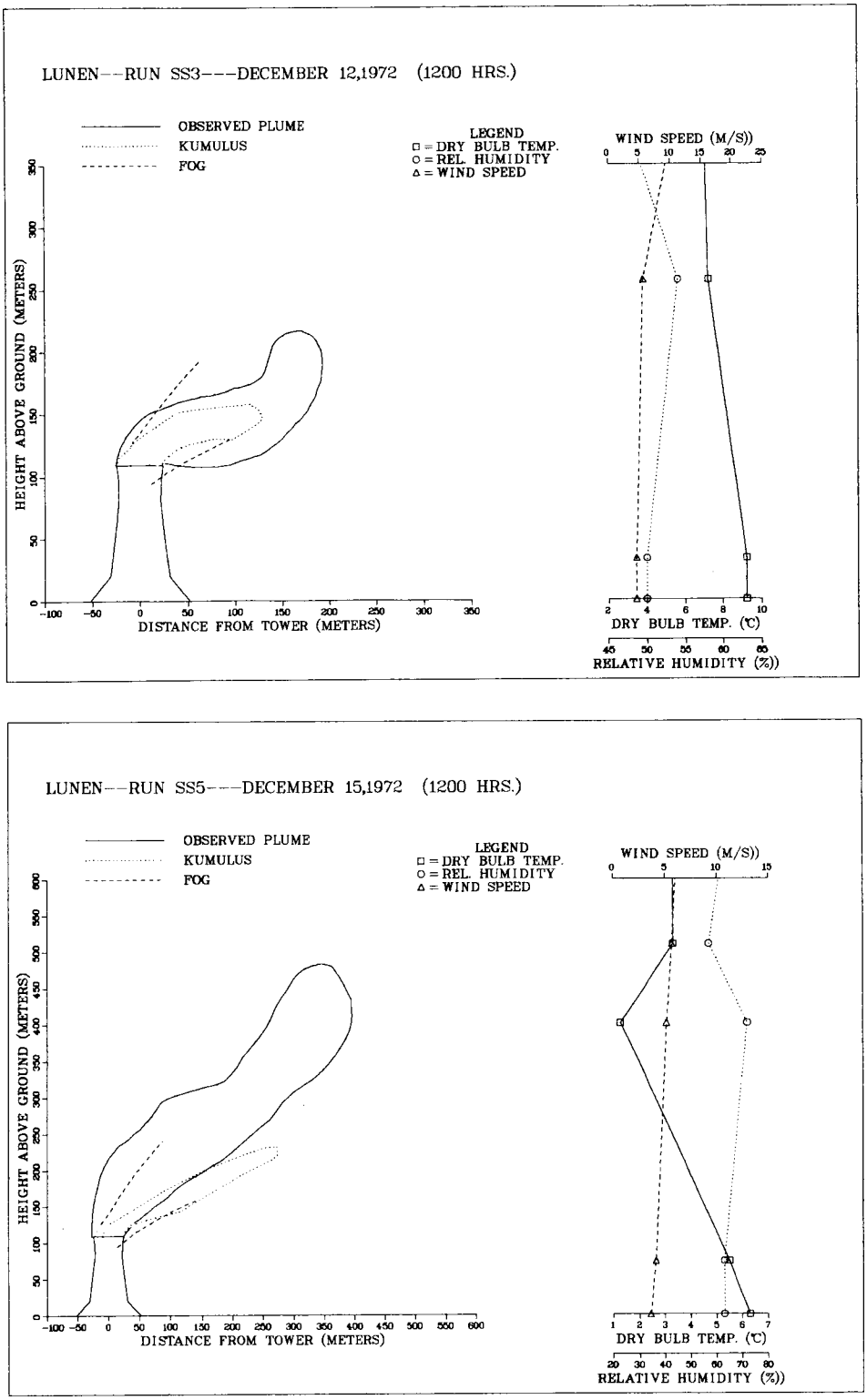

Figure 5-4. Comparison of predictions of KUMULUS and FOG models to observed visible-plume outlines at Lünen . . . cases SS3 and SS5.

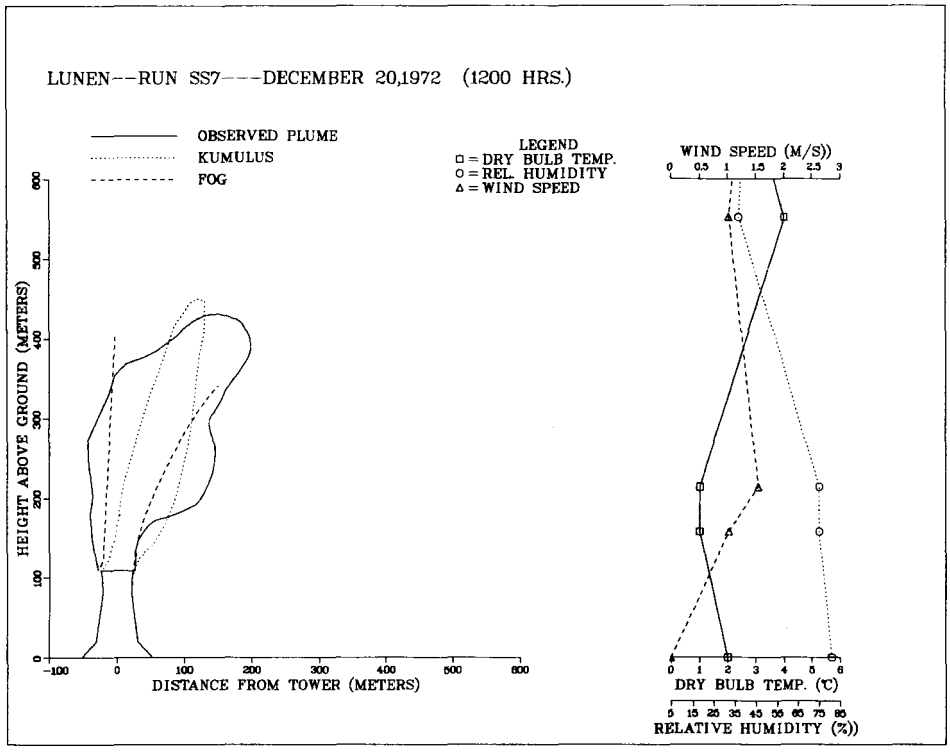

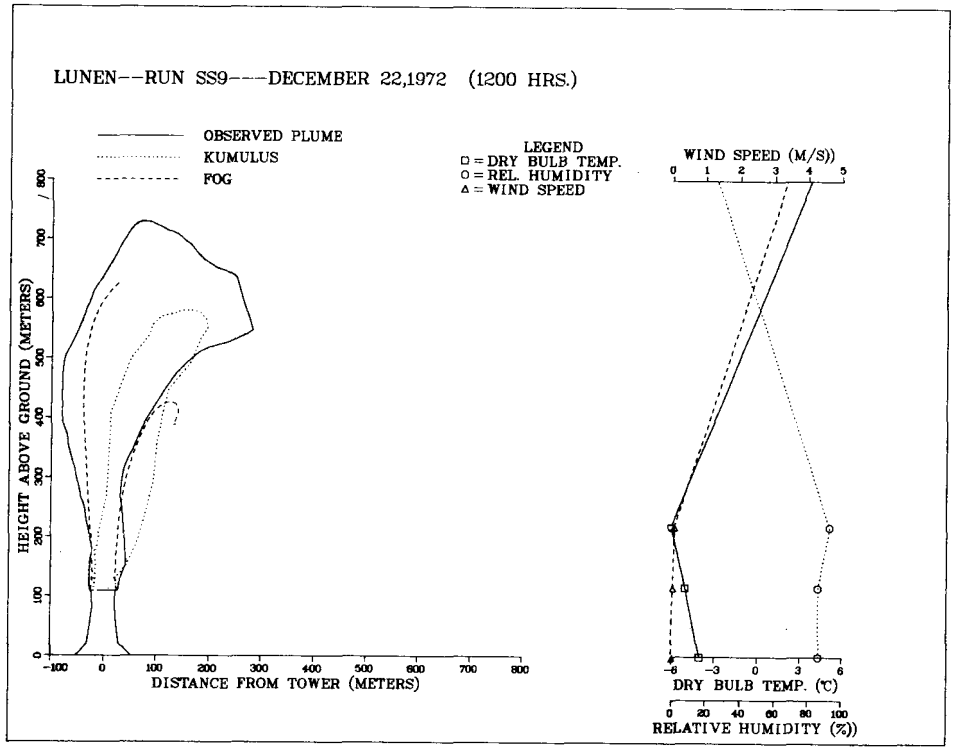

Figure 5-5. Comparison of predictions of KUMULUS and FOG models to observed visible-plume outlines at Lünen . . . cases SS7 and SS9.

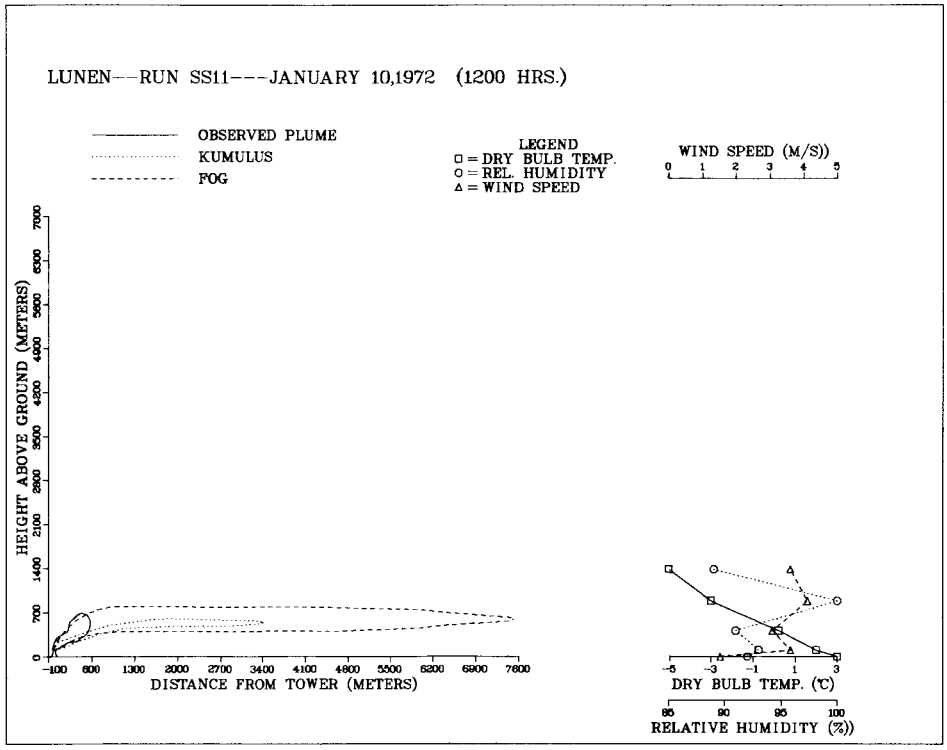

Figure 5-6. Comparison of predictions of KUMULUS and FOG models to observed visible-plume outline at Lünen . . . case SS11.

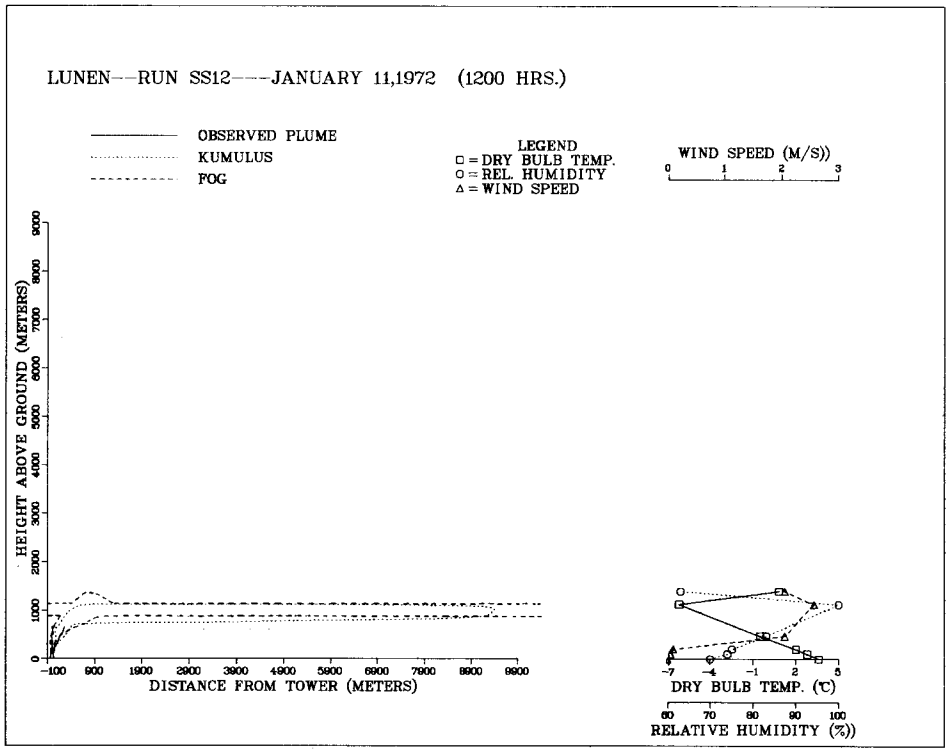

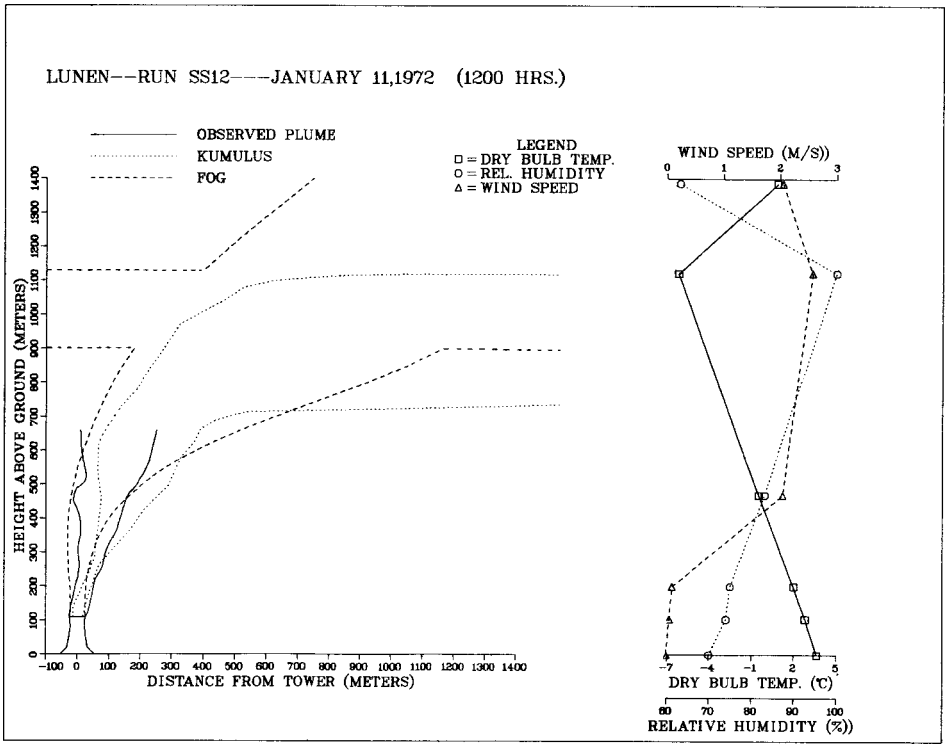

Figure 5-7. Comparison of predictions of KUMULUS and FOG models to observed visible-plume outlines at Lünen . . . case SS12.

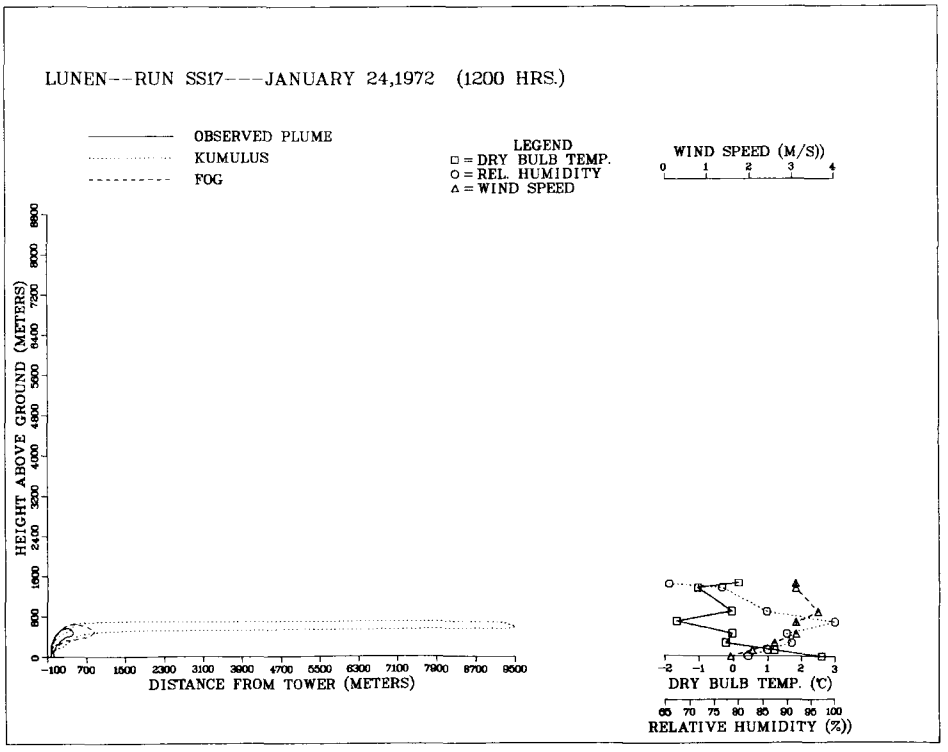

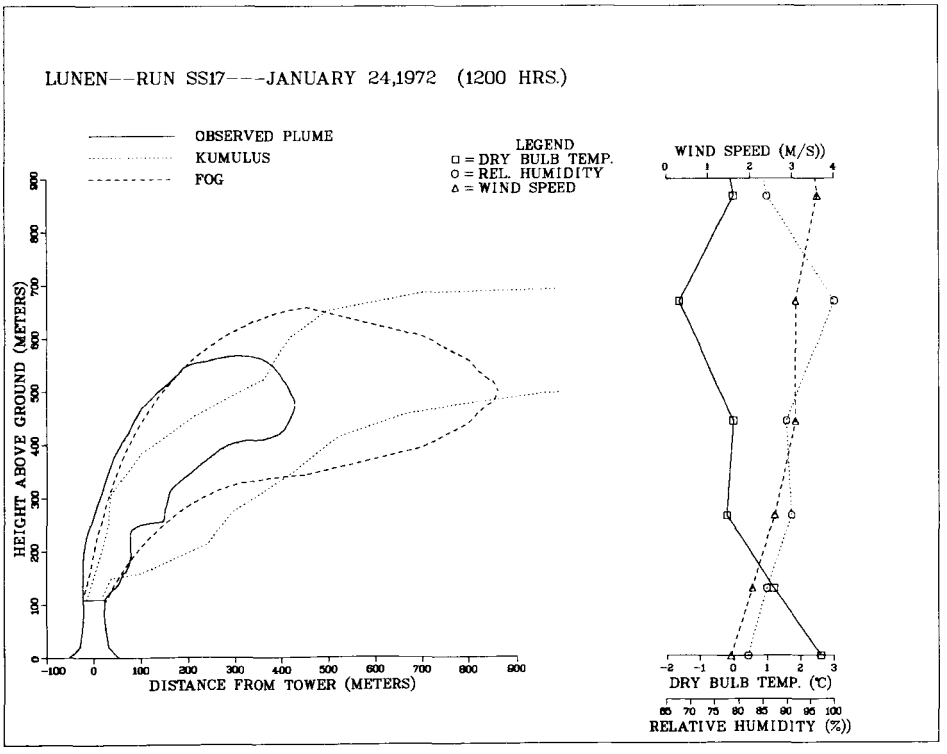

Figure 5-8. Comparison of predictions of KUMULUS and FOG models to observed visible-plume outlines at Lünen . . . case SS17.

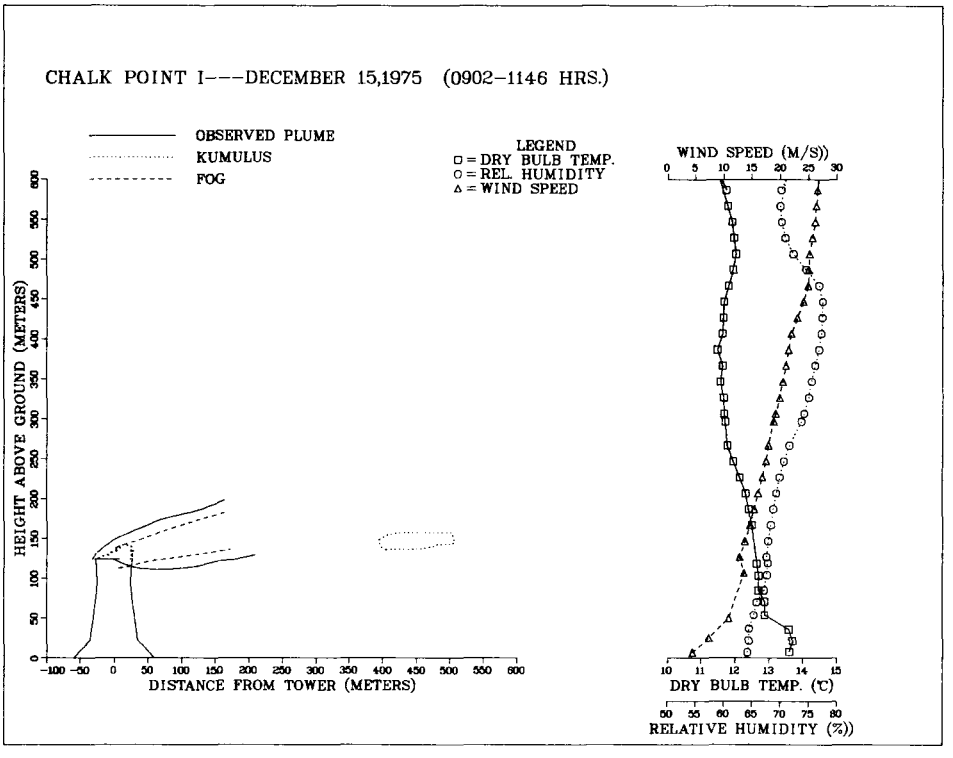

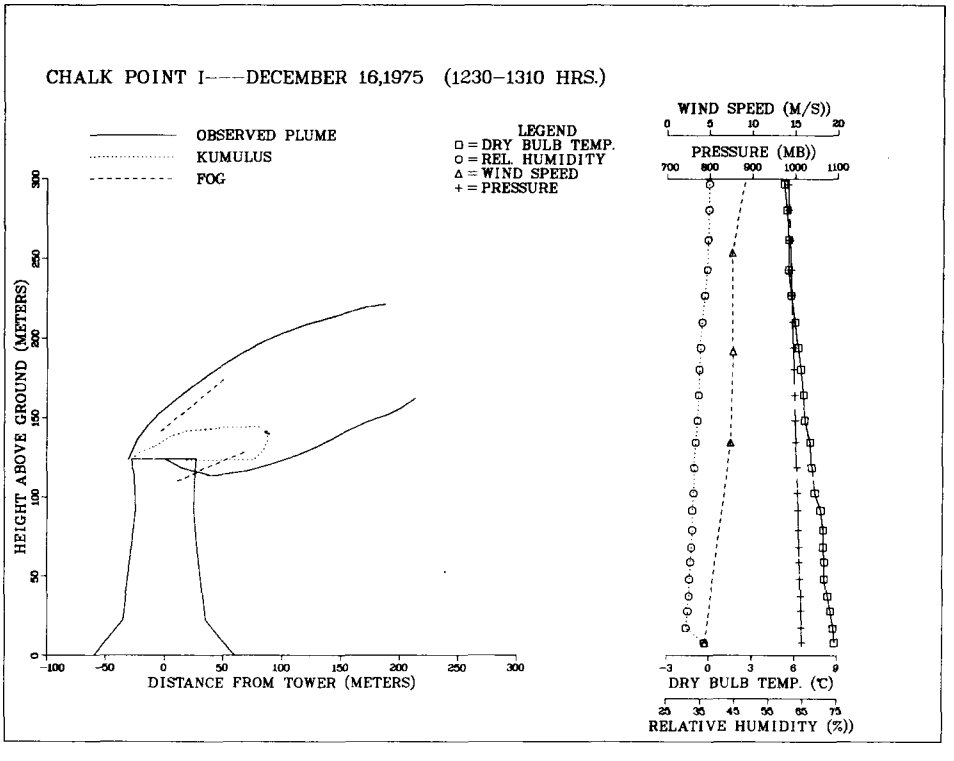

Figure 5-9. Comparison of predictions of KUMULUS and FOG models to observed visible-plume outlines at Chalk Point . . . cases CP1D15AV and CP1D16P1.

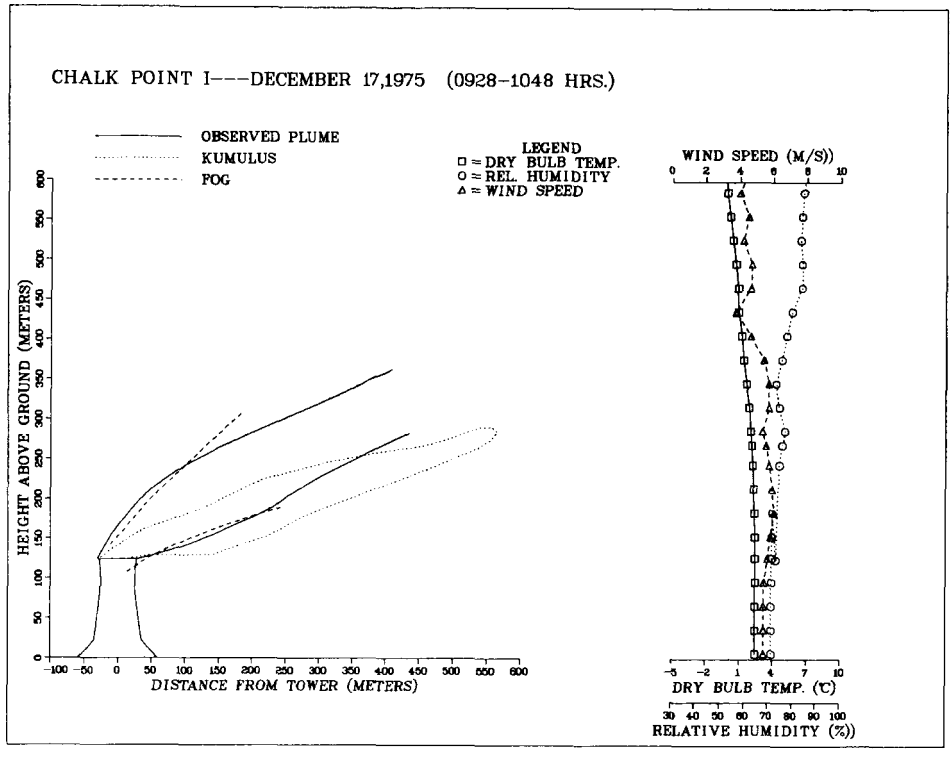

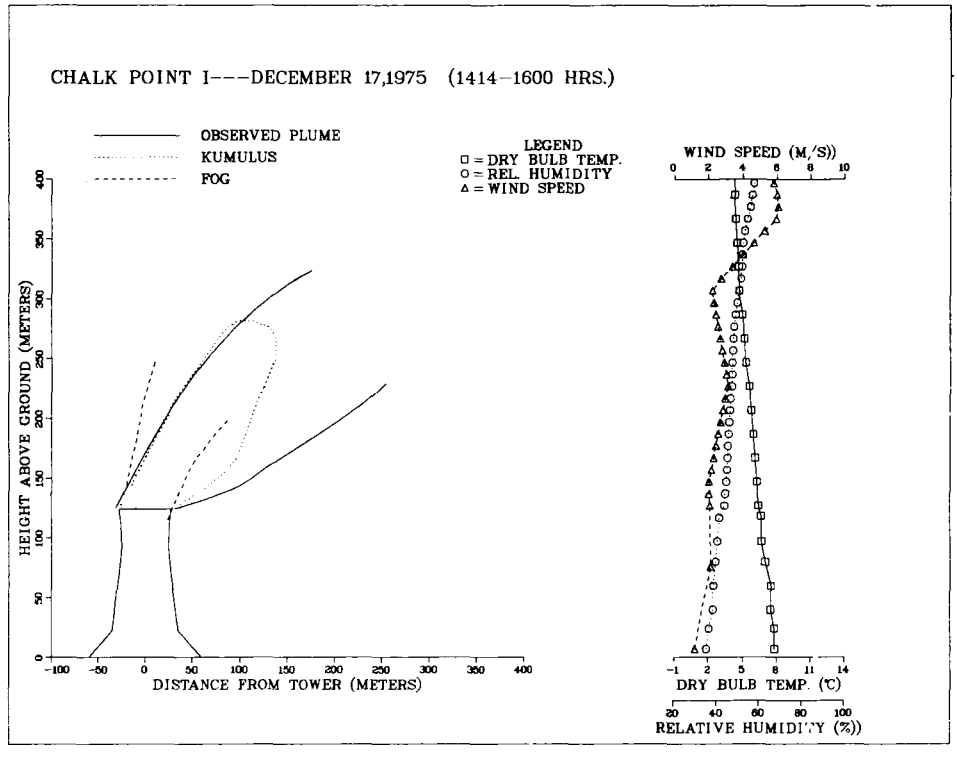

Figure 5-10. Comparison of predictions of KUMULUS and FOG models to observed visible-plume outlines at Chalk Point . . . cases CP1D17A1 and CP1D17A2.

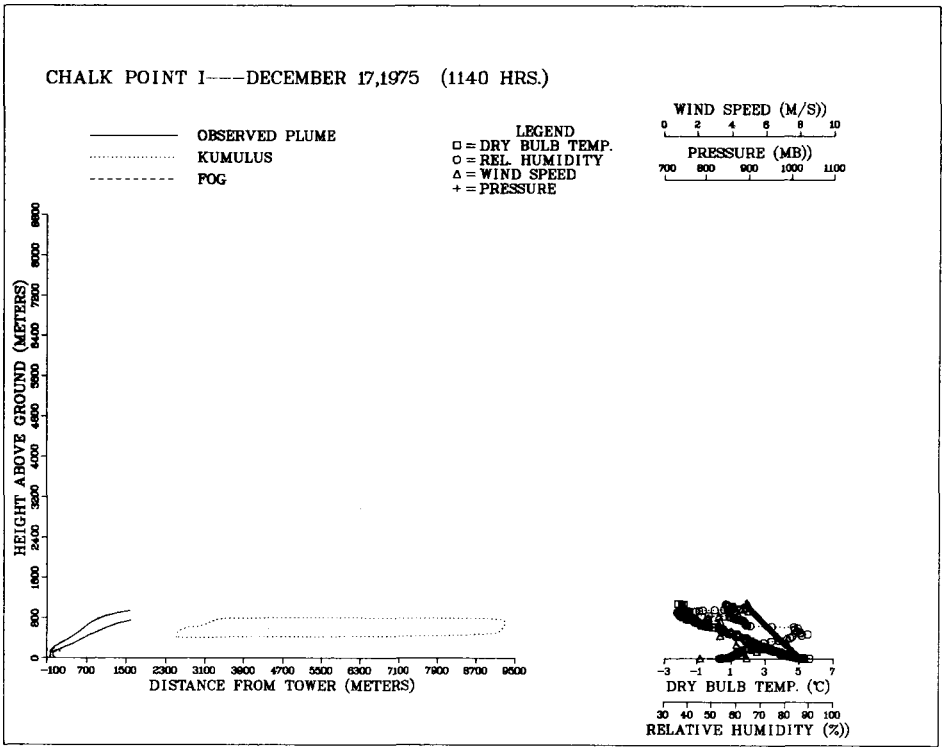

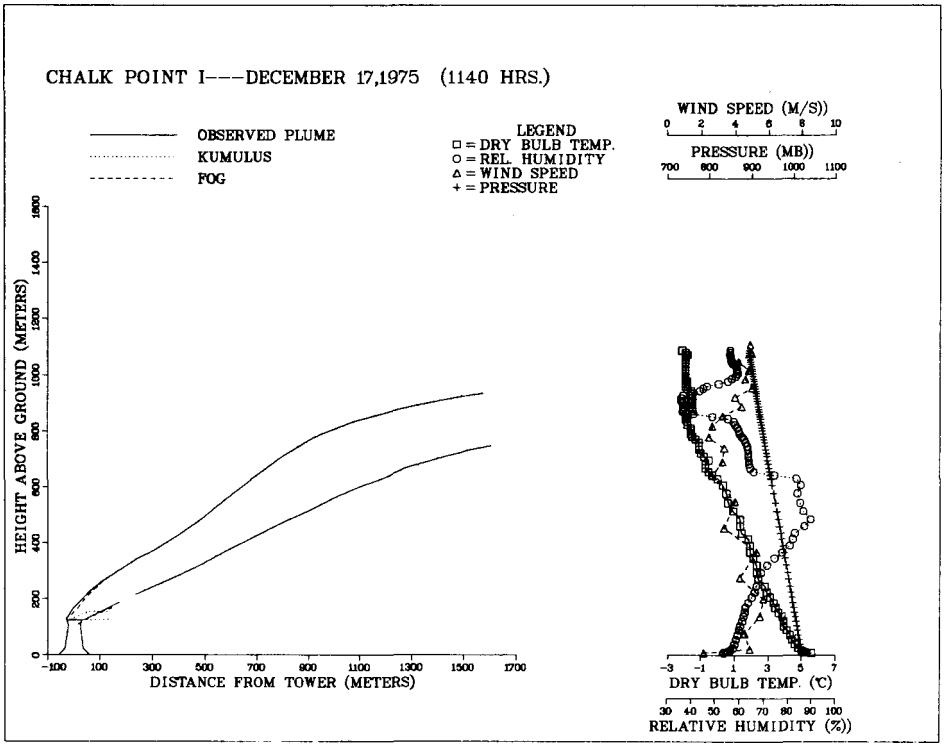

Figure 5-11. Comparison of predictions of KUMULUS and FOG models to observed visible-plume outlines at Chalk Point . . . case CP1D17P2.

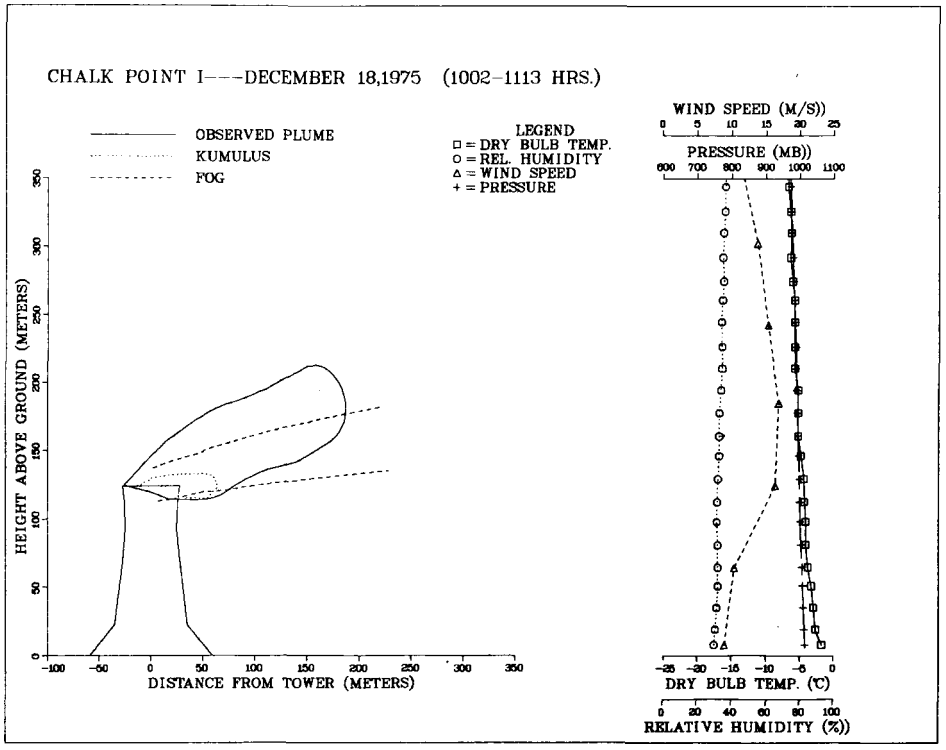

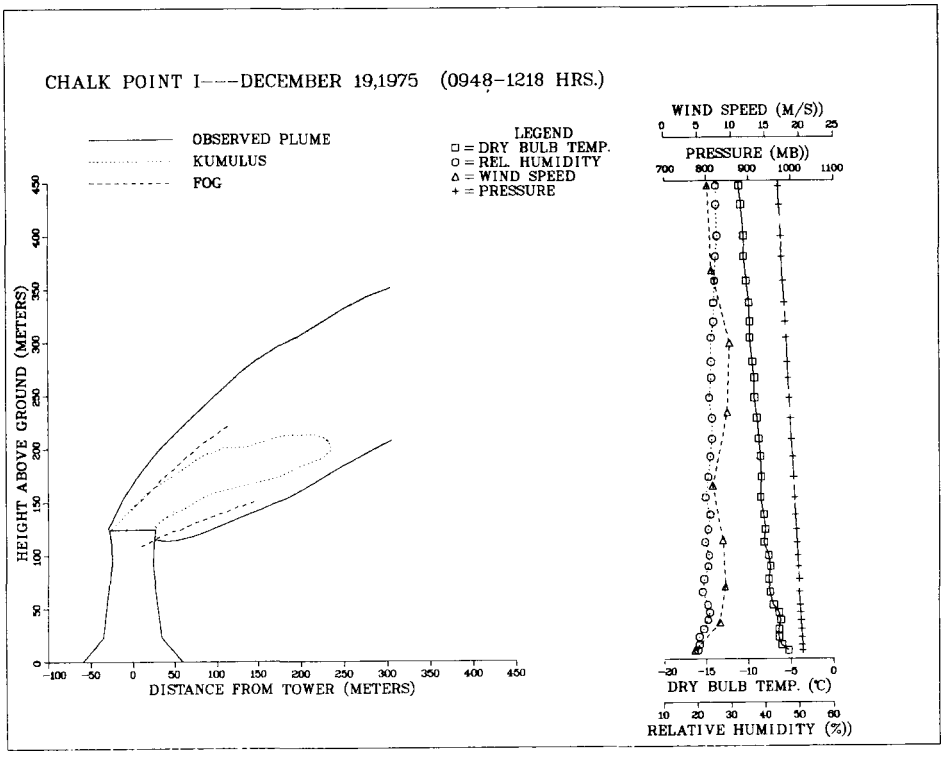

Figure 5-12. Comparison of predictions of KUMULUS and FOG models to observed visible-plume outlines at Chalk Point . . . cases CP1D18P1 and CP1D19P1.

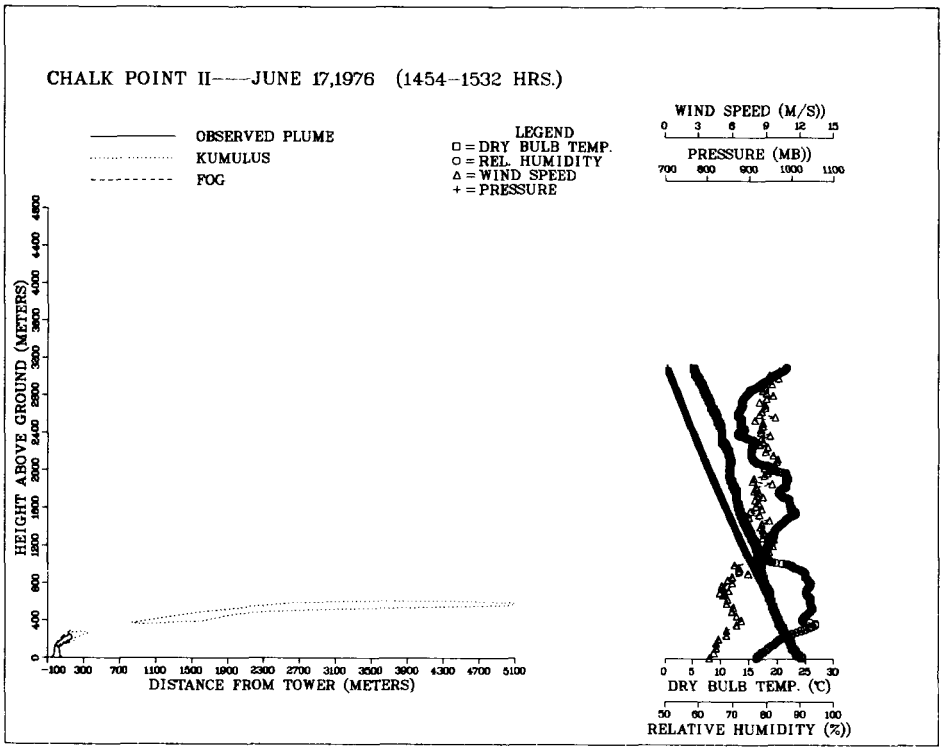

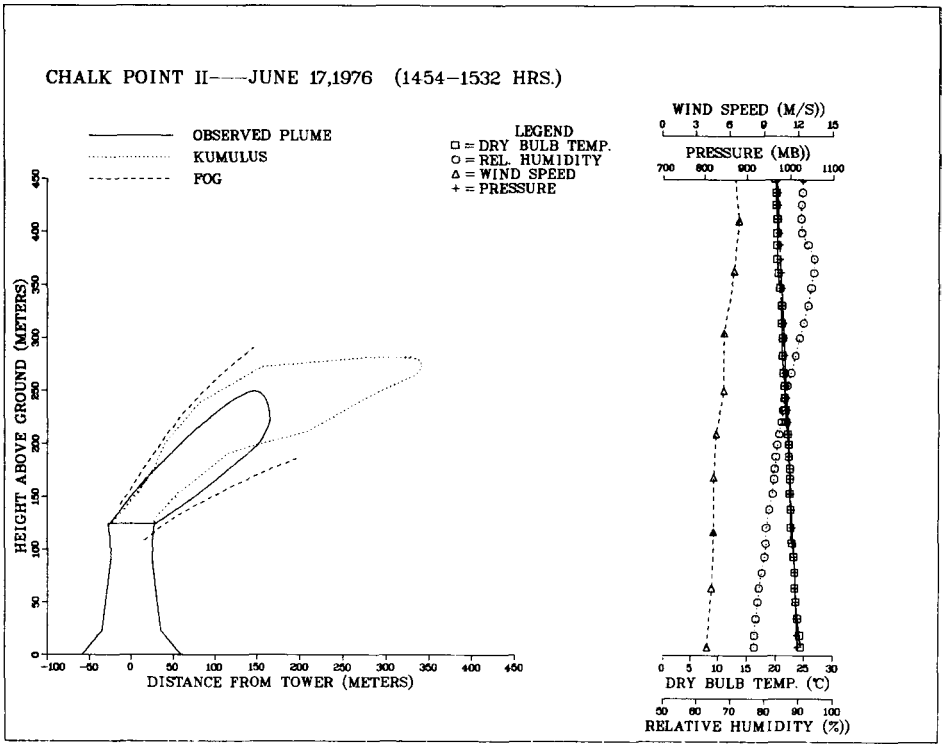

Figure 5-13. Comparison of predictions of KUMULUS and FOG models to observed visible-plume outlines at Chalk Point . . . case CP2J17.

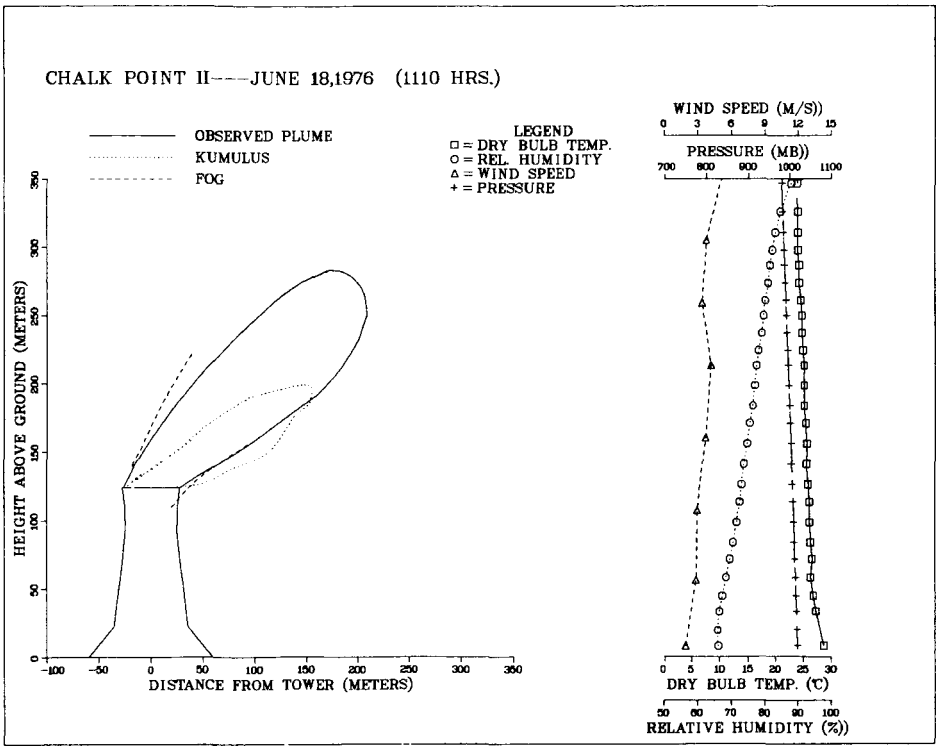

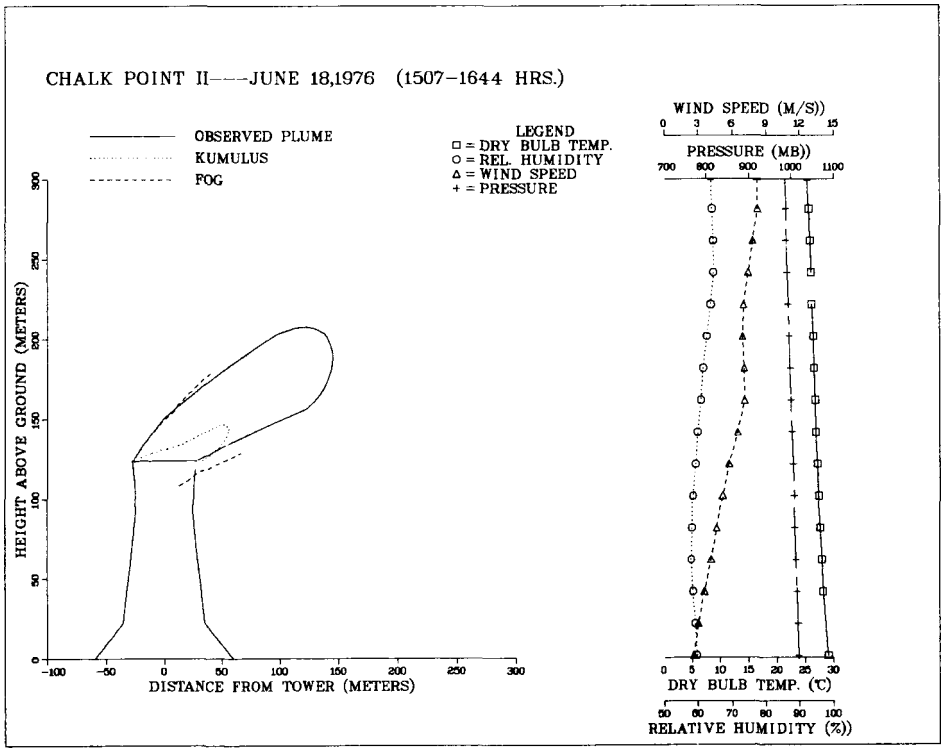

Figure 5-14. Comparison of predictions of KUMULUS and FOG models to observed visible-plume outlines at Chalk Point . . . cases CP2J13P1 and CP2J18A2.

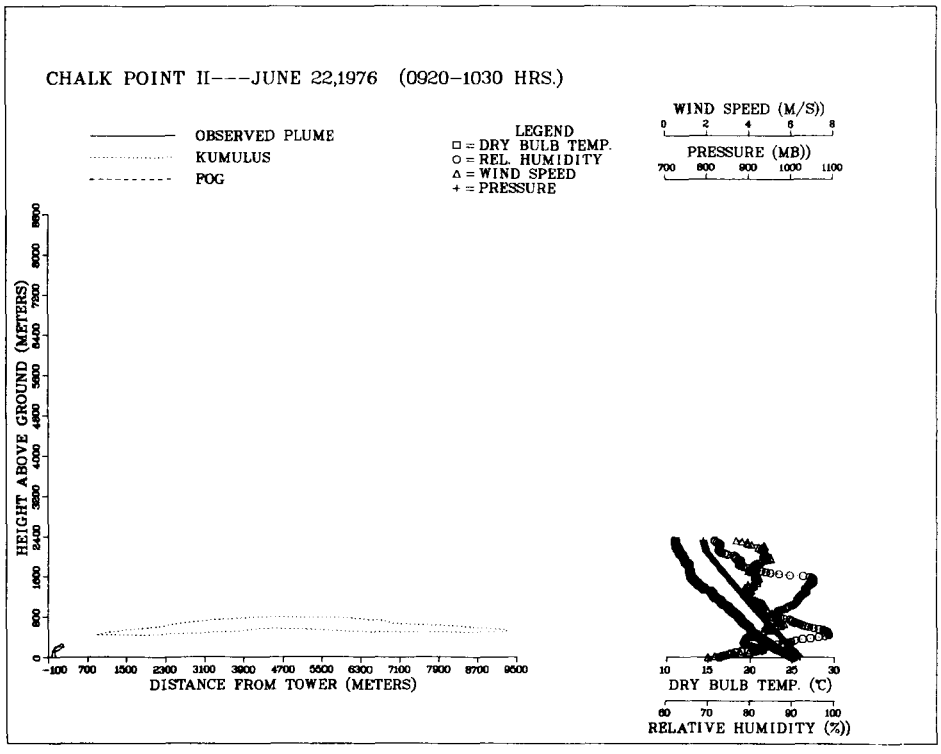

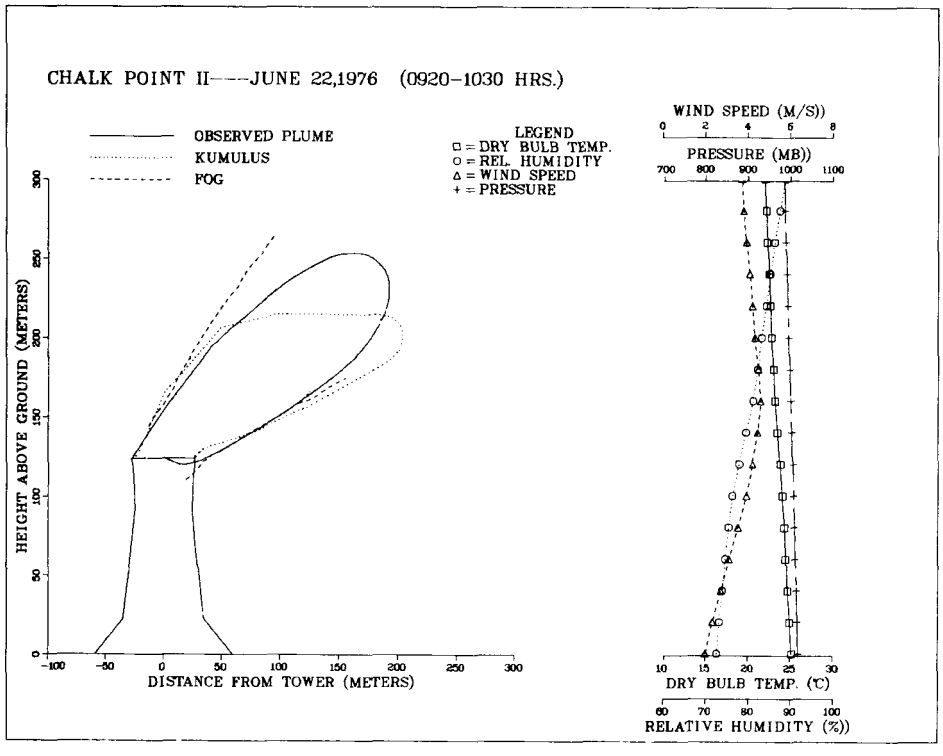

Figure 5-15. Comparison of predictions of KUMULUS and FOG models to observed visible-plume outlines at Chalk Point . . . case CP2J22.

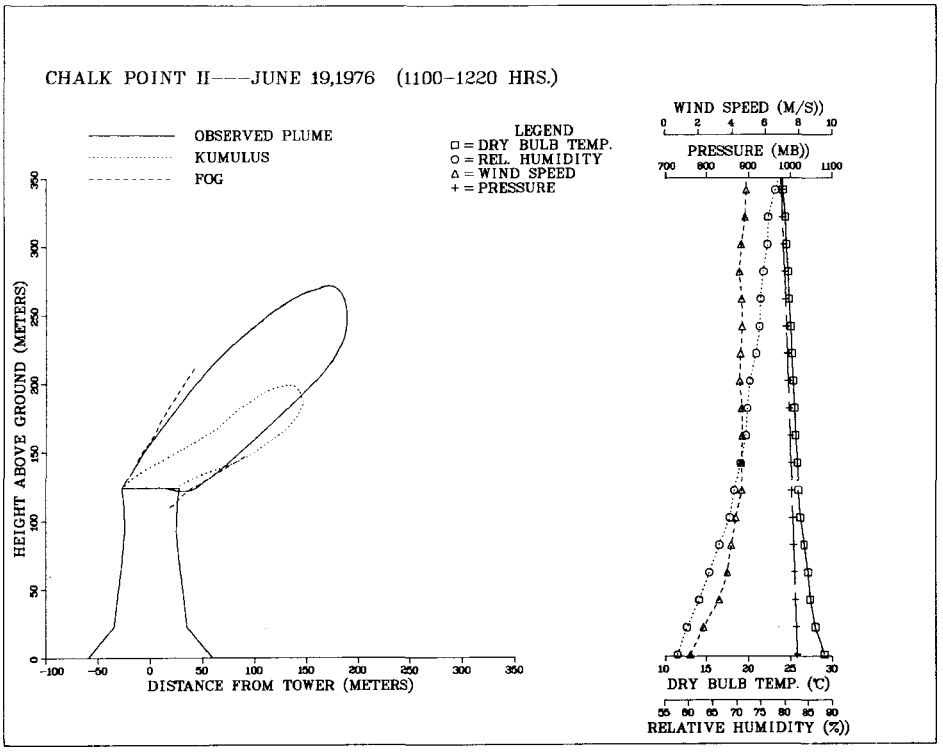

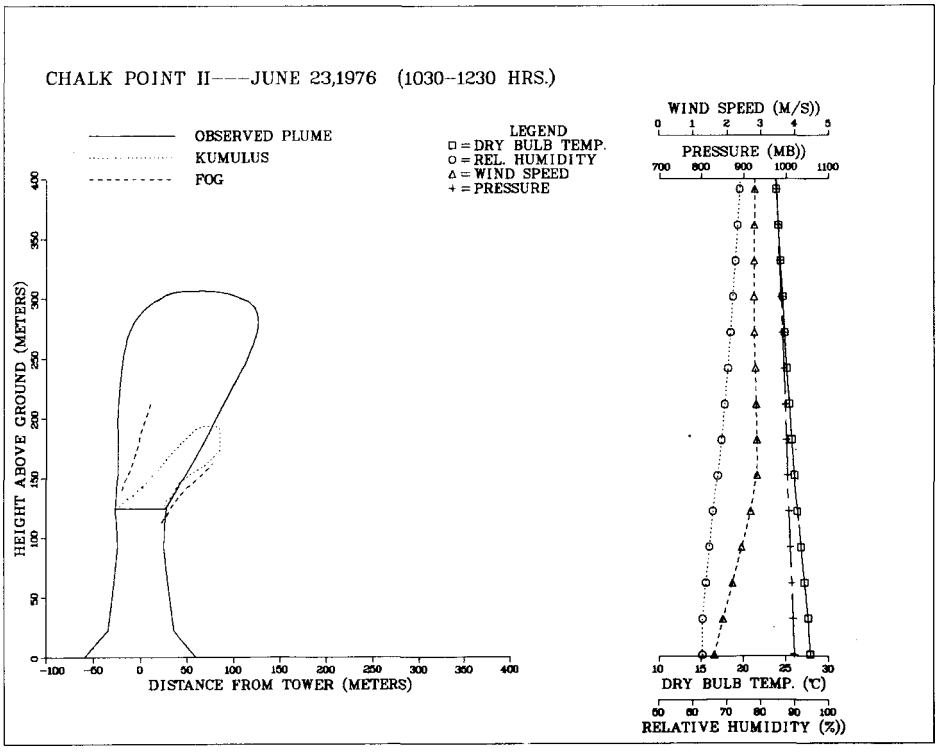

Figure 5-16. Comparison of predictions of KUMULUS and FOG models to observed visible-plume outlines at Chalk Point . . . cases CP2J19 and CP2J23.

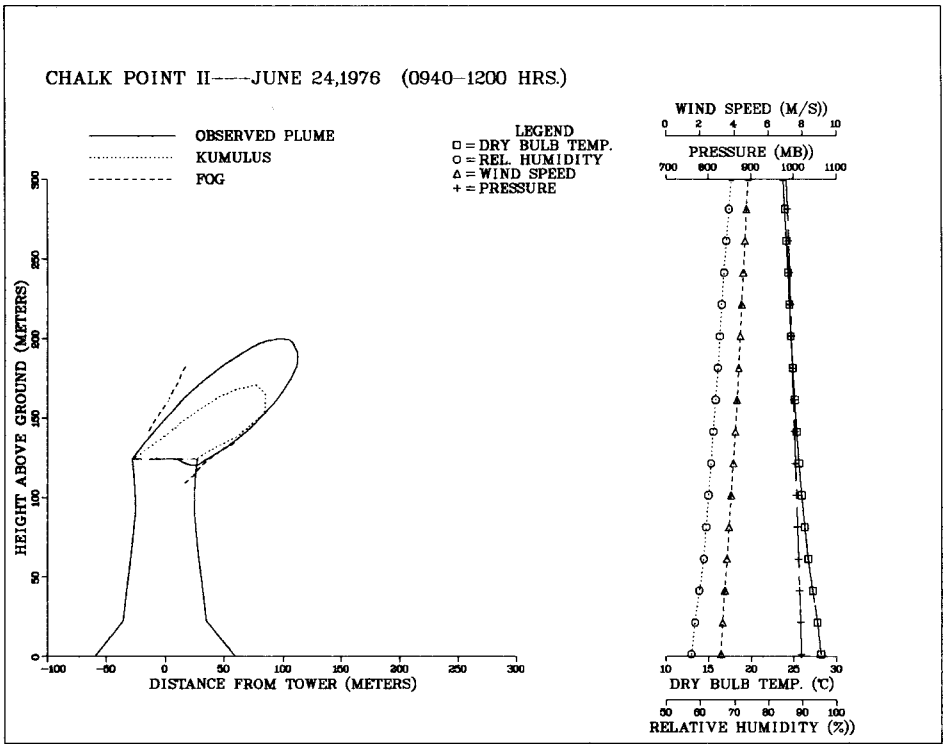

Figure 5-17. Comparison of predictions of KUMULUS and FOG models to observed visible-plume outline at Chalk Point . . . case CP2J24.

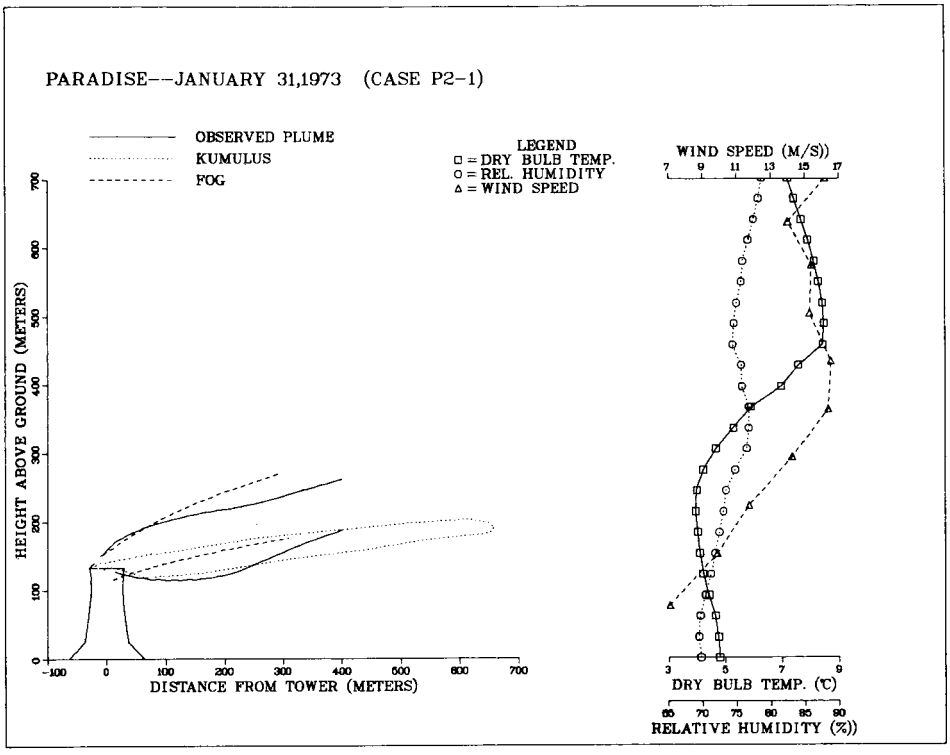

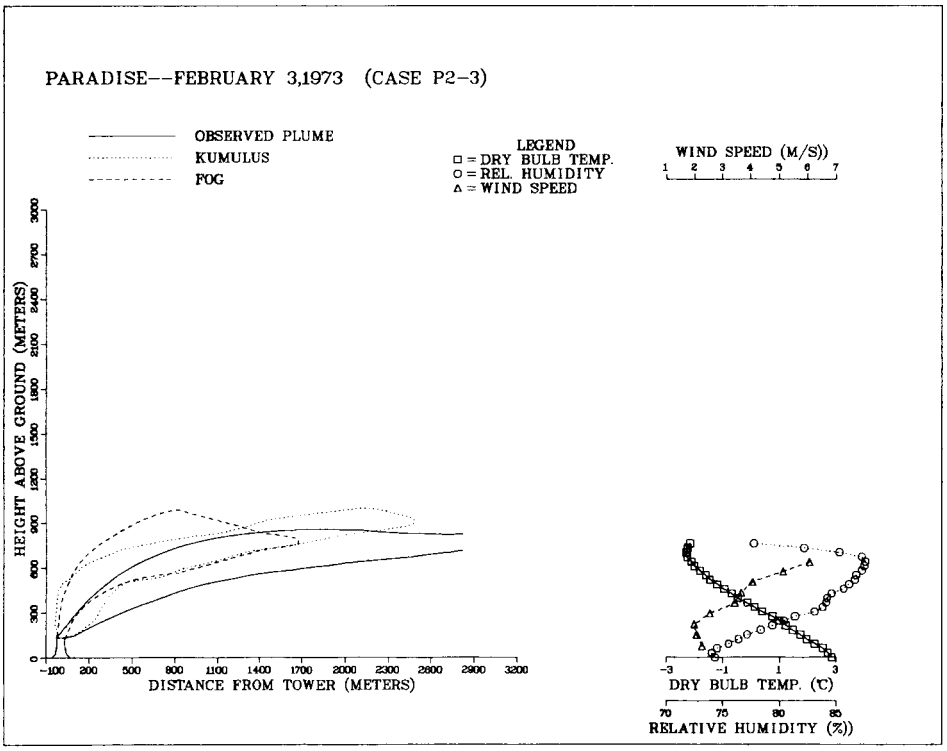

Figure 5-18. Comparison of predictions of KUMULUS and FOG models to observed visible-plume at Paradise . . . cases P2-1 and P2-3.

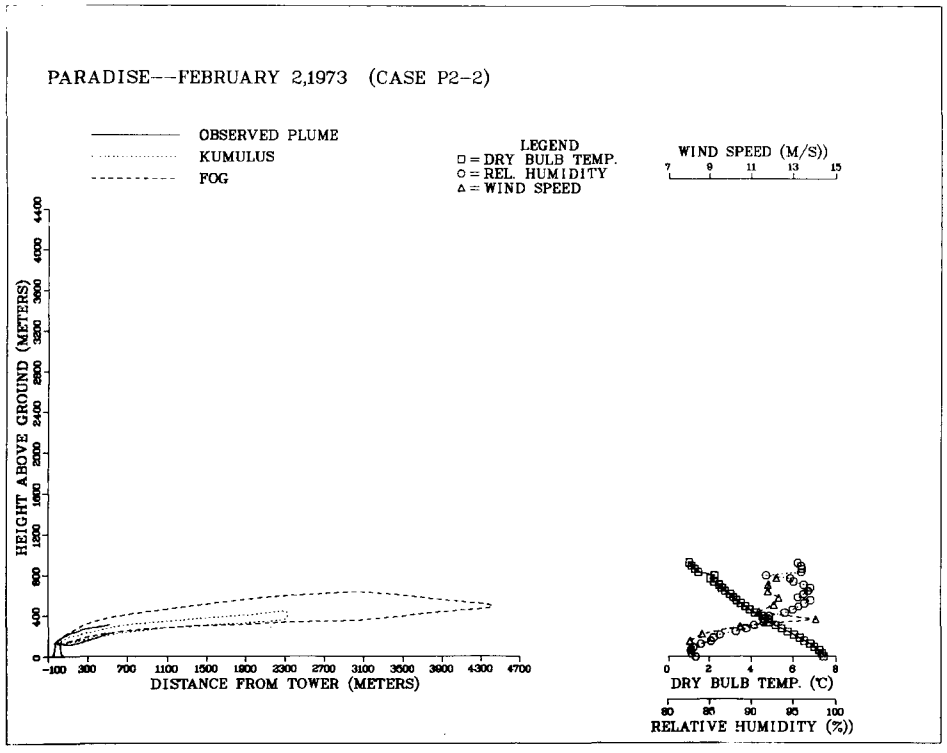

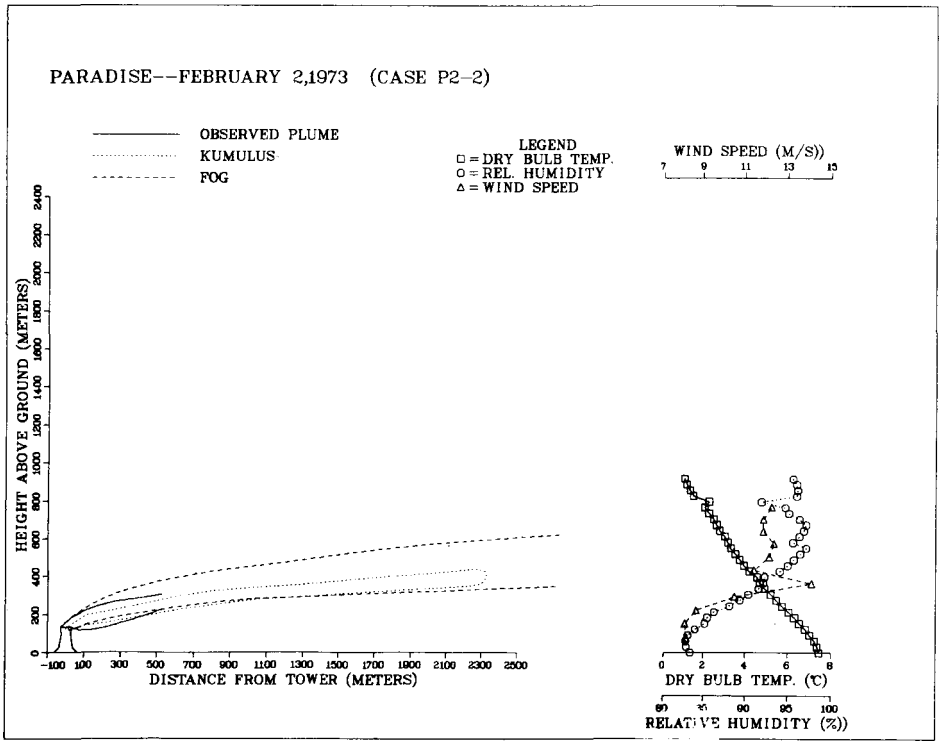

Figure 5-19. Comparison of predictions of KUMULUS and FOG models to observed visible-plume outline at Paradise . . . case P2-2.

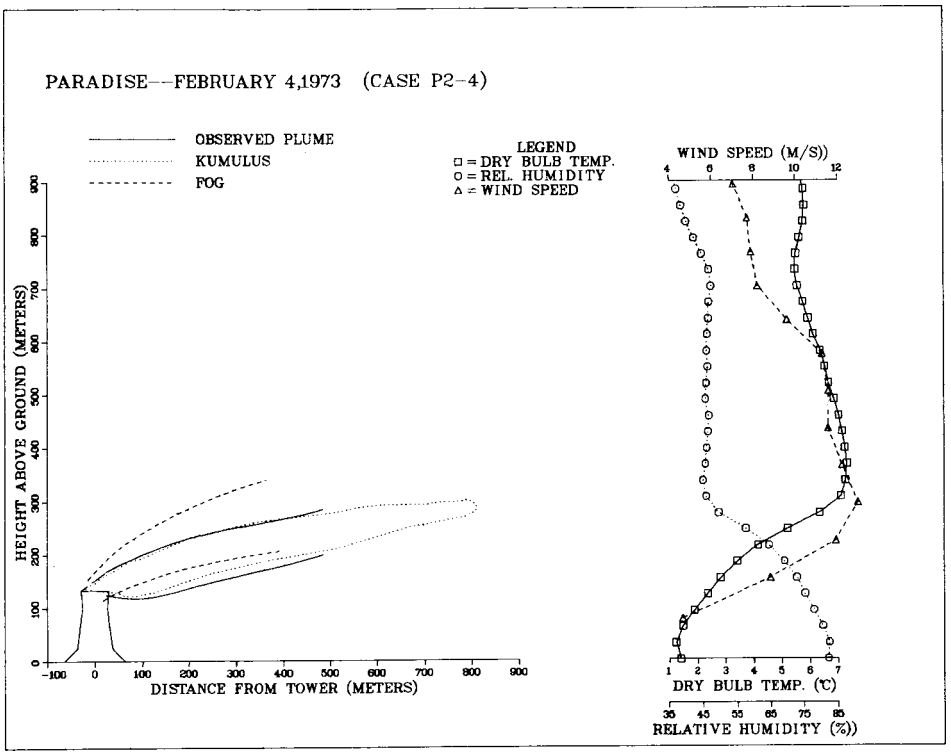

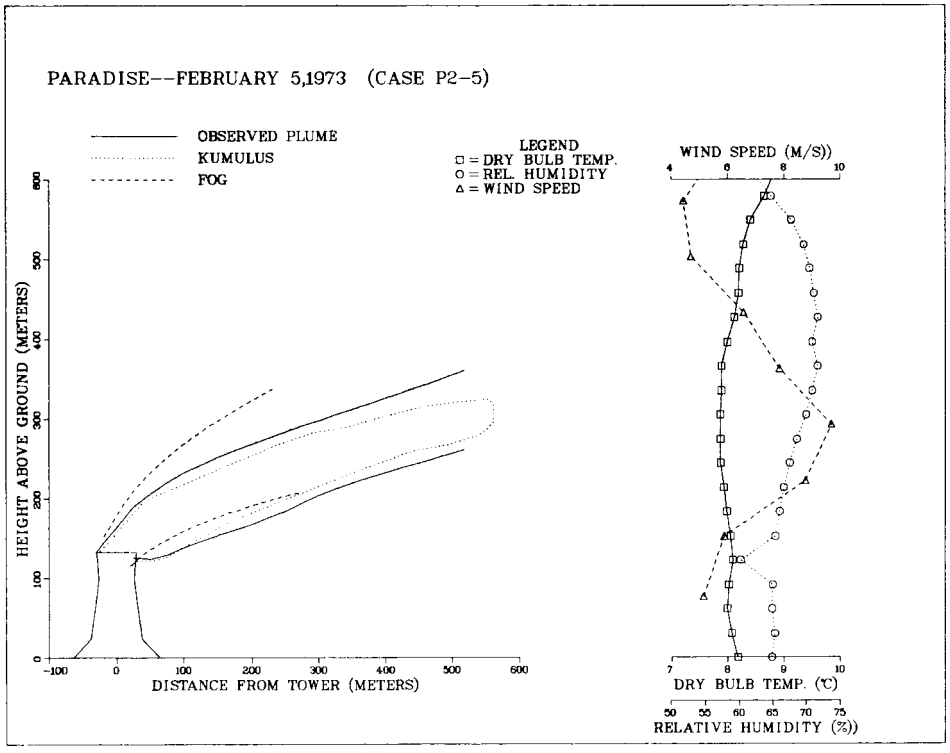

Figure 5-20. Comparison of predictions of KUMULUS and FOG models to observed visible-plume outlines at Paradise . . . cases P2-4 and P2-5.

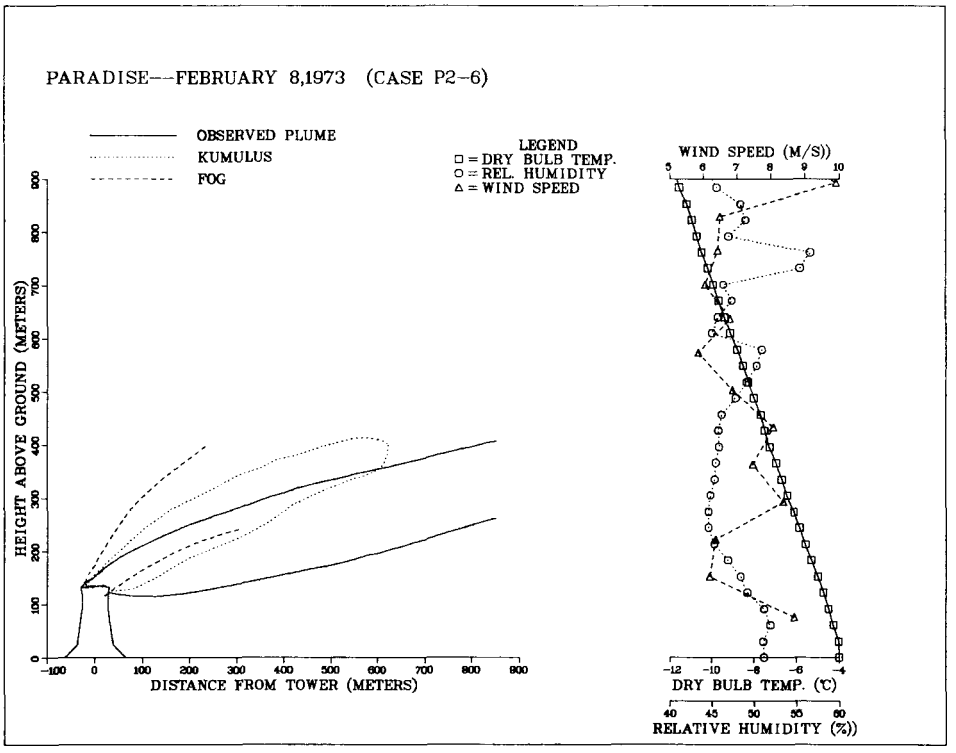

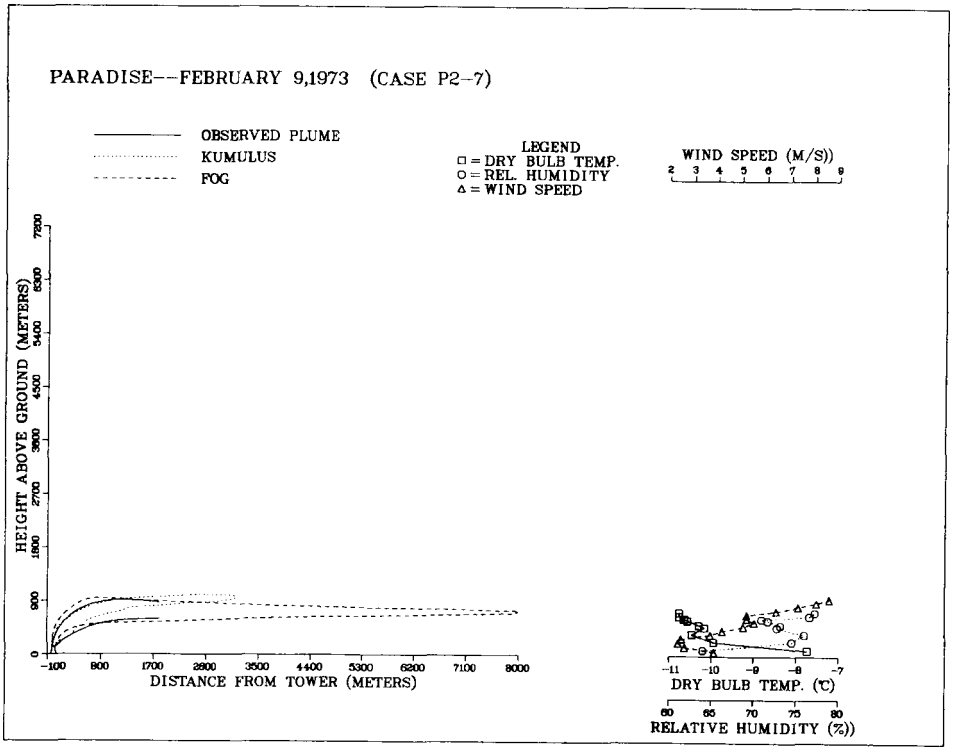

Figure 5-21. Comparison of predictions of KUMULUS and FOG models to observed visible-plume outlines at Paradise . . . cases P2-6 and P2-7.

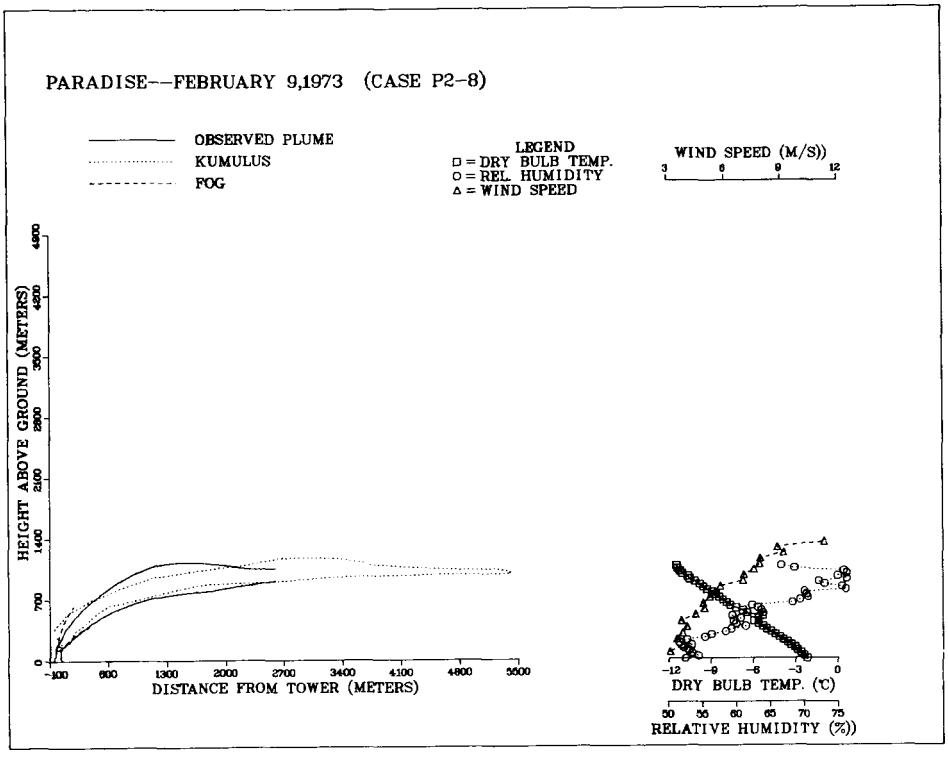

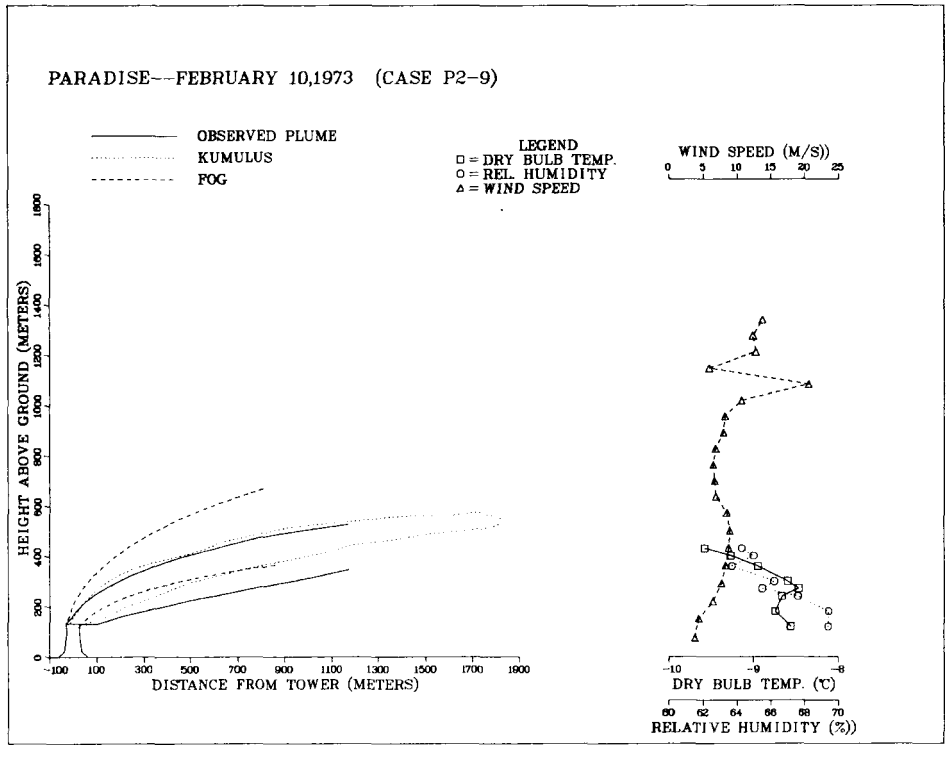

Figure 5-22. Comparison of predictions of KUMULUS and FOG models to observed visible-plume outlines at Paradise . . . cases P2-8 and P2-9.

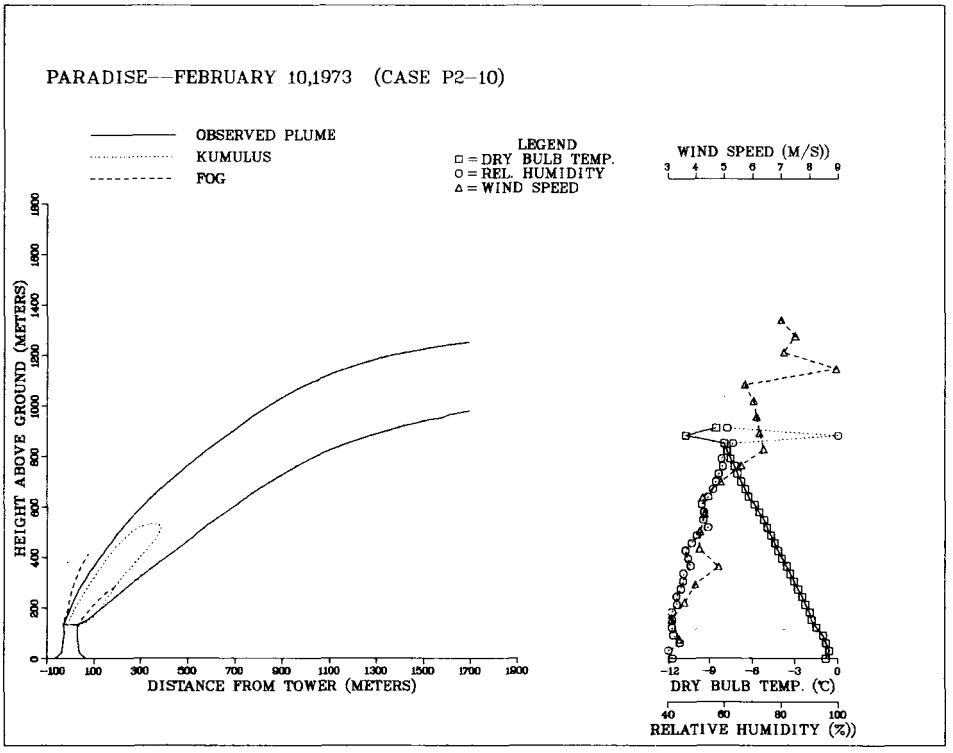

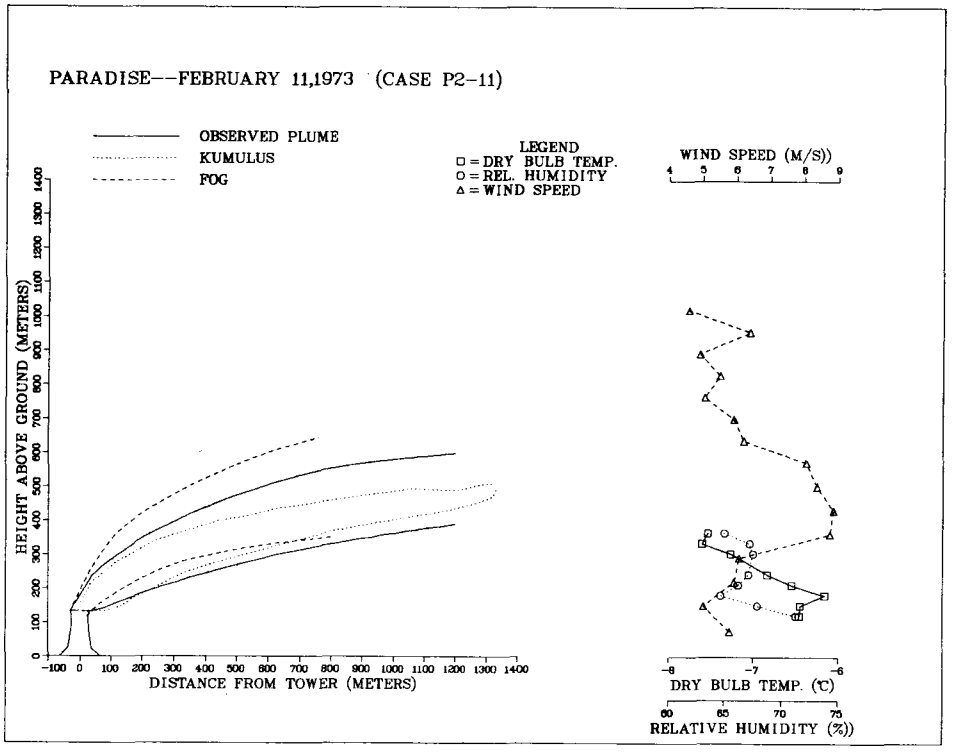

Figure 5-23. Comparison of predictions of KUMULUS and FOG models to observed visible-plume outlines at Paradise . . . cases P2-10 and P2-11.

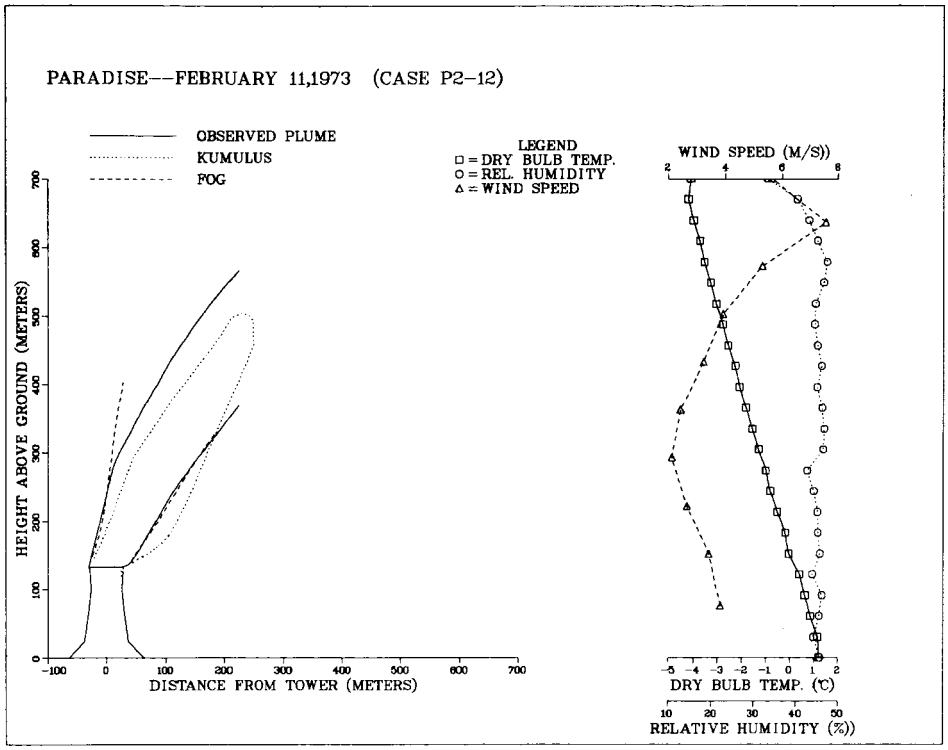

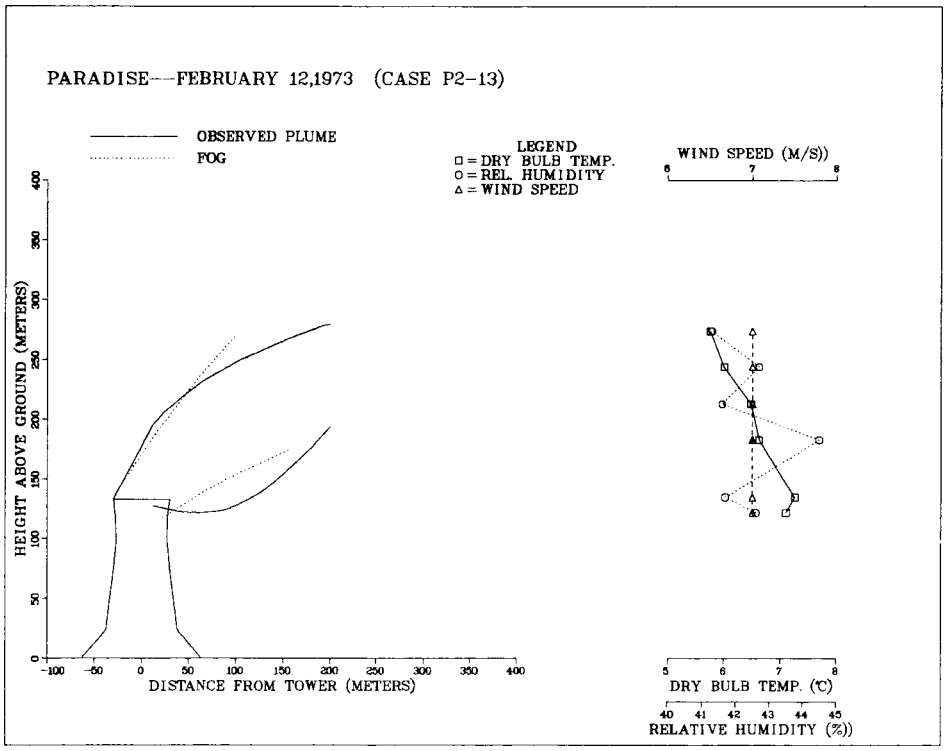

Figure 5-24. Comparison of predictions of KUMULUS and FOG models to observed visible-plume outlines at Paradise . . . cases P2-12 and P2-13.

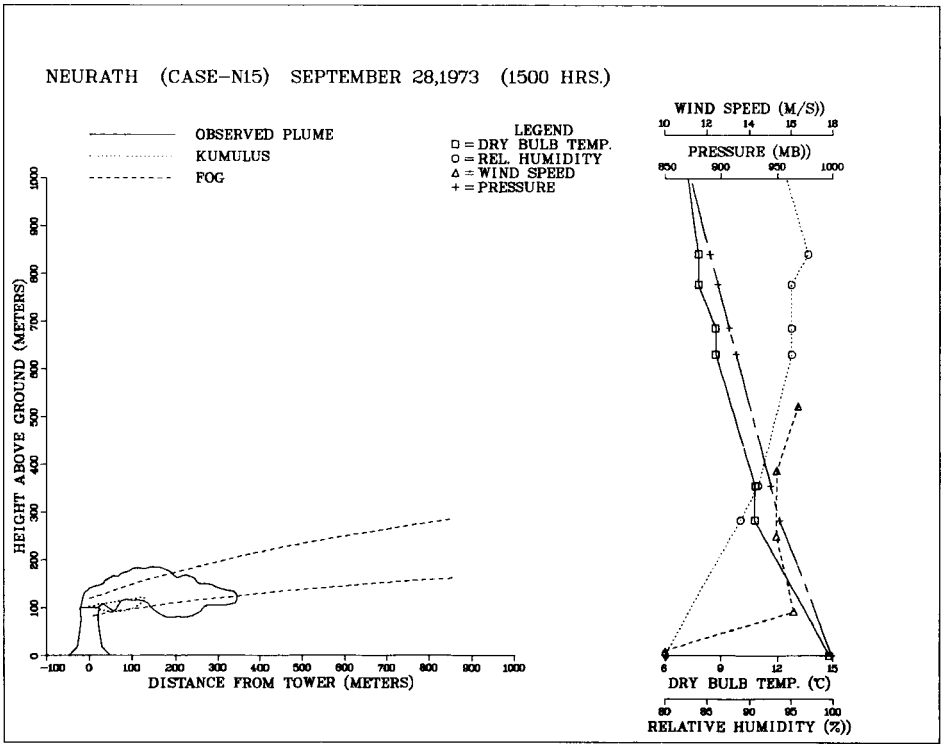

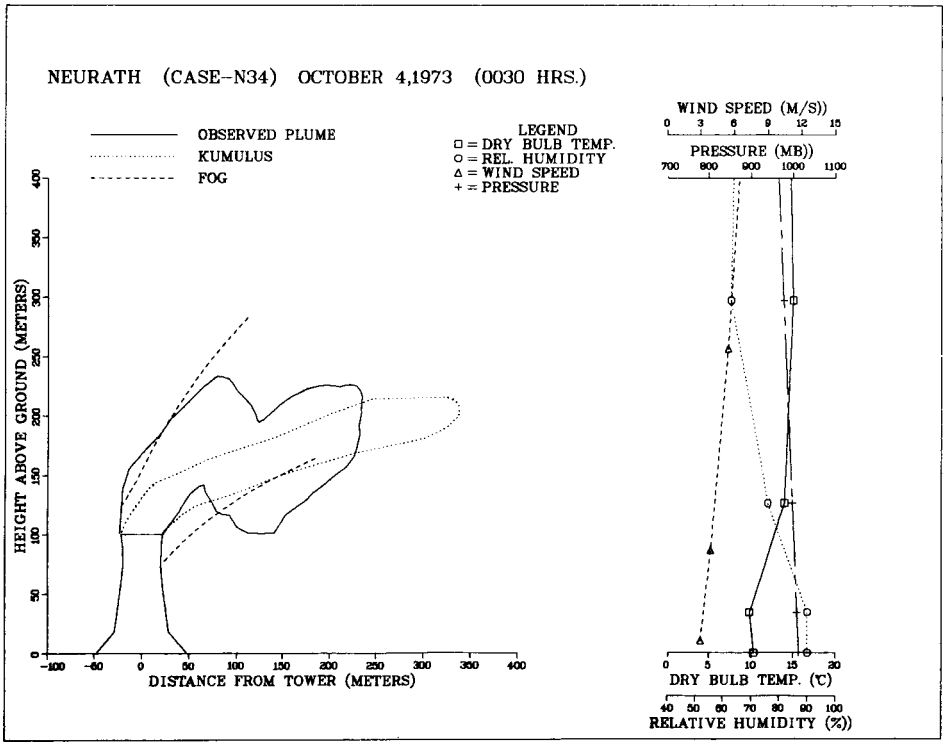

Figure 5-25. Comparison of predictions of KUMULUS and FOG models to observed visible-plume outlines at Neurath . . . cases N15 and N34.

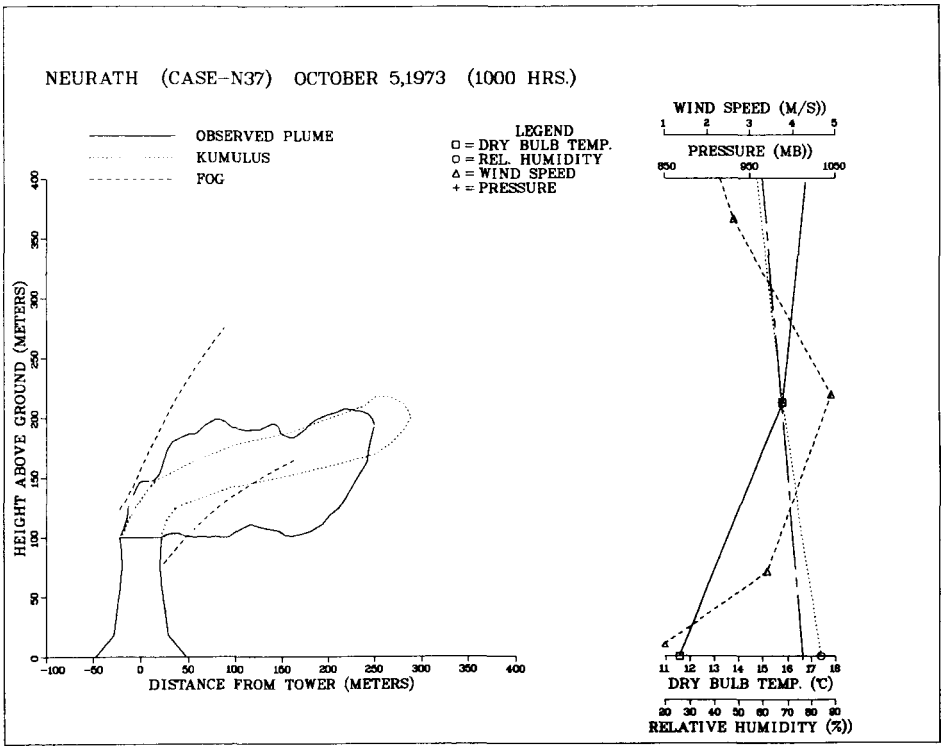

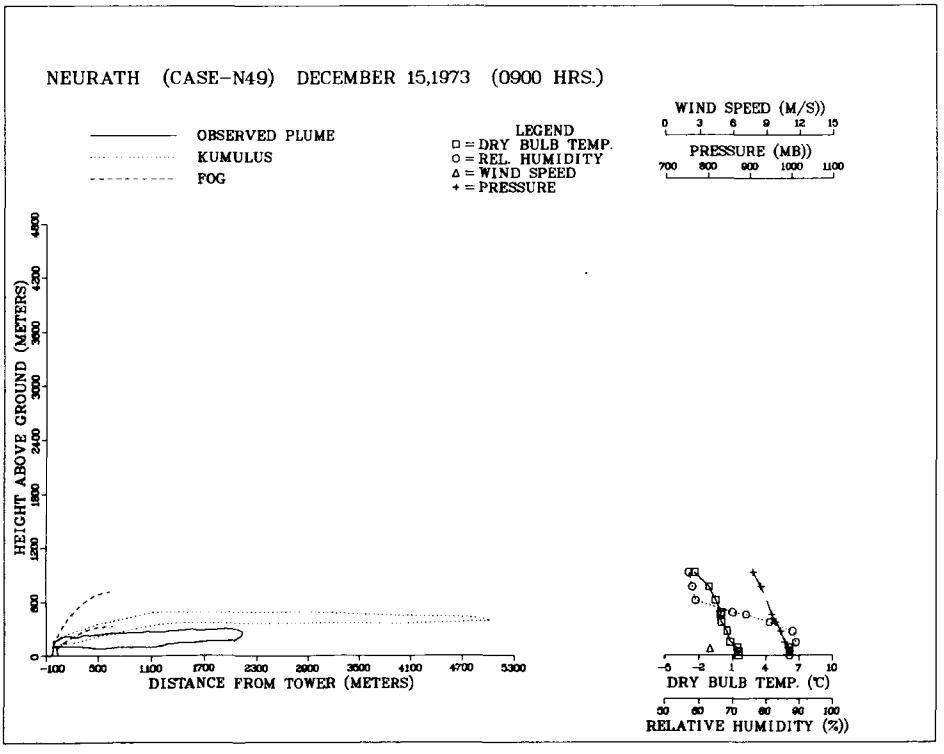

Figure 5-26. Comparison of predictions of KUMULUS and FOG models to observed visible-plume outlines at Neurath . . . cases N34 and N49.

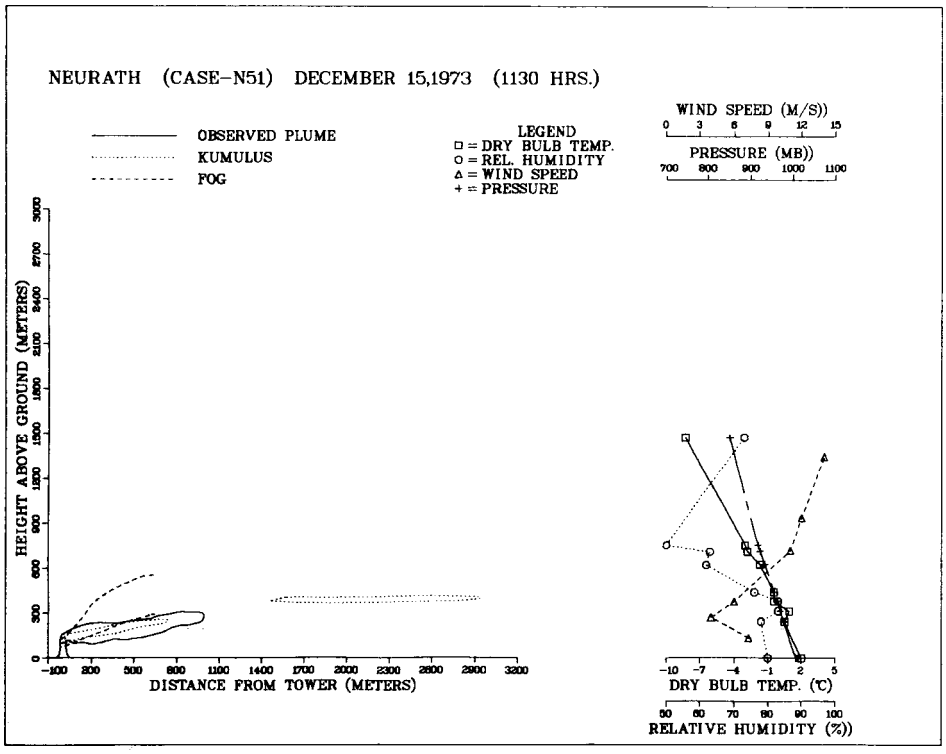

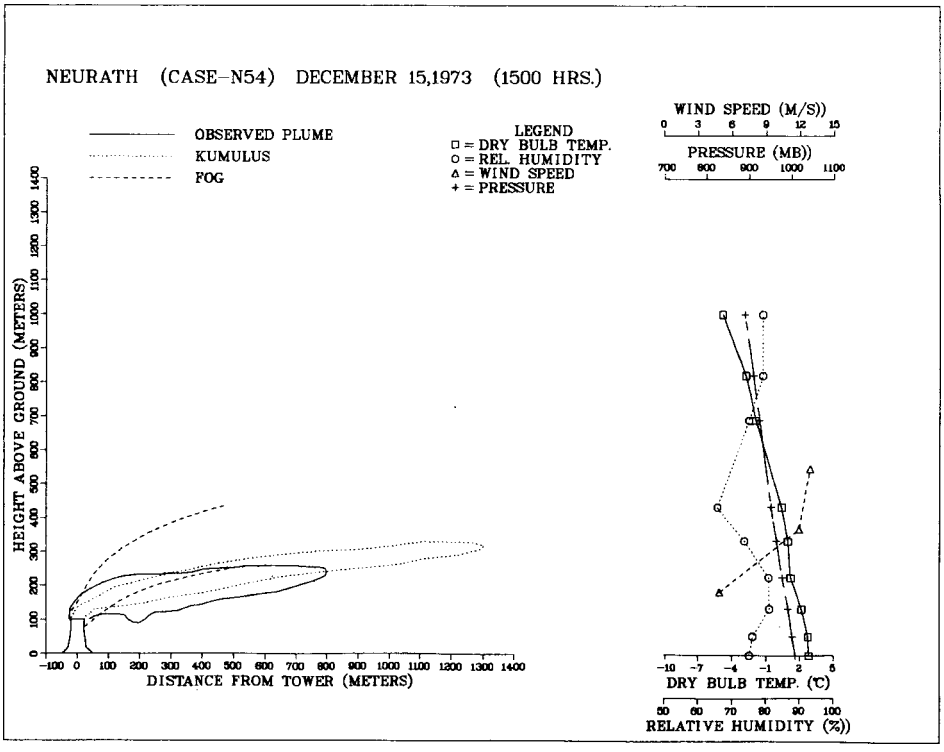

Figure 5-27. Comparison of predictions of KUMULUS and FOG models to observed visible-plume outlines at Neurath . . . cases N51 and N54.

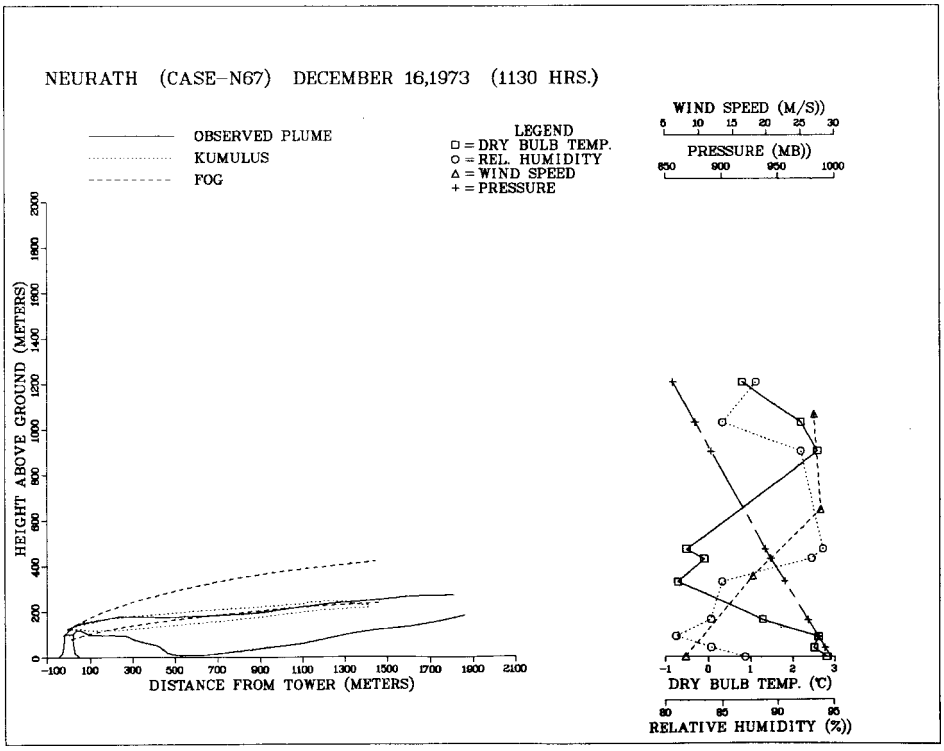

Figure 5-28. Comparison of predictions of KUMULUS and FOG models to observed visible-plume outline at Neurath . . . case N67.

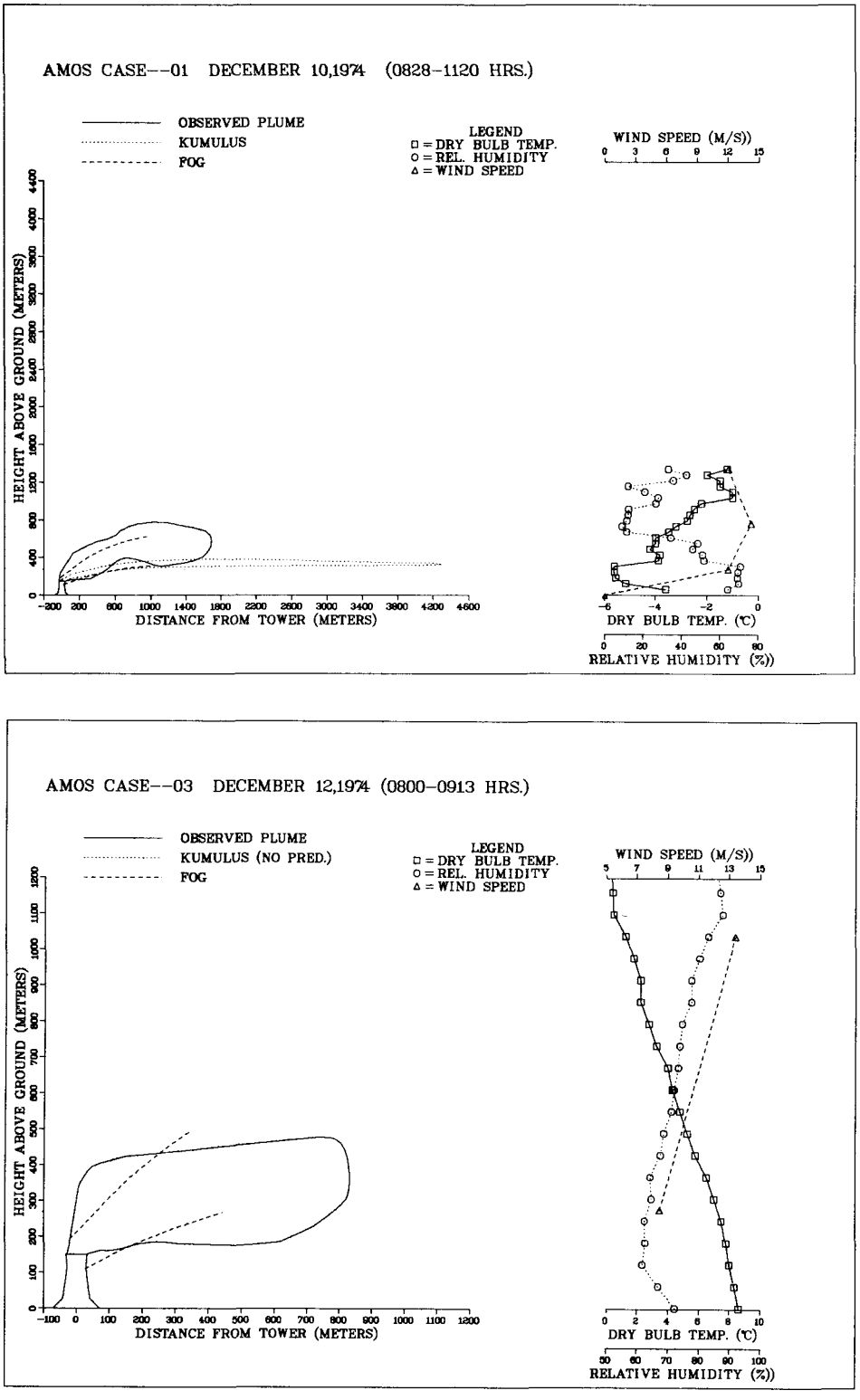

Figure 5-29. Comparison of predictions of KUMULUS and FOG models to observed visible-plume outlines at Amos . . . cases A1 and A3.

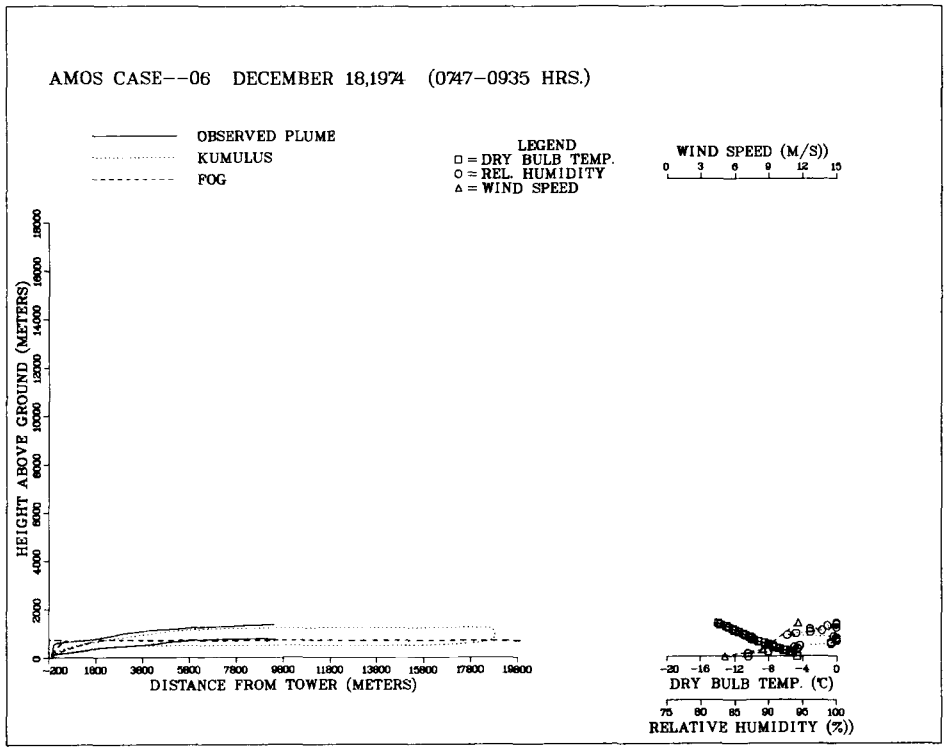

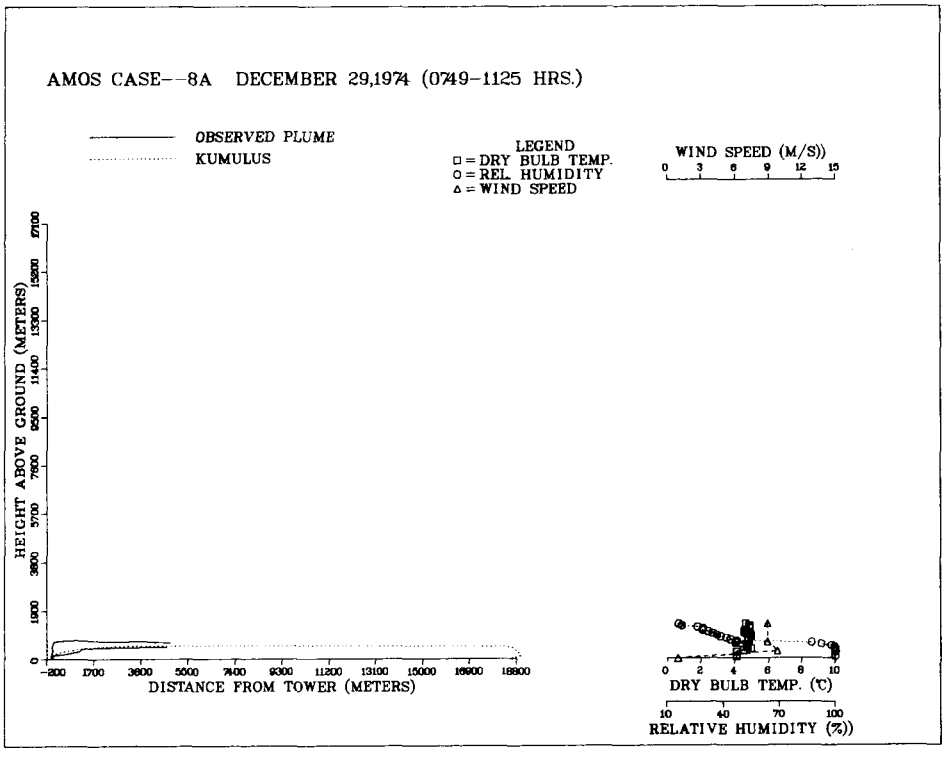

Figure 5-30. Comparison of predictions of KUMULUS and FOG models to observed visible-plume outlines at Amos . . . cases A6 and A8A.

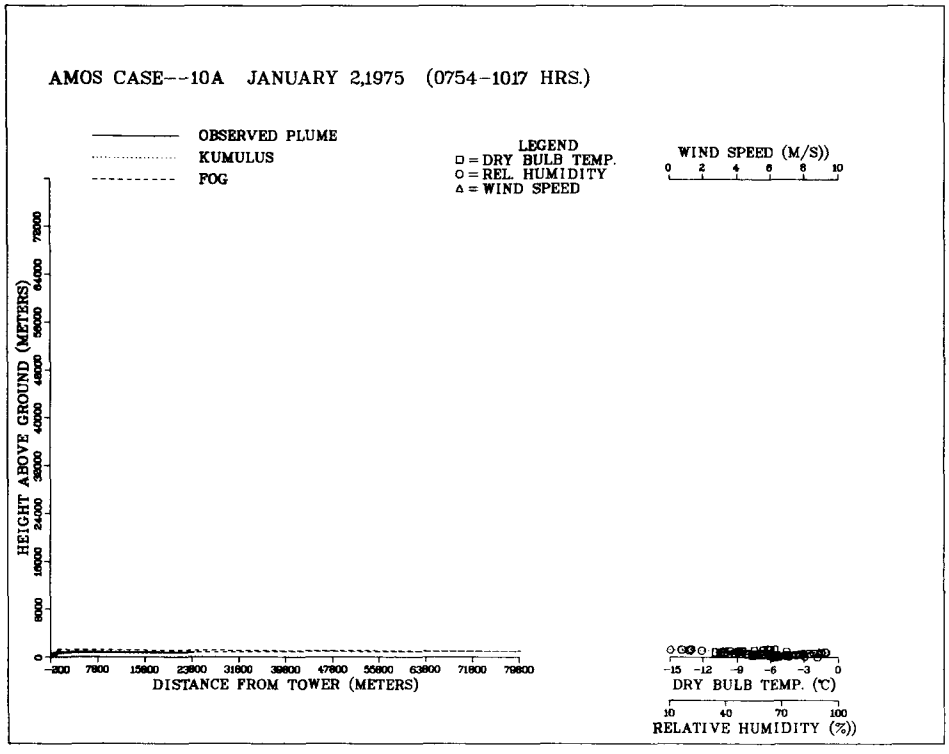

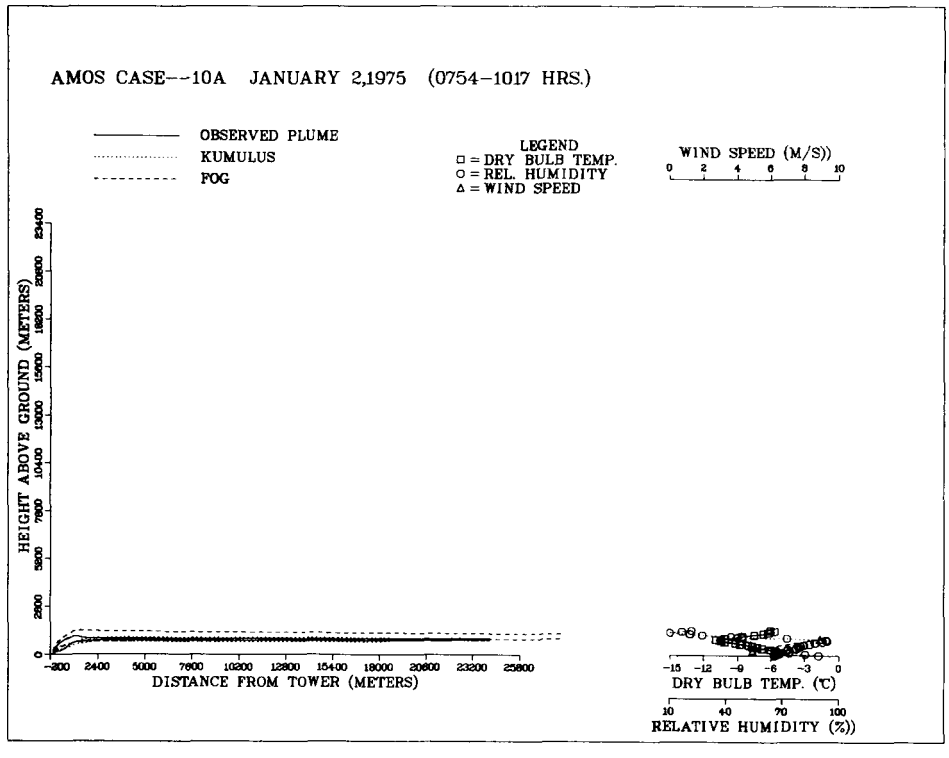

Figure 5-31. Comparison of predictions of KUMULUS and FOG models to observed visible-plume outlines at Amos . . . case A10A.

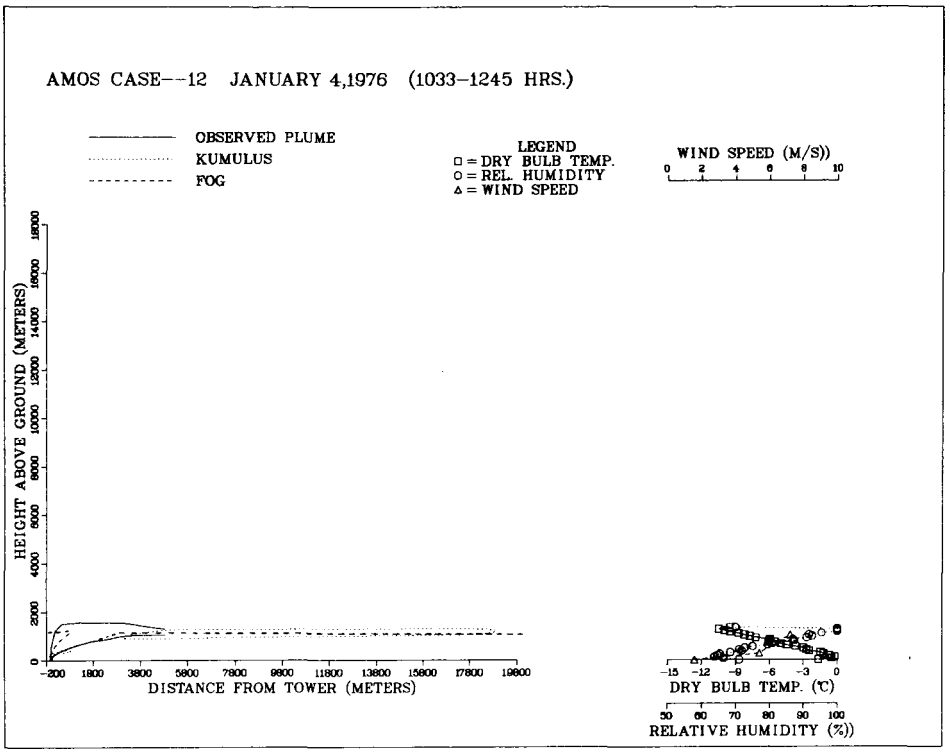

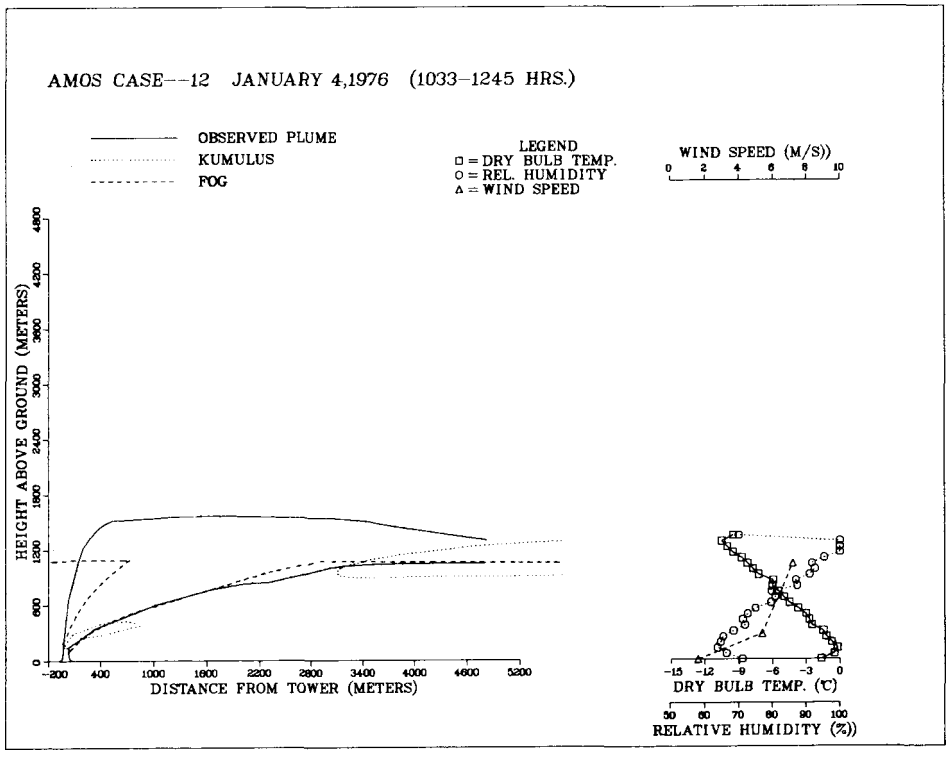

Figure 5-32. Comparison of predictions of KUMULUS and FOG models to observed visible-plume outlines at Amos . . . case A12.

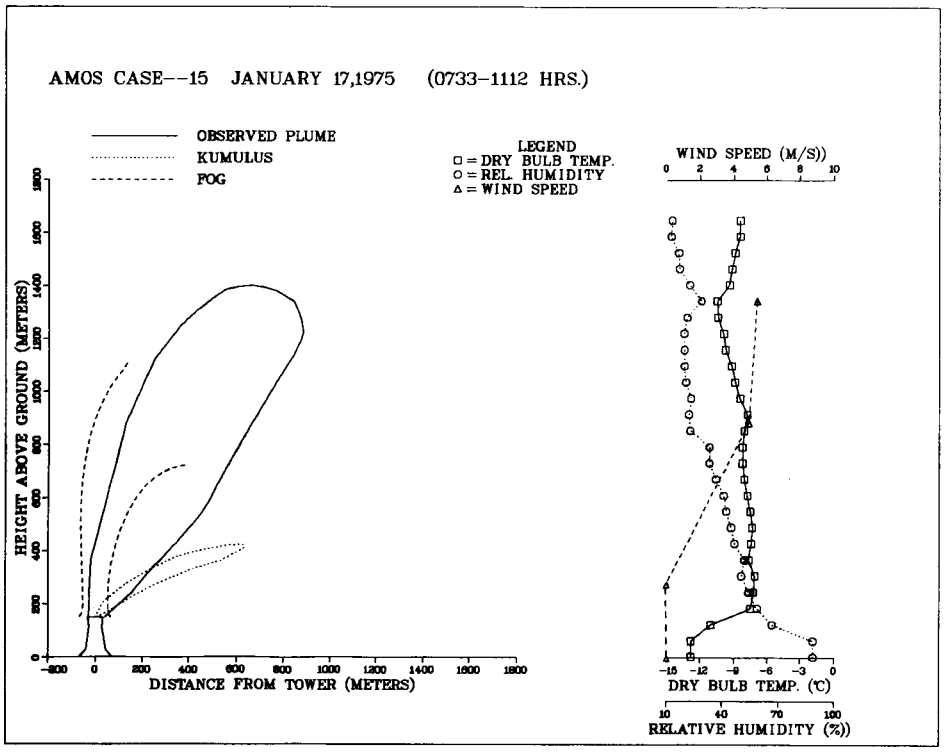

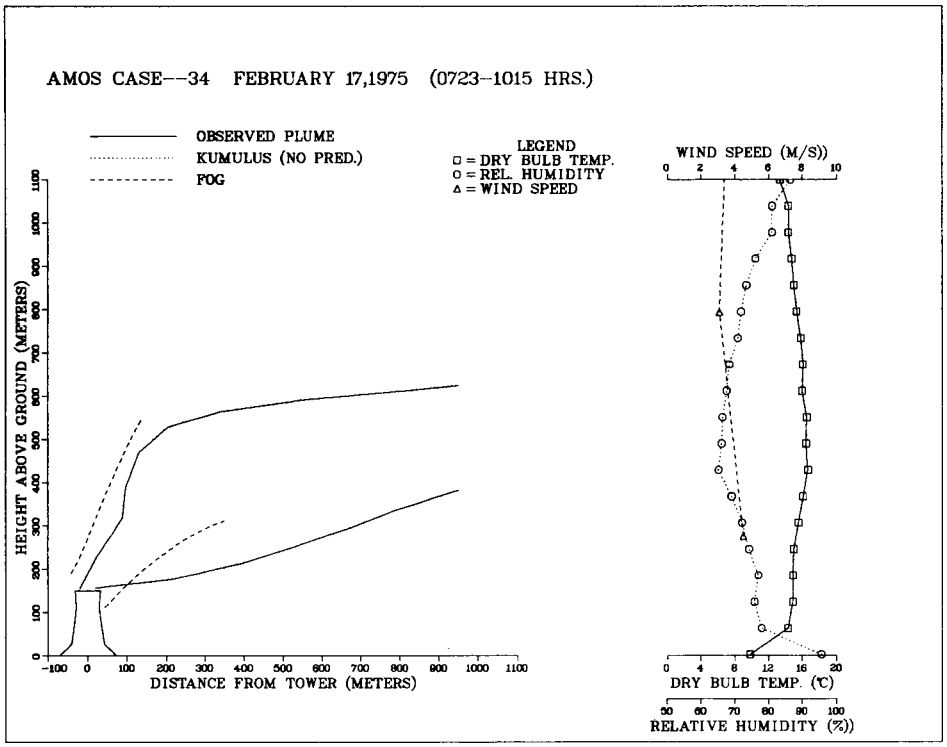

Figure 5-33. Comparison of predictions of KUMULUS and FOG models to observed visible-plume outlines at Amos . . . cases A15 and A34.

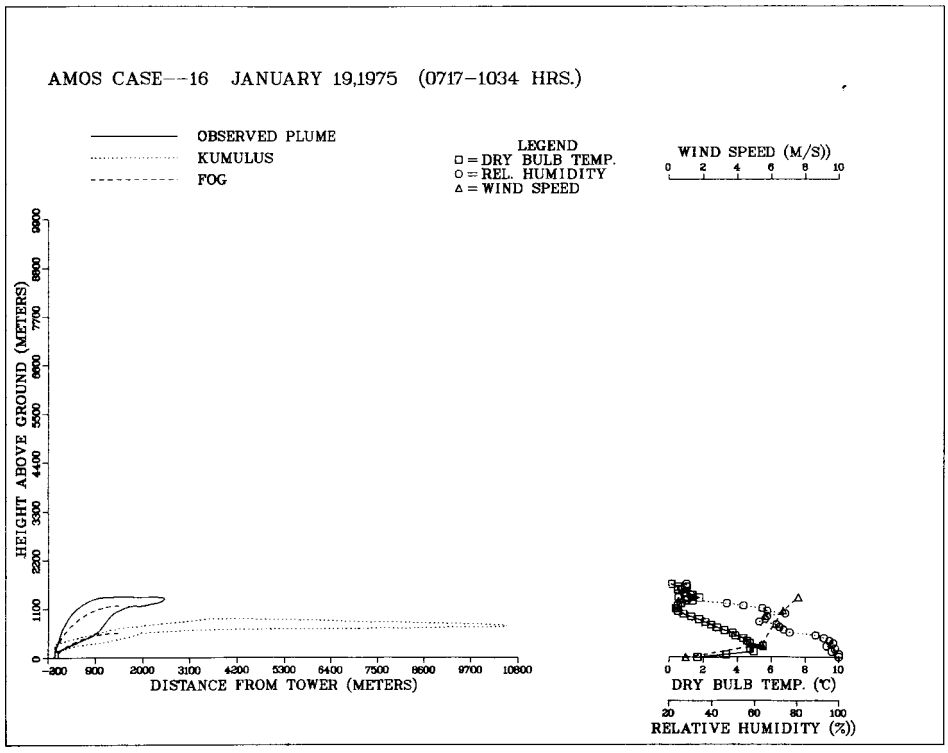

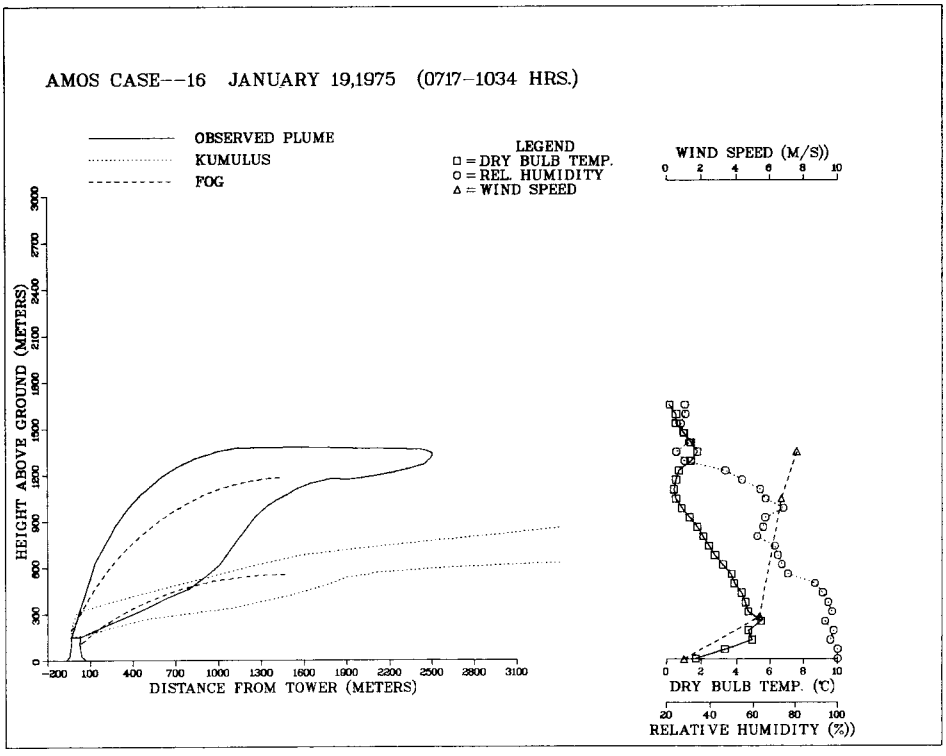

Figure 5-34. Comparison of predictions of KUMULUS and FOG models to observed visible-plume outlines at Amos . . . case A16.

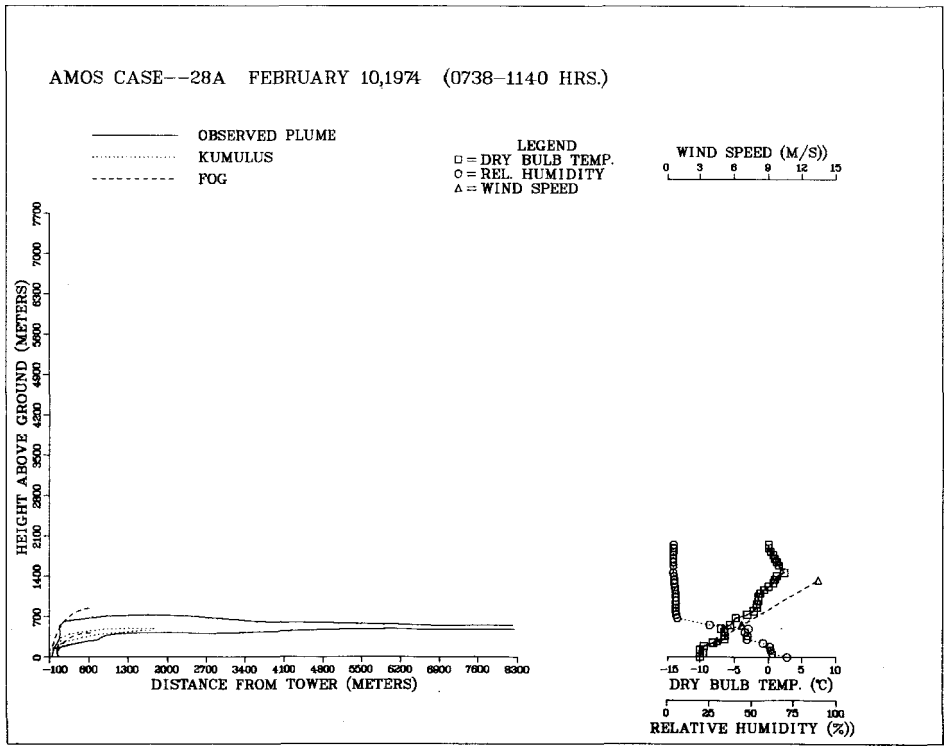

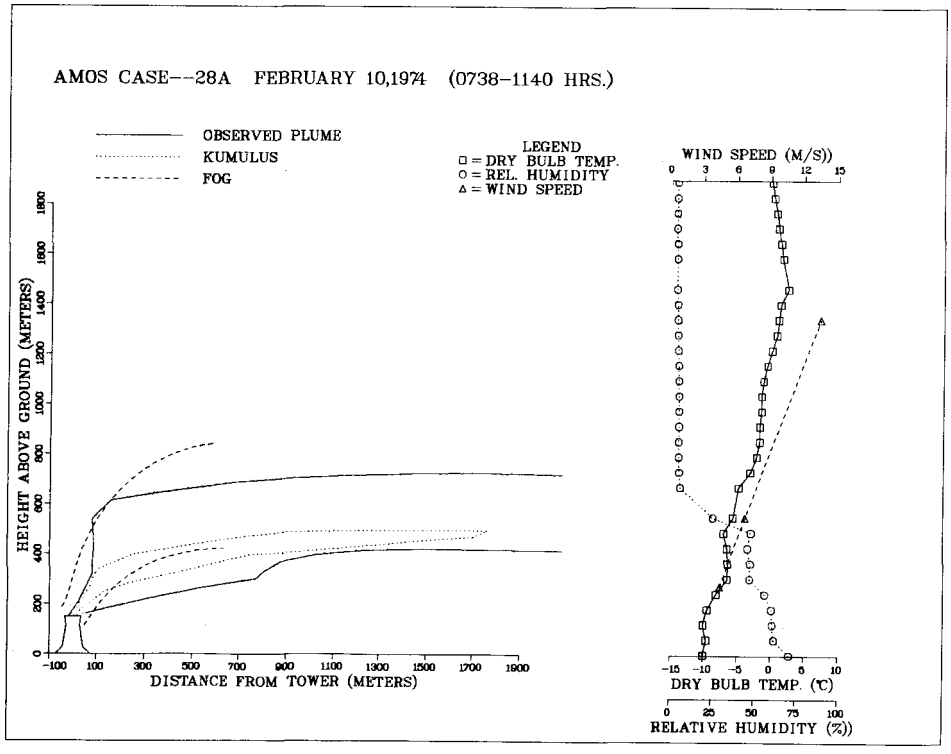

Figure 5-35. Comparison of predictions of KUMULUS and FOG models to observed visible-plume outlines at Amos . . . case A28A.

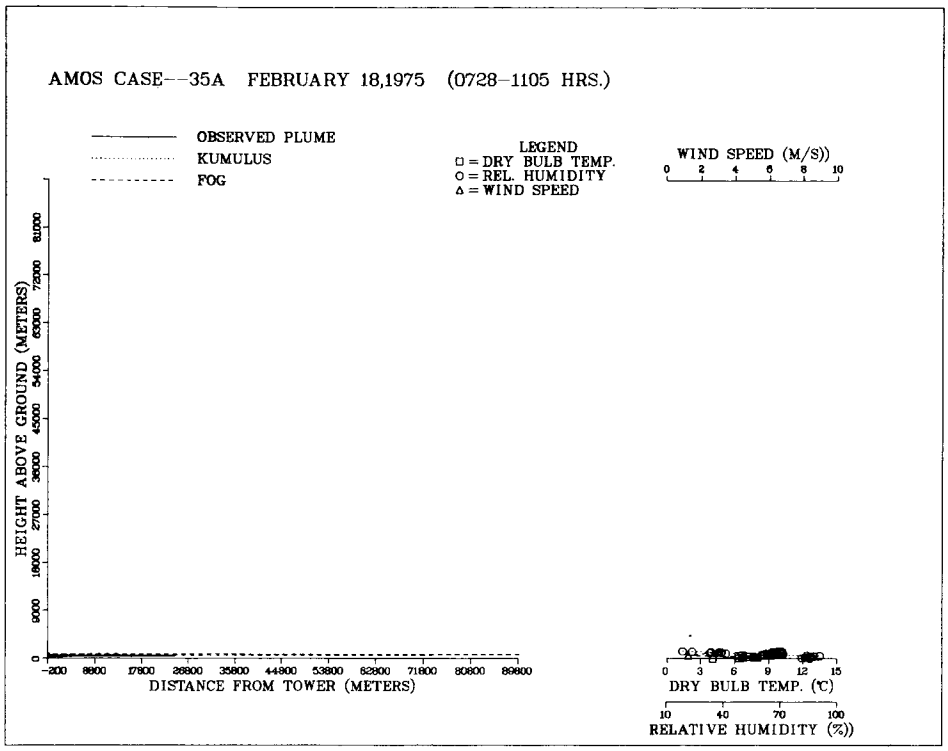

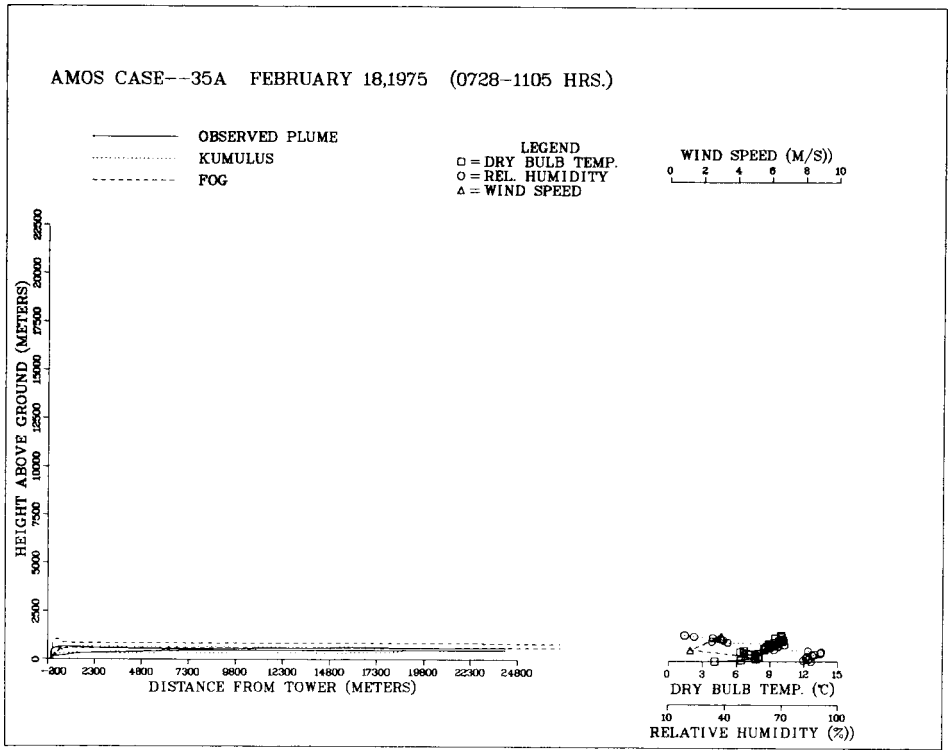

Figure 5-36. Comparison of predictions of KUMULUS and FOG models to observed visible-plume outlines at Amos . . . case A35A.

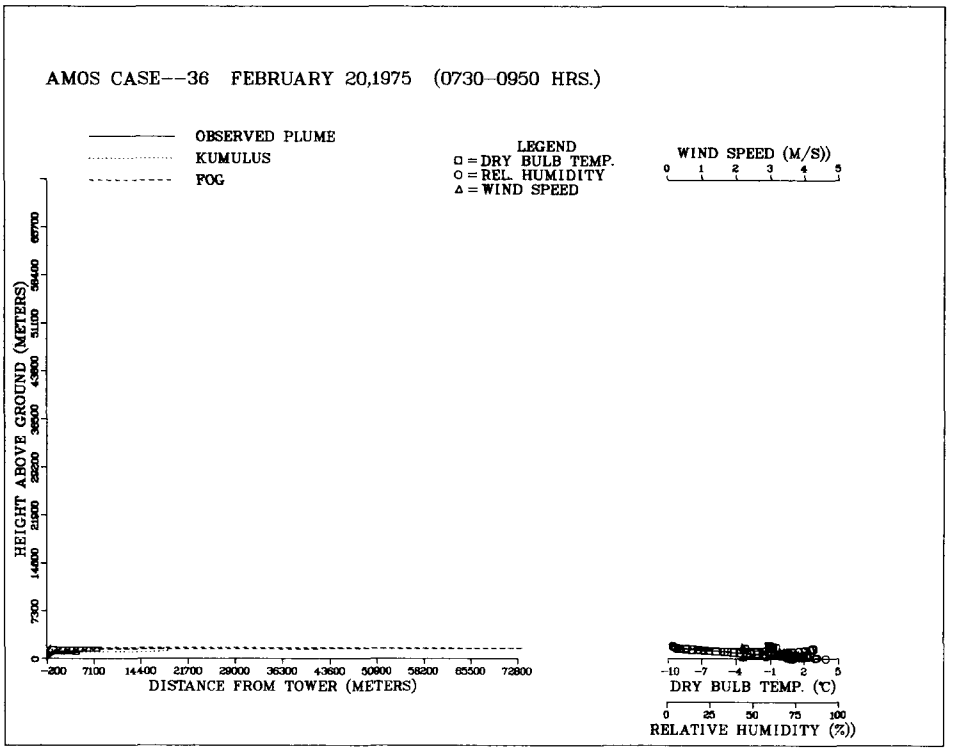

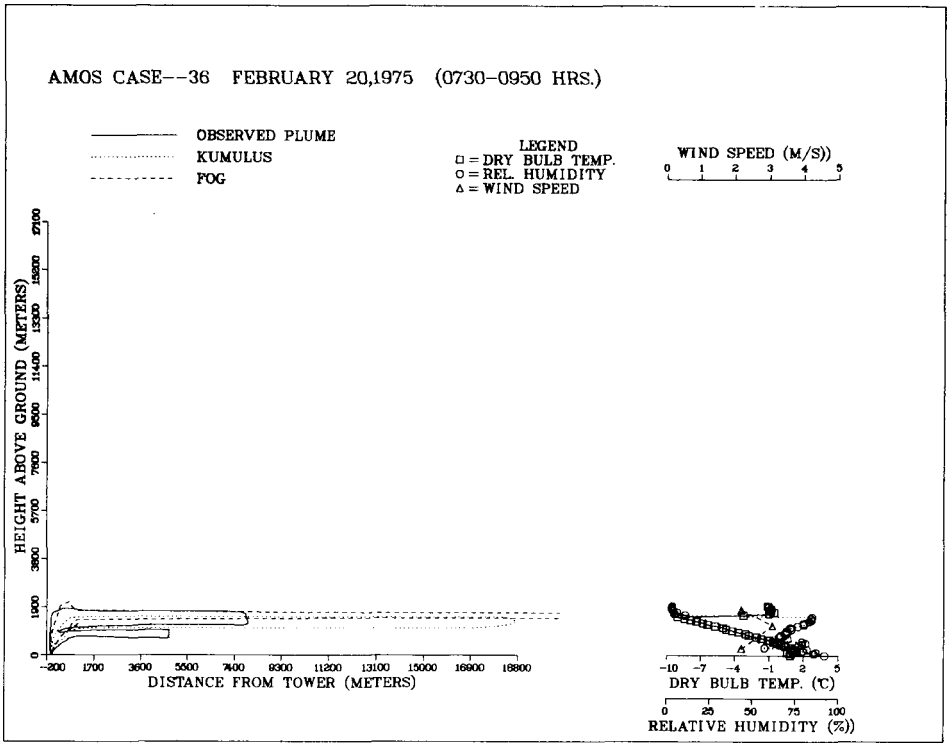

Figure 5-37. Comparison of predictions of KUMULUS and FOG models to observed visible-plume outlines at Amos . . . case A36.

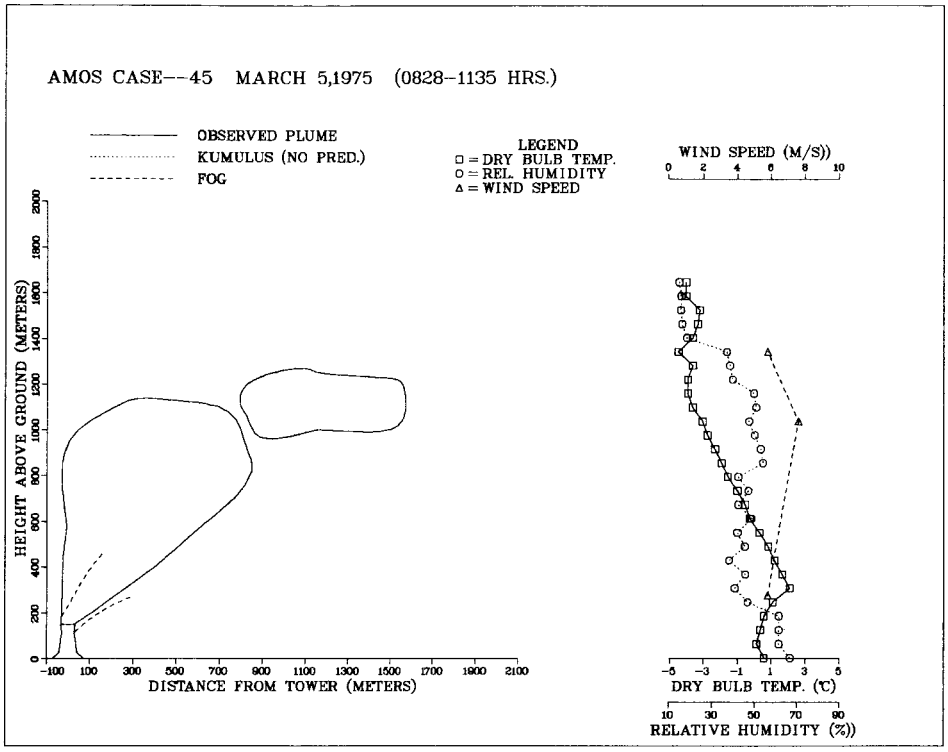

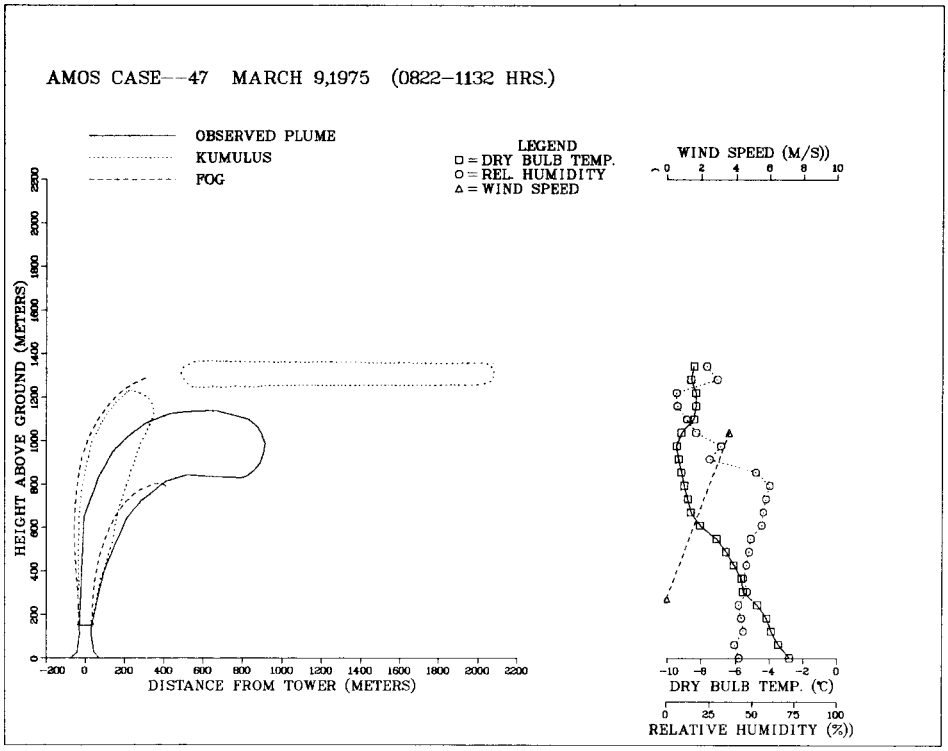

Figure 5-38. Comparison of predictions of KUMULUS and FOG models to observed visible-plume outlines at Amos . . . cases A45 and A47.

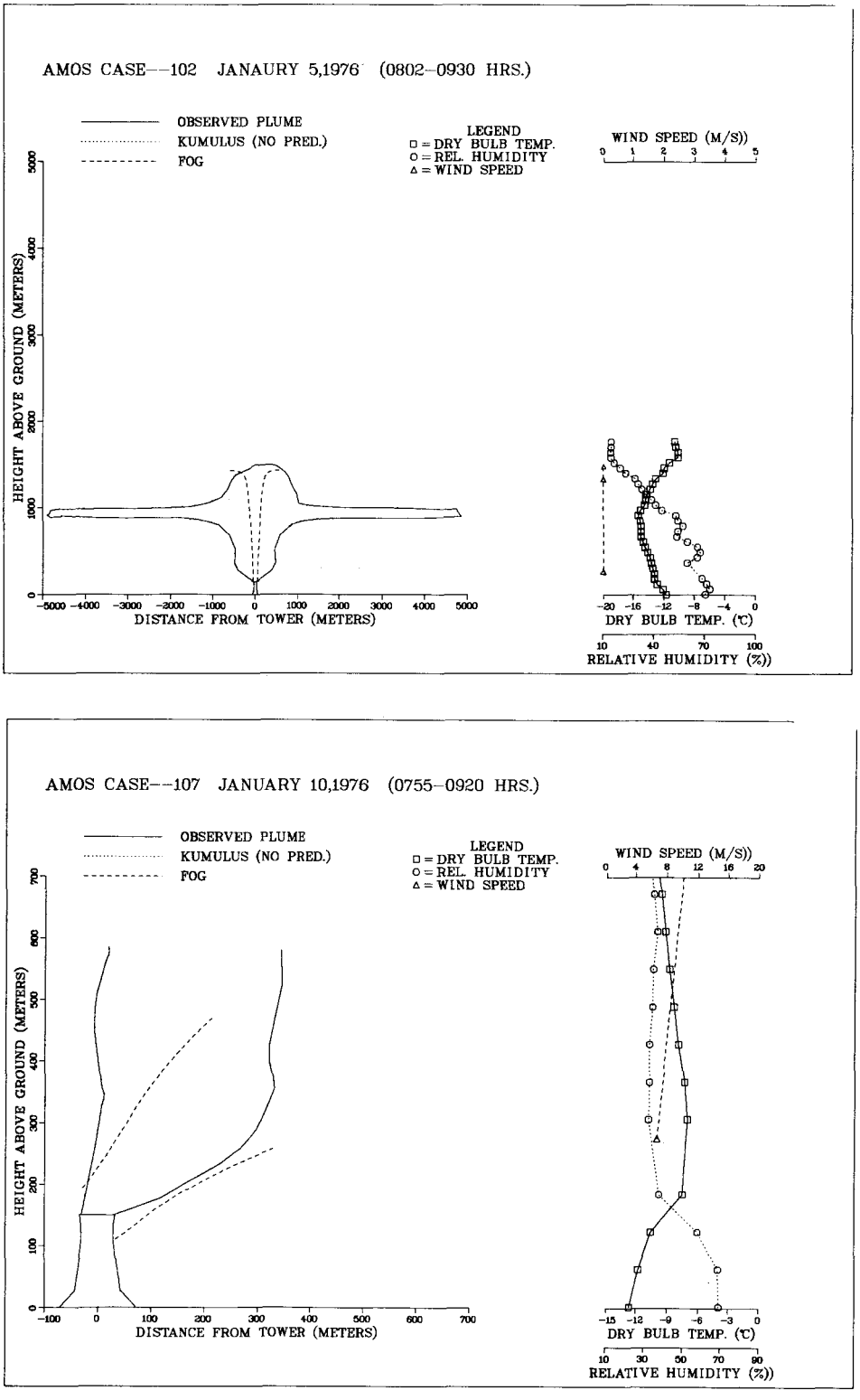

Figure 5-39. Comparison of predictions of KUMULUS and FOG models to observed visible-plume outlines at Amos . . . cases A102 and A107.

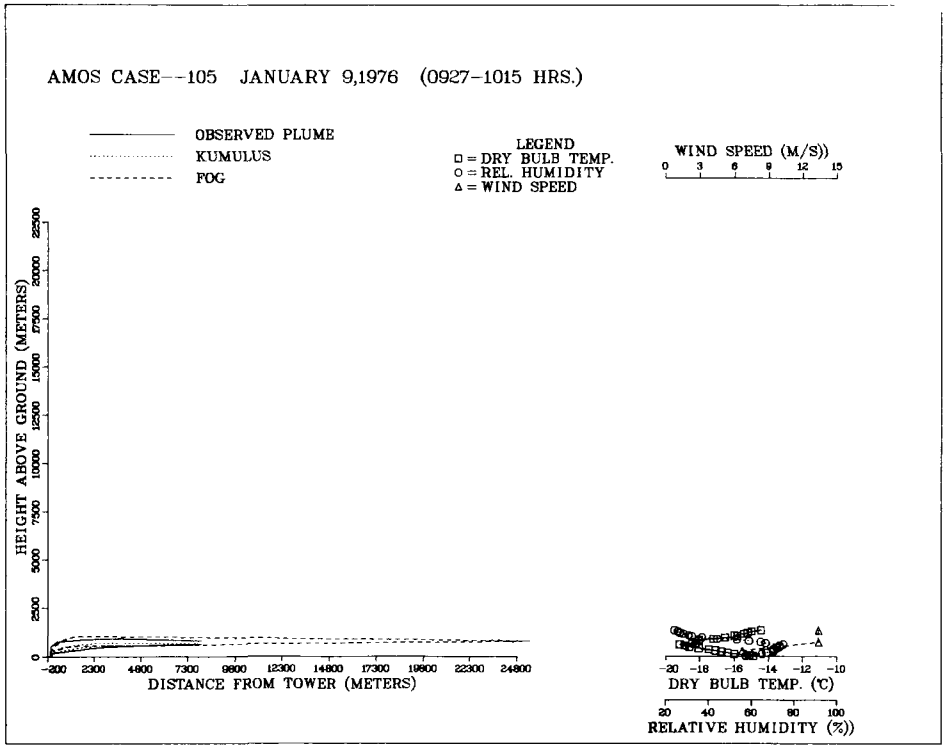

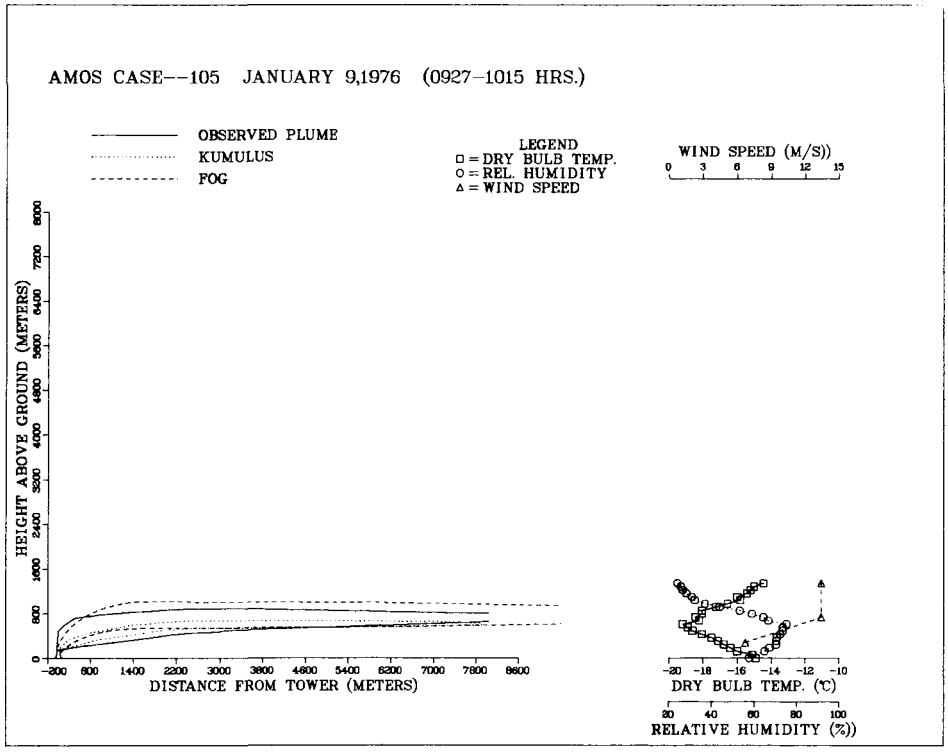

Figure 5-40. Comparison of predictions of KUMULUS and FOG models to observed visible-plume outlines at Amos . . . case A105A.

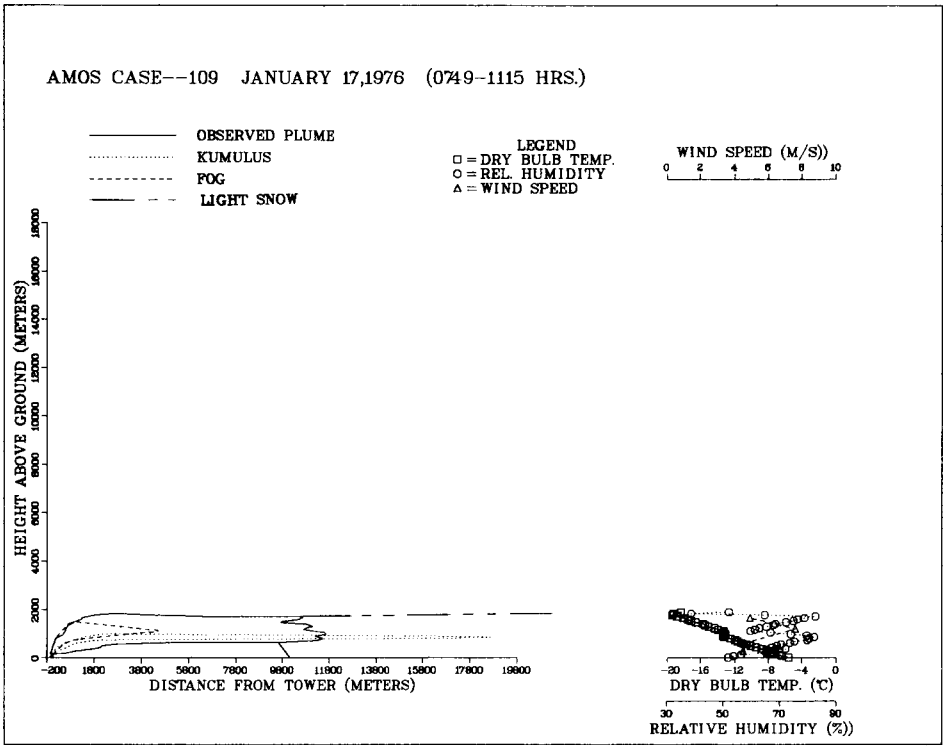

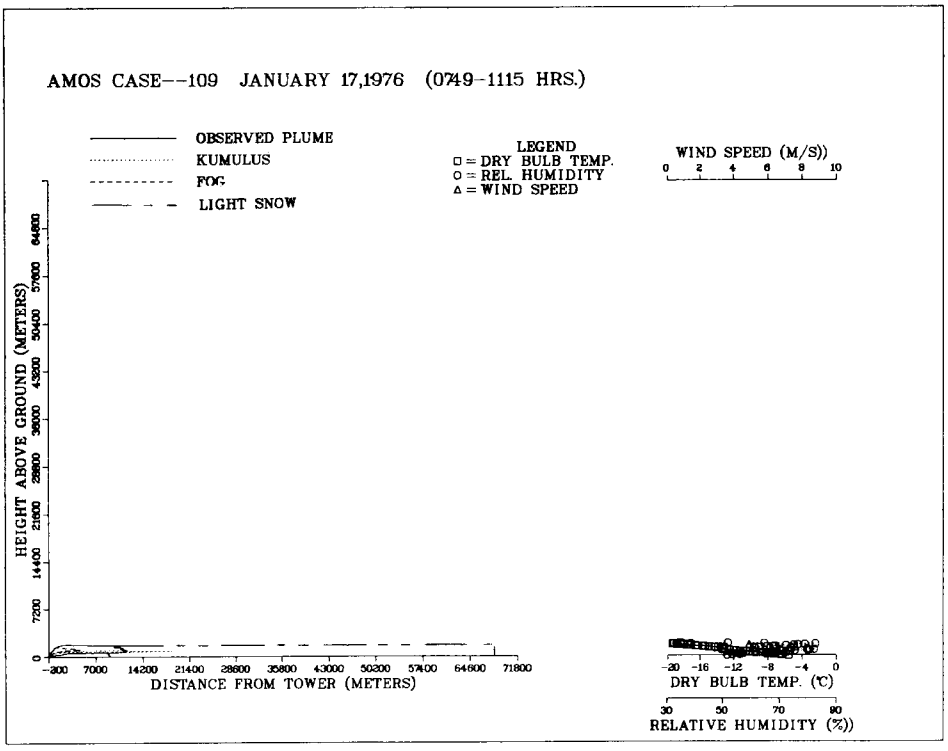

Figure 5-41. Comparison of predictions of KUMULUS and FOG models to observed visible-plume outlines at Amos . . . case A109.

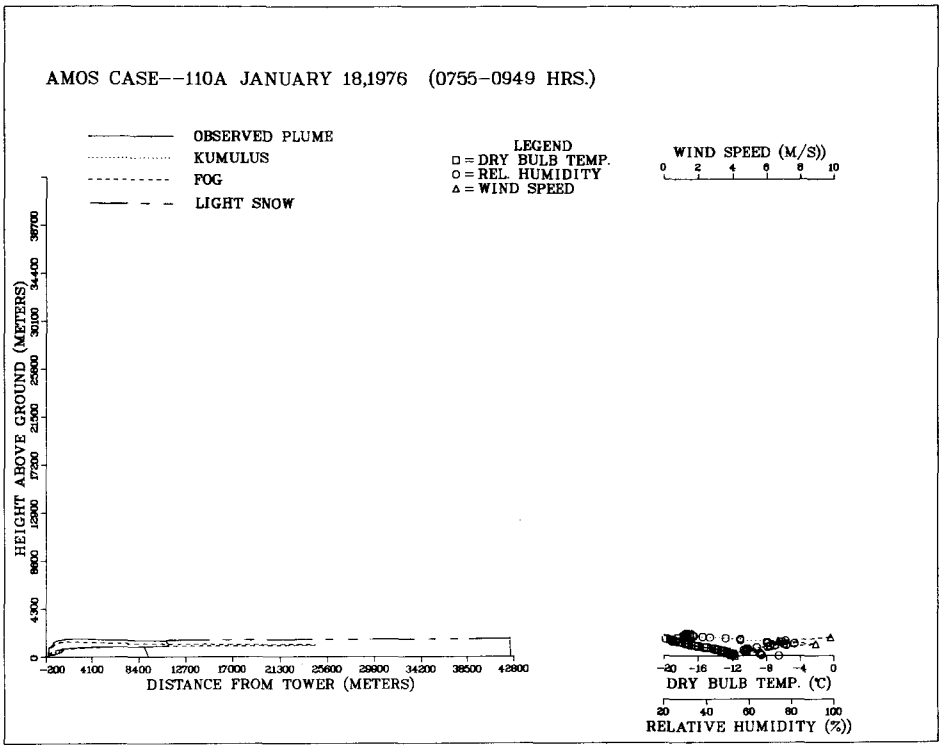

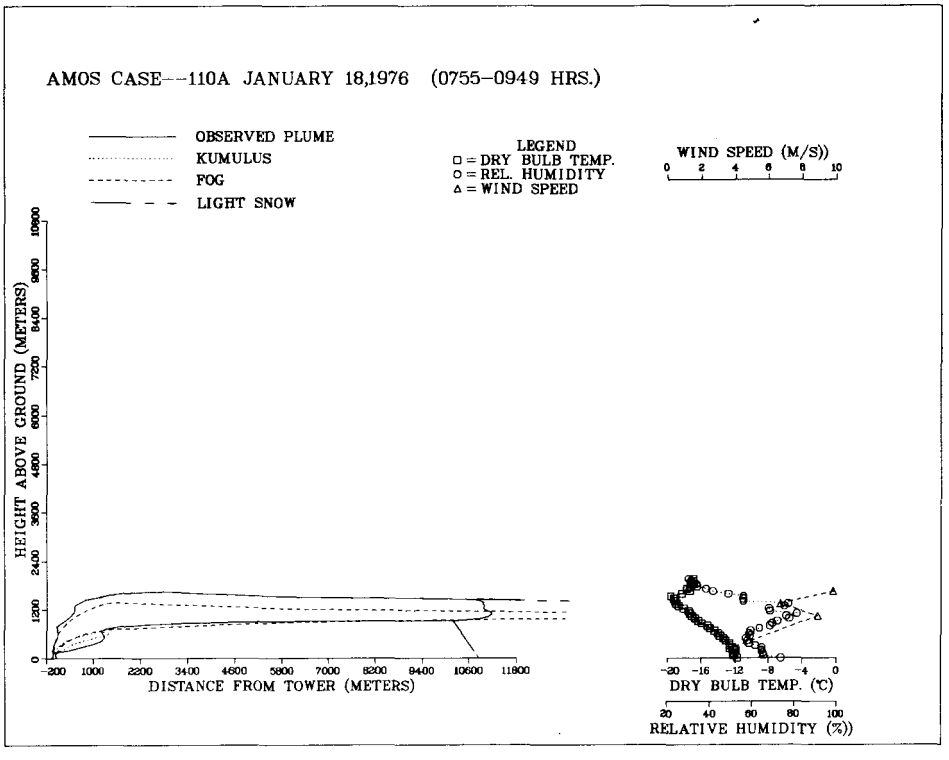

Figure 5-42. Comparison of predictions of KUMULUS and FOG models to observed visible-plume outlines at Amos . . . case A110A.

BEFORE CALIBRATION

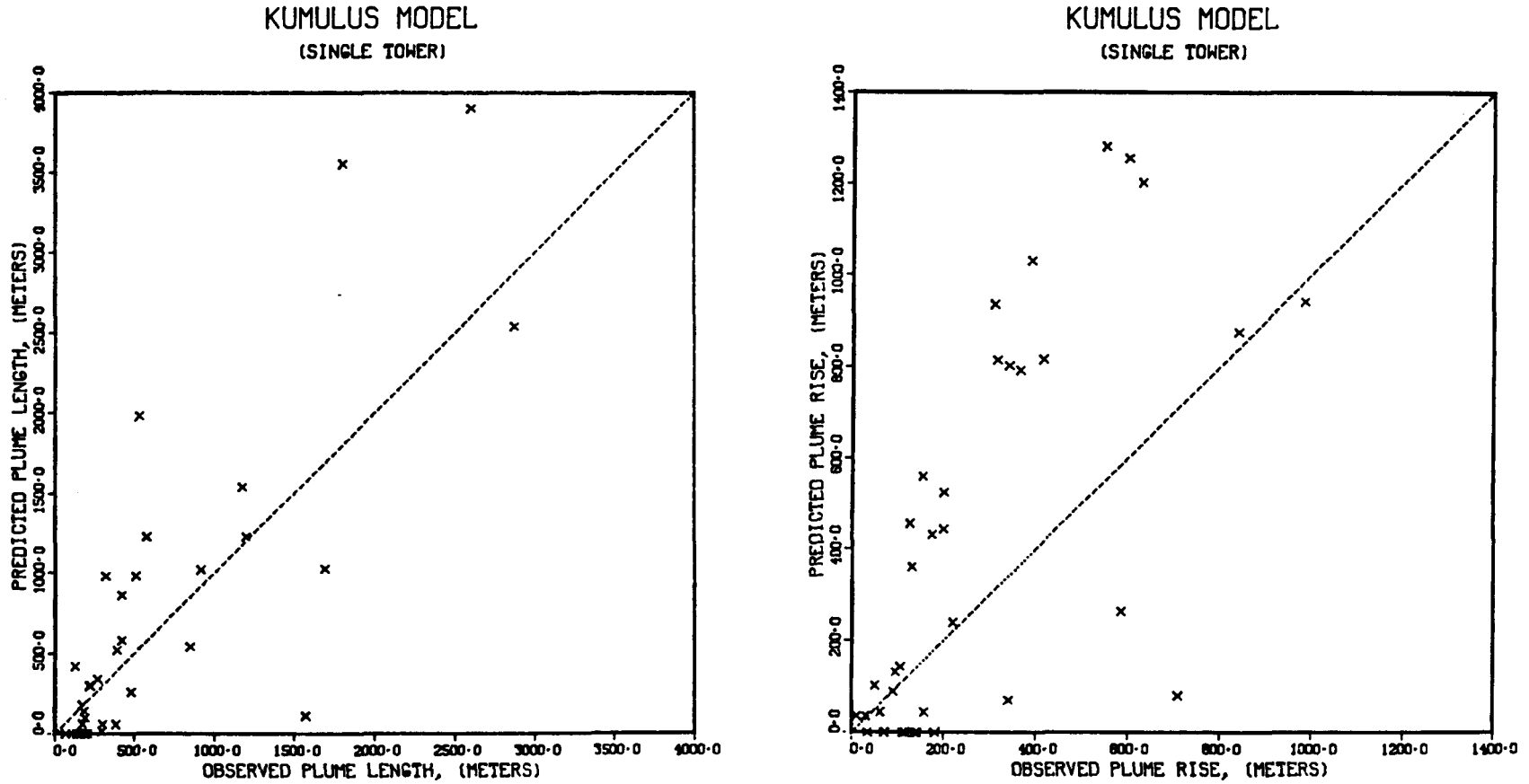

Figure 5-43. Comparison of KUMULUS model predictions of visible-plume length and rise to single tower visible plume data from Lünen, Chalk Point and Paradise (before calibration).

AFTER CALIBRATION

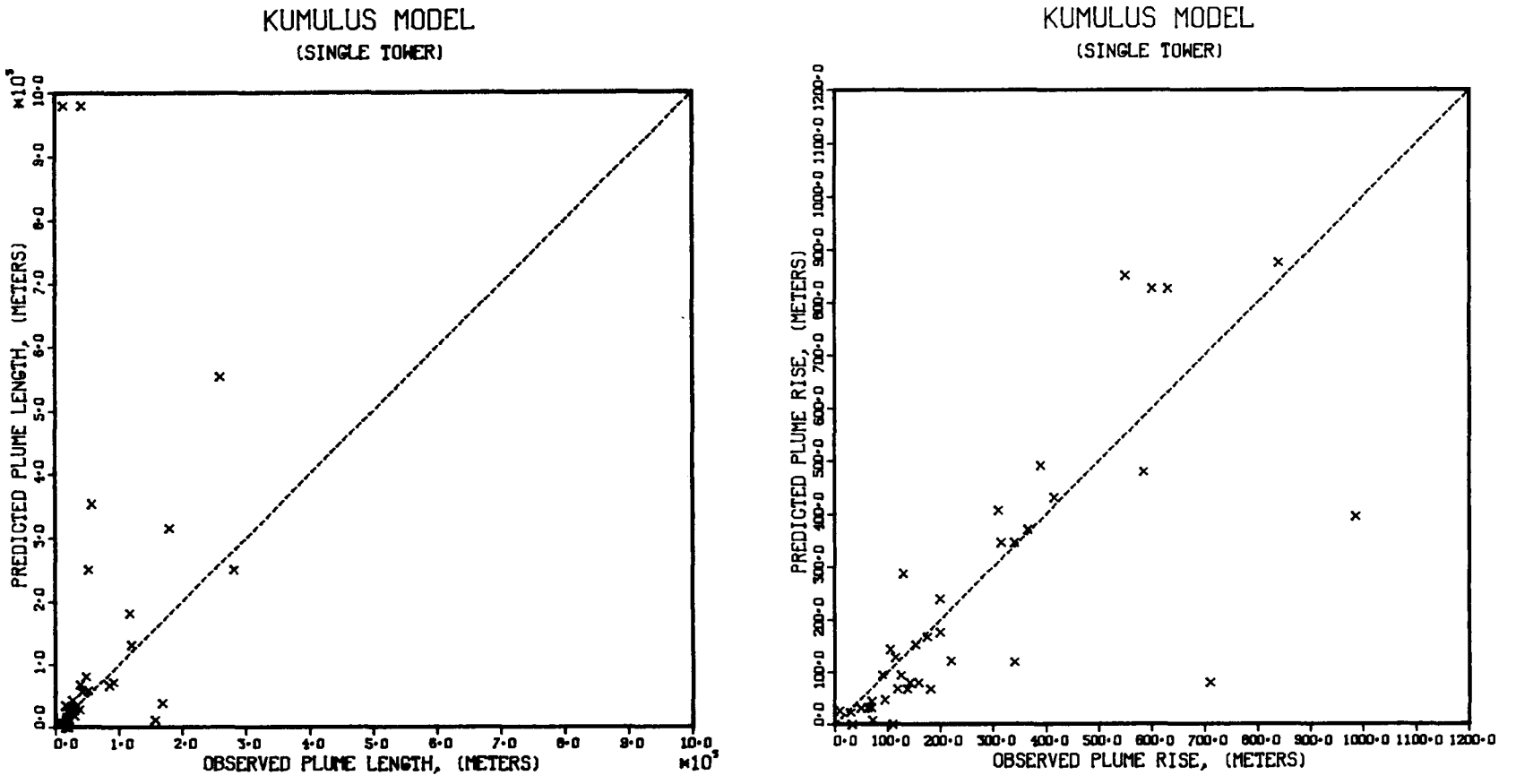

Figure 5-44. Comparison of KUMULUS model predictions of visible-plume length and rise to single tower visible plume data from Lünen, Chalk Point and Paradise (after calibration).

AFTER CALIBRATION

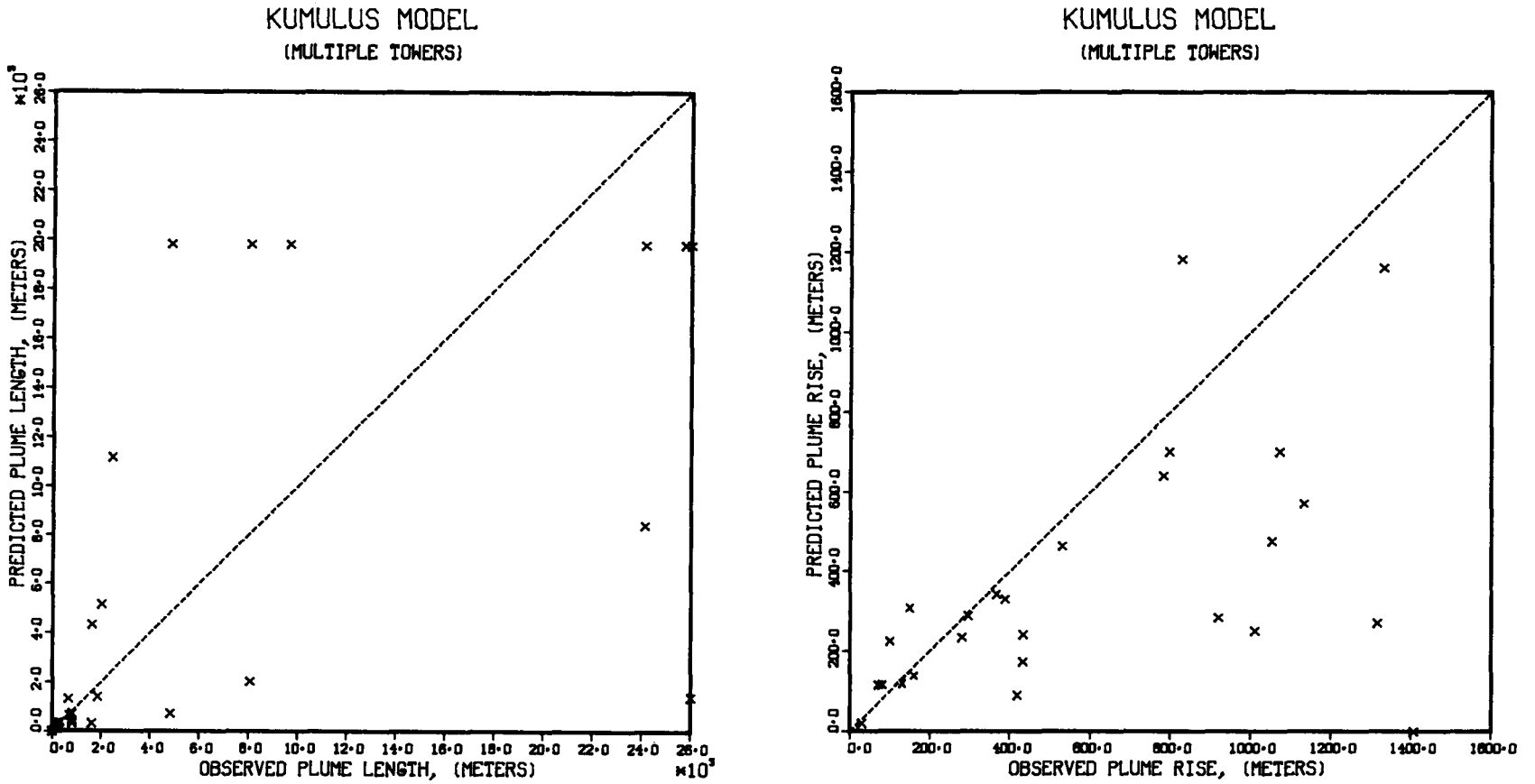

Figure 5-45. Comparison of KUMULUS model predictions of visible-plume length and rise to multiple tower visible plume data from Neurath and Amos (after calibration).

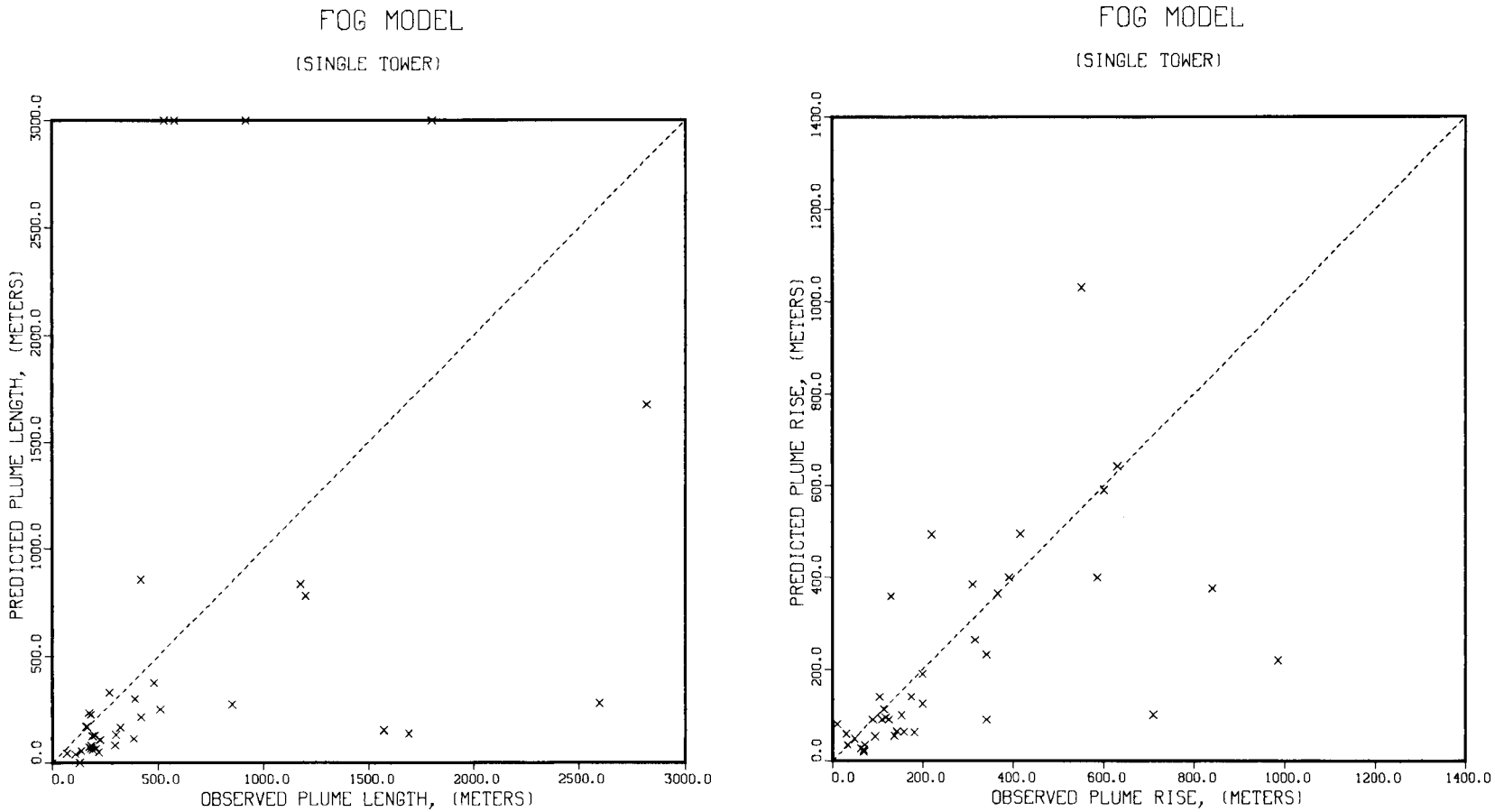

Figure 5-46. Comparison of FOG model predictions of visible-plume length and rise to single tower visible plume data from Lünen, Chalk Point, and Paradise.

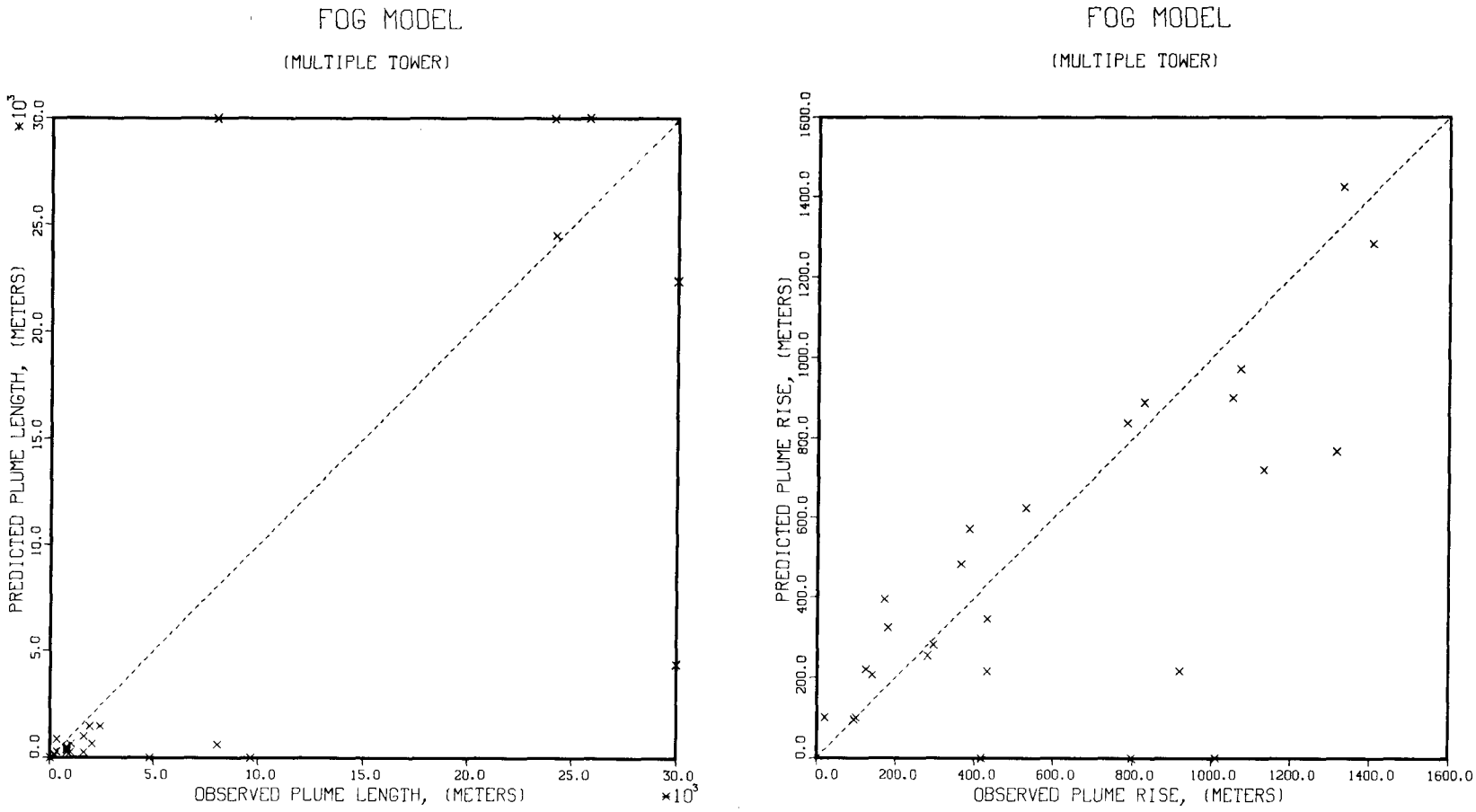

Figure 5-47. Comparison of FOG model predictions of visible-plume length and rise to multiple tower visible plume data from Neurath and Amos.

Section 6

SPECIAL STUDIES

NIEDERAUSSEM STUDY (1)

Each of the field studies presented in the earlier sections of this report represents measurement periods encompassing a short term, typically a few hours. The Neideraussem investigation is a climatological study aimed at assessing long-term physical and biological impacts of cooling towers in the near vicinity of a power plant. Of interest at Niederaussem were plume shadowing, visible-plume persistence, ground-level temperature and moisture increases, local increases in precipitation, leaf-wetting duration, and the potential for damaging effects of fluorine to local cultivated plants. Special consideration was given at the Niederaussem site for determining any damaging effects on cultivated plants by hydrogen fluoride immissions. That study should be of most interest to those involved in the environmental impact assessment of cooling towers on the environment. As far as we are aware, the Niederaussem study is the only climatological investigation of cooling tower impacts available.

The site chosen for this study was this coal-fired power station at Niederaussem, which had a capacity of 1500 MW_e at the time. The plant is situated on relatively flat terrain except for two railroad embankments and the Garsdorf strip mine beginning about 1.2 km away in the southwest. The plant cooling installation consists of three natural-draft cooling towers, each for a unit of 300 MW_e, and six mechanical-draft wet cooling towers of total capacity 600 MW_e, with a total water throughput of 191,700 m^3/h.

Ejection of water vapor does not take place solely from the cooling towers. Because of the high water content of the brown coal, considerable quantities of water vapor are removed by the chimneys with the chimney gas. Waste heat is emitted directly to the air by means of the chimneys, the boiler house, as well as by the cooling towers. For this reason, the meteorological influences on the environment can be considered only for the power station as a whole, and not just for the cooling towers alone.

The measurement technique employed was the so-called double-station method in which

there is one meteorological station on the side of the power station sheltered by the wind and one station on the windward side. Two station pairs (Figure 6-1) were set up with the lines joining them perpendicular to one another: stations A and C are in the north-northeast and south-southwest directions, respectively, and stations B and D are in the east-southeast and west-northwest directions, respectively. Each station was 650 m from the center of the cooling tower complex except for station D which had to be set up at a distance of 580 m because of adjoining cultivation. Also, station B had to be set up on a railway embankment 7 m high, due to the presence of fields on both sides of it. Stations A, C and D were all on land which was used agriculturally.

Each of the four stations was equipped with a hygrothermograph in a weather shed for determining the temperature and relative humidity of the air at a height of 2 m, and a mechanical anemometer (Woelfle type) for wind direction and wind intensity. There also was a star pyranometer for overall radiation, a leaf wetting recorder (of Woelfle-type, 1 m high), rain gauges, and, in some cases, pluviographs at each station A-D. An additional precipitation measurement profile was obtained from the four other stations. The profile extended over a distance of up to 6.3 km from the cooling towers to the east-northeast (see stations N_2-N_5 in Figure 6-1).

Measurements were taken from September 1, 1972 through June 30, 1974. The additional precipitation profile was available from January 1973. Recordings of wind, air temperature, relative humidity and leaf wetting were taken on a hourly basis. Hourly values of radiation were obtained from four fixed pyranometers and occasionally, half-hour values were acquired. Occasionally, a pyranometer on a moving vehicle was used for synoptic studies. For the precipitation, at all stations, the cumulative values between two successive monitoring periods were available (these periods were three to four days). In addition to these measurements, other measurements of different types were made with devices mounted on a vehicle. Observations also were made of the cooling tower plumes during the station monitoring trips after December 1973. Conclusions from each of the separate studies will now be given.

Plume Shadowing Effects

The decrease of a portion of the overall radiation (short wave from the sun and sky) due to the presence of the visible cooling-tower plume has raised some concern especially if the plume is above agricultural land. It is interesting to focus

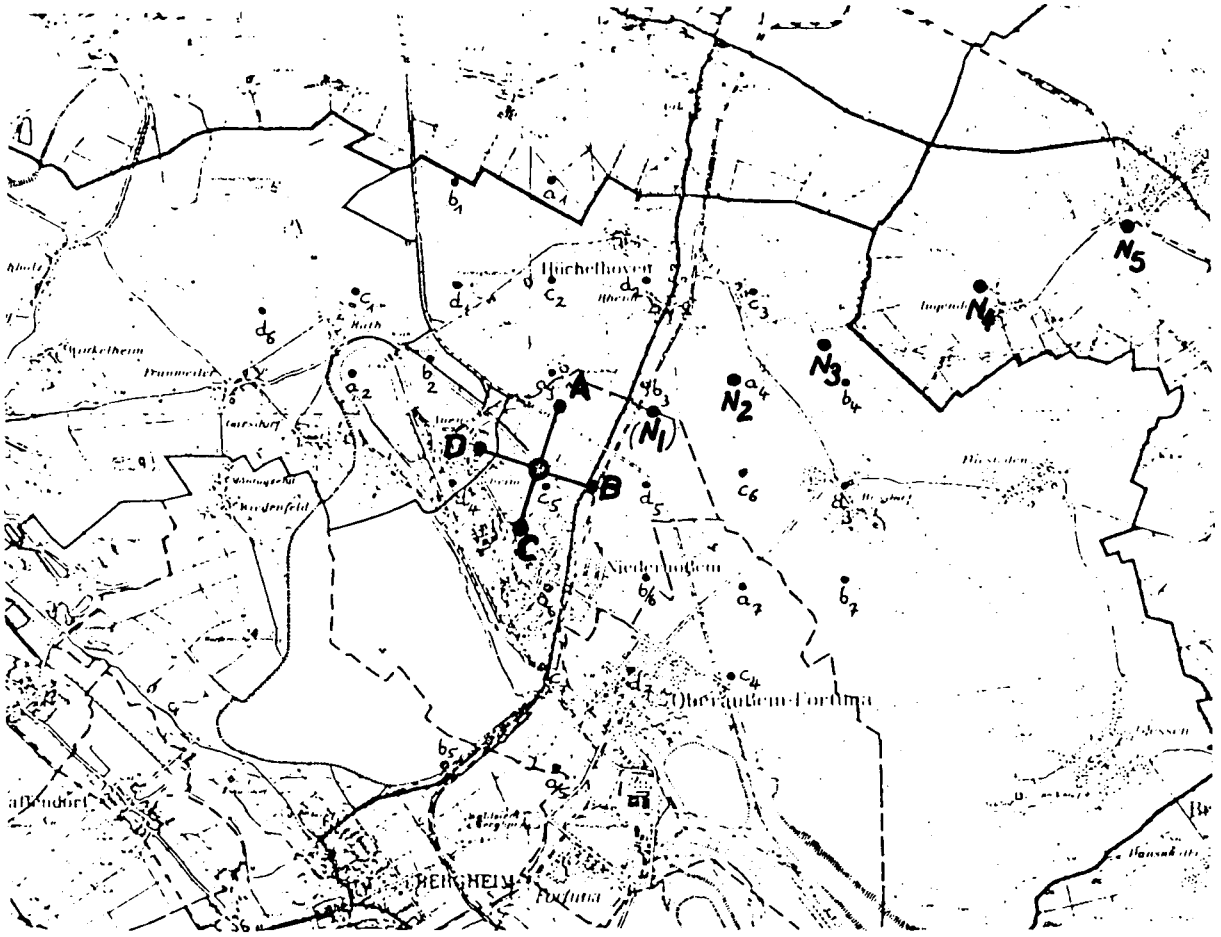

Figure 6-1. Survey map of Niederaussem and surroundings with the A, B, C, and D measuring stations shown. N_1 through N_5 are the additional precipitation measurement stations.

on data representing two sky conditions in order to present an intercomparison of the different kinds of shadowing effects on the environment that are possible. Figure 6-2 shows the distribution of the overall illumination in the environment of the cooling towers on a sunny autumn day with a weak northeast wind. In the core shadow, the illumination was reduced by about 60 to 65% in comparison to the illumination prevailing at an undisturbed comparison point. The reduction is only about 5% directly beneath the plume. The area south of the plume had a 5 to 10% increase in illumination due to the reflection of the light by the mist droplets in the plume.

Figure 6-3 shows the overall illumination measured on a cloudy autumn day with weak northeast winds. The reduction in illumination in the narrow core directly below the plume is about 20%, whereas, with increasing distance and decreasing shadowing, the reduction drops to about 5% at a distance of 350 m on the southeast side or at 500 m on the northwest side.

The data showed that the instantaneous values of radiation losses can be considerable due to plume shadowing. The average loss with time, however, is only slight, since the shadow changes its position with the direction of the wind and the position of the sun. The reduction of radiation caused by the shadowing coming from the cooling tower plume is only noticeable in the immediate vicinity of the power station. If we start from a point 200 m northeast of the cooling towers, the radiation losses for a 500 m circle are about 5-25%, and from there points distant by 1000 m, the radiation losses are less than 1% to about 5%, and beyond 1000 m, they are practically imperceptibly slight. Interestingly, the maximum radiation losses due to shadowing occur during parts of the year when light intensities for maximum assimilation by plants are already exceeded by large amounts.

An interesting feature of plume shadowing was discovered. As we observe for individual cumulus clouds in nature, the irradiation along the sunny side of the plume is increased by 5-10% across a considerable area by reflection by the plume fog droplets, which appear to be white. A planimetric measurement of shadowing areas and amounts and radiation increases and amounts showed that the total loss of brightness caused by the plume under sunny conditions was reduced by 20% because of this reflection phenomenon.

From the shadowing data, the investigators concluded that, from the point of view of plant physiology, the effects of the light reduction caused by the plume, at ground locations, is less than often supposed. Given the relationship between

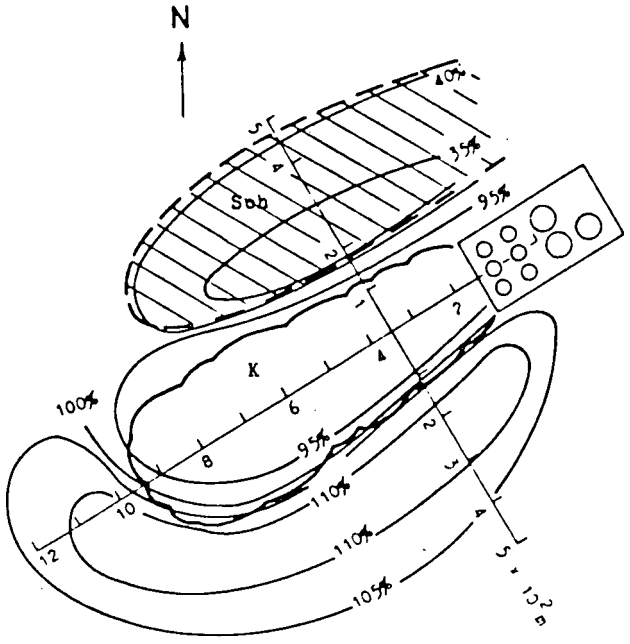

Figure 6-2. Overall illumination in the neighborhood of the cooling tower plume at Niederaussem in percent of undisturbed illumination for a sky without clouds. (K represents the plume).

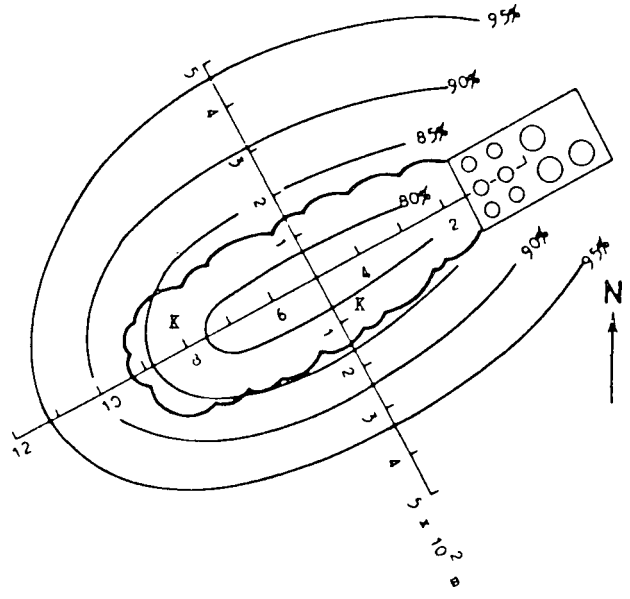

Figure 6-3. Overall illumination in the neighborhood of the cooling tower plume at Niederaussem in percent of the undistributed illumination for a completely overcast sky. (K represents the plume).

intensity of illumination and rate of assimilation, which at high light intensities already is far into the saturation range, shadowing light losses are of no consequence for growth. Also, the average radiation loss with time is only slight, since the shadow changes its position with the direction of the wind and the position of the sun.

Temperature and Relative Humidity Effects

As stated above, Stations A-D had hygrothermographs with measurements made every hour. Each hydrothermograph was in a weather shed (the so-called Giessener shed) located 2 m above ground. A mechanical anemometer (method of Woelfle) was used for determining wind magnitude and direction. The relatively large errors possible with use in a hair hygrometer for relative humidity might mask the kinds of variations seen between upwind and downwind locations. In the A-D orientation, one station was always upwind of the downwind station of interest as a result of the orientation of stations A - D.

It was necessary to determine when the individual stations were on the leeward side or on the windward side of the power plant. The assumption was made that the station was on the leeward (or windward) side if the wind came from (or went to) the direction of the cooling towers, or deviated from this by up to 22.5° counter-clockwise. This assumption was made in order to account for the clockwise rotation of the wind direction with respect to height. Out of the total number of hourly measurements of wind direction, 7,022 counted hours yielded a leeward hour distribution for the individual stations, as shown in Figure 6-4.

Station B exhibits the greatest number of leeward hours which means nothing more than the known predominance of westerly winds. Station D which is opposite, is found in the lee of the power station with the second greatest frequency, while the two other stations, C and A, have only 16.5% and 6.5%, respectively, of the total leeward hour count.

For each of the hours counted, the differences in air temperature were determined between the station on the side exposed to the wind and the station on the lee side. These differences were associated to the time intervals: 12 midnight-6 am, 6 am-12 noon, 12 noon-6 pm, and 6 pm-12 midnight. The mean values of the air temperature differences between the lee side and windward side, $\Delta T = T_{Lee} - T_{Windward}$, were computed and were plotted as function of time of day (6-hour intervals) over

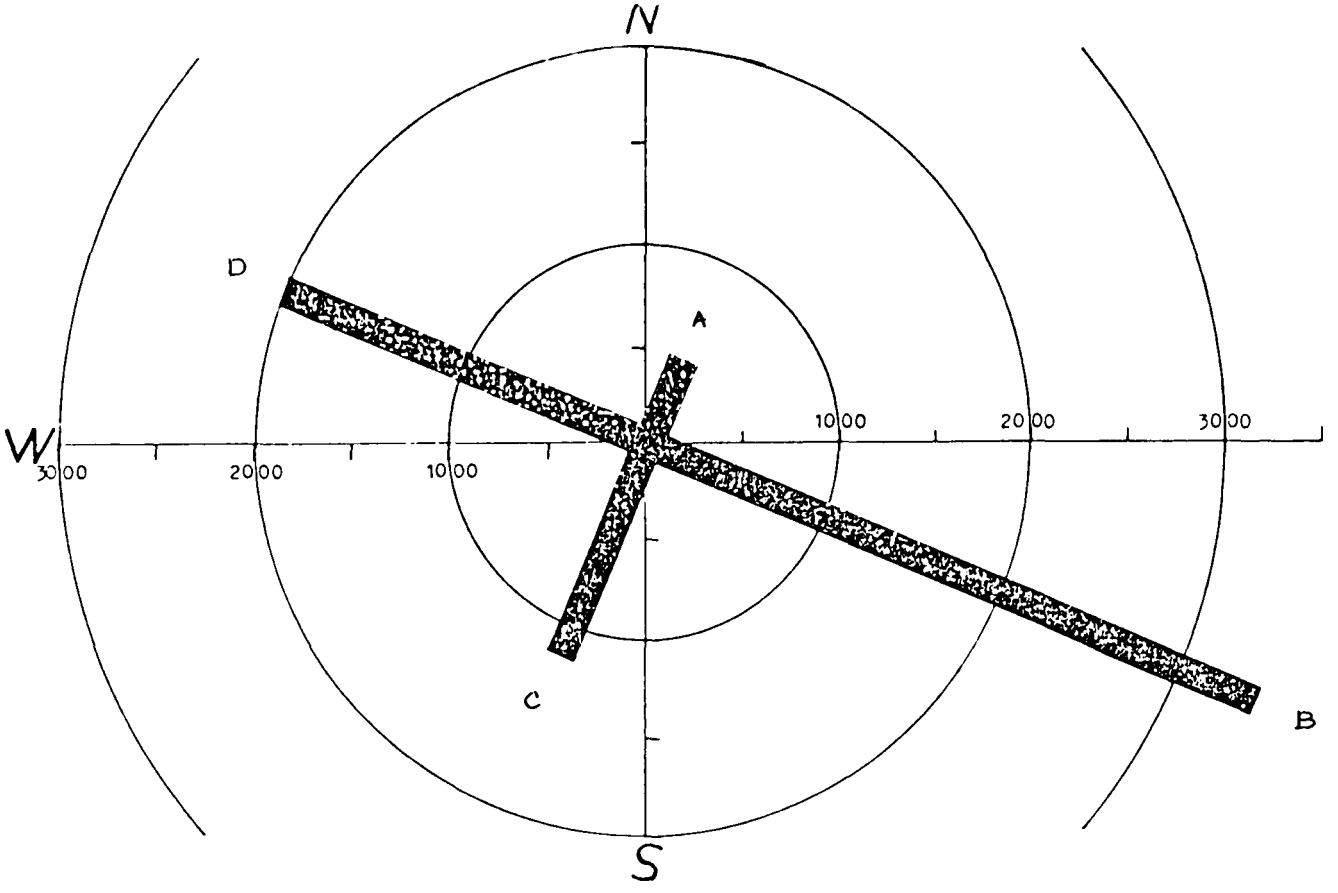

Figure 6-4. Leeward measurement hours for the stations A-D in the total time interval from September 1972 to June 1974 at Niederaussem. The columns are plotted in the direction of the stations from the cooling towers outward.

the total time period of the study (Figure 6-5). A daily cycle can be clearly seen in Figure 6-5 with a maximum for ΔT at night between 12 midnight and 6 am of 0.70°C; then, in the day, a decrease to 0.25°C (6am-12 noon) and 0.06°C (12 noon-6 pm) and, finally, as night falls, a sharp increase to 0.54°C (6pm-12 midnight).

Temperatures are almost always higher on the lee side of the power station due to the waste heat of the power station and probably mostly from the boiler house. It is the more stable conditions at night that keeps the heat from the plant nearer the ground in contrast to daytime where more unstable conditions occur leading to a greater rise of the heat. Station C showed the greatest increase in temperature from the upwind side and station A showed the least increase in temperature from its upwind side. We would expect station B to have the greatest temperature increase by making a correspondence with Figure 6-4. This discrepancy is due to the extent to which the air movement is impaired at the individual stations by obstructions in the environment (principally buildings). For station C, the air movement is the most strongly impaired and for station A, it is the least impaired.

The same procedure as used for temperature differences was also applied to relative humidity differences. A daily cycle for relative humidity differences (lee side minus upwind side) was noticed as well and is plotted (Figure 6-6). It is very clear that these differences were almost exclusively negative, meaning that on the lee side of the power station, the relative humidity is less than on the side exposed to the wind. In addition, differences are greater during the night (between 1.5 - 2.5%) than the day (below 0.5%). The lowering of the relative humidity on the lee side, in comparison to the side exposed to the wind can be simply explained by the higher temperature on the lee side. The total water content (difference between lee and windward sides) is slightly positive in the summer and negative in the winter. However, for the orders of magnitude seen, we are surely dealing with some uncertainties with regard to measurement and evaluation and accuracy. The investigators concluded that the influences of the cooling tower plumes show less effect on lee side temperature and humidity than other heat sources and of these heat sources, the boiler plant contributes probably the most.

Local Precipitation Effects

Stations A-D measured total precipitation (drift plus rainfall plus snowfall). In addition, a precipitation measurement profile was obtained from 4 other stations (N2, N3, N4, N5) from Jan. 20, 1973 which extended over a distance of up to 6.3 km from the cooling tower in the east-northeast direction. Monitoring for all 8 stations was carried out regularly twice weekly.

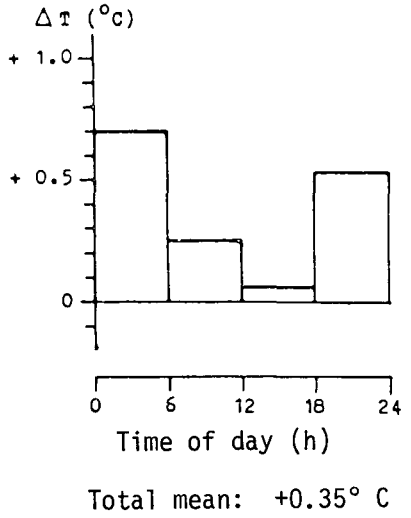

Total mean: +0.35° C

Figure 6-5. Mean values of the air temperature differences between the lee side and the windward side at the Niederaussem cooling towers as a function of time of day (6-hour intervals) for the total time period (Sept. 72-June 74).

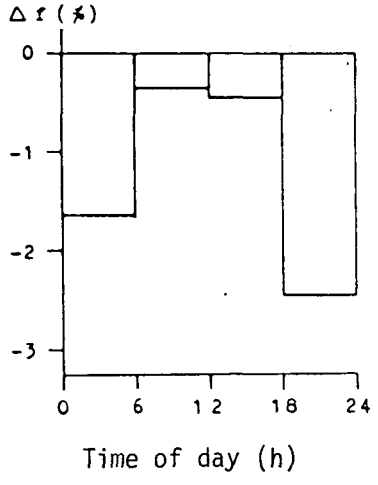

Total mean: -1.1%

Figure 6-6. Mean values of the difference of the relative humidity between the lee side and the windward side at the Niederaussem cooling towers as a function of time of day (6-hour intervals) for the total time period (Sept. 72-June 74).

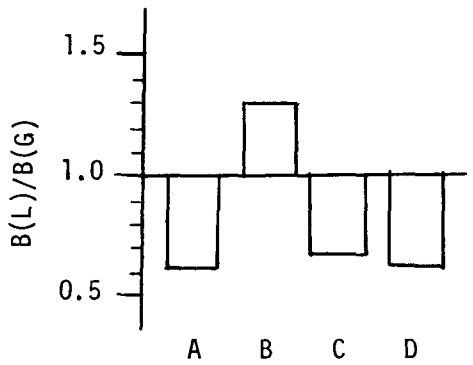

Figure 6-7. Ratio of relative leeward wetting duration to relative total wetting duration for stations A-D at the Niederaussem cooling towers for the total time period (Sept. 72-June 74).

Number of leeward hours for each station:

A	439
B	3403
C	1059
D	1967

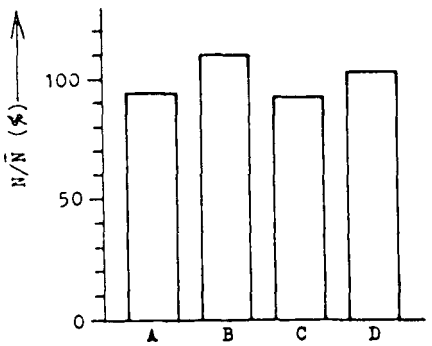

Figure 6-8. Ratio of the precipitation sums of the stations A-D to the mean precipitation sum for stations A-D at the Niederaussem cooling towers for the total time period (Sept. 72-June 74).

The precipitation measurements were carried out with rain gauges and on some occasions, with pluviographs. Readings were taken every three or four days at each station. Spatial variations in precipitation were accounted for in the location of the rain gauges (4 points in a 650 m circle about the cooling tower complex center and 4 points in a straight line out to 6.3 km). Temporal variations were determined only from twice weekly measurements over a period of two years.

It was found that the cooling tower plume occasionally led to an intensification of the precipitation in the immediate vicinity of the cooling tower complex. In almost every season, greater precipitation appeared at station B which was most frequently on the lee side of the power station. However, it was not possible to determine the extent to which this was attributable to the special position of this measurement point on the railway embankment. Reliable quantitative data could not be presented on the basis of the precipitation measurements available. Definitive conclusions could not be reached due to the special location of station B and the lack of careful statistical analysis of the data. However, circumstantial evidence exists of local increased precipitation including the higher precipitation measurements at B (Figure 6-7) and the occasional recording of increased snowfall under the cooling tower plume.

The results seem to indicate that the precipitation around the cooling towers is a little higher than at a greater distance. This average increase of a few millimeters per year could be seen especially on the main lee side of the station.

Improvements in the measurement techniques could have been made in the following areas:

(a) many more rain gauges located further from the plant than 6.3 km

(b) continuous recording of rainfall would have been more valuable in order to test the effects of individual storms.

(c) Station B had to be set up 580 m from the tower complex due to adjoining vegetation. It was set up on a railway embankment 7 m high which was more likely, due to its location, to accumulate precipitation than the other gauges.

Visible Plume Length

Observations (by sight alone) were made for 53 days to determine whether or not the visible plume was above the measurement station (of A-D) located in the leeward position of the wind. The data were acquired from Dec. 17, 1973 to June 30, 1974 during bi-weekly monitoring trips. These observations were always made in the afternoon and thus are only representative for this time. Only 23 of the total cases did a visible plume reach to the station or beyond (i.e. plume length $\geq$ 650 m),

which gives us 43% of the cases observed. Out of the 30 remaining observation days, 16 of the visible plumes (=30%) disappeared shortly after exit from the cooling towers. The size of this data base is not large enough to provide definite estimates on plume length climatology.

Table 6-1 shows the percentage distribution of visible plume lengths as a function of the seasons. The frequency of longer plumes decreases from the winter to the summer, from 65% to 19%. However, because of the relatively low number of cases, we should not overrate these percentages. Noteworthy is the high number of cases (56%) in which, in the summer, the visible plume disappears almost immediately after exiting the cooling towers (plume length < 200 m). In the winter, this was the case only in 10% of the observation days.

The investigators did assume that the leeward position was established on the basis of the ground wind conditions and accordingly, cases occur in which, in spite of the leeward position and adequate length, the plume was not above the station, because the wind directions close to the ground and at the height of the plume varied more from one another than was assumed. For this reason, the time in which a cooling tower plume was present above a leeward station was, with high probability, below 50% of the total number of leeward hours in all seasons. This situation was noted, but it was of no consequence except in the unusual case where the plume touches the ground. Such a phenomenon was seldom observed and thus, it can be concluded that there are no such effects to be concerned with as relates the cooling tower plume.

The study could have been strengthened by the acquisition of more data more often during the day than just afternoons and over longer periods of time to improve the statistics.

Additional Studies

Three additional types of measurements were made which will be briefly discussed. The first measurement subprogram was set up to determine whether the large quantities of water released from the cooling towers lead to a more frequent and longer lasting wetting of plants in the vicinity of the towers. Such an effect could cause a delay in the drying up of the soil before tillage ; it could cause a reduction in the efficiency and time of use for plant protectives as well as aid in the development and reproduction of pests. Leaf-wetting recorders were set up at each station 1 meter above the ground. Recordings were made hourly to see

Table 6-1.

Percentage distribution of visible plume lengths as a function of season at Niederaussem.

	Visible Plume length		
	>650m	<200m	Number of observations
Winter (12/73 - 2/74)	65%	10%	20
Spring (March, April 74)	41%	30%	17
Summer (May, June 1974)	19%	56%	16
Total (12/73 - 6/74)	43%	30%	53%

Notes: (a) Visible plumes < 200 m in length are essentially those which disappear slmost immediately after exit from the cooling tower.

(b) The monitoring trips were used in the afternoon and therefore the plume observations are thus only representative for this time of day.

if leaf-wetting occurred. These measurements were used to form ratios based on the number of hours that each station was in a leeward position. B(G) represented the ratio of the total number of wetting hours to the total measurement hours. B(L) represented the ratio of leeward wetting hours to the total leeward measurement hours. An influence of cooling tower emissions on the leaf wetting could then be determined when the ratio B(L)/B(G) was formed and then plotted for each station as a function of season. It was found that for stations A, C and D, the wetting in the leeward position is always lower than the total wetting. As a result, an increase of the wetting duration from the cooling towers could thus be excluded.

Station B showed an opposite effect. The leeward wetting, except for the summer of 1974, was always more than 1.5 times the total wetting. This can be explained by the fact that station B is on the lee side of the power station with respect to the predominant west-northwest winds. For these wind directions, there is a high percentage of the total precipitation and thus, the frequency of precipitation and wetting is greater than for the other wind directions. When averaging B(L)/B(G) over the entire measurement period (Figure 6-8), the relationship with station B is clearly seen. The results of an individual station cannot be considered alone. The mean of two opposite stations or of all four stations is more meaningful. The mean of all four stations (Table 6-2) was computed for the total time of measurement to follow suit with the temperature and relative humidity results. Here the ratio is always less than 1, i.e. the leeward wetting is less than the total wetting.

The result: not an increase, but a decrease of the relative wetting duration on the lee side of the power station (in the seasonal means, a decrease of 6-24%; in the total mean, a decrease of about 21%) can be explained if we compare it with the result for air temperature and humidity. Here an increase of the temperature on the leeward side (of an average of 0.35°C) appeared, and a decrease of the relative humidity by 1.1%. In addition, as we have often mentioned, on the leeward side, a more intense mixing is probably present. This all contributes to greater evaporation and hence to a more rapid drying, of both the measurement sensors of the recorder and of the vegetation. This leads, on the whole, to a shortening of the leaf-wetting time. Since temperature increase and decrease of the relative humidity are caused by the combination of the thermal power station and the cooling towers, the shortening of the wetting duration cannot be stated as based on the effects of the cooling towers alone.

Table 6-2.

Ratio of relative leeward wetting duration to relative total wetting duration B(L)/B(G) and deviation of this ratio from 1 at Niederaussem.

Period	Winter		Summer		Autumn/Spring	
	$\frac{B(L)}{B(G)}$	$1-\frac{B(L)}{B(G)}$	$\frac{B(L)}{B(G)}$	$1-\frac{B(L)}{B(G)}$	$\frac{B(L)}{B(G)}$	$1-\frac{B(L)}{B(G)}$
1972/1973	0.94	0.06	0.79	0.21	0.78	0.22
1973/1974	0.76	0.24	0.94	0.06	0.90	0.10

Total period (September 1972 - June 1974)

$\frac{B(L)}{B(G)}$	$1-\frac{B(L)}{B(G)}$
0.79	0.21

The second study dealt with the determination of whether and to what extent the cooling tower emissions can cause a delay in the drying of cultivation near the power station. Only grains were studied since the region near the power plant is almost entirely dedicated to farming. Samples were taken from an area west-northwest of the power station, comprising about 20 km^2, up to a distance of 7 km from the cooling towers. Winter barley was chosen to be examined for water content and no definite relationship could be seen between the water content of the grain and distance from the cooling towers. Likewise, samples of winter wheat were taken and again, no strong relationship was found. The water content did vary from 12-37% for the barley and 10-33% for the wheat, but it is thought that the field differences caused by the variety, soil, sewing period, and terrain climate are the influences on the changes in water content.

A more detailed study was done on these samples with a classification by distance into three groups. A deduction could not be made that there was a definite influence of the cooling tower emissions on the ear moisture.

Sample-taking was repeated a year later at a distance of up to 4.7 km from the cooling towers with the same method as before. Samples were taken from all directions except west because of the strip mines there. Several calculations were made (explained in detail in Ref. (1)) which pointed to the same results as the year before. It can be said that on the leeward side of the power station, there is no indication of an increase or decrease in ear moisture content. There are indications of a reduction of the water content on the leeward side, but these are by no means statistically certain. The differences must be attributed to other factors, such as grain varieties, fertilizers, soil types and climate to name a few, and not to the cooling tower emissions.

The third additional study dealt with the hydrogen fluoride emissions and their effect on the air and vegetation. The study of hydrogen fluoride impacts on plants was undertaken because:

(a) power stations employing coal may be emitters of fluoride (such is not yet confirmed for brown coal power plants, however), and

(b) even small traces of hydrogen fluoride gas are able to cause direct damage to the stomata of plants, and, through the medium of the plant, can lead to excessive (and, under certain circumstances, toxic) absorption of fluoride by animals. After several days of action, average HF concentrations of less than 1 $\mu g/m^3$ air can lead to enrichments of fluoride in plant organs containing chlorophyll.

A detailed description can be found in the original text. Only the results will be given here.

The two-year studies of fluoride concentrations in the air in a 3 km circle of the plant in the region of the thermal electric power station of Niederaussem produced the following results:

- In the first measurement year the fluoride quantities in the air were found higher and more frequently elevated than those in the second measurement year. Accordingly, the characteristic immission magnitudes in the first measurement year were also greater than in the second measurement year. In the second measurement year, the characteristic magnitudes were far below the legally established limiting values.

- An increased fluoride load because of the thermal electric power station cannot be demonstrated; there seems to be a somewhat higher load in the total area.

- A relationship between higher fluoride content and season of the year cannot be demonstrated.

- It is not demonstrable with certainty that higher fluoride values are present for a higher relative humidity.

- In the vegetation period of 1973, pea plants were cultured seven times in succession and the fluoride content was determined in the roots, stems, leaves, and in the associated soil. The maximum fluoride content was always in the pea roots, and the fluoride content was always lowest in the pea stems, since these only assume the function of transporting the absorbed fluoride. The fluoride content in the pea leaves was subject to great variations, and at the same time was dependent on the quantity of dust deposits containing fluoride.

- The average values of the soil, root, stem and leaf fluoride content were greater for all four stations in Niederaussem than at a comparison station in Bonn, and this indicates a greater fluoride load in this area.

No relationship between the fluoride content of the plant and the duration of wetting of the leaves was definitely established.

STUDY ON BACTERIA EMISSIONS FROM COOLING TOWERS (2-8)

A comprehensive study was carried out in the Federal Republic of Germany to assess the possibility of germs being emitted from cooling towers when waste water was being used for cooling the power plant condensers. The study encompassed many field tests on existing wet cooling towers supplemented with tests carried out on a laboratory cooling tower. The short review presented below of the results of that study is based on the synopsis in English given in Ref (6). Several reports in German (2-6) present all the details.

Two major questions are of interest. The first relates to the spreading of germs from the cooling towers and the possible direct or indirect risk to the population. The second relates to the propagation of micro-organisms in the cooling water itself due to the presence of increased cooling water temperatures and a supply of nutrients in the cooling water. Field studies investigating these two questions were carried out at prototype towers under different seasons and under various atmospheric conditions. The object of the field studies was to identify both qualitatively and quantitatively the most important types of micro-organisms (a) at a number of locations inside the cooling tower, (b) in the cooling water, and (c) outside the tower in its immediate vicinity.

Field Experiments

The test methods used were designed mainly to detect bacteria of medical importance. Clearly the bacterial content of the cooling water is determined primarily by the quality of the surface water fed in to the plant. Whether bacteria multiply or reduce in number in the cooling water depends on the type of water treatment, the type and quantity of organic material in the cooling water, the water temperature, and the additives and biocides used for conditioning.

It was found that in the cooling water, the total CFU values (CFU = colony-forming units) can increase by a factor of 30 compared with values in the incoming surface water to the plant as a sole result of cooling water temperature increases. Entero-bacteria multiply in the cooling water, but only when heavy contamination with organic material is present. Without such contamination, no multiplication takes place at increased water temperatures. On the other hand, however, a rise in germ count in

the case of certain micro-organisms such as, for example, Pseudomonas aeruginosa, can also be promoted without very large amounts of organic materials in the cooling water but due to the addition of conditioning materials.

Now the findings on the pathogenic micro-organisms emitted at the tower top will be summarized. Evaluations of measurements at tower tops and from river water samples indicates that under unfavorable conditions when there is a total germ emission rate at the tower top of 10^8/sec, there is a discharge of 10^7 coliform bacteria as well as (theoretically) 10^3 salmonella and 10 tuberculosis pathogens as well as 200 virions per second. The authors felt that the number of virions was too high because viruses are predominately deposited on solids and unusually large particles which are not discharged with the cooling tower plume vapor. Accounting for other factors which cause damage to aerosol-borne germs in the plume, the authors felt justified to reduce as well the numbers of intestinal bacteria including salmonella by 10 in each case.

Thus the rate of emission of pathogens is smaller (100/sec of salmonella, 10/sec of tuberculosis pathogens, 20/sec of virions) over the area of 700-3700 m^2 (cross-section of the cooling tower at the top). During the time in which they remain in the atmosphere, the bacteria which are predominantly found individually in the aerosols, are then also subjected to additional vitiation (due to changes in the relative humidity, desiccation, solar radiation, open-air factor, temperature). This is a result of their travel through the plumes where the plume is spreading and mixing depending upon the local ambient wind and temperature. The above vitiating influences have a more pronounced effect at high temperatures and with solar radiation, i.e. at those times during which the cooling towers are more frequently operated in Germany because of increased river water temperatures or as a result of low water levels.

Whereas the influences discussed above lead to a reduction in the concentrations, it must also be recognized that continuous rain will wash away bacteria contained in the plume, which could result in <u>increased</u> immission in the immediate vicinity of the towers. It was found, however, that under these environmental conditions there was no increased germ count to be observed immediately above the ground.

If all the effects on the micro-organisms in the atmosphere mentioned above are taken into account, then it is not surprising that even when searching through large volumes of air, the authors were not able to isolate pathogens. Notably, the 3.5 m^3 of air per measuring point sucked in over a period of 5 minutes using

slot collectors was far above the average quantity which an adult person inhales per hour (0.54 m^3).

Theoretical Predictions

Upon superficial observation, the estimated emission rates appear to lead to fears of serious immission. In order to confirm the ground-level measurements, mathematical computation was also used to determine what concentration of germs occurs in the air above the ground and what immissions can theoretically be caused on the ground. In these calculations, an assumption of unfavorable conditions was made. These predictions were compared with the measured results which covered not only the dispersal in the atmosphere, but also the behavior of sedimented germs on plants and in the earth.

It turned out that the experimentally measured immission rates were not larger than the values predicted, but varied in concentration between 10 and 200 CFU m^{-3} in regions which can be measured in areas of low or no anthropogenic influence. The maximum, long-term surface concentrations which result under such conditions amounts to about 2.3×10^5 CFU m^{-2}. This relatively low additional concentration (approx. 10^{-3}%) will hardly be evident since a normal concentration found on earth and grass samples is about 10^{10} CFU m^{-2}.

Furthermore, laboratory investigations to confirm the results of the field measurements have indicated the mortality rate of micro-organisms under idealized conditions. Information was acquired from these investigations concerning the relation between the mortality rate and the thermodynamic as well as flow conditions in the cooling tower.

Lab Experiments

The lab measurements were carried out with a pure culture of E. coli. They allow the following conclusions to be drawn:

In the super-saturated cooling-tower plume, the colony-forming capability of bacteria carried in the drops does not alter very much. With an unsaturated plume, however, a differentiation must be made between two types of reactions. The lab experiments, in which the germ suspension was sprayed into unsaturated air without mixing secondary air, revealed no dependence of the rate of reduction upon the actual value of the plume relative humidity. In contrast, the experiments in which the germ-bearing

droplets were vaporized due to the mixture of an unsaturated secondary air flow revealed a clear reduction in colony-forming capability with decreasing relative humidity. This latter case is of importance for dispersal and immission of airborne germs from cooling towers to the extent that also here, the visible plume, at first charged with drops, is dried by the admixture of unsaturated ambient air. Here the micro-organisms do not behave uniformly; enterobacteria and Pseudomonas aeruginosa are, for example, more strongly reduced than sporogenic organisms.

Test results and propagation calculations have both equally confirmed that as a result of the considerable spreading in the propagation of the cooling-tower plume a measurable germ contribution caused by the cooling-tower emission can be ruled out. Where, nevertheless, there is a growth of individual bacteria from the cooling-tower vapor on the ground or solid surfaces, then experience shows that they rapidly perish unless they accidentally reach a source of nourishment which also allows the growth of greatly vitiated micro-organisms.

Discussion of Environmental Impact

The total germ content and the number of facultative pathogenic micro-organisms in the plume is dependent primarily on the quality of the incoming cooling water. For this reason the problem of germ propagation through the operation of cooling towers is directly related to the level of treatment of the waste water prior to discharge into the surface waters. Where the circulating water contains large quantities of pathogens, then, as expected, there is an increased discharge of germs at the top of the cooling tower although not above a maximum value. In the case of high contamination, an improvement in the water quality is possible by sand filtration and precipitation of suspended substances as well as, where necessary, through the addition of antimicrobial substances.

At a given contamination of the cooling water, the germ content in the plume is further determined to a large extent by the drift eliminator. As the investigations have shown, the discharge of germs at the top of the cooling tower - even with a high germ content of the circulation water - does not exceed a maximum value when modern drift eliminators are used. Whereas in the case of cooling towers without drift eliminators, a considerably higher emission is to be expected. In the region of the drift eliminator, there is a quantitative but no germ-specific reduction, i.e. with a relatively high proportion of facultative pathogenic micro-organisms in the cooling water there is first of all a relatively equivalent proportion to be expected in the plume. From the germ content in the plume from cooling towers with

well-designed drift eliminators, a recalculation for the content of pathogens produced values which (after dispersion in the atmosphere and after the effects of vitiating factors) indicated the expectation of such a low immission that the risk of an infection through inhalation or deglutition is negligibly small. In practice, no danger is to be expected. Also the possibility of a multiplication of sedimented germs on or in nutritional plants in the wider vicinity can probably be excluded.

In the immediate vicinity of the cooling towers, on the other hand, increased germ counts through the discharge of spray water must theoretically be expected. Furthermore, a relatively increased concentration through germs being washed out of the plume with rain would also be theoretically conceivable. To prevent these indirect risks, the investigators state that it is in any case sufficient in the immediate vicinity (150 m around cooling tower installations) to ban the cultivation of fruit and vegetables which are consumed uncooked. They also recommend that no meat, meat products, milk and other easily perishable foodstuffs should be stored openly in this area.

Only in the case of cooling towers with no or badly-designed drift eliminators can one expect higher bacterial discharge and thus also increased risk.

Concerning the discharge of cooling water which passed through the cooling tower into rivers and other water bodies, results indicated no significant increase in the colony counts. Such a generalization will not necessarily apply to rivers under low speeds without further analysis.

Compared with the possibilities of other methods of transmission of pathogens from surface water or sewage, the discharge of germs from cooling towers is of only minor importance. For example, bathing in surface waters carries a far greater risk through the ingestion of 50 ml of water. But since, in spite of the ingestion of water of a comparatively high germ content, bathing has been found to produce only a few epidemics, it is unlikely that there is any kind of danger from the ingestion of the cooling tower aerosol.

Relevant germ-containing aerosols were not evident in the vicinity of cooling towers despite the collection of large volumes.

Furthermore, the source of emission is usually at a height of more than 100 meters. The micro-organisms are thus present for a longer duration in the air and, as a result, there is a greater reduction in the germs reaching the ground compared with sources close to the ground.

Study Conclusions and Discussion

Based on the present level of knowledge, the investigators state that it is possible to equip and operate cooling plants in such a way that there is no risk of infection. For the assessment from the health physics point of view of a planned cooling installation at a particular location, the microbiological and chemical values of the cooling water made available are of primary importance. With careful technical design of the cooling plant together with appropriate regard to the specific circumstances of the location (population density, topography, climate), a health physics assessment is possible. But since the crucial data are frequently only obtainable during actual operation, an acceptance test may occasionally be necessary. The investigators state that, in any case, the requirement must be that there will be no danger due to micro-organisms or chemicals resulting from operation of the cooling plant beyond that which is already encountered from other sources. Where such a risk exists, a reduction in the risk must be achieved through additional technical equipment or modifications or adoption of the chemical additives to the circulating water. Furthermore, the authors state that it must be ensured through methodical operation that the superheating in the surface water or the release of permissible quantities of chemicals are not considerably exceeded even for short periods. Above all, in the case of low velocity river water, the possibility of a sudden contamination or poisoning of the cooling water as the result of an accident must be separately and adequately evaluated.

REFERENCES

1. H. Berge, E. King, and D. Lorenz. Water Vapor Immissions in the Region of a Conventional Thermal Power Station Fortschr. - Ber. VDI-Z. Series 15, No. 6. 1975, pp. 175.

2. J. Borneff, G. Ernst, H.-P. Werner and D. Wurz. Microbial Emission, Immission and Changes in the Germ Count in the Cooling Towers I. Communication: Introduction to the Problem Posed. Zbl. Bakt. Hyg., I. Abt. Orig. B 169, 1-38 (1979)

3. H. -P. Werner, E. Baer, G. Dibelius, H. Dittrich, A. Ederhof, W. Egler, G. Ernst, W. Roller and D. Wurz. Microbial Emission, Immission and Changes in the Germ Count in the Cooling Water during Operation of Wet Cooling Towers II. Communication: Measuring Methods, Emission Values and Changes in the Germ Count in the Cooling System. Zbl. Bakt. Hyg., I. Abt. Orig. B 169, 39-134 (1979).

4. E. Baer, J. Billing, G. Ernst, H. -P. Werner and D. Wurz. Microbial Emission, Immission and Changes in the Germ Count in the Cooling Water during Operation of Wet Cooling Towers III. Communication: Laboratory Tests for the Determination of the Reduction Kinetics of Escherichia coli in Cooling Tower Plumes. Zbl. Bakt. Hyg., I. Abt. Orig. B 169, 135-163 (1979).

5. K. Botzenhart, W. Egler, Y. Attar, G. Ernst, P. Fischer, L. Krizek and D. Wurz. Microbial Emission, Immission and Changes in the Germ Count in the Cooling Water during Operation of Wet Cooling Towers IV. Communication: Microbial Immission in the Vicinity of Wet Cooling Towers. Zbl. Bakt. Hyg., I. Abt. Orig. B 169, 164-205 (1979).

6. J. Borneff, G. Ernst, H. -P. Werner, K. Botzenhart, E. Thofern and D. Wurz. Microbial Emission, Immission and Changes in the Germ Count in the Cooling Water during Operation of Wet Cooling Towers V. Communication: Synopsis and Assessment Zbl. Bakt. Hyg., I. Abt. Orig. B 169, 206-223 (1979).